



Measurement of the nuclear inelastic cross sections of antinuclei with ALICE and implications for indirect Dark Matter searches

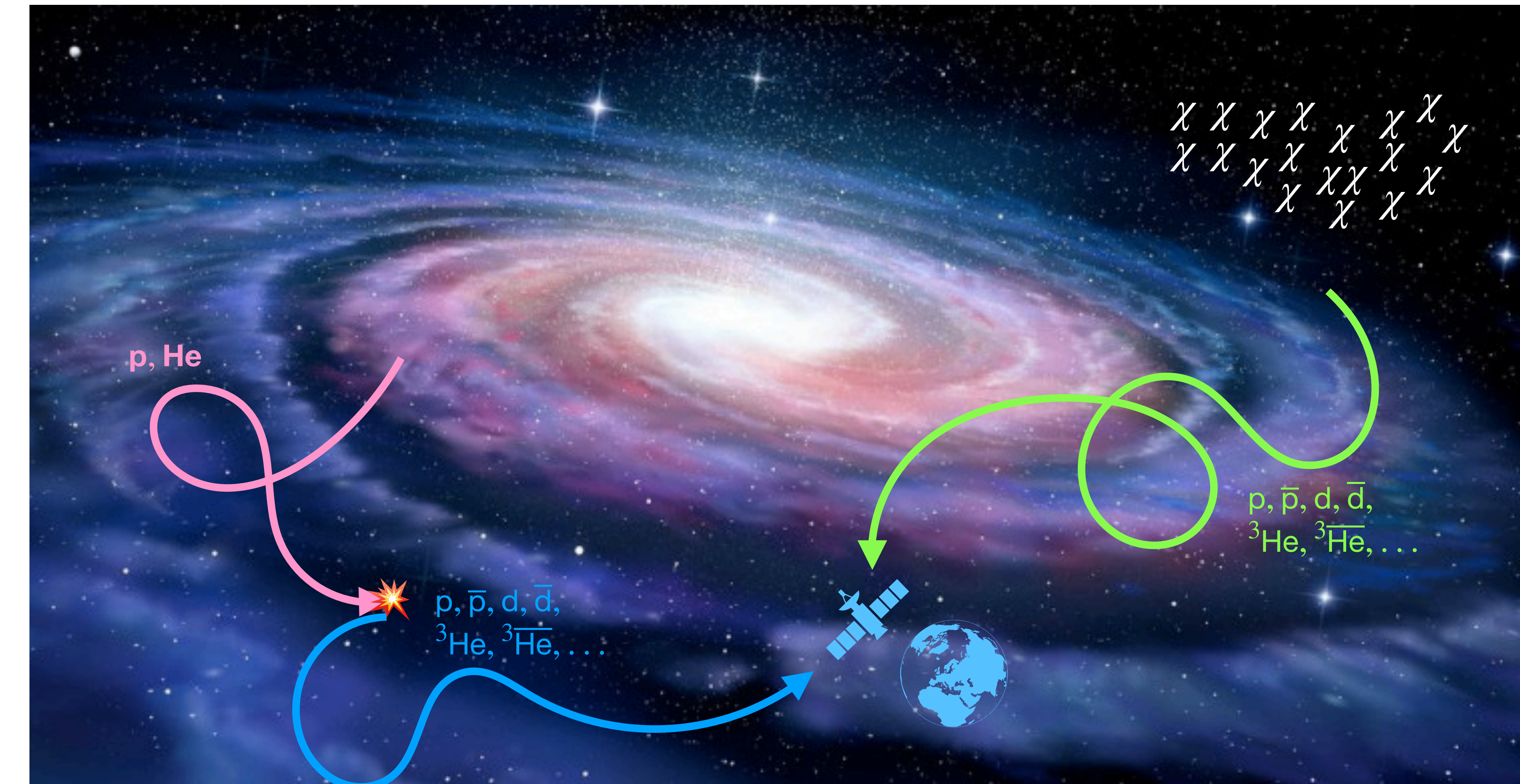
Stephan Koenigstorfer
Technische Universität München
on behalf of the ALICE Collaboration

ICHEP 2020 | PRAGUE

Introduction

Cosmic ray antinuclei

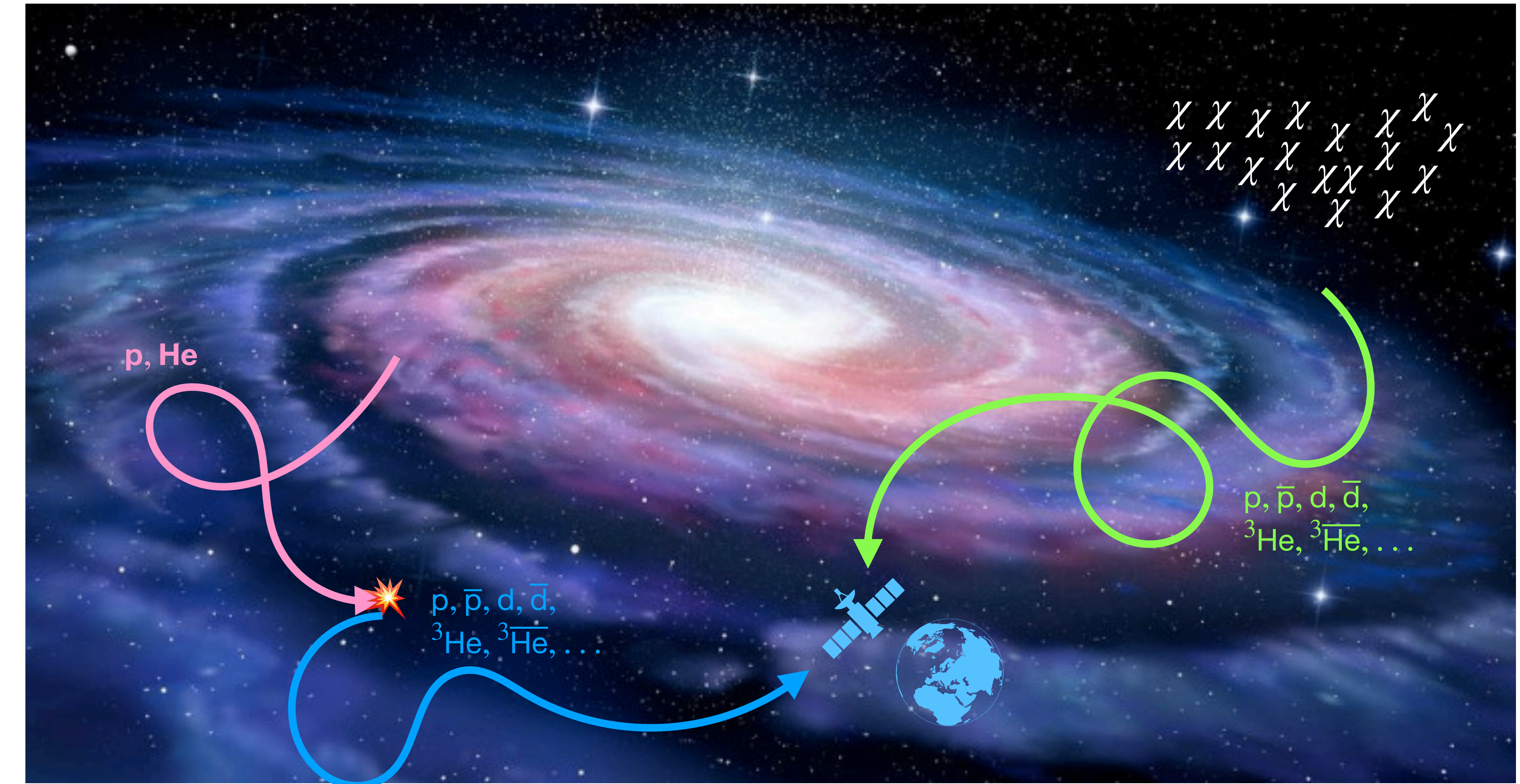
- unique Dark Matter probe



Introduction

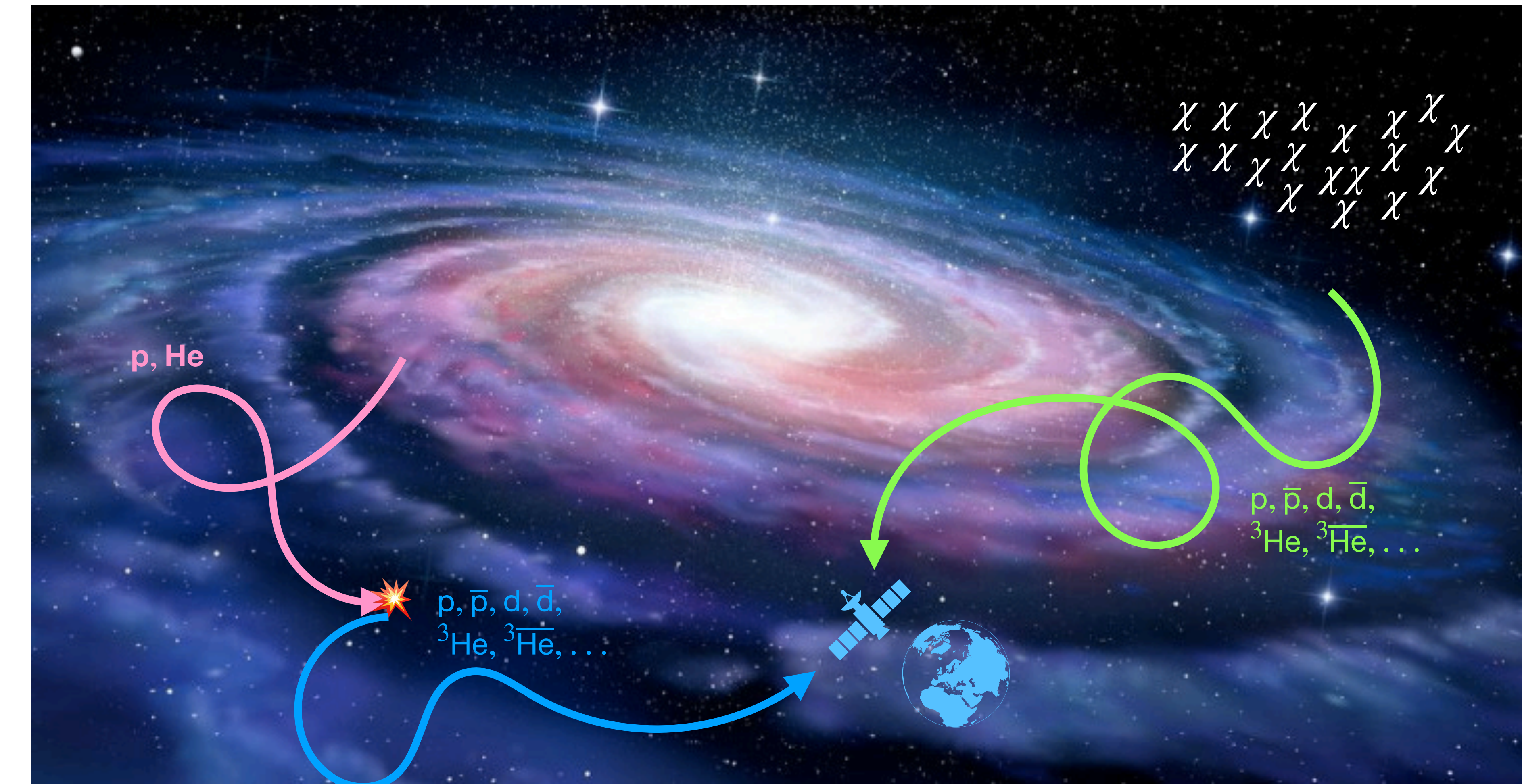
Cosmic ray antinuclei

- unique Dark Matter probe
 - Low background from secondary production is expected



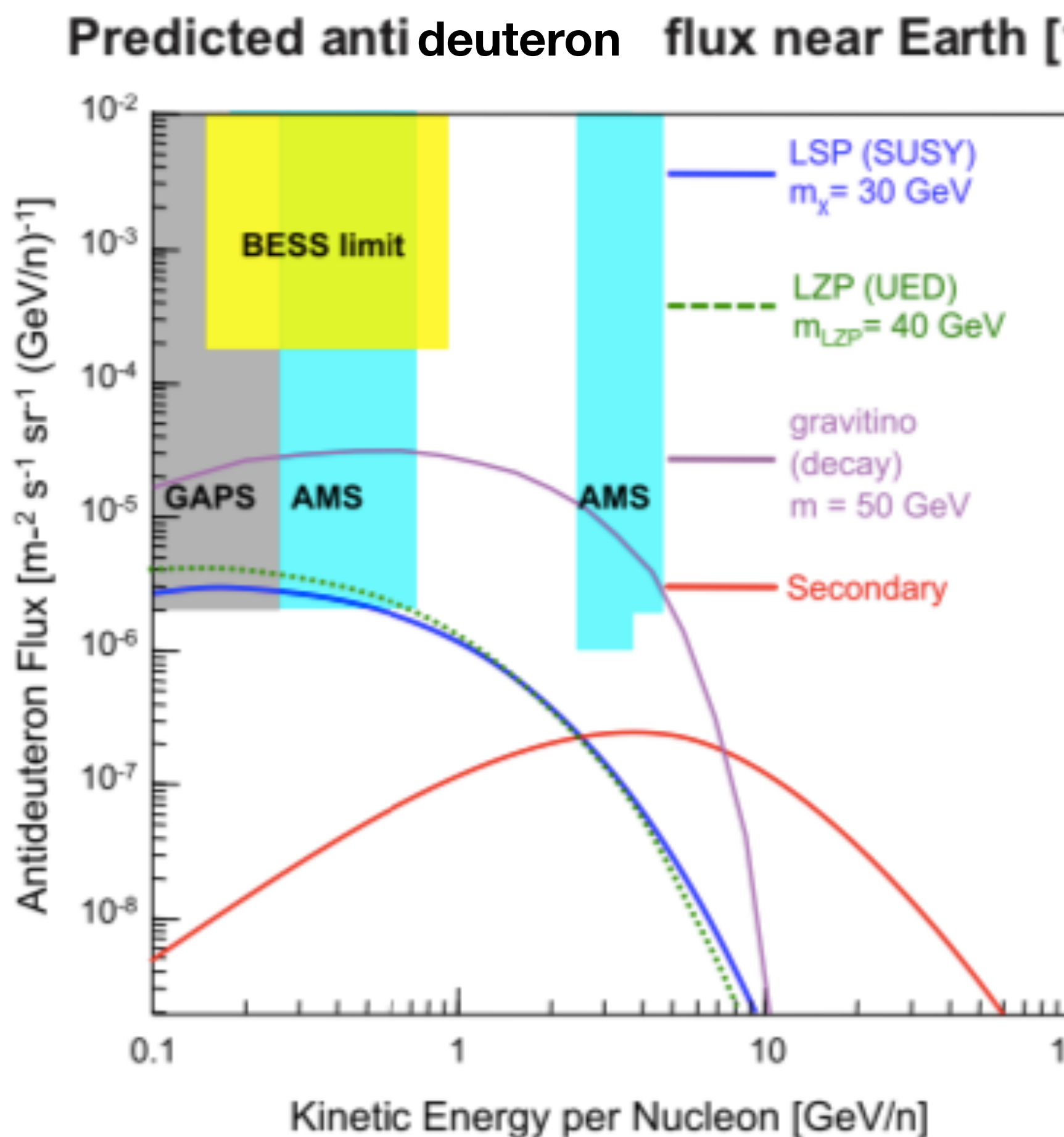
Introduction

- Cosmic ray antinuclei
- unique Dark Matter probe
 - Low background from secondary production is expected
 - Need to determine exact primary and secondary fluxes!

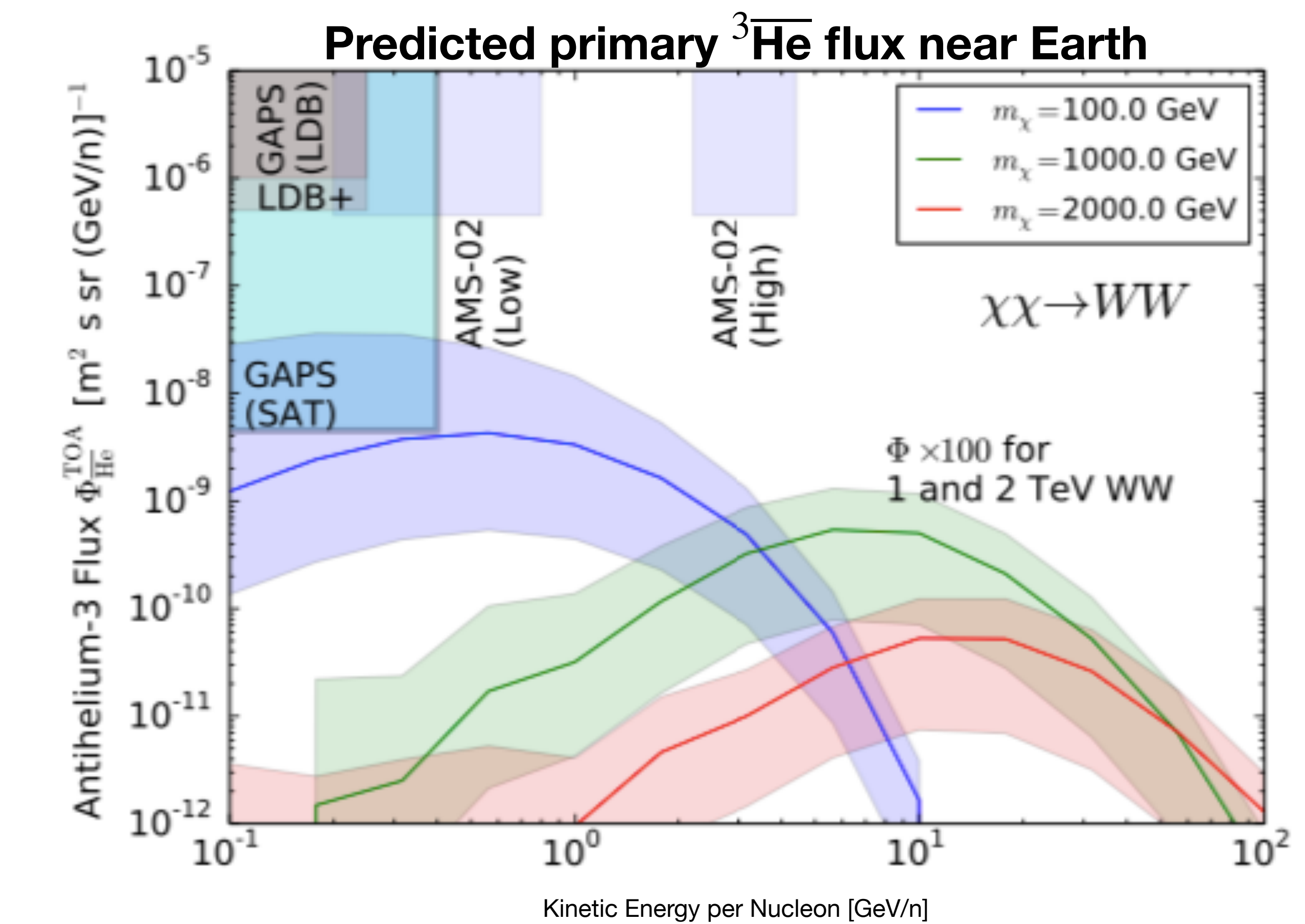
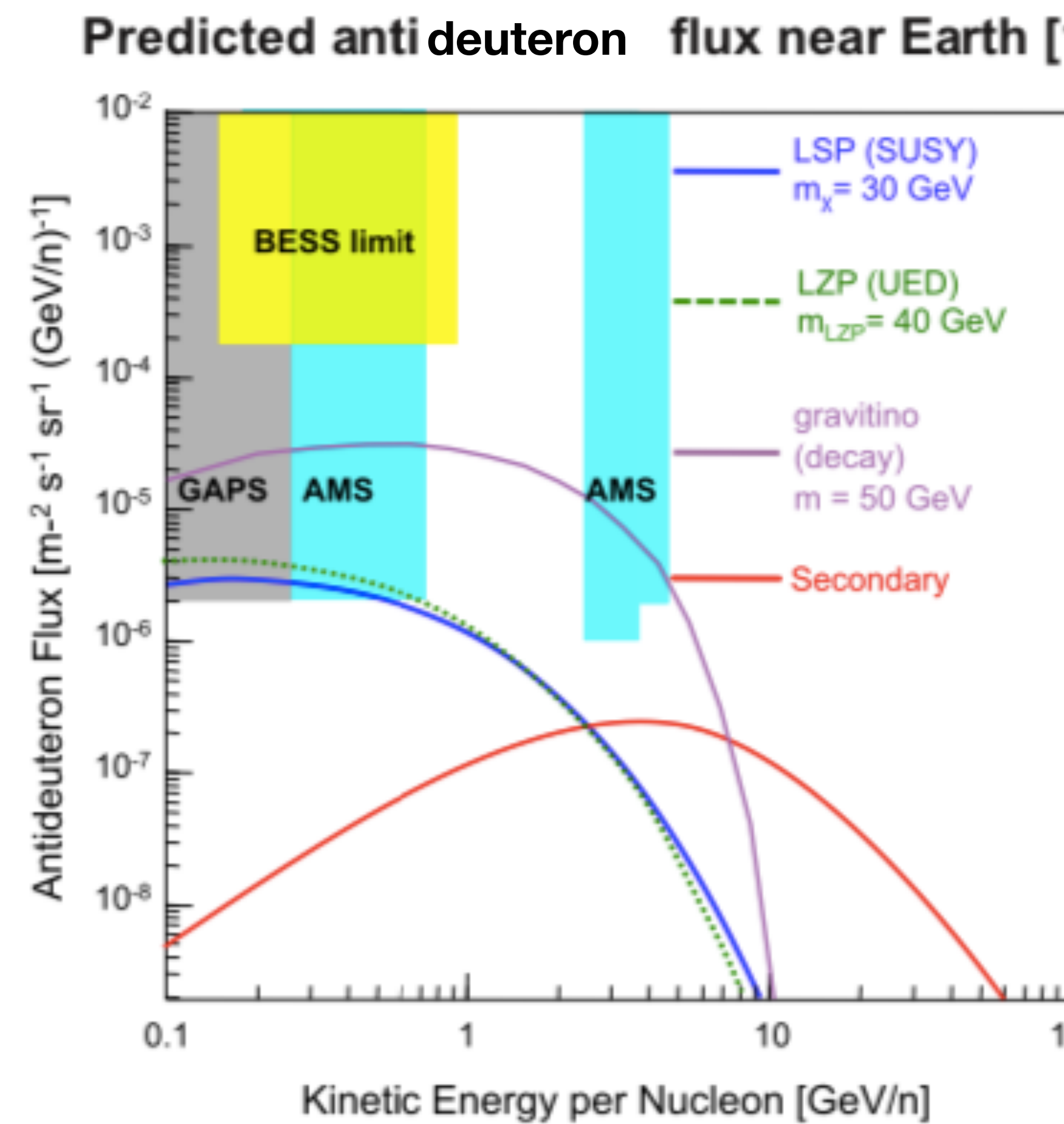


Predicted antinuclei fluxes near earth

Predicted antinuclei fluxes near earth



Predicted antinuclei fluxes near earth



Content of this talk

- What is needed to calculate cosmic ray antinuclei fluxes
- Current status of antinuclei inelastic cross section measurements
- The ALICE experiment
- Method to determine antinuclei inelastic cross sections with ALICE
- Antiproton, antideuteron and ${}^3\overline{\text{He}}$ inelastic cross section
- Possible implications for indirect Dark Matter searches

A long way to the detectors

A long way to the detectors

Interstellar Medium



- Injected primary cosmic ray (CR) spectra
- Production of secondary CR in interstellar medium
- Transport
- Absorption and (re-)acceleration

Local interstellar flux

A long way to the detectors

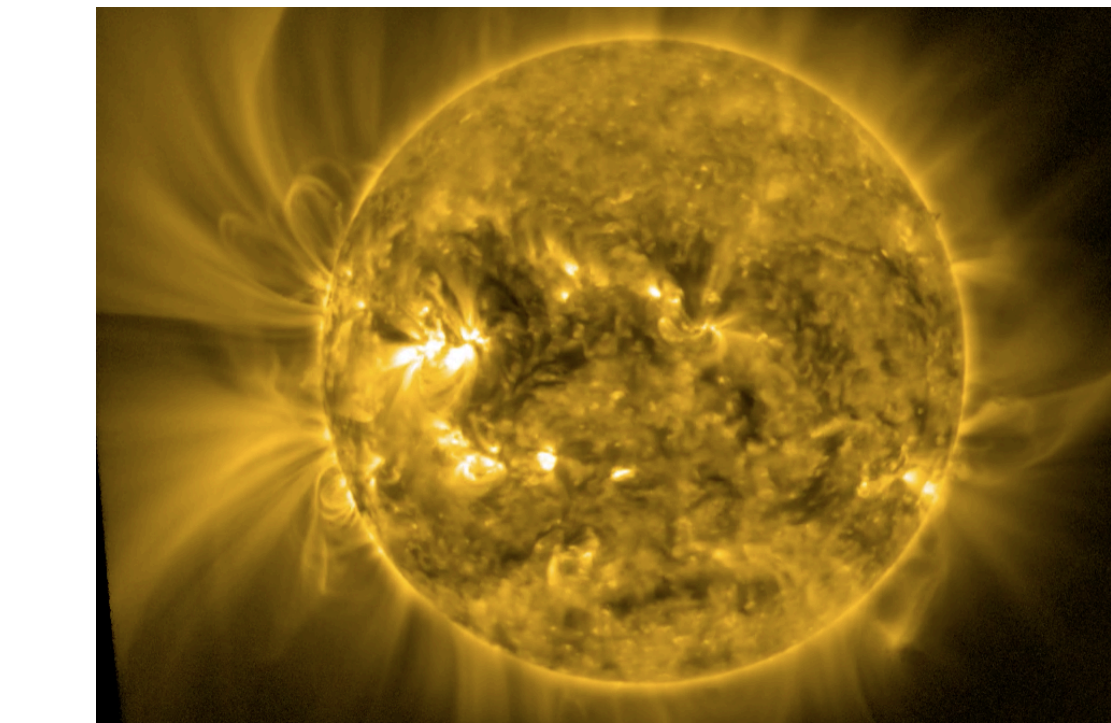
Interstellar Medium



- Injected primary cosmic ray (CR) spectra
- Production of secondary CR in interstellar medium
- Transport
- Absorption and (re-)acceleration

Local interstellar flux

Heliosphere



- Solar wind shielding
- Most dominant effect at low momenta
- Time dependence of activity

Solar modulated flux

A long way to the detectors

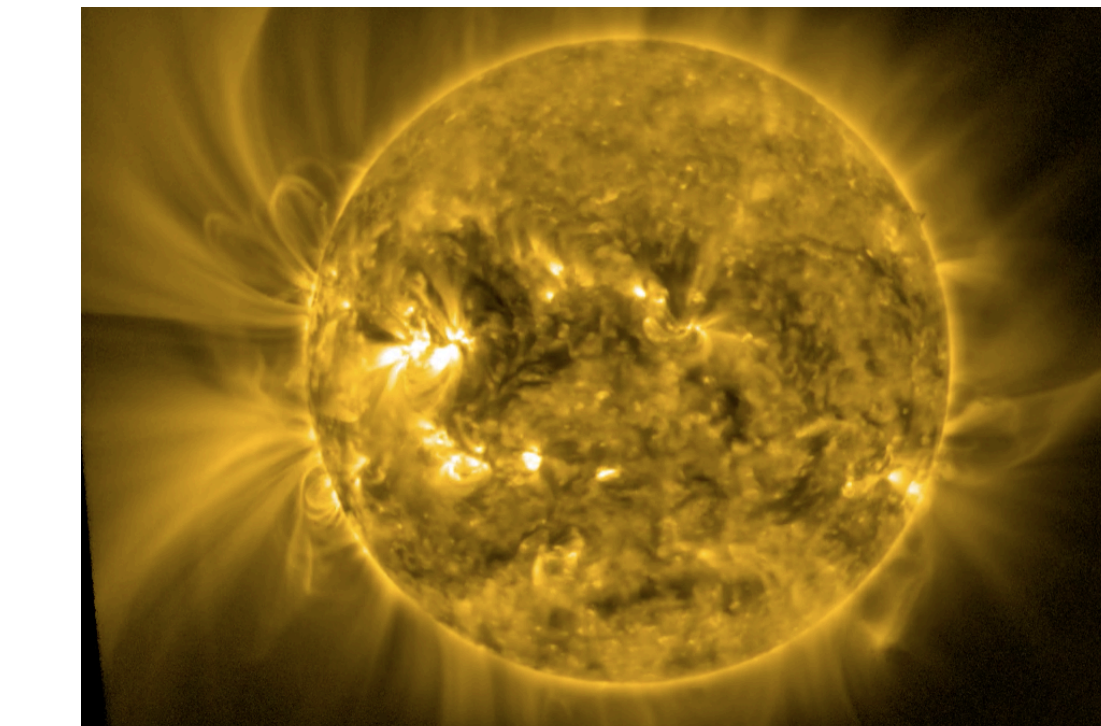
Interstellar Medium



- Injected primary cosmic ray (CR) spectra
- Production of secondary CR in interstellar medium
- Transport
- Absorption and (re-)acceleration

Local interstellar flux

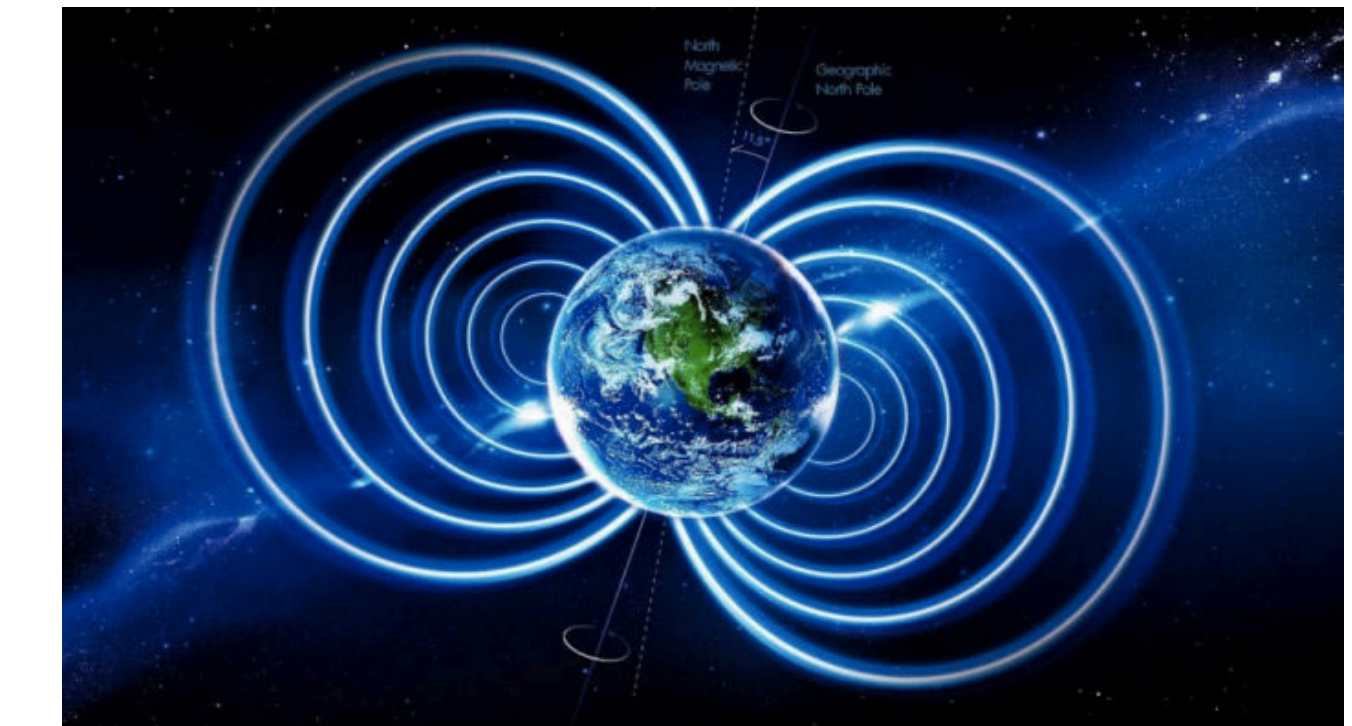
Heliosphere



- Solar wind shielding
- Most dominant effect at low momenta
- Time dependence of activity

Solar modulated flux

Near Earth environment



- Shielding/deflection by Earth's magnetic field
- Background production and absorption in Earth's atmosphere

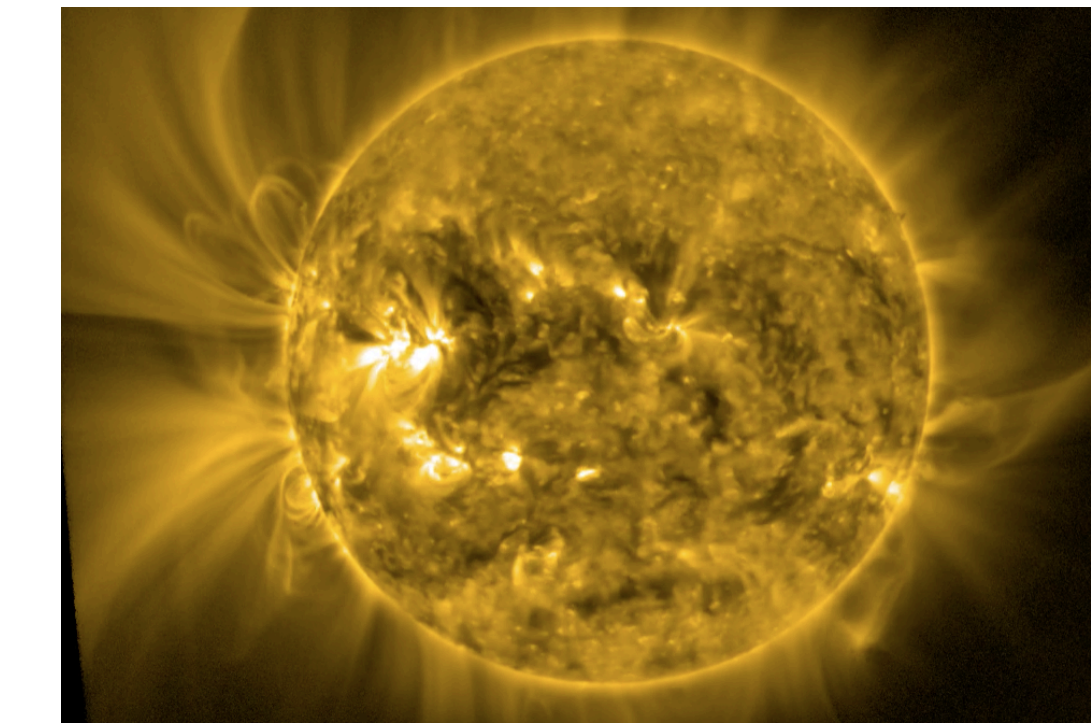
Flux at experiment

A long way to the detectors

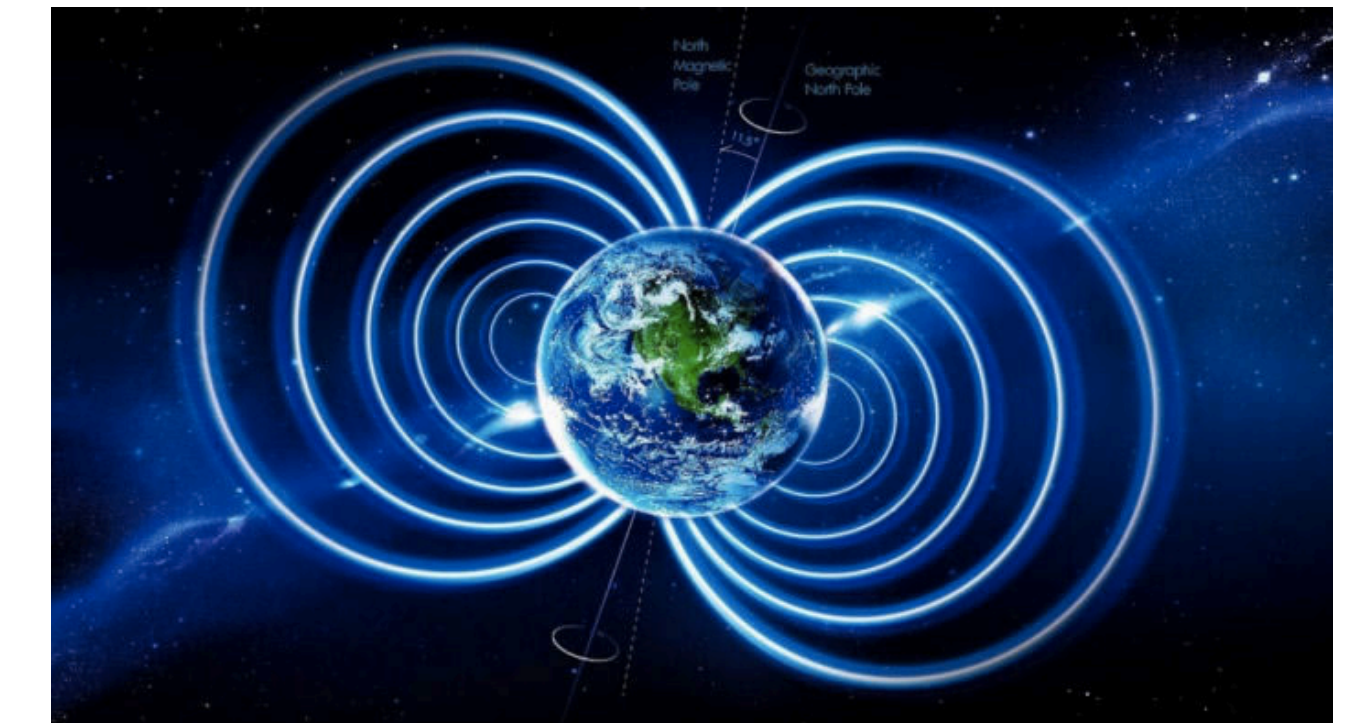
Interstellar Medium



Heliosphere



Near Earth environment



Steps in calculating antinuclei fluxes:

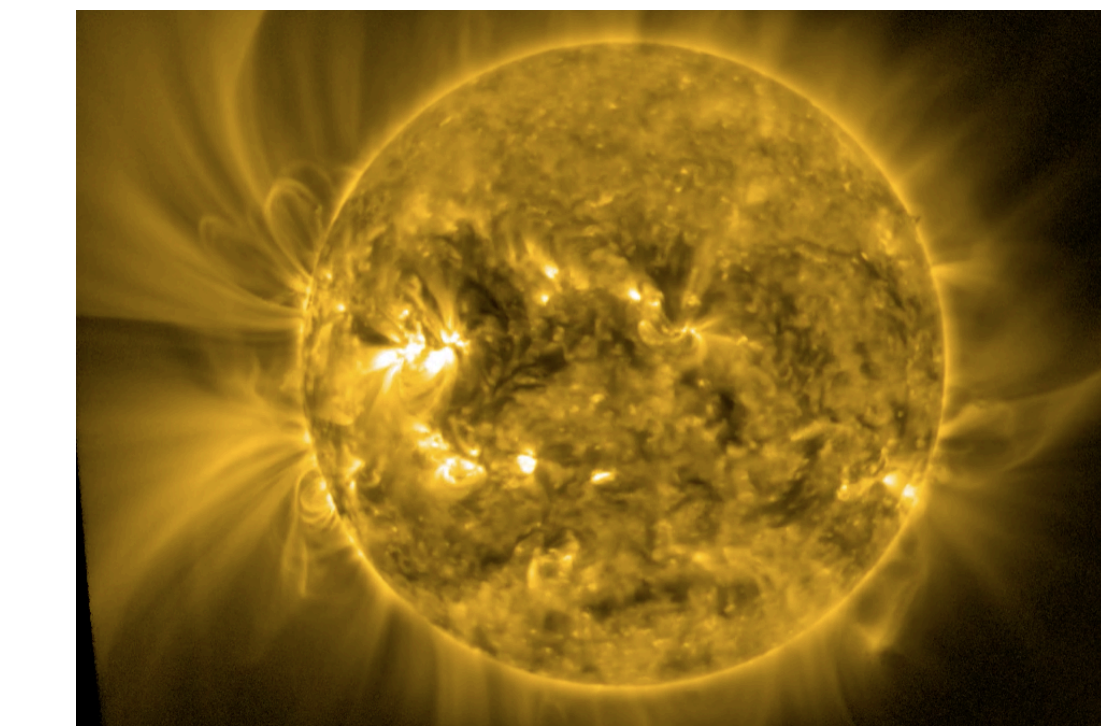
- Propagation: Common for all (anti)particles
- Annihilation in interstellar medium and Earth's atmosphere
- Production of antinuclei in pp, p \bar{p} , p-He, \bar{p} -He, ...

A long way to the detectors

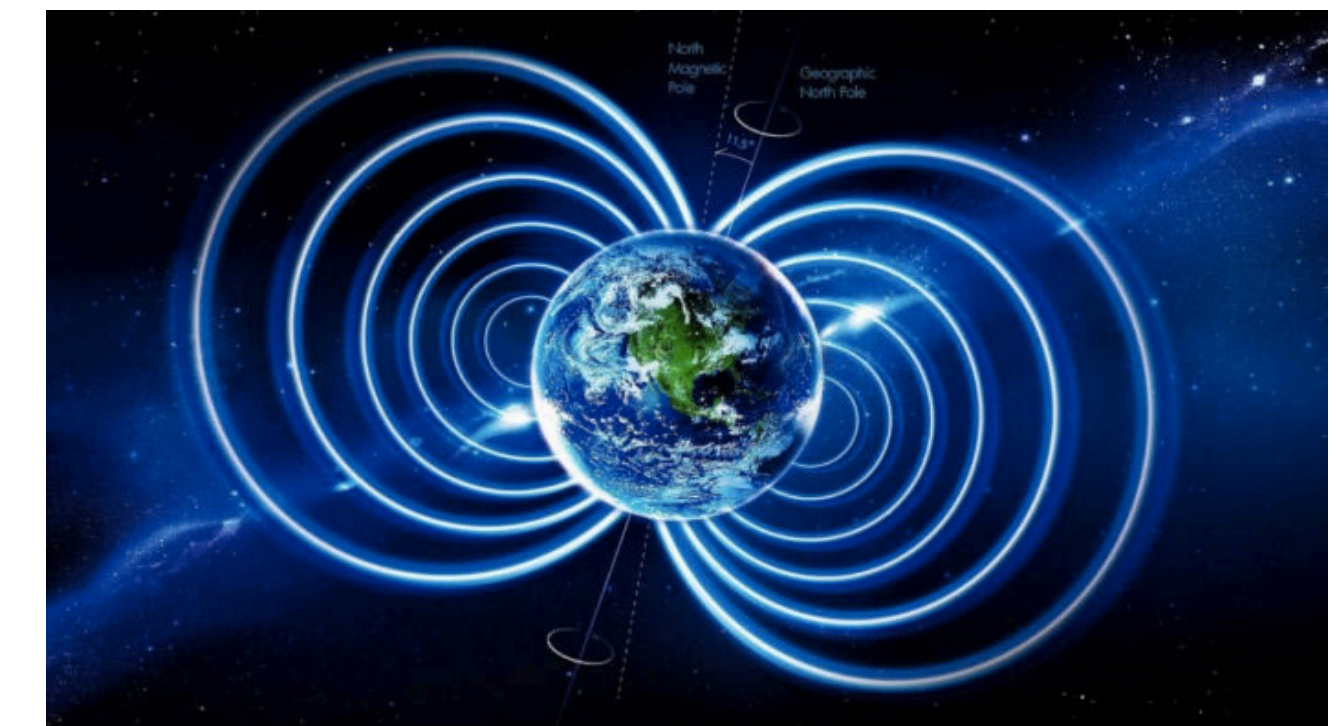
Interstellar Medium



Heliosphere

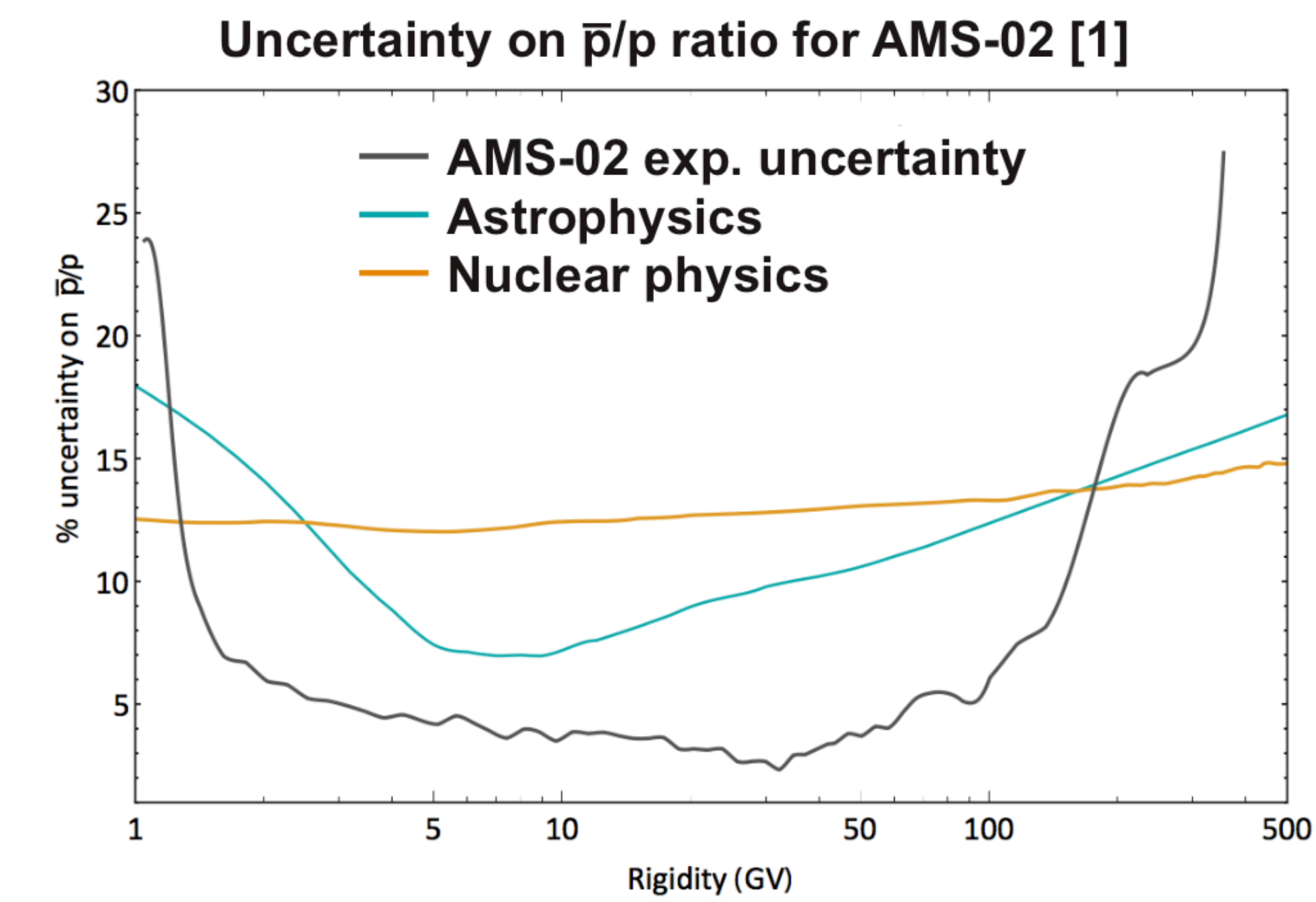


Near Earth environment



Steps in calculating antinuclei fluxes:

- Propagation: Common for all (anti)particles
- Annihilation in interstellar medium and Earth's atmosphere
- Production of antinuclei in $p\bar{p}$, $p\bar{p}$, $p\text{-He}$, $\bar{p}\text{-He}$, ...

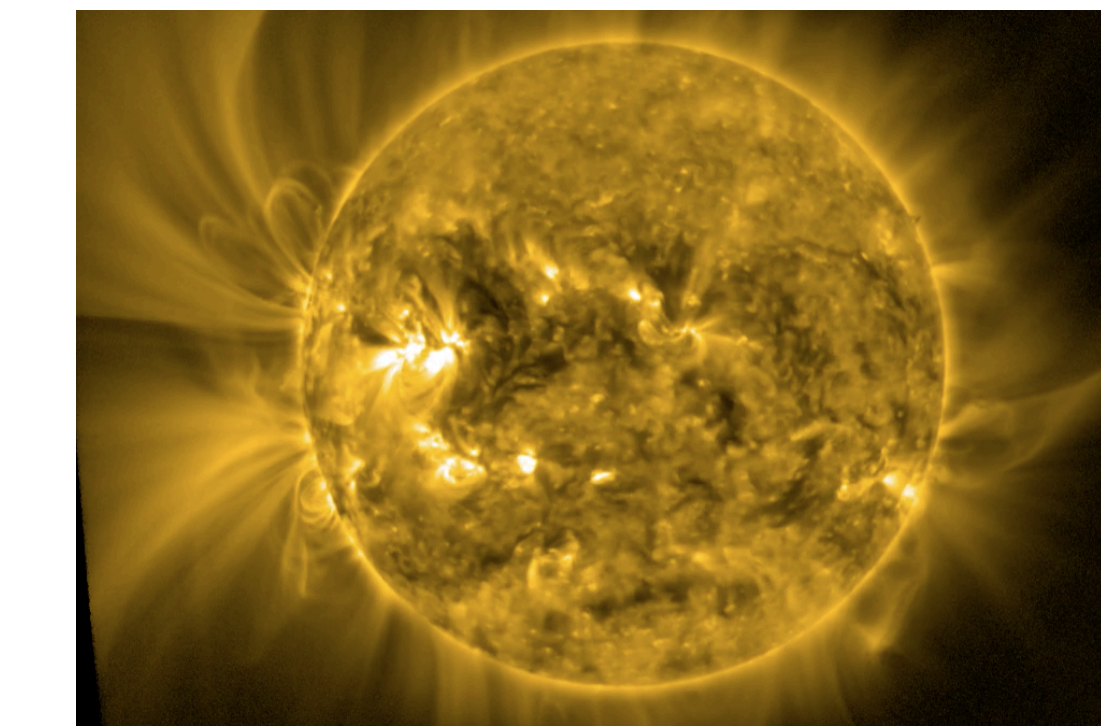


A long way to the detectors

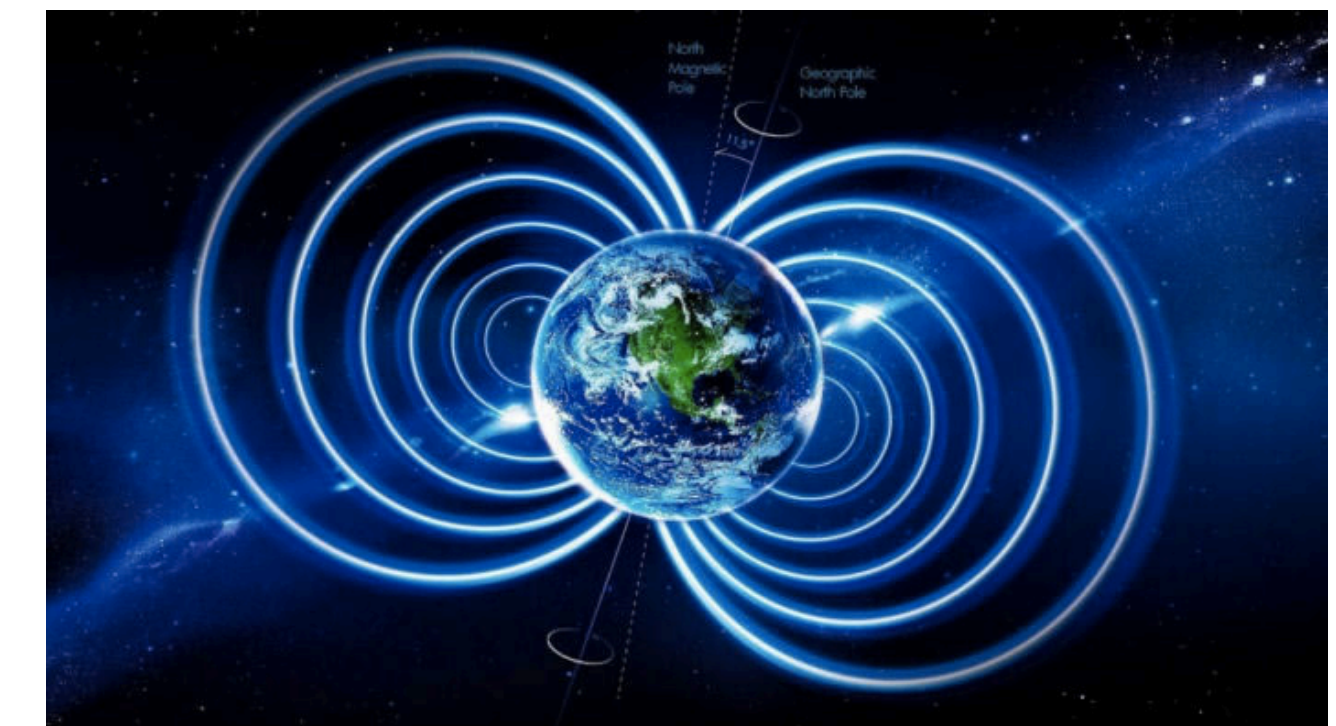
Interstellar Medium



Heliosphere



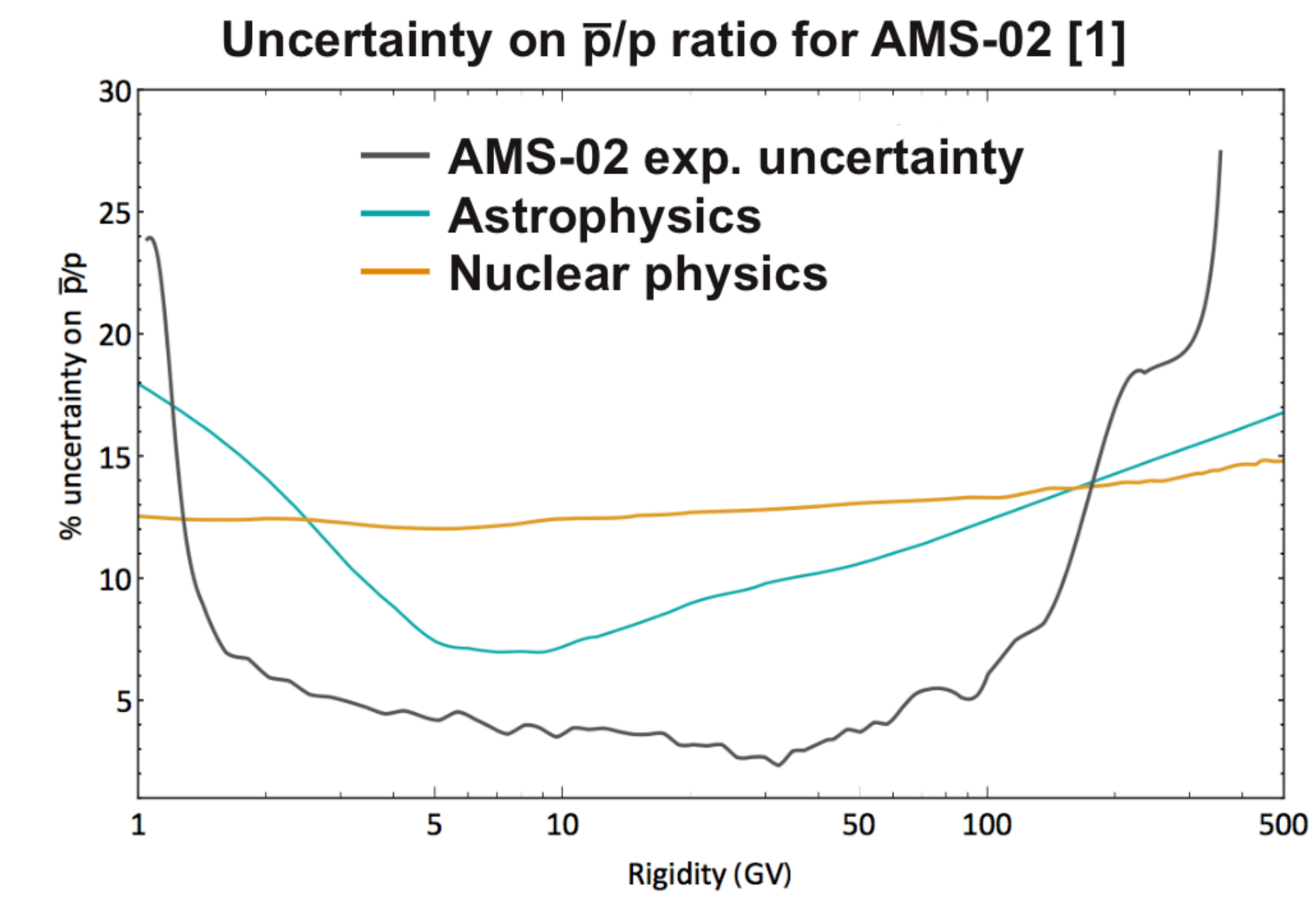
Near Earth environment



Steps in calculating antinuclei fluxes:

- Propagation: Common for all (anti)particles
- Annihilation in interstellar medium and Earth's atmosphere
- Production of antinuclei in pp, p \bar{p} , p-He, \bar{p} -He, ...

Precise nuclear inelastic cross sections are needed to reduce large uncertainties from nuclear physics!

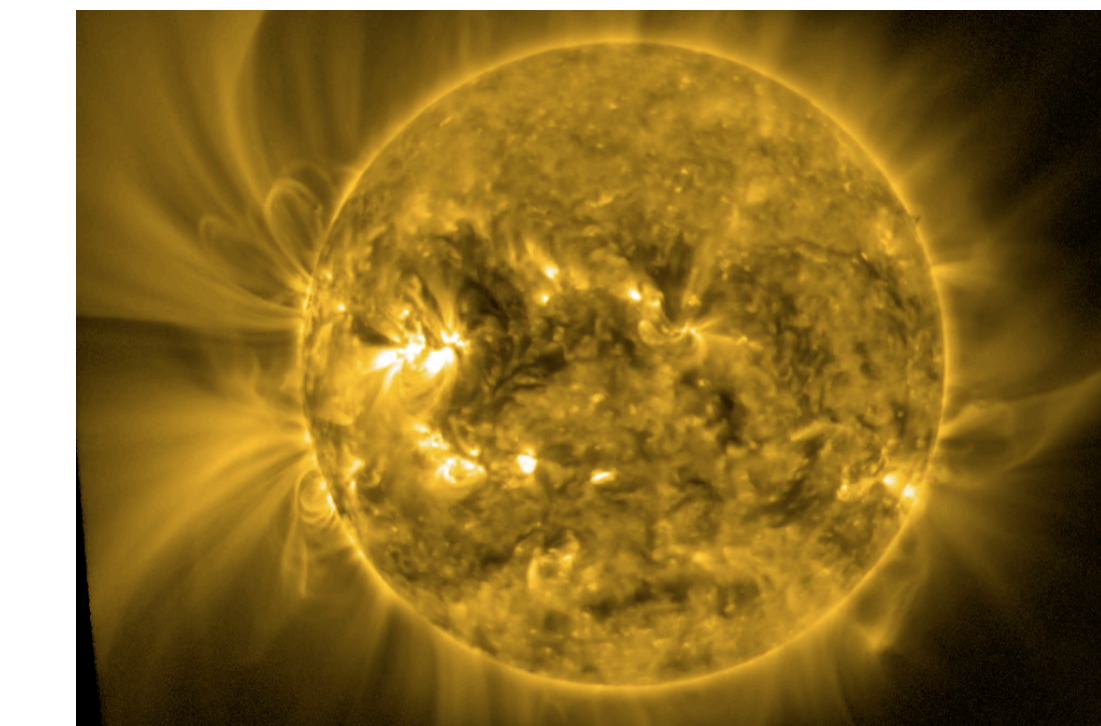


A long way to the detectors

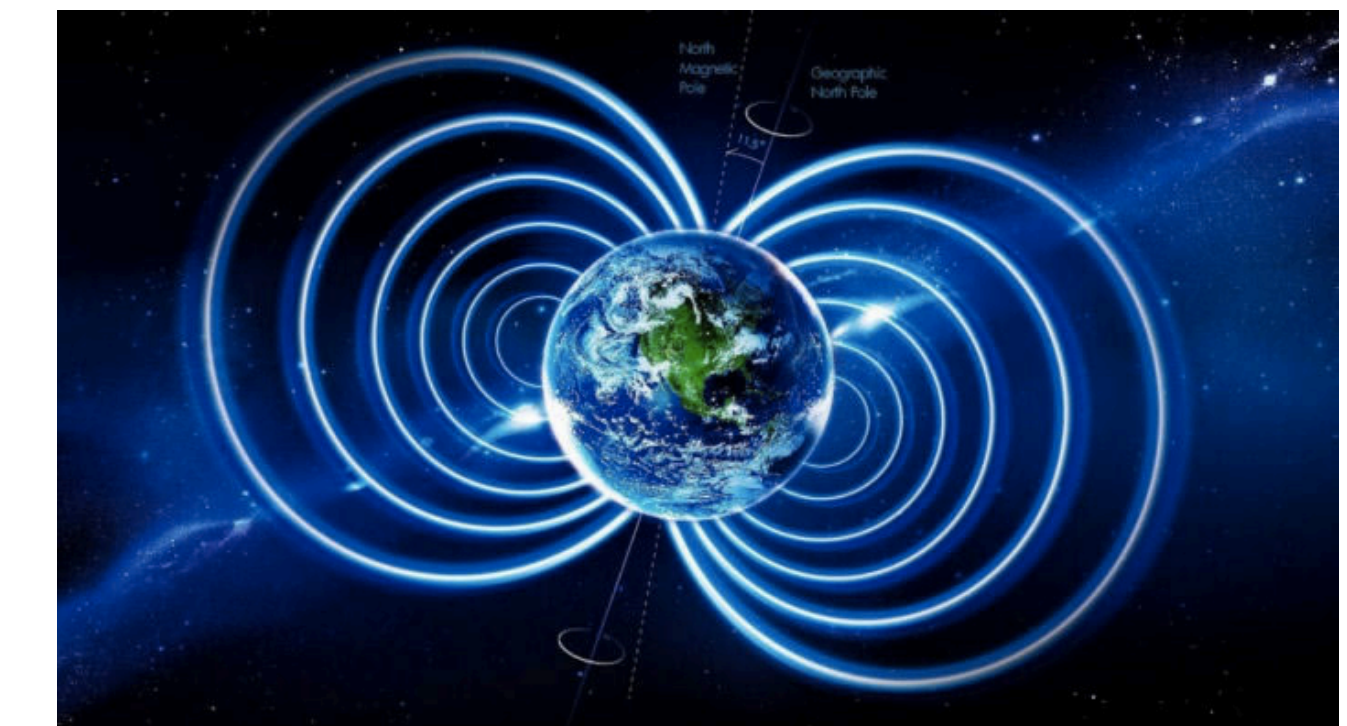
Interstellar Medium



Heliosphere



Near Earth environment

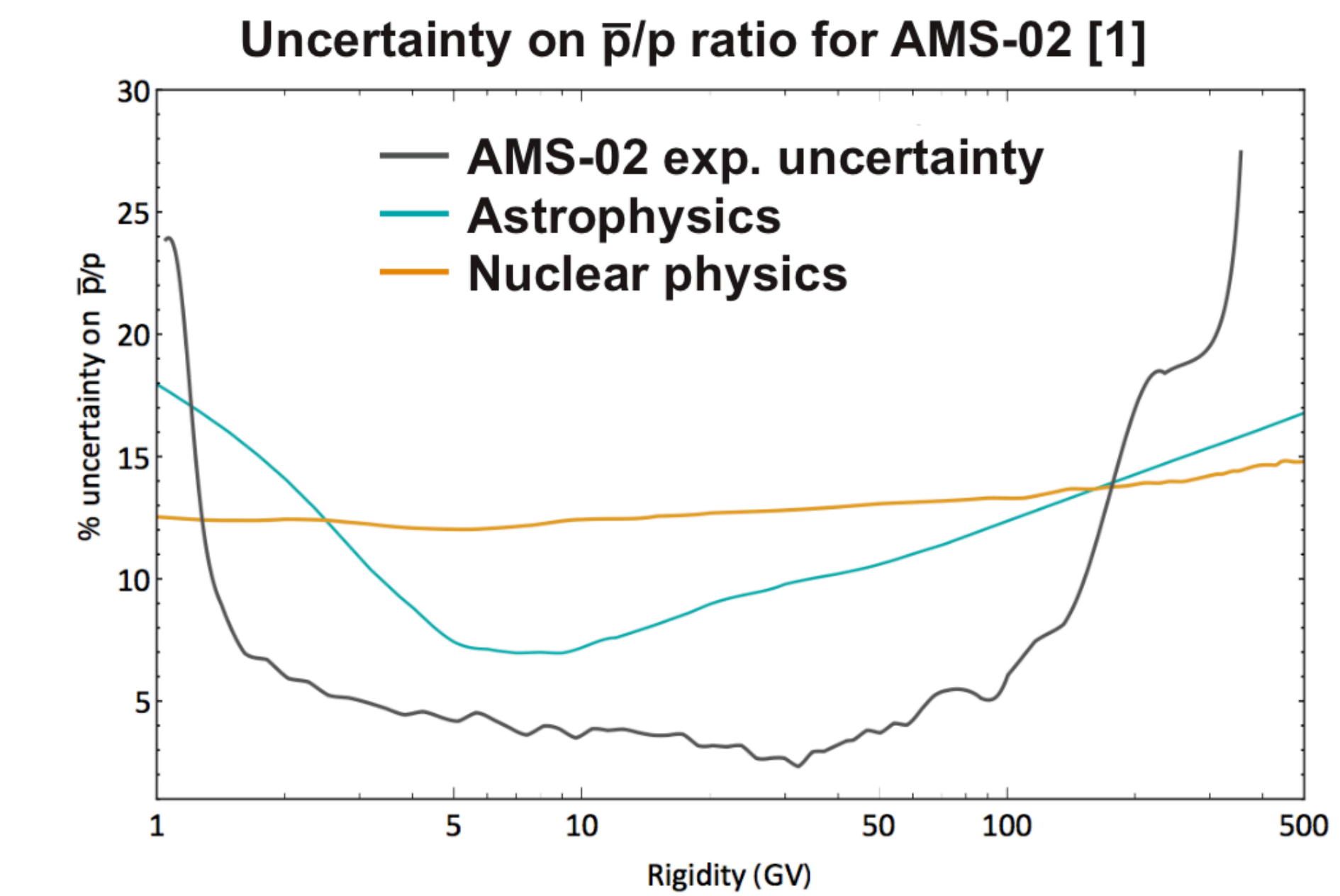


Steps in calculating antinuclei fluxes:

- Propagation: Common for all (anti)particles
- Annihilation in interstellar medium and Earth's atmosphere
- Production of antinuclei in $p\bar{p}$, $p\bar{p}$, $p\text{-He}$, $\bar{p}\text{-He}$, ...

Precise nuclear inelastic cross sections are needed to reduce large uncertainties from nuclear physics!

This talk

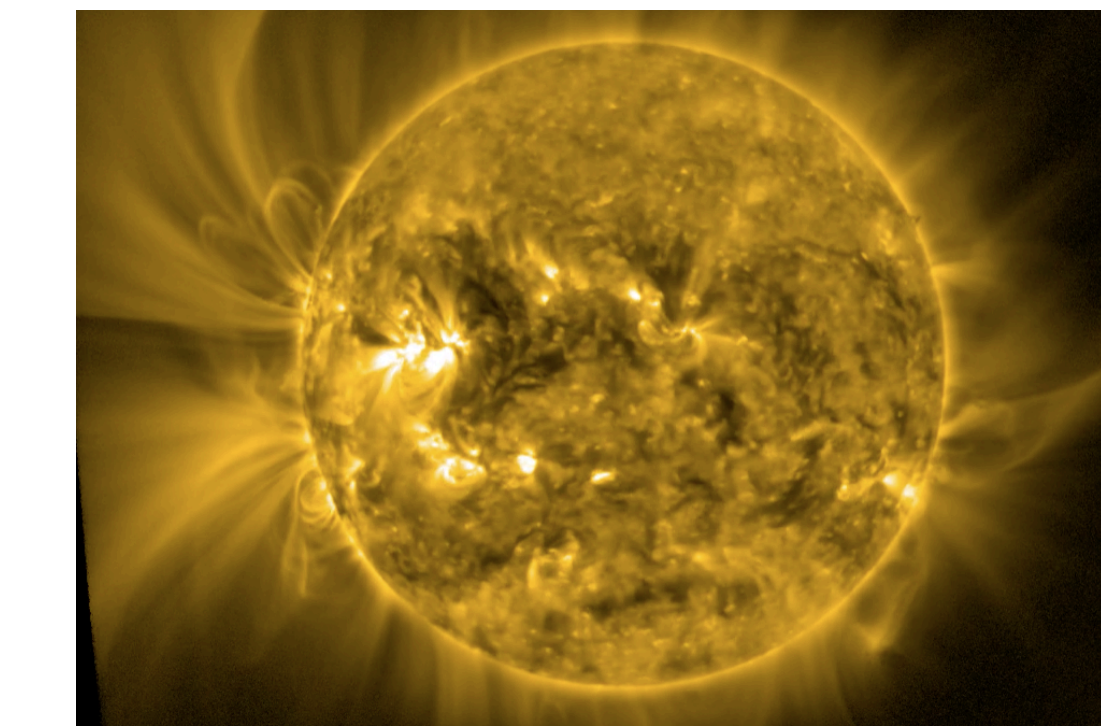


A long way to the detectors

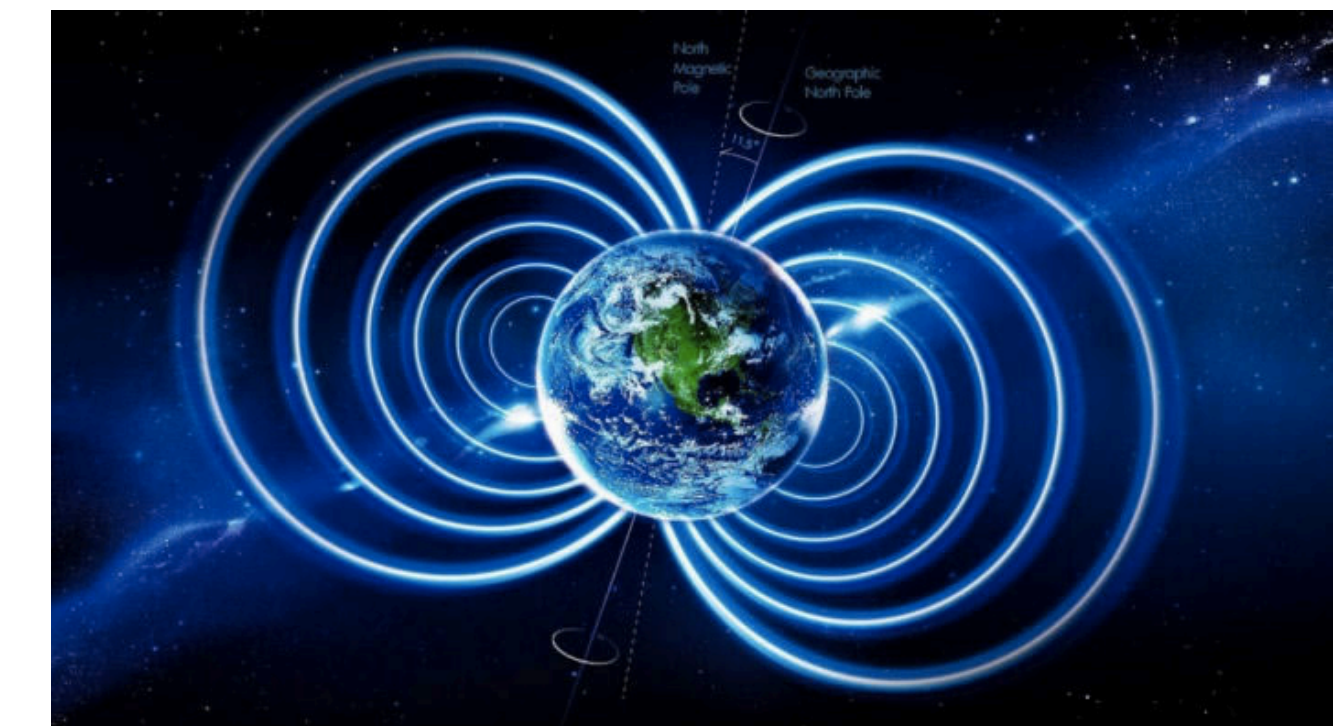
Interstellar Medium



Heliosphere



Near Earth environment



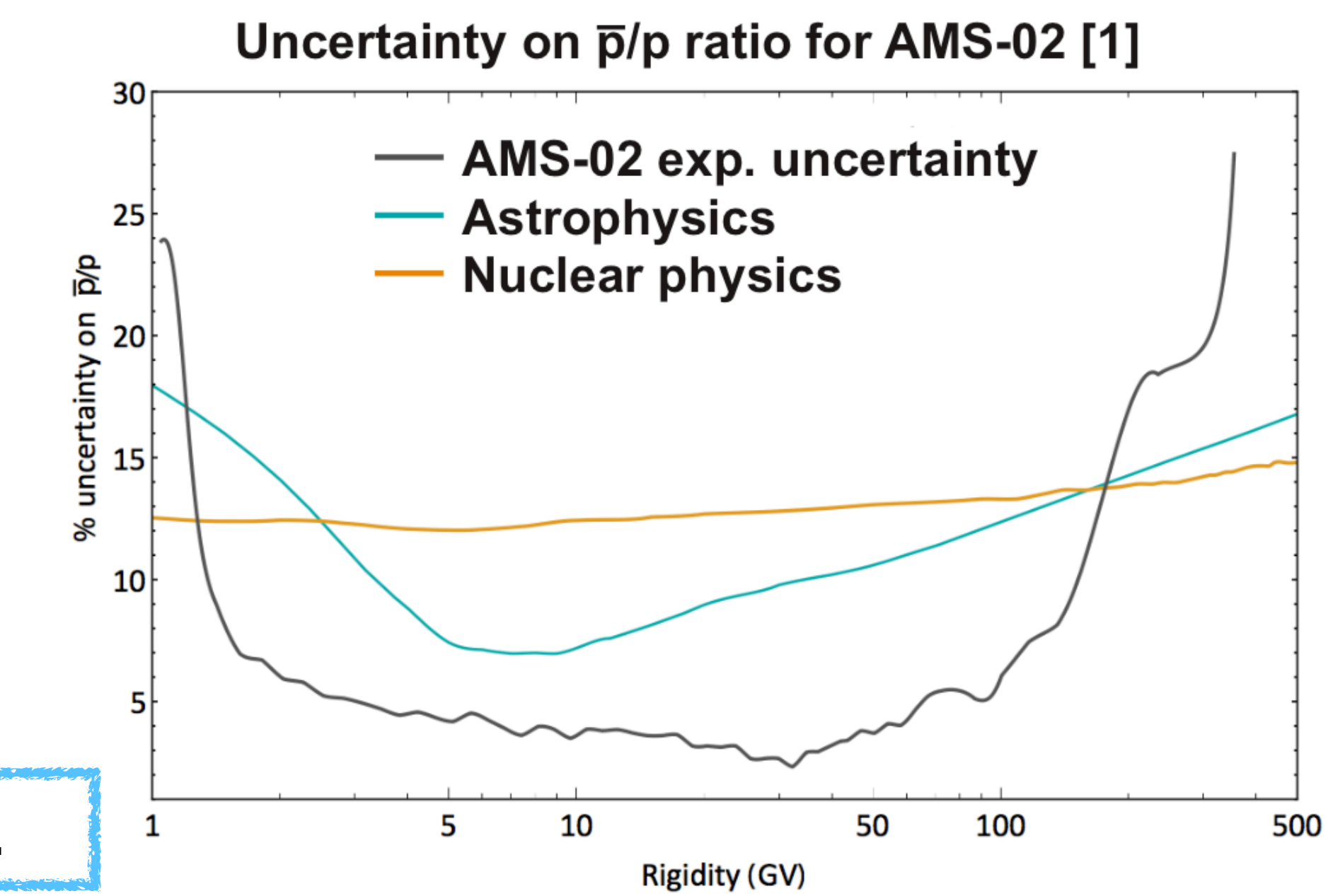
Steps in calculating antinuclei fluxes:

- Propagation: Common for all (anti)particles
- Annihilation in interstellar medium and Earth's atmosphere
- Production of antinuclei in $p\bar{p}$, $p\bar{p}$, $p\text{-He}$, $\bar{p}\text{-He}$, ...

Precise nuclear inelastic cross sections are needed to reduce large uncertainties from nuclear physics!

This talk

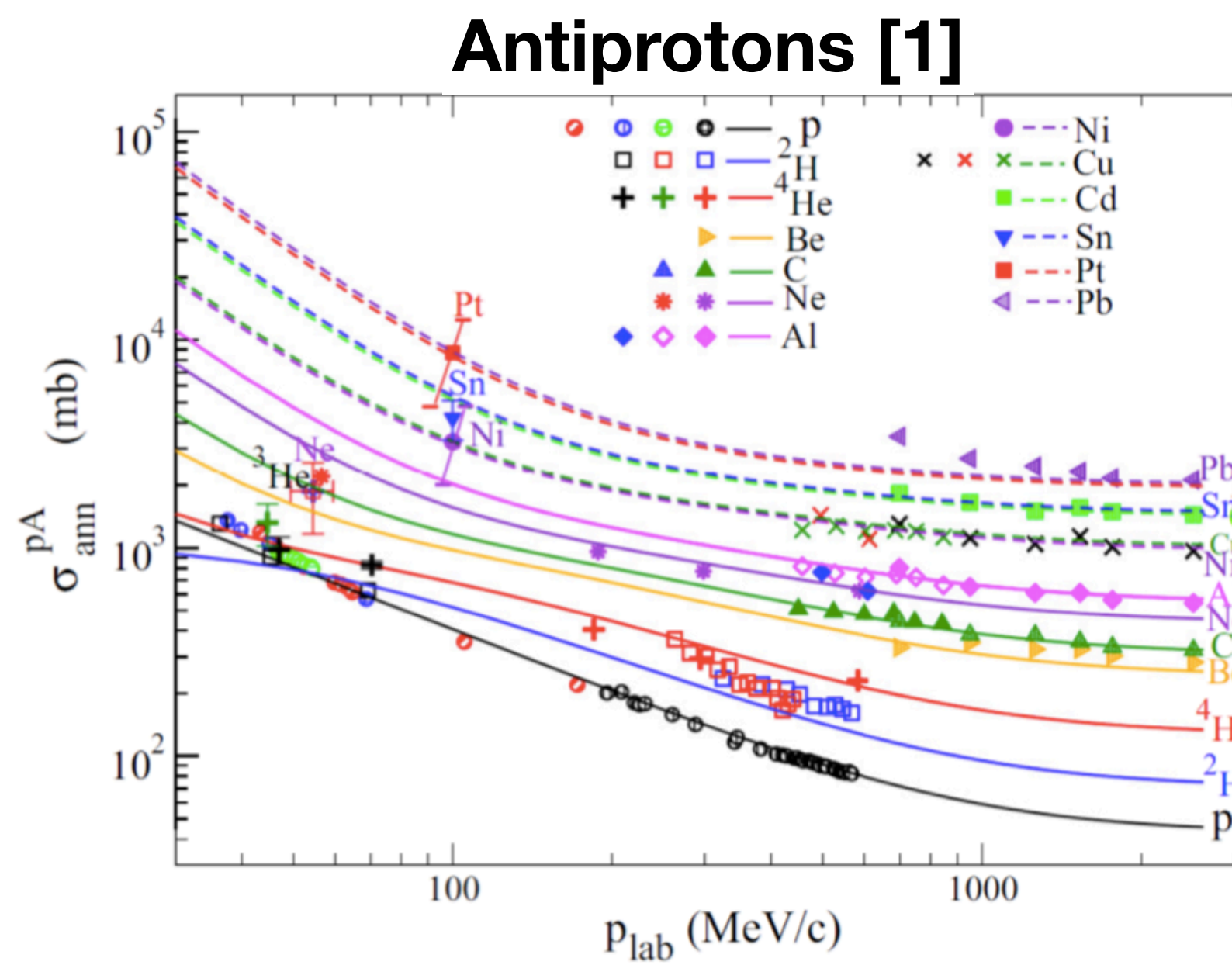
Talks by S. Hornung and C. Pinto.



Current status of antinuclei inelastic cross sections

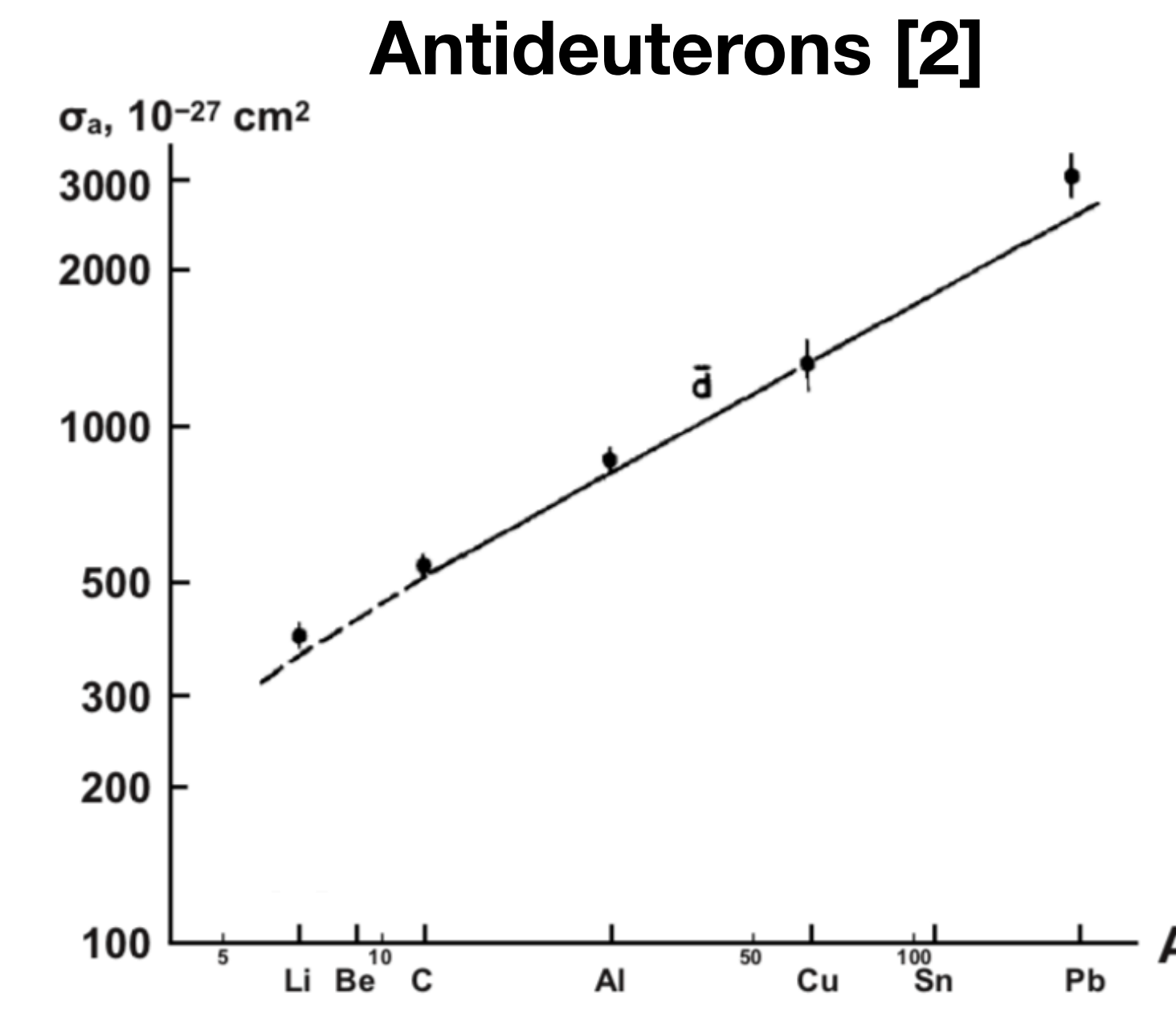
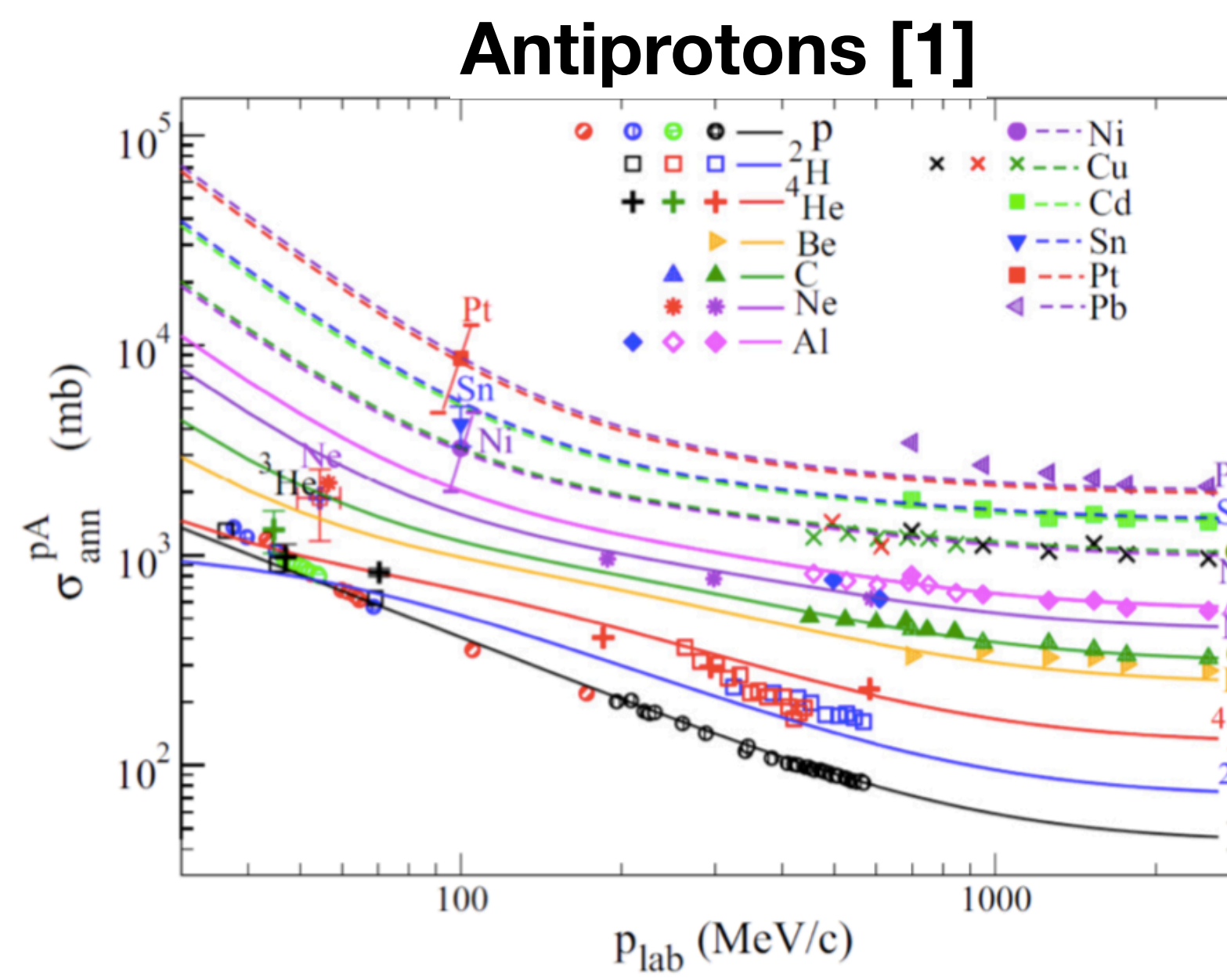
Current status of antinuclei inelastic cross sections

- Antiproton inelastic cross section is well known.



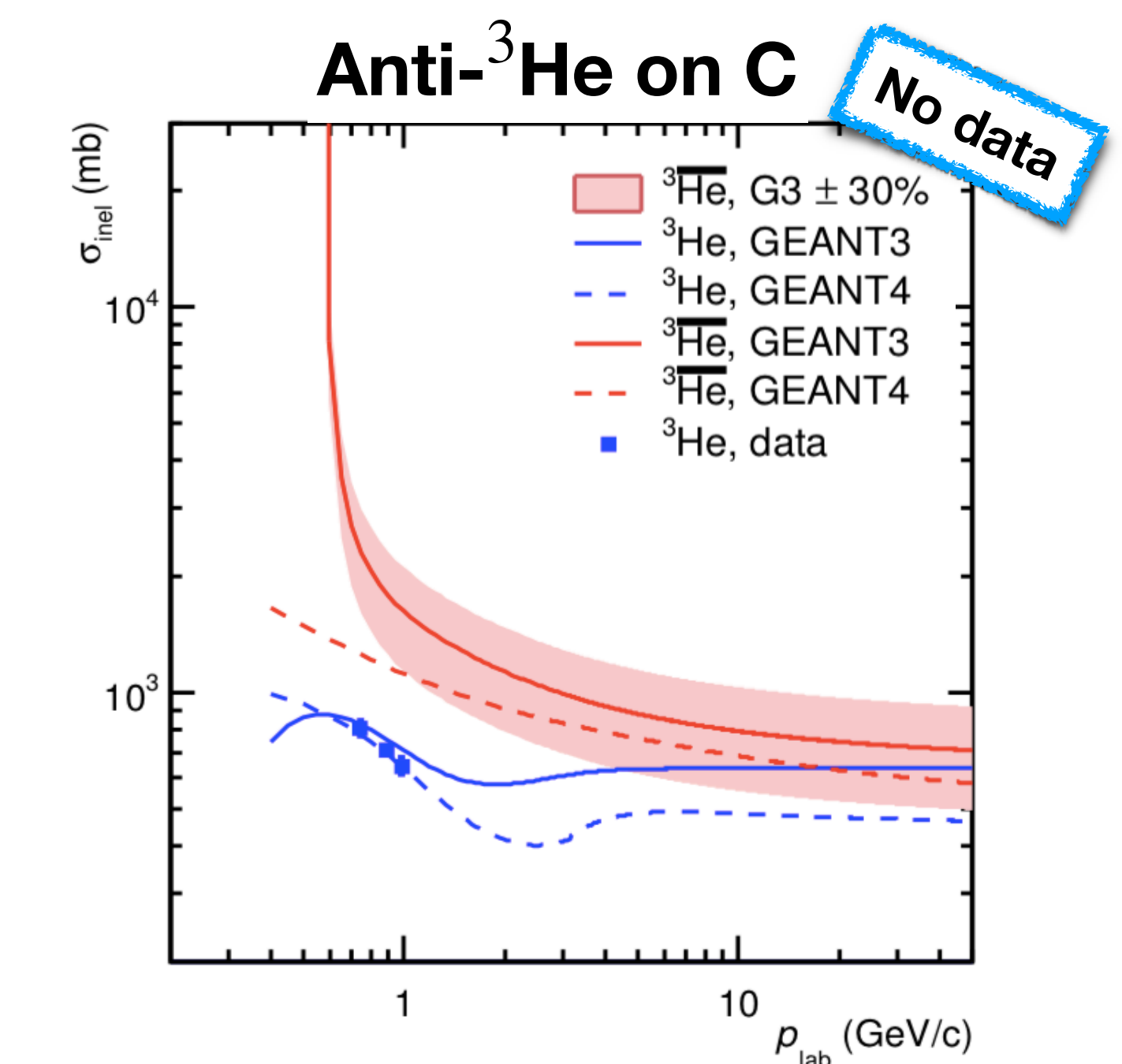
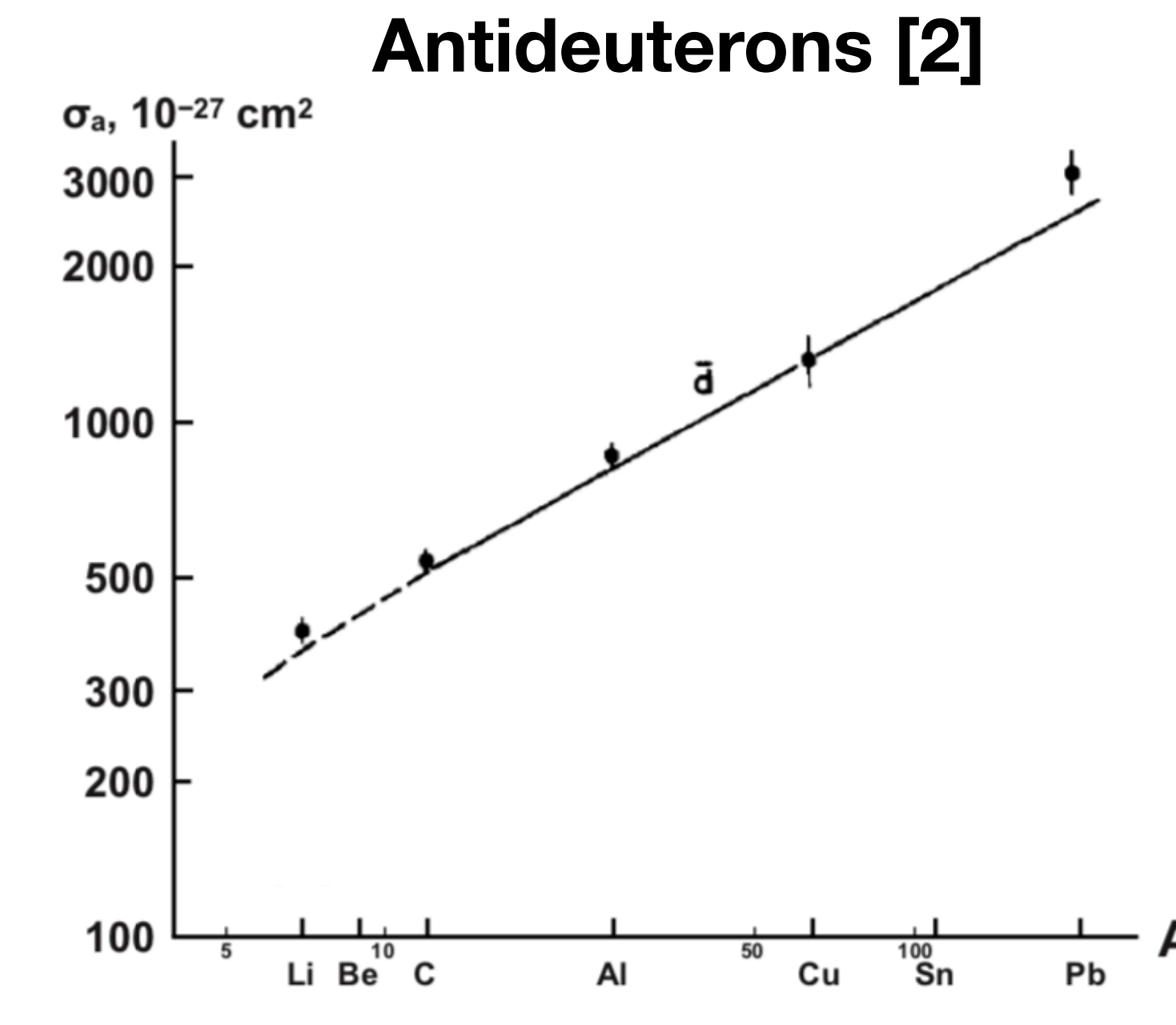
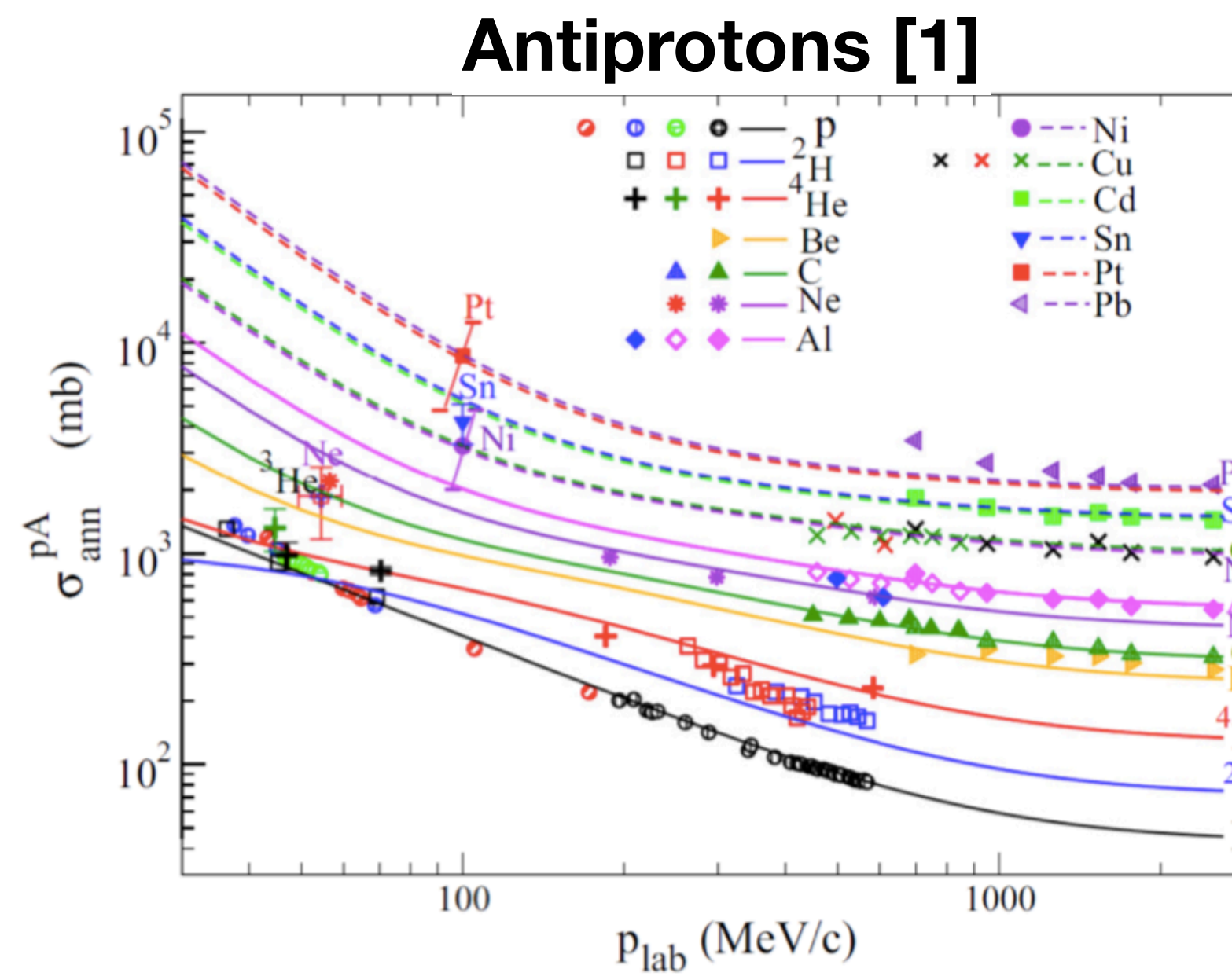
Current status of antinuclei inelastic cross sections

- Antiproton inelastic cross section is well known.
- Antideuteron inelastic cross section is poorly known at low energies.



Current status of antinuclei inelastic cross sections

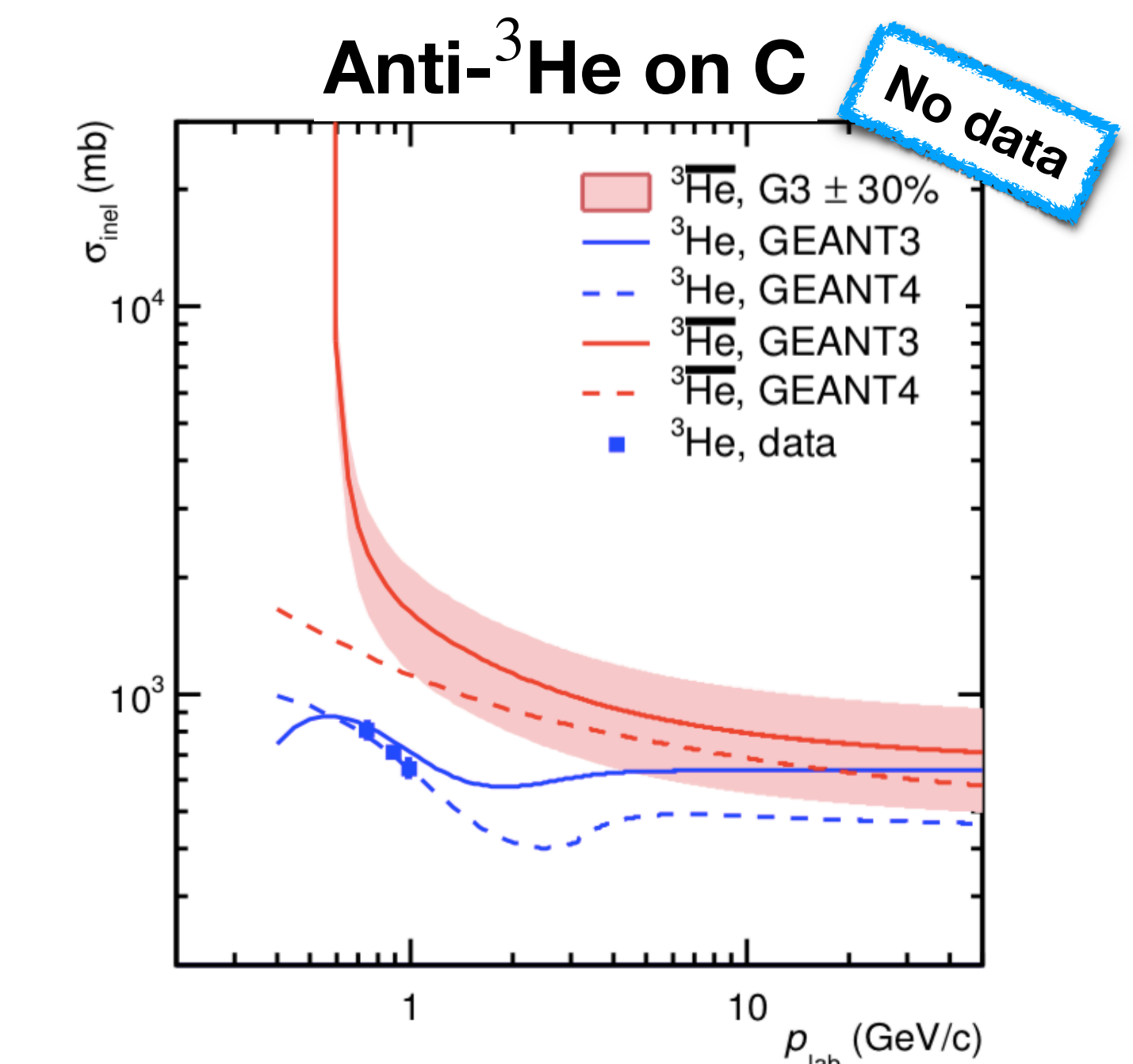
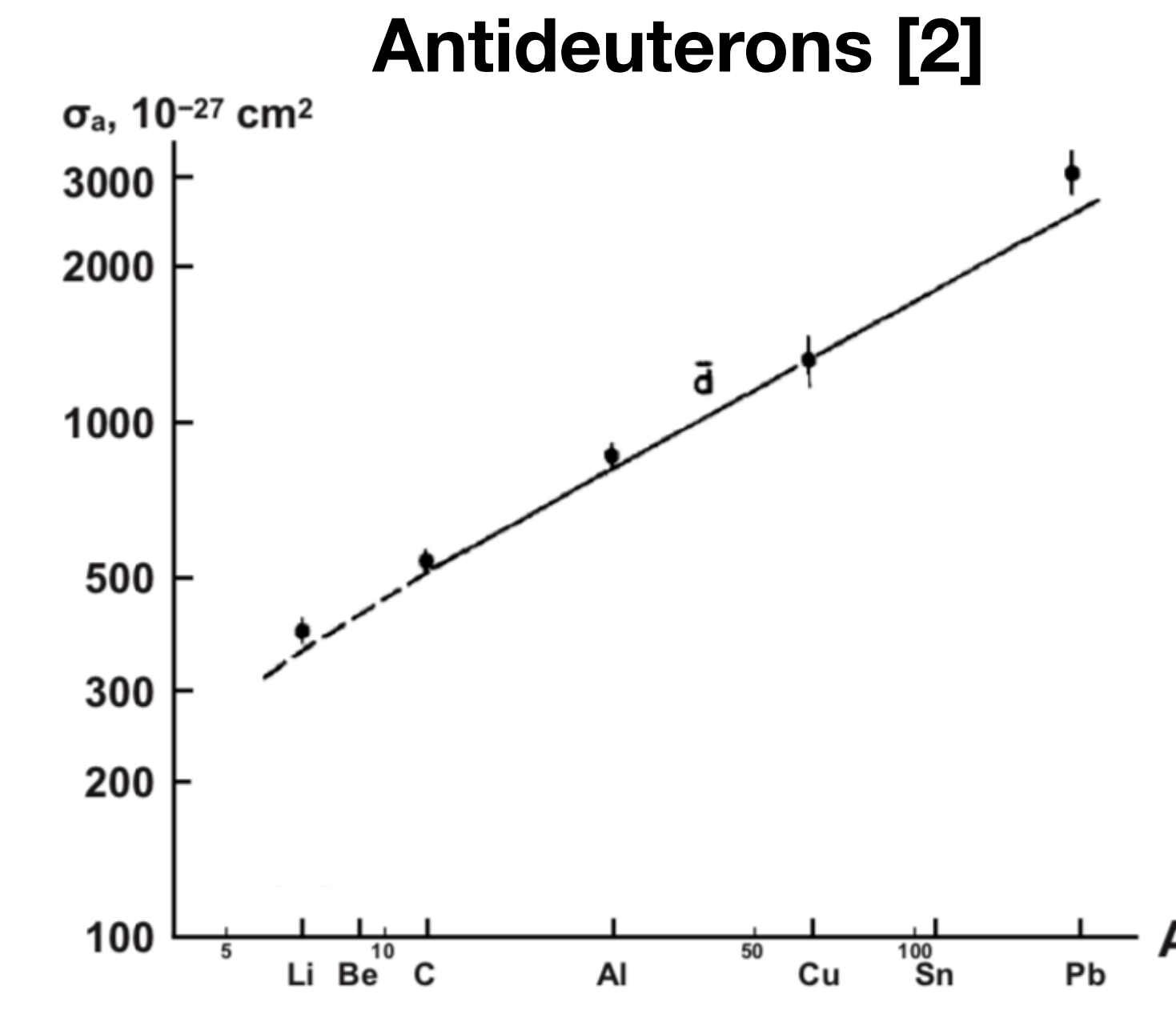
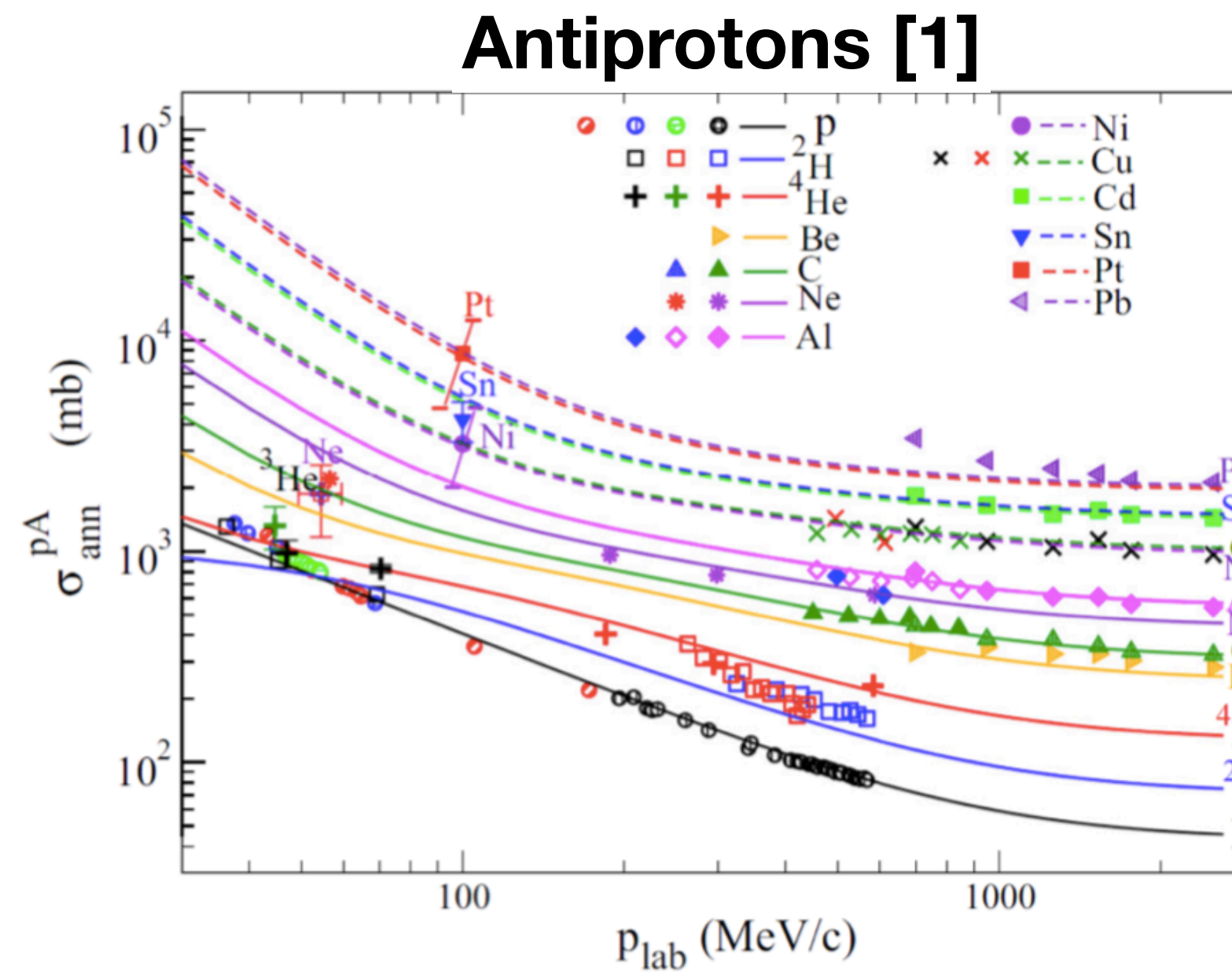
- Antiproton inelastic cross section is well known.
- Antideuteron inelastic cross section is poorly known at low energies.
- Antihelium inelastic cross section has never been measured before.



Current status of antinuclei inelastic cross sections

- Antiproton inelastic cross section is well known.
- Antideuteron inelastic cross section is poorly known at low energies.
- Antihelium inelastic cross section has never been measured before.

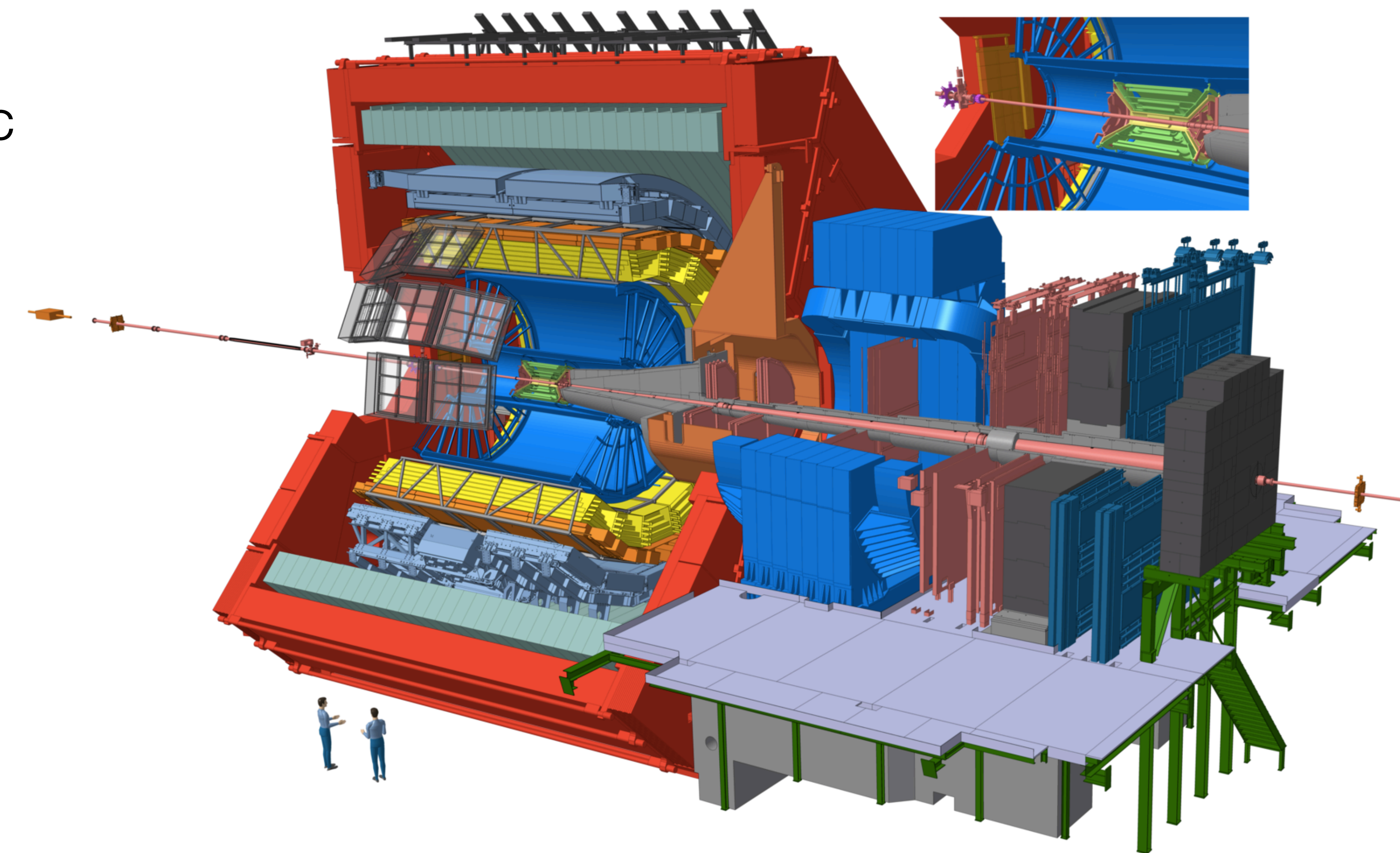
→ Use *ALICE* to measure antinuclei inelastic cross sections!



The ALICE experiment at CERN

General-purpose (heavy-ion) experiment at the Large Hadron Collider

- Excellent tracking and particle identification (PID) capabilities
- Most suitable detector at the LHC study the physics of (anti)nuclei



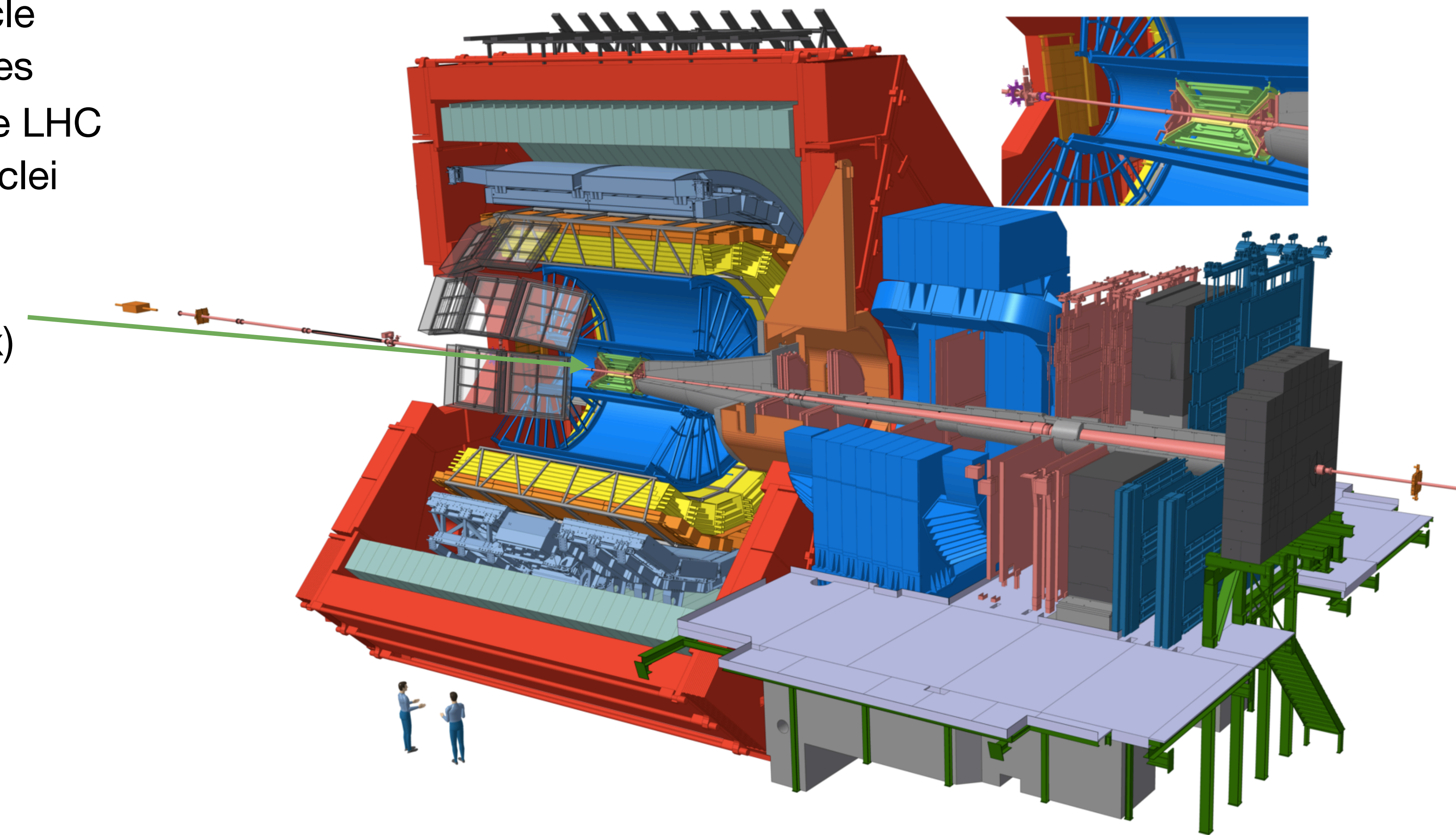
The ALICE experiment at CERN

General-purpose (heavy-ion) experiment at the Large Hadron Collider

- Excellent tracking and particle identification (PID) capabilities
- Most suitable detector at the LHC study the physics of (anti)nuclei

Inner Tracking System (ITS)

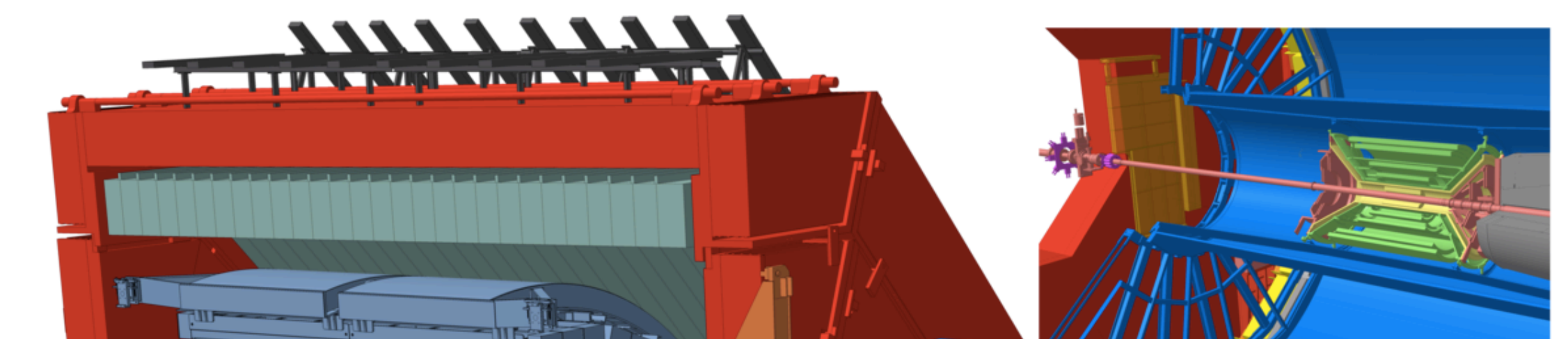
- Tracking, vertex, PID, (dE/dx)



The ALICE experiment at CERN

General-purpose (heavy-ion) experiment at the Large Hadron Collider

- Excellent tracking and particle identification (PID) capabilities
- Most suitable detector at the LHC study the physics of (anti)nuclei

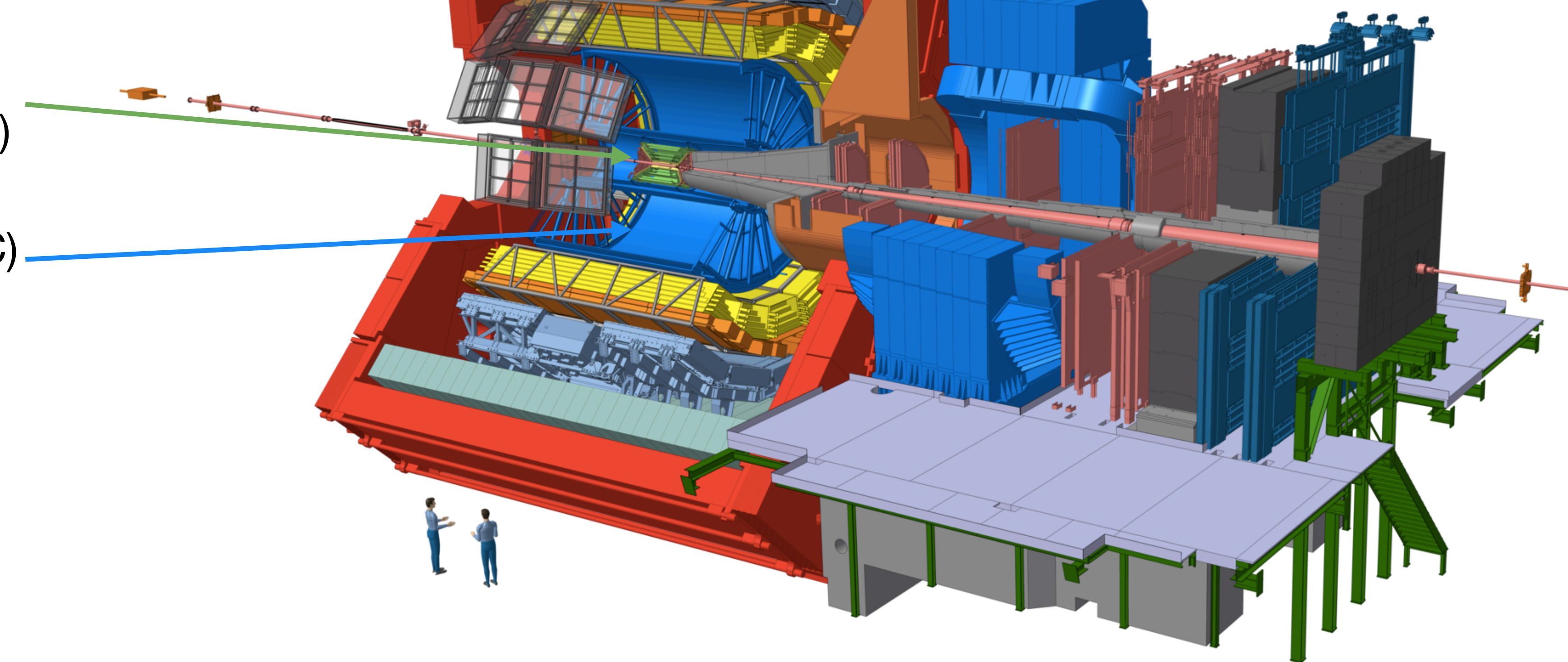


Inner Tracking System (ITS)

- Tracking, vertex, PID, (dE/dx)

Time Projection Chamber (TPC)

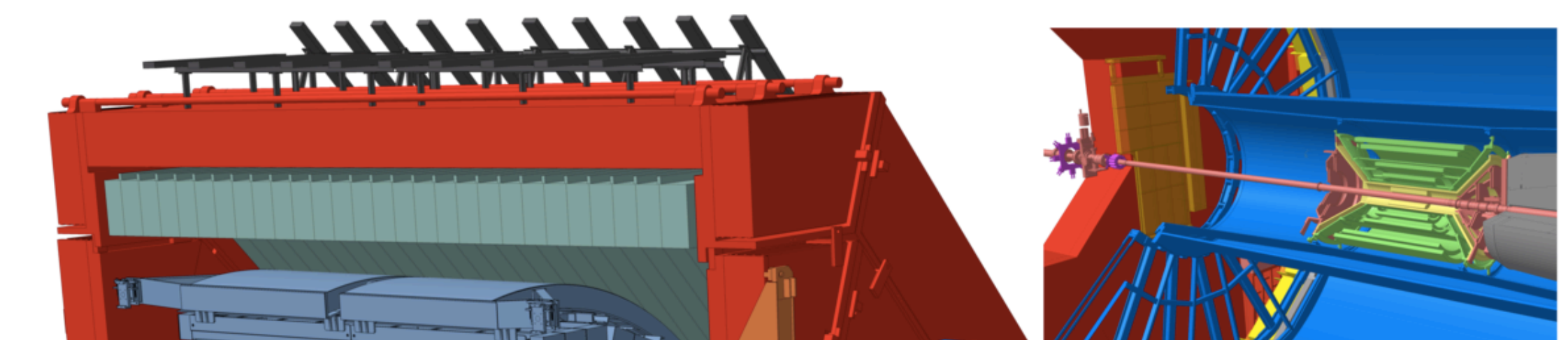
- Tracking, PID (dE/dx)



The ALICE experiment at CERN

General-purpose (heavy-ion) experiment at the Large Hadron Collider

- Excellent tracking and particle identification (PID) capabilities
- Most suitable detector at the LHC study the physics of (anti)nuclei



Inner Tracking System (ITS)

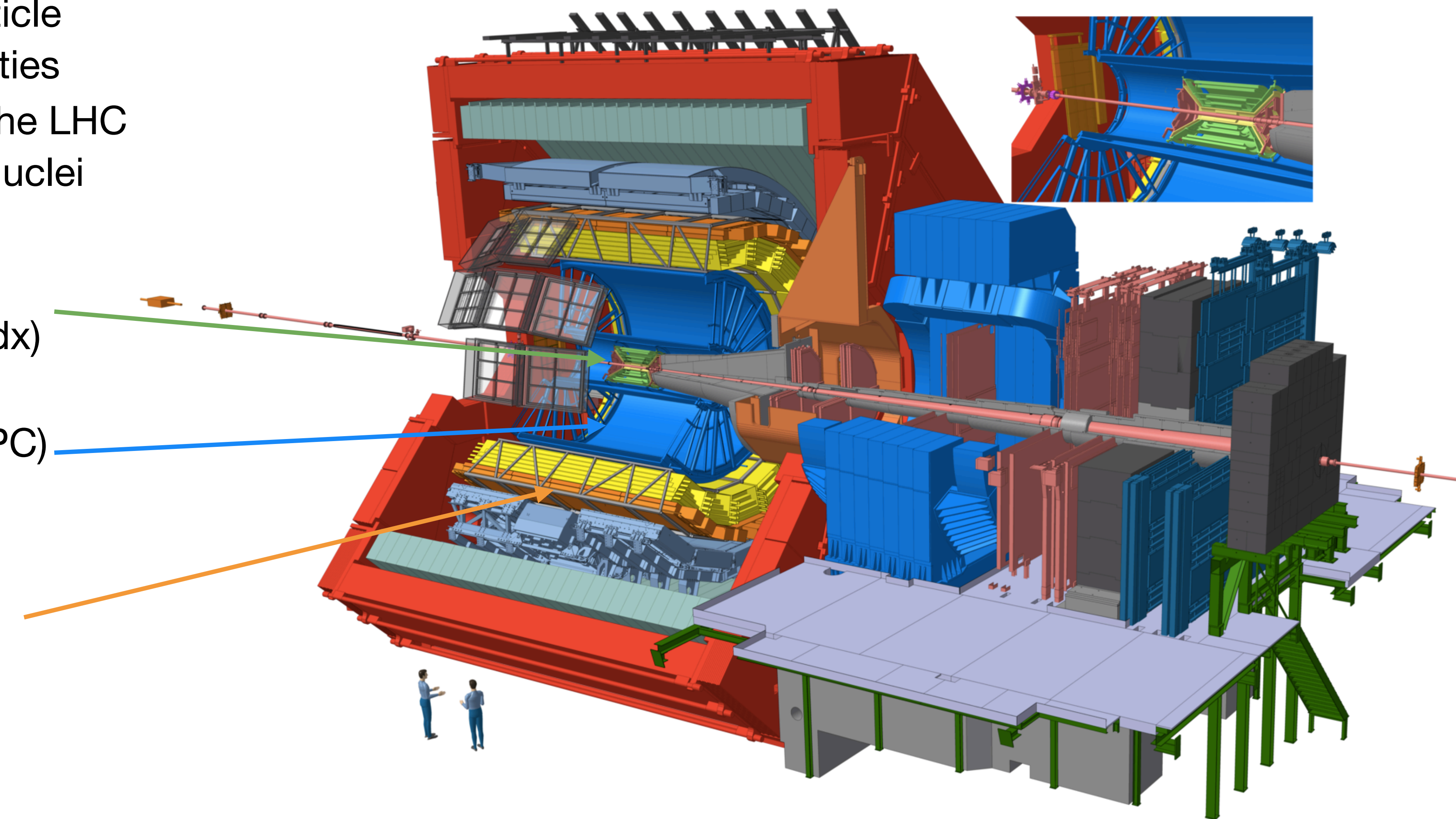
- Tracking, vertex, PID, (dE/dx)

Time Projection Chamber (TPC)

- Tracking, PID (dE/dx)

Time of Flight detector (TOF)

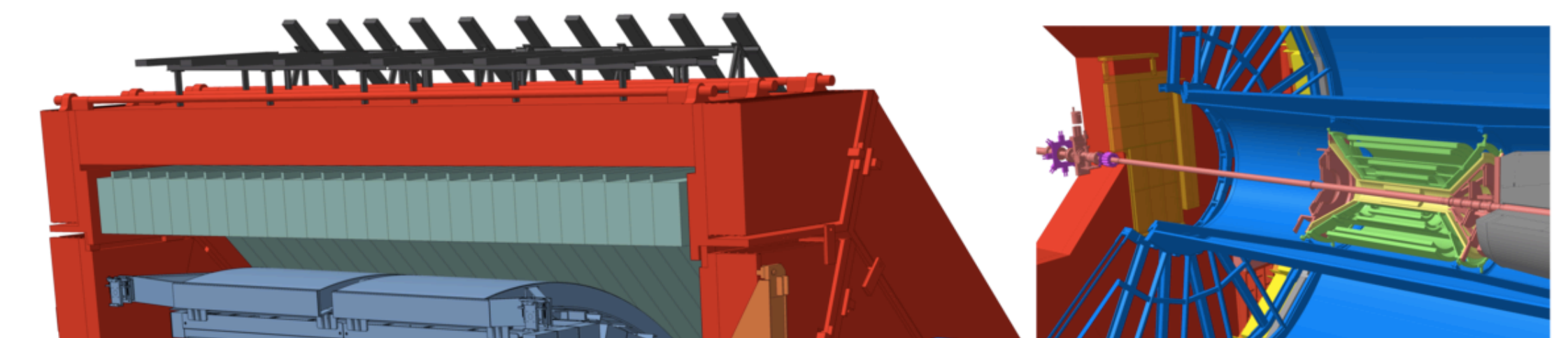
- PID (TOF measurement)



The ALICE experiment at CERN

General-purpose (heavy-ion) experiment at the Large Hadron Collider

- Excellent tracking and particle identification (PID) capabilities
- Most suitable detector at the LHC study the physics of (anti)nuclei



Inner Tracking System (ITS)

- Tracking, vertex, PID, (dE/dx)

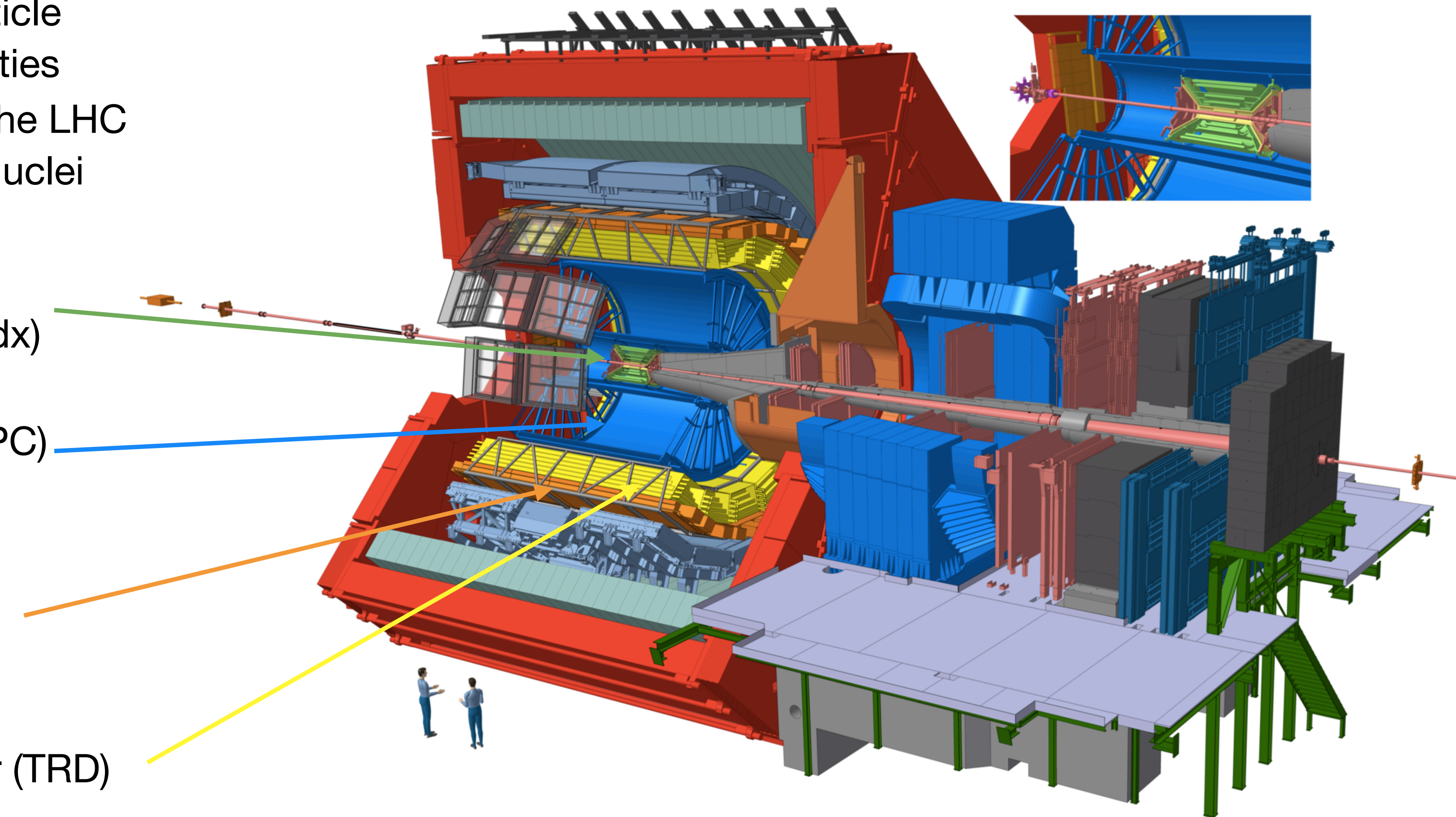
Time Projection Chamber (TPC)

- Tracking, PID (dE/dx)

Time of Flight detector (TOF)

- PID (TOF measurement)

Transition Radiation Detector (TRD)



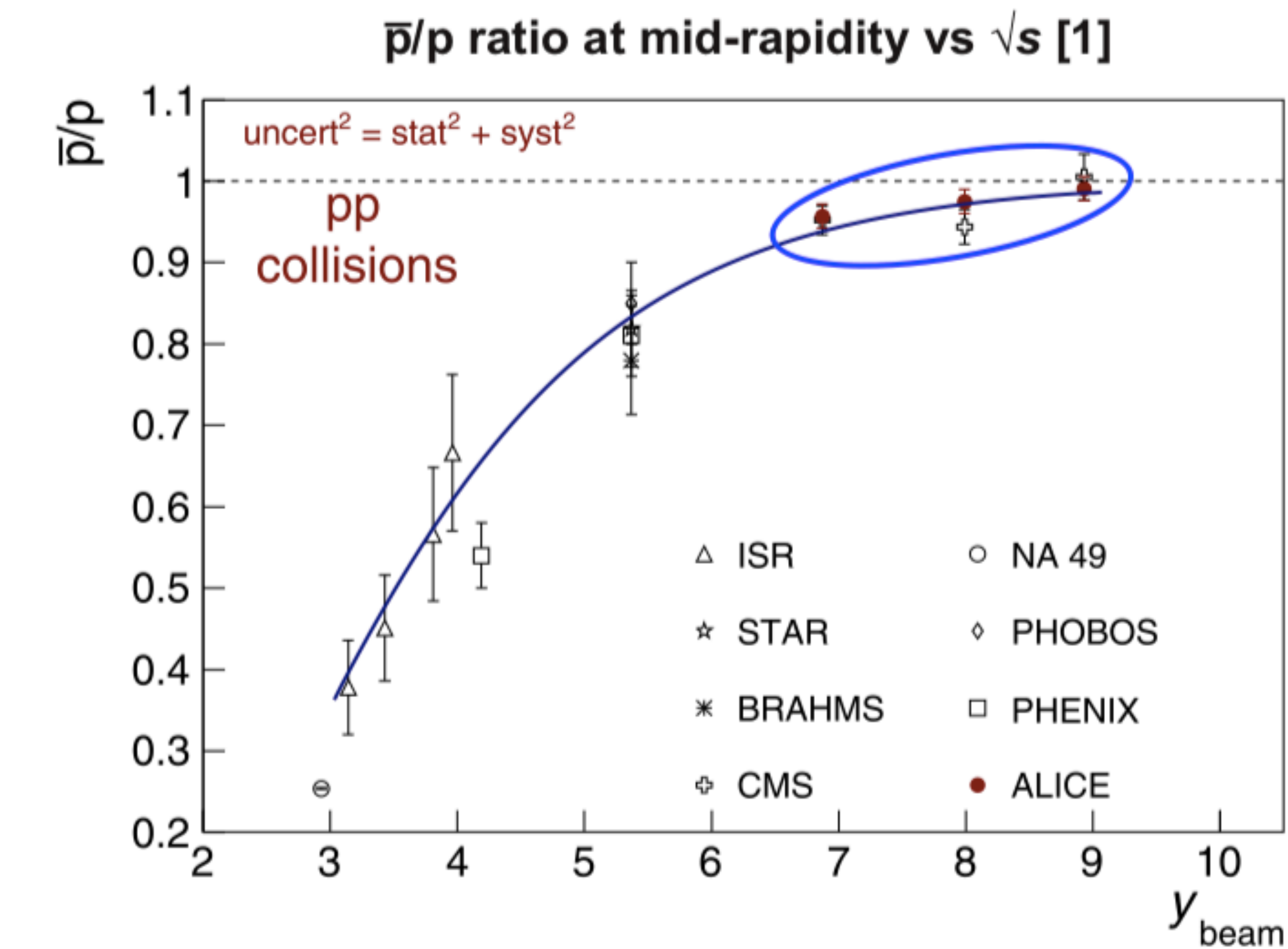
Use the LHC as an antimatter factory...

At LHC energies, particles and antiparticles are produced in almost equal amounts.

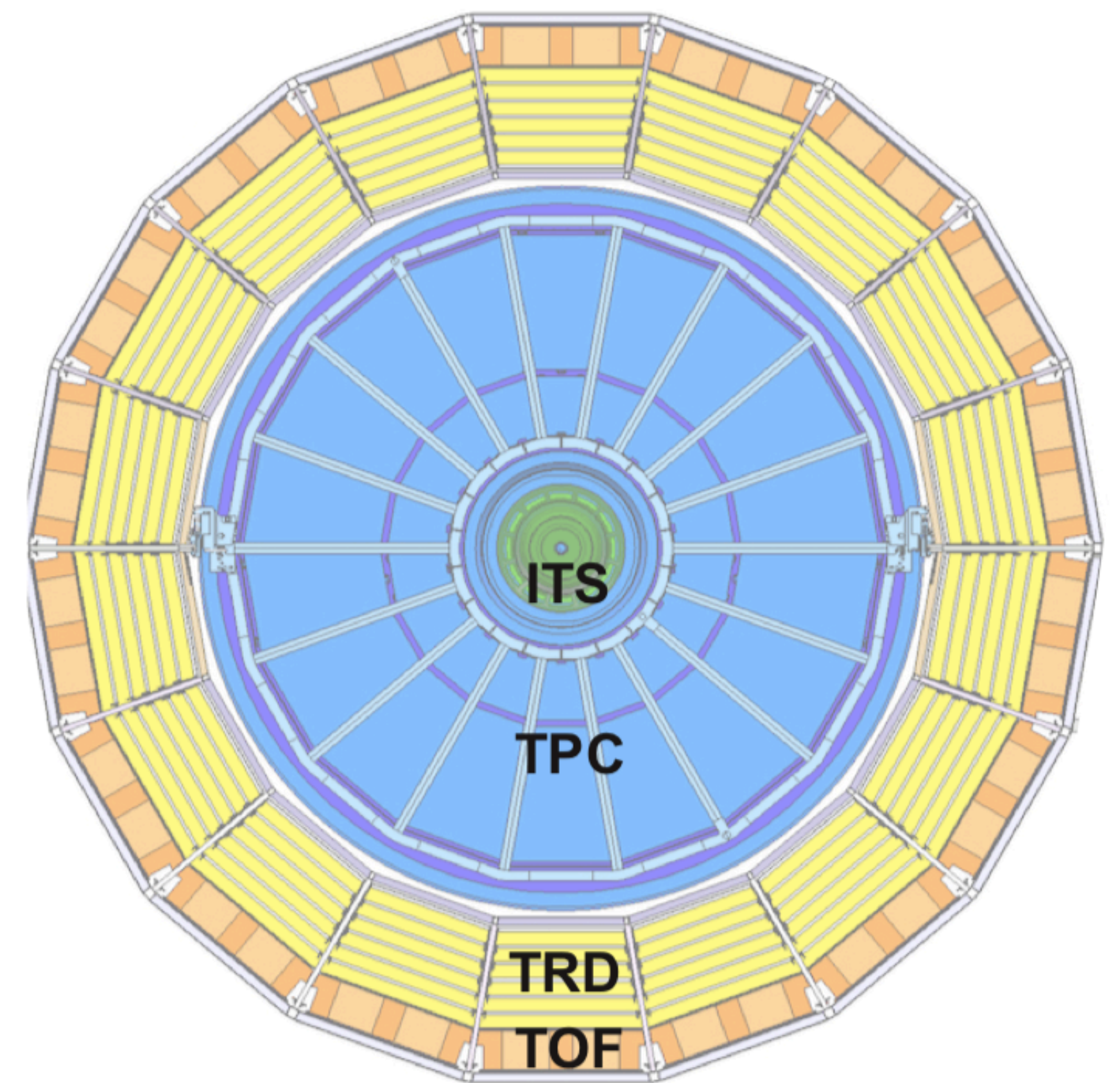
- Primordial antimatter-to-matter ratio approaches unity with increasing \sqrt{s}

This talk:

- (Anti)- ${}^3\text{He}$ results from high multiplicity pp collisions at $\sqrt{s} = 13 \text{ TeV}$, $\sim 10^9$ events
- (Anti)proton and (anti)deuteron results from p-Pb collisions at $\sqrt{s_{\text{NN}}} = 5.02 \text{ TeV}$, $\sim 300 \text{ M}$ events.

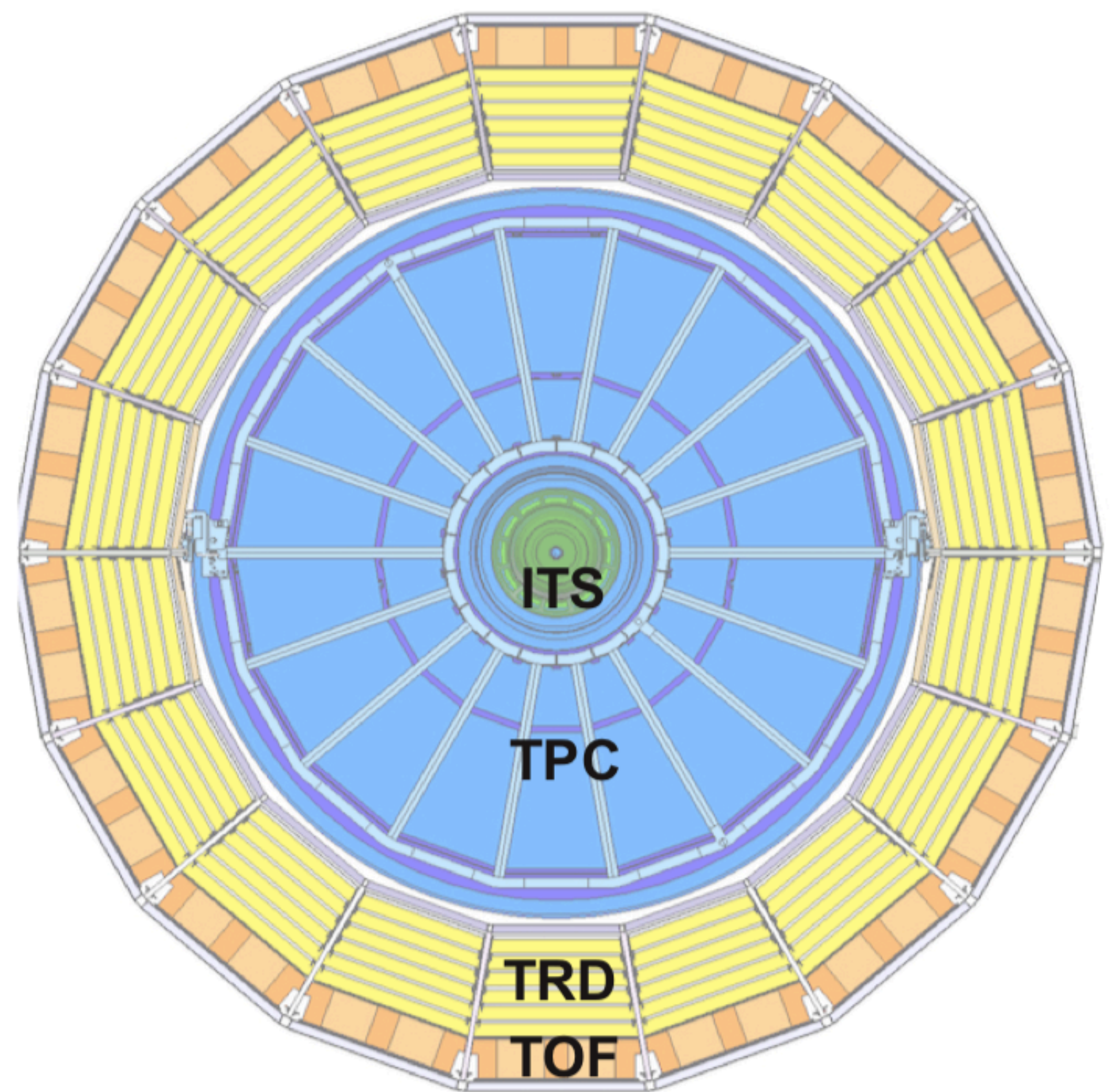


... and the ALICE detector material as a target



... and the ALICE detector material as a target

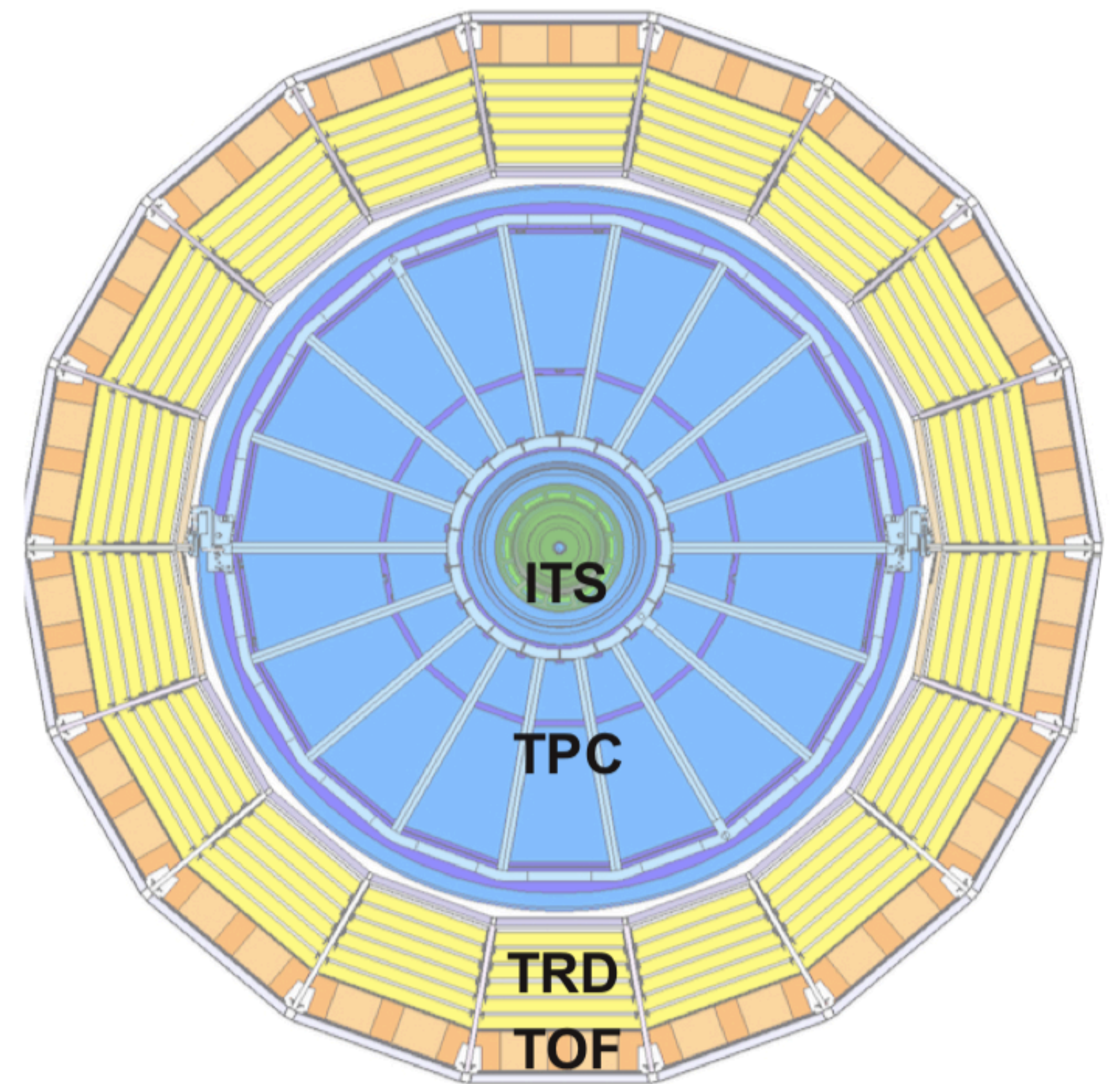
ALICE material budget at mid-rapidity [1]:



... and the ALICE detector material as a target

ALICE material budget at mid-rapidity [1]:

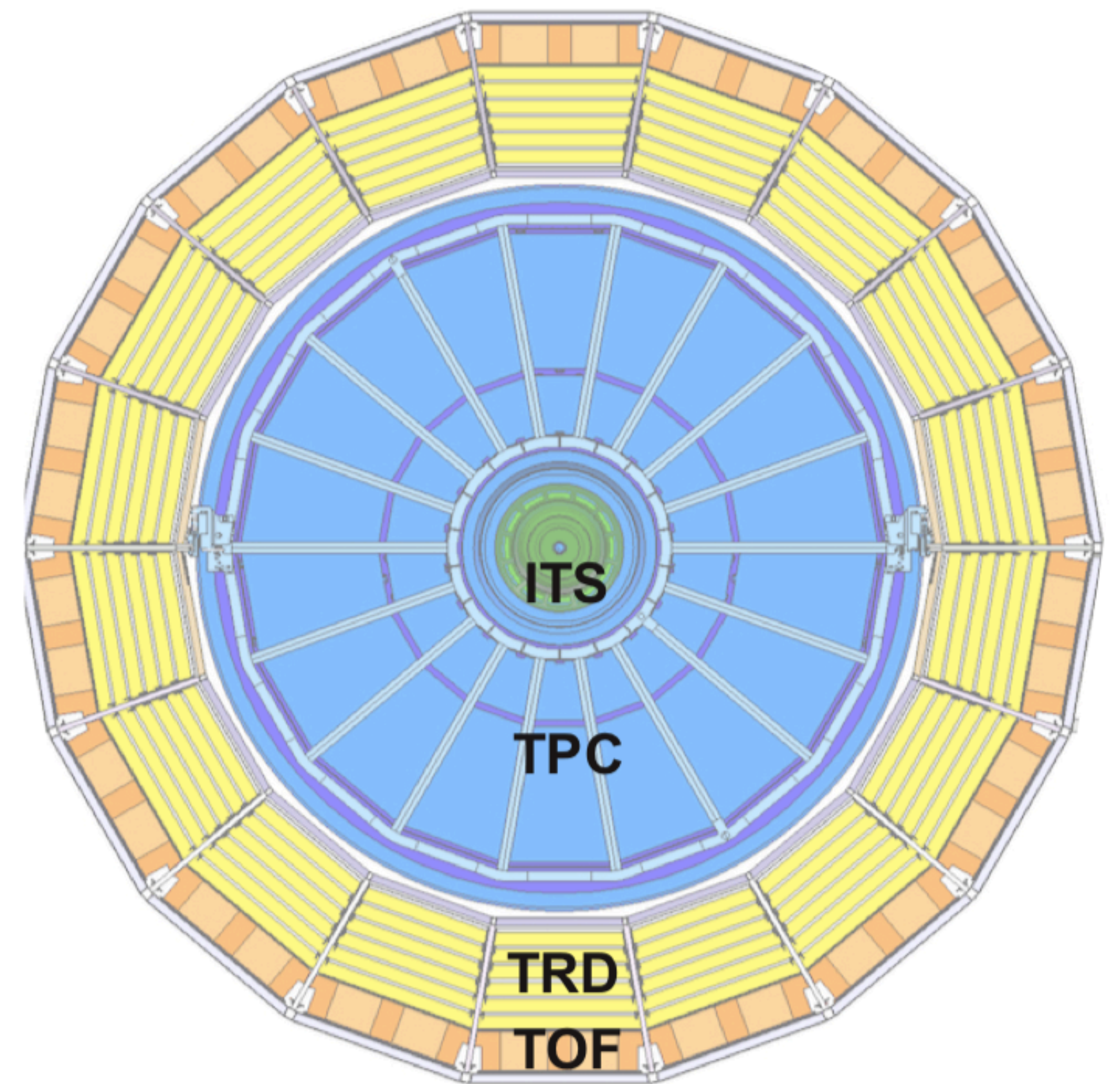
- **Beryllium beam pipe ($\sim 0.3\% X_0$)**



... and the ALICE detector material as a target

ALICE material budget at mid-rapidity [1]:

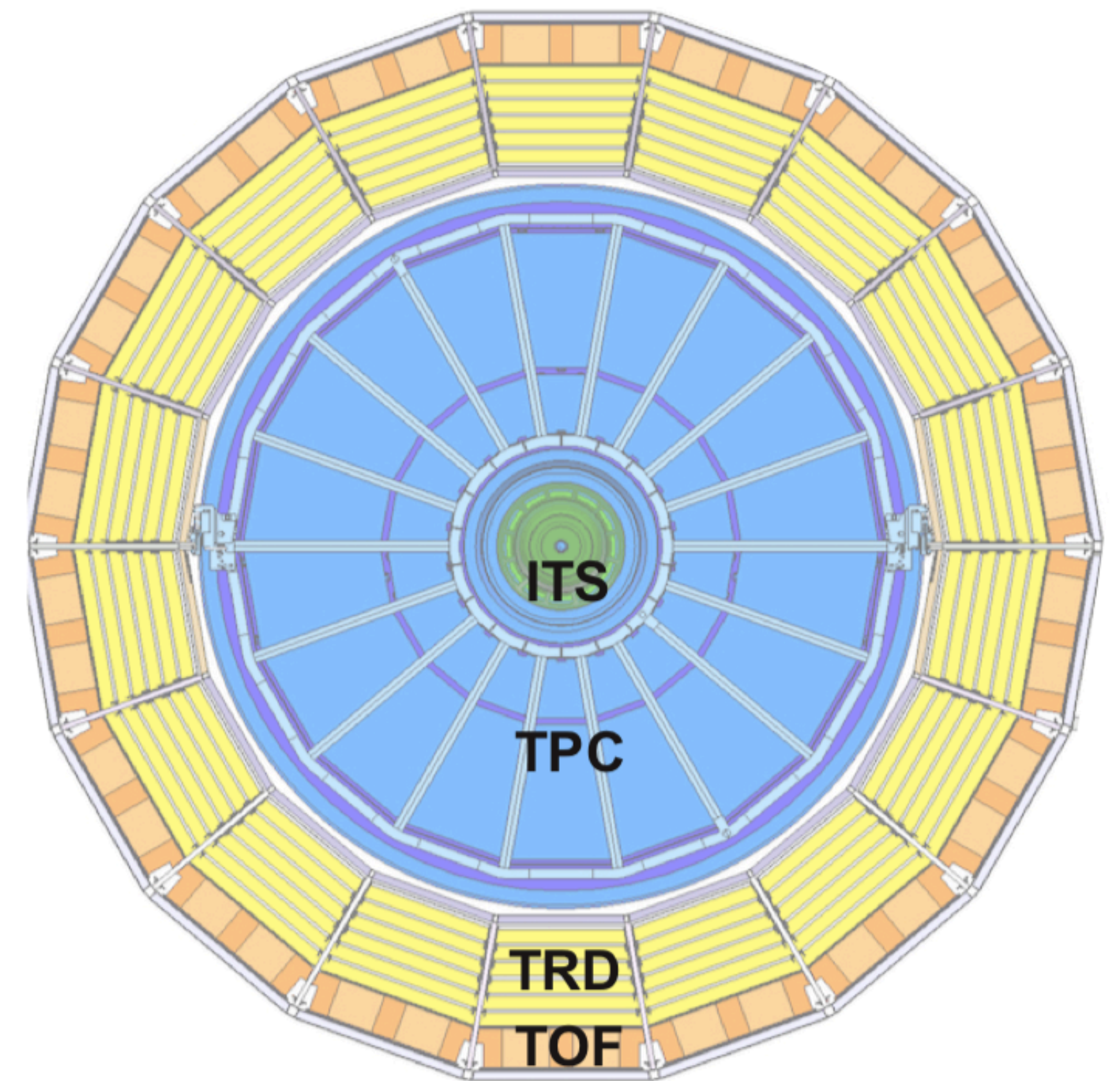
- **Beryllium beam pipe ($\sim 0.3\% X_0$)**
- **ITS ($\sim 8\% X_0$)**



... and the ALICE detector material as a target

ALICE material budget at mid-rapidity [1]:

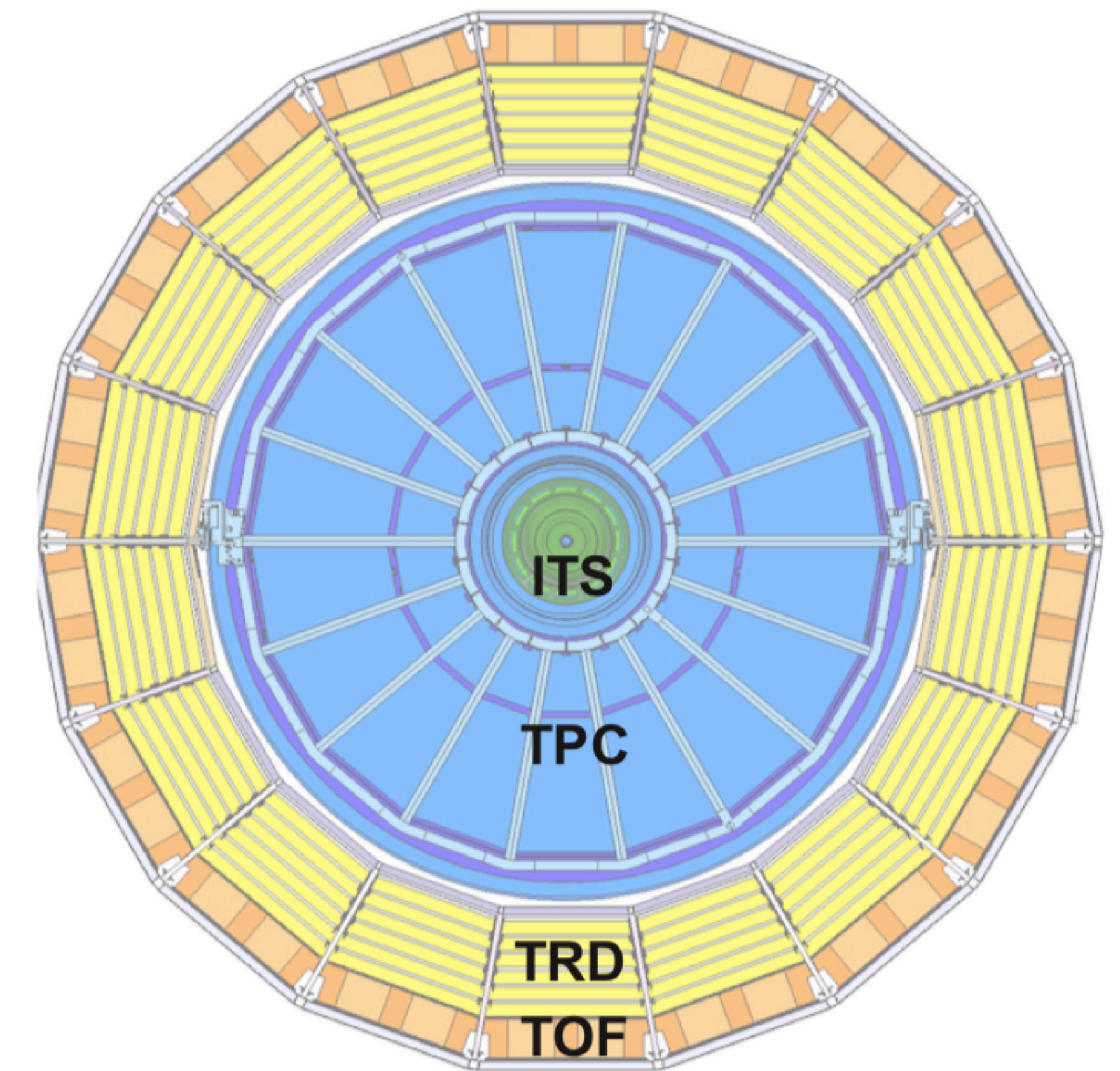
- **Beryllium beam pipe ($\sim 0.3\% X_0$)**
- **ITS ($\sim 8\% X_0$)**
- **TPC ($\sim 4\% X_0$)**



... and the ALICE detector material as a target

ALICE material budget at mid-rapidity [1]:

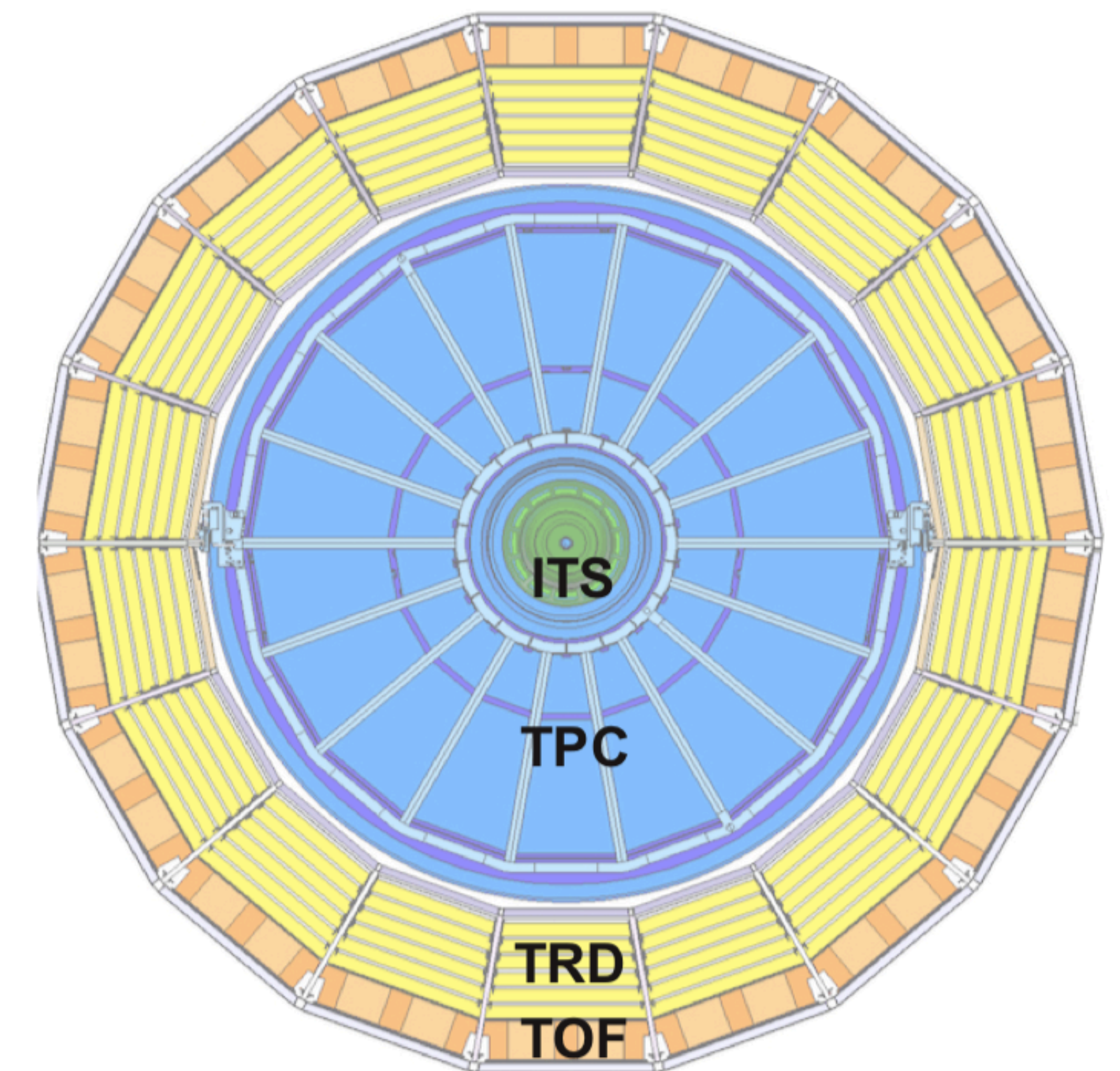
- **Beryllium beam pipe ($\sim 0.3\% X_0$)**
- **ITS ($\sim 8\% X_0$)**
- **TPC ($\sim 4\% X_0$)**
- **TRD ($\sim 25\% X_0$)**



... and the ALICE detector material as a target

ALICE material budget at mid-rapidity [1]:

- **Beryllium beam pipe ($\sim 0.3\% X_0$)**
- **ITS ($\sim 8\% X_0$)**
- **TPC ($\sim 4\% X_0$)**
- **TRD ($\sim 25\% X_0$)**
- **Space frame ($\sim 20\% X_0$ between TPC and TOF)**

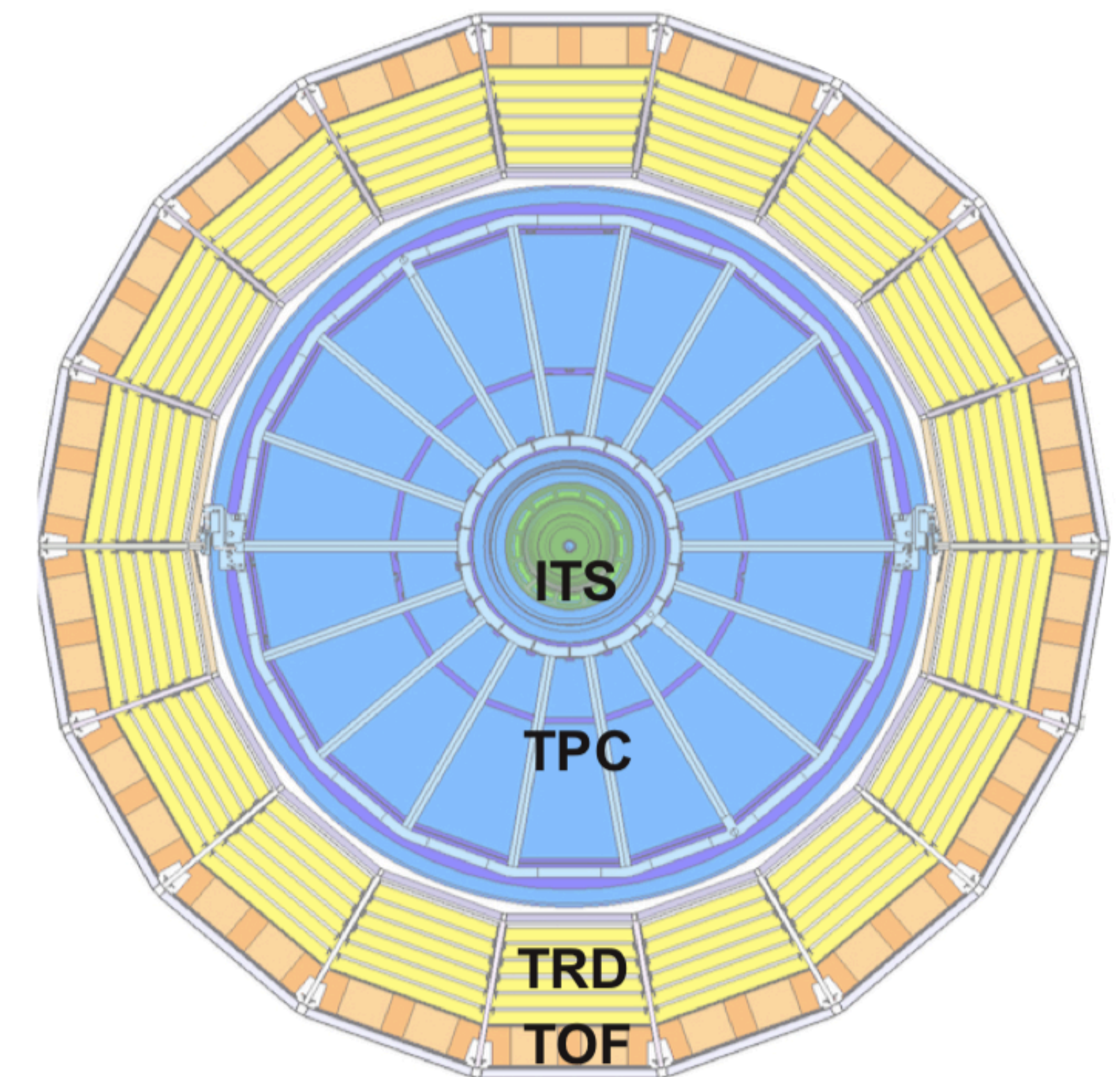


... and the ALICE detector material as a target

ALICE material budget at mid-rapidity [1]:

- **Beryllium beam pipe ($\sim 0.3\% X_0$)**
- **ITS ($\sim 8\% X_0$)**
- **TPC ($\sim 4\% X_0$)**
- **TRD ($\sim 25\% X_0$)**
- **Space frame ($\sim 20\% X_0$ between TPC and TOF)**

Idea: use raw reconstructed antiparticle-to-particle ratios (\bar{p}/p , \bar{d}/d , ${}^3\overline{\text{He}}/{}^3\text{He}$)

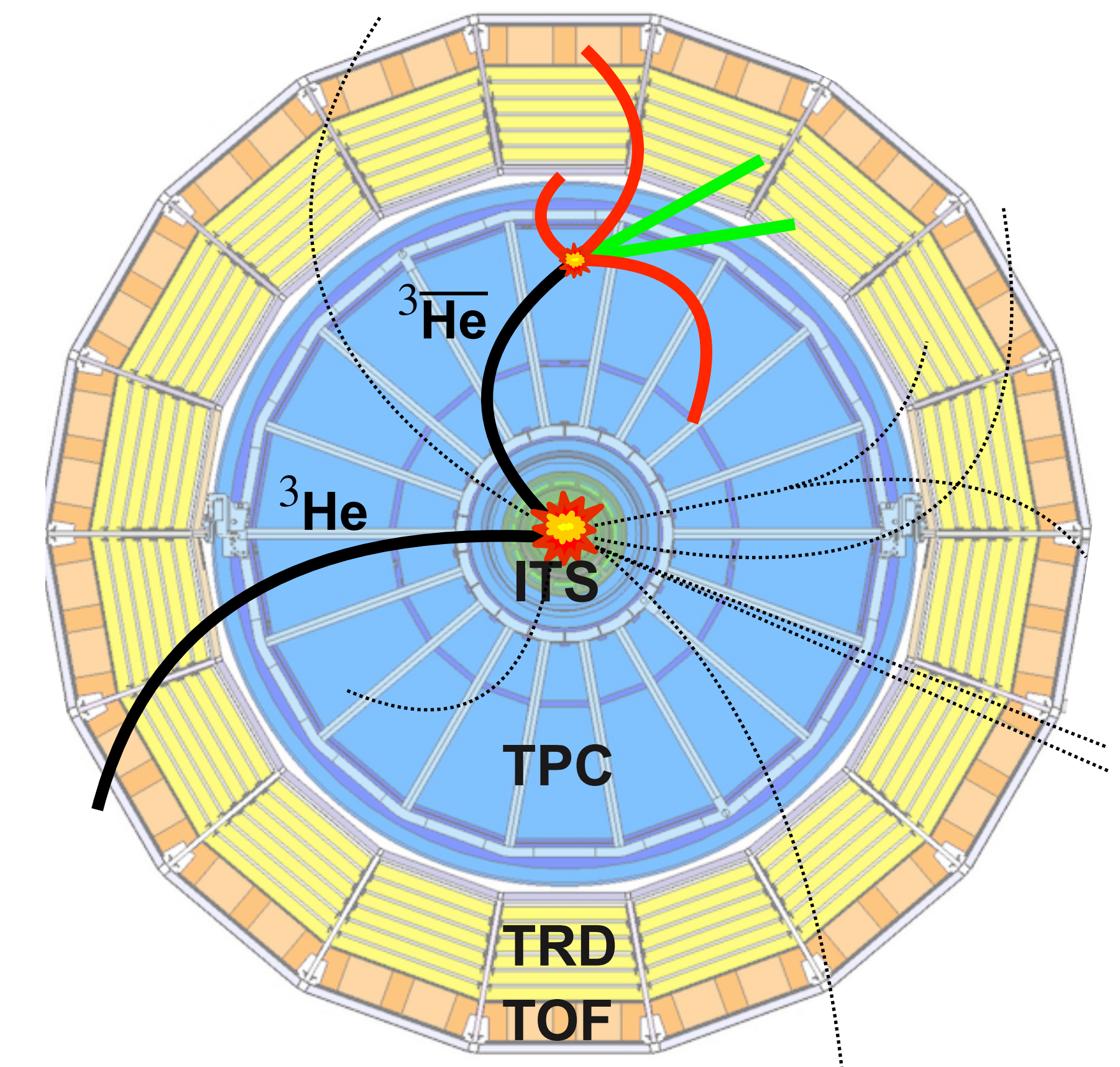


... and the ALICE detector material as a target

ALICE material budget at mid-rapidity [1]:

- **Beryllium beam pipe ($\sim 0.3\% X_0$)**
- **ITS ($\sim 8\% X_0$)**
- **TPC ($\sim 4\% X_0$)**
- **TRD ($\sim 25\% X_0$)**
- **Space frame ($\sim 20\% X_0$ between TPC and TOF)**

Idea: use raw reconstructed antiparticle-to-particle ratios (\bar{p}/p , \bar{d}/d , ${}^3\overline{\text{He}}/{}^3\text{He}$)



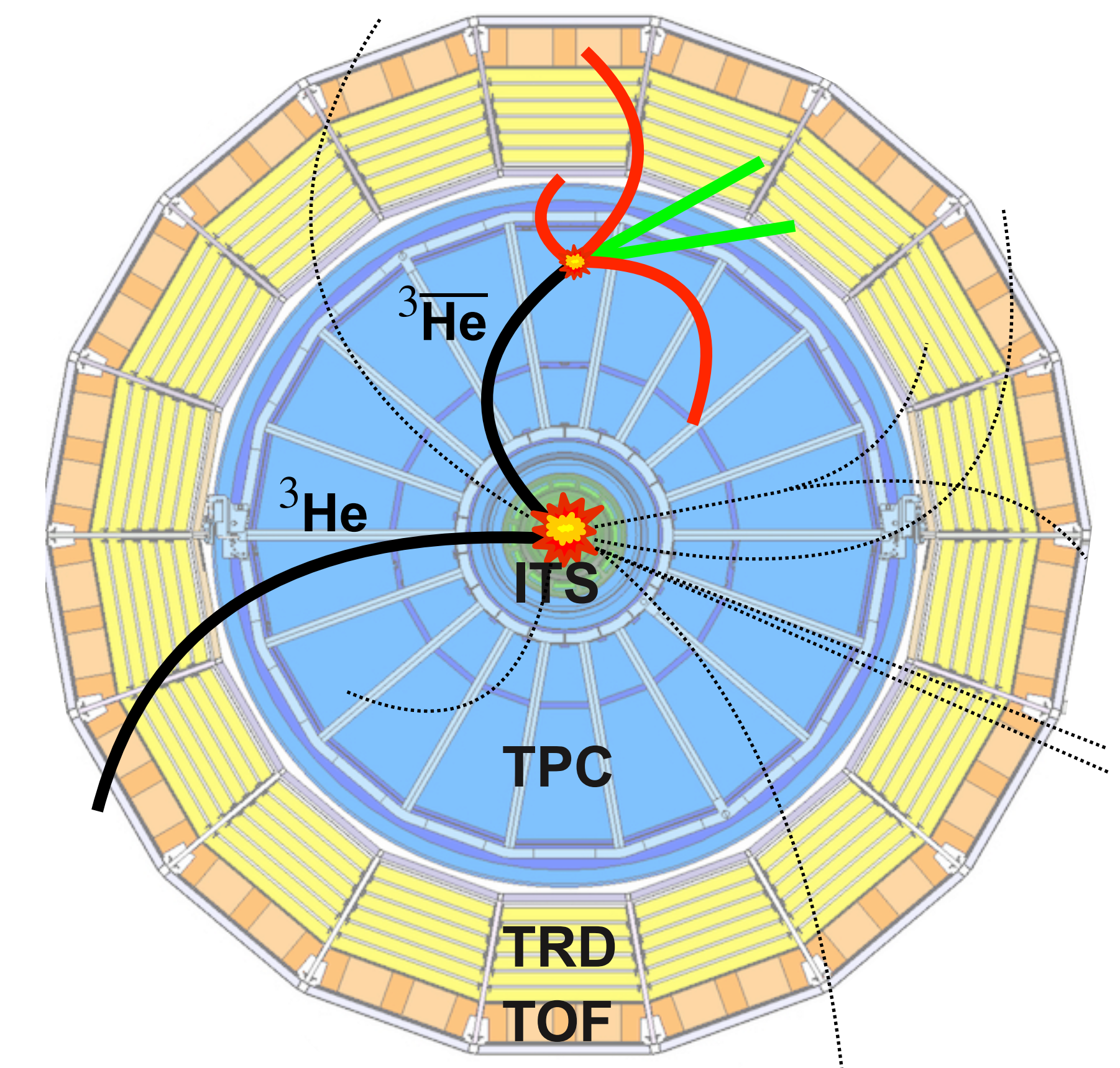
... and the ALICE detector material as a target

ALICE material budget at mid-rapidity [1]:

- **Beryllium beam pipe ($\sim 0.3\% X_0$)**
- **ITS ($\sim 8\% X_0$)**
- **TPC ($\sim 4\% X_0$)**
- **TRD ($\sim 25\% X_0$)**
- **Space frame ($\sim 20\% X_0$ between TPC and TOF)**

Idea: use raw reconstructed antiparticle-to-particle ratios (\bar{p}/p , \bar{d}/d , ${}^3\overline{\text{He}}/{}^3\text{He}$)

- No correction due to detector efficiency or absorption from material.



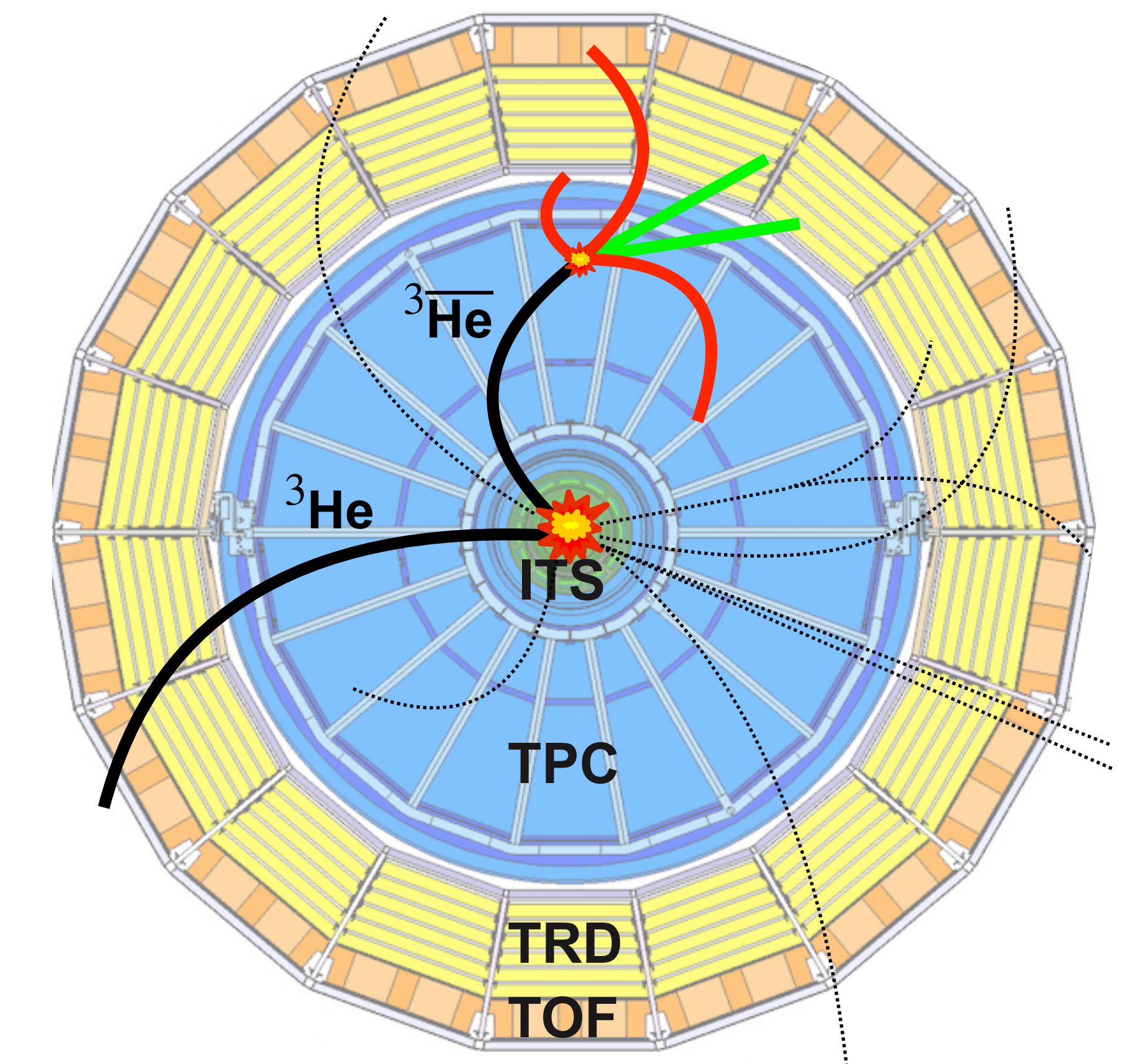
... and the ALICE detector material as a target

ALICE material budget at mid-rapidity [1]:

- **Beryllium beam pipe ($\sim 0.3\% X_0$)**
- **ITS ($\sim 8\% X_0$)**
- **TPC ($\sim 4\% X_0$)**
- **TRD ($\sim 25\% X_0$)**
- **Space frame ($\sim 20\% X_0$ between TPC and TOF)**

Idea: use raw reconstructed antiparticle-to-particle ratios (\bar{p}/p , \bar{d}/d , ${}^3\overline{\text{He}}/{}^3\text{He}$)

- No correction due to detector efficiency or absorption from material.
- Correct for secondary (anti)particles from weak decays and spallation processes.



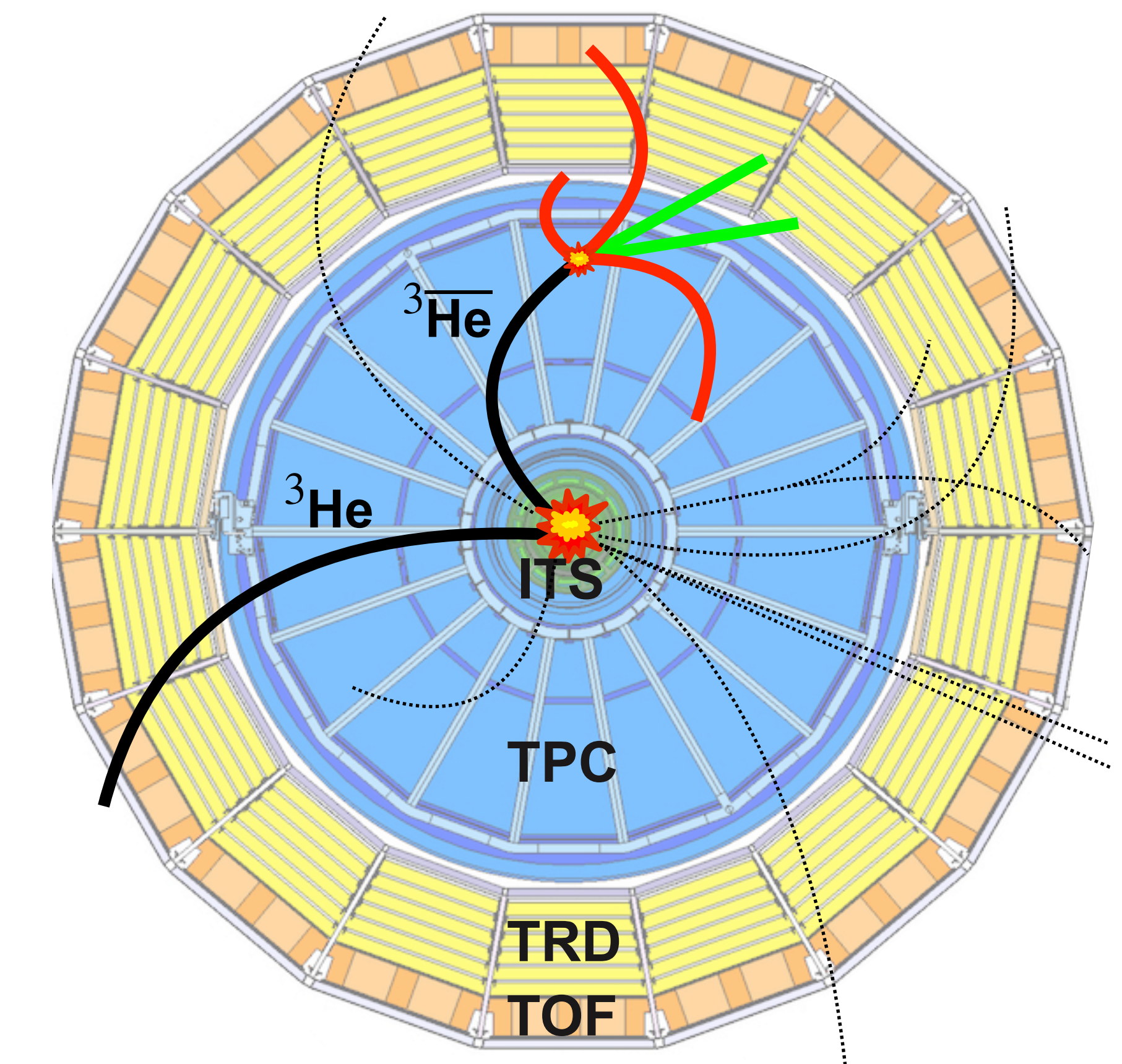
... and the ALICE detector material as a target

ALICE material budget at mid-rapidity [1]:

- **Beryllium beam pipe ($\sim 0.3\% X_0$)**
- **ITS ($\sim 8\% X_0$)**
- **TPC ($\sim 4\% X_0$)**
- **TRD ($\sim 25\% X_0$)**
- **Space frame ($\sim 20\% X_0$ between TPC and TOF)**

Idea: use raw reconstructed antiparticle-to-particle ratios (\bar{p}/p , \bar{d}/d , ${}^3\overline{\text{He}}/{}^3\text{He}$)

- No correction due to detector efficiency or absorption from material.
- Correct for secondary (anti)particles from weak decays and spallation processes.
- Measure σ_{inel} via comparison with detailed Monte Carlo simulations using Geant4.



Particle identification in TPC and TOF

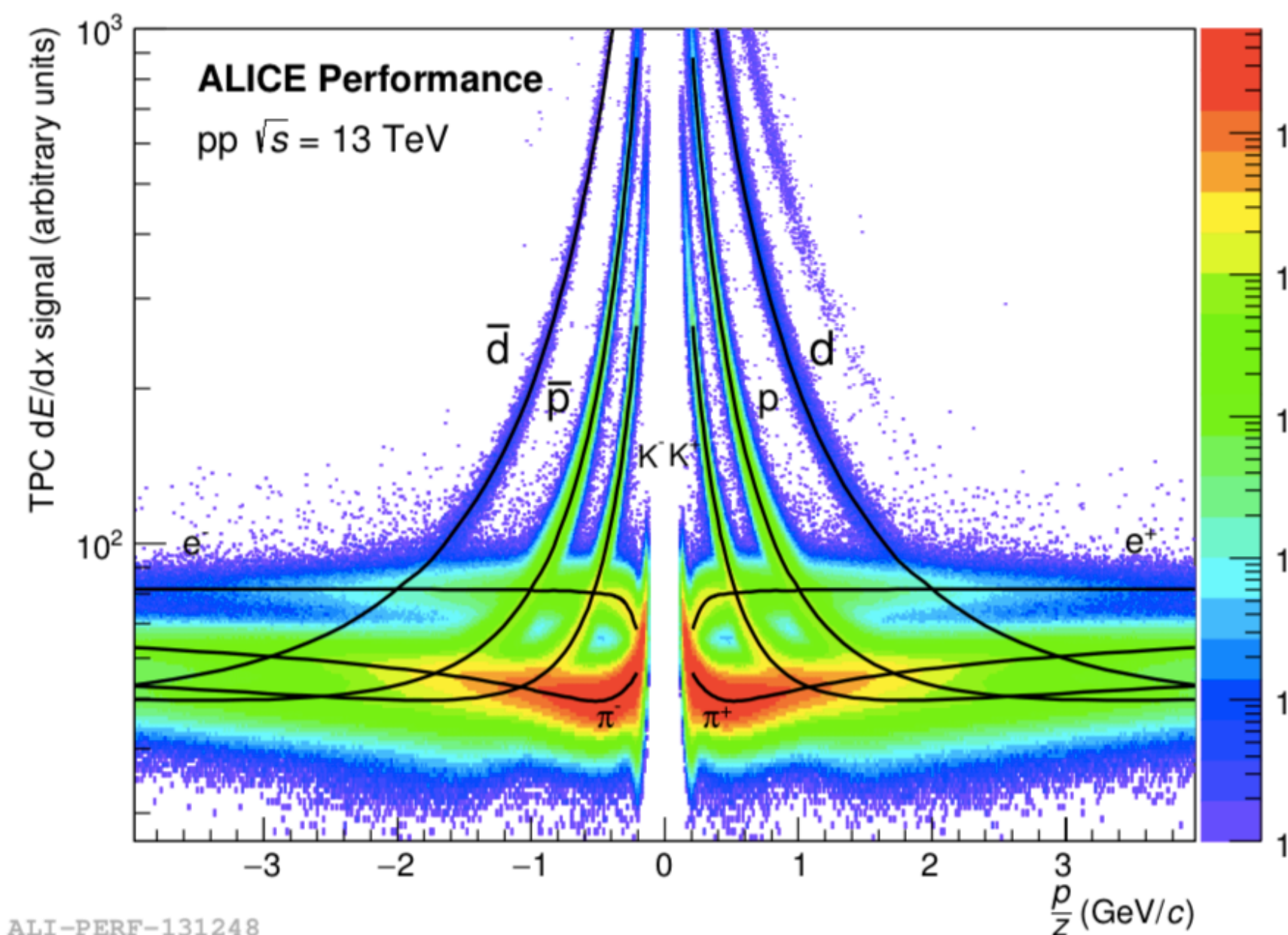
Complementary information from TPC and TOF detectors allows to select high purity (anti)particles:

Particle identification in TPC and TOF

Complementary information from TPC and TOF detectors allows to select high purity

(anti)particles:

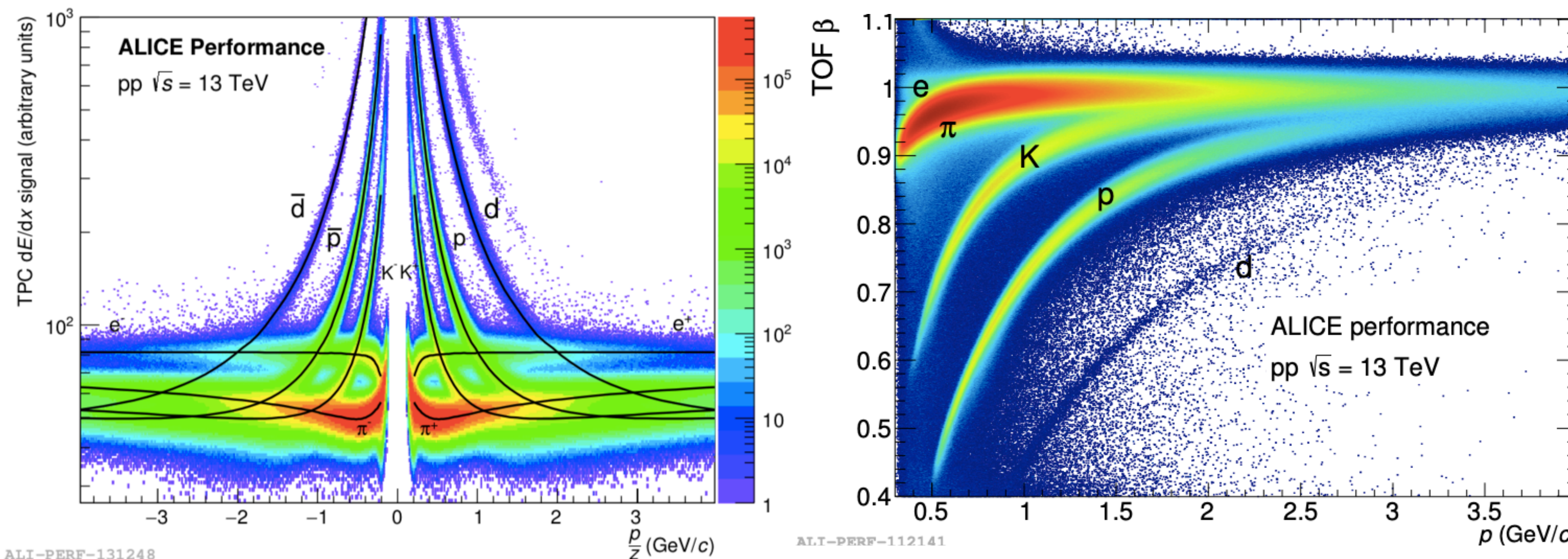
- TPC: dE/dx in gas



Particle identification in TPC and TOF

Complementary information from TPC and TOF detectors allows to select high purity (anti)particles:

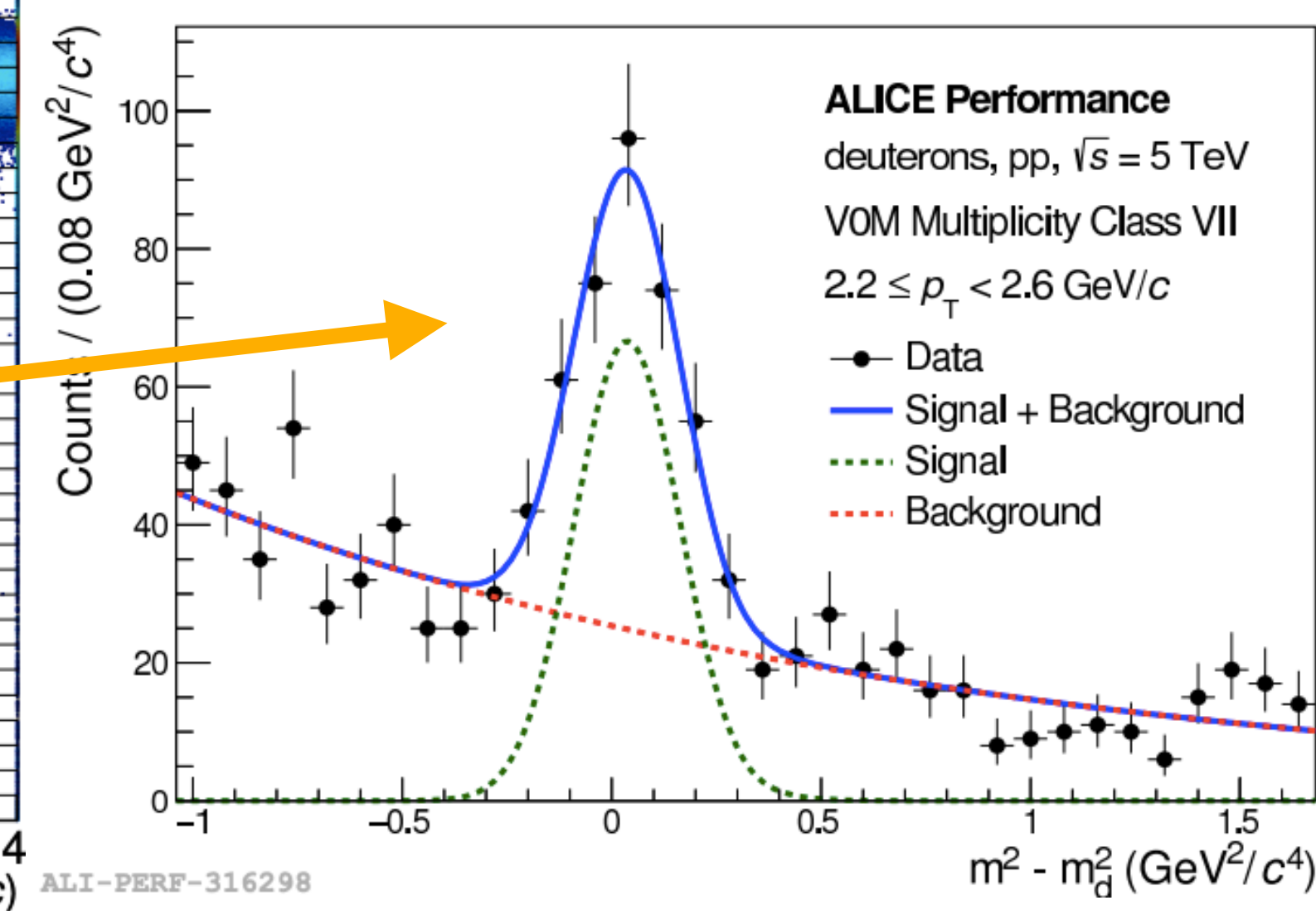
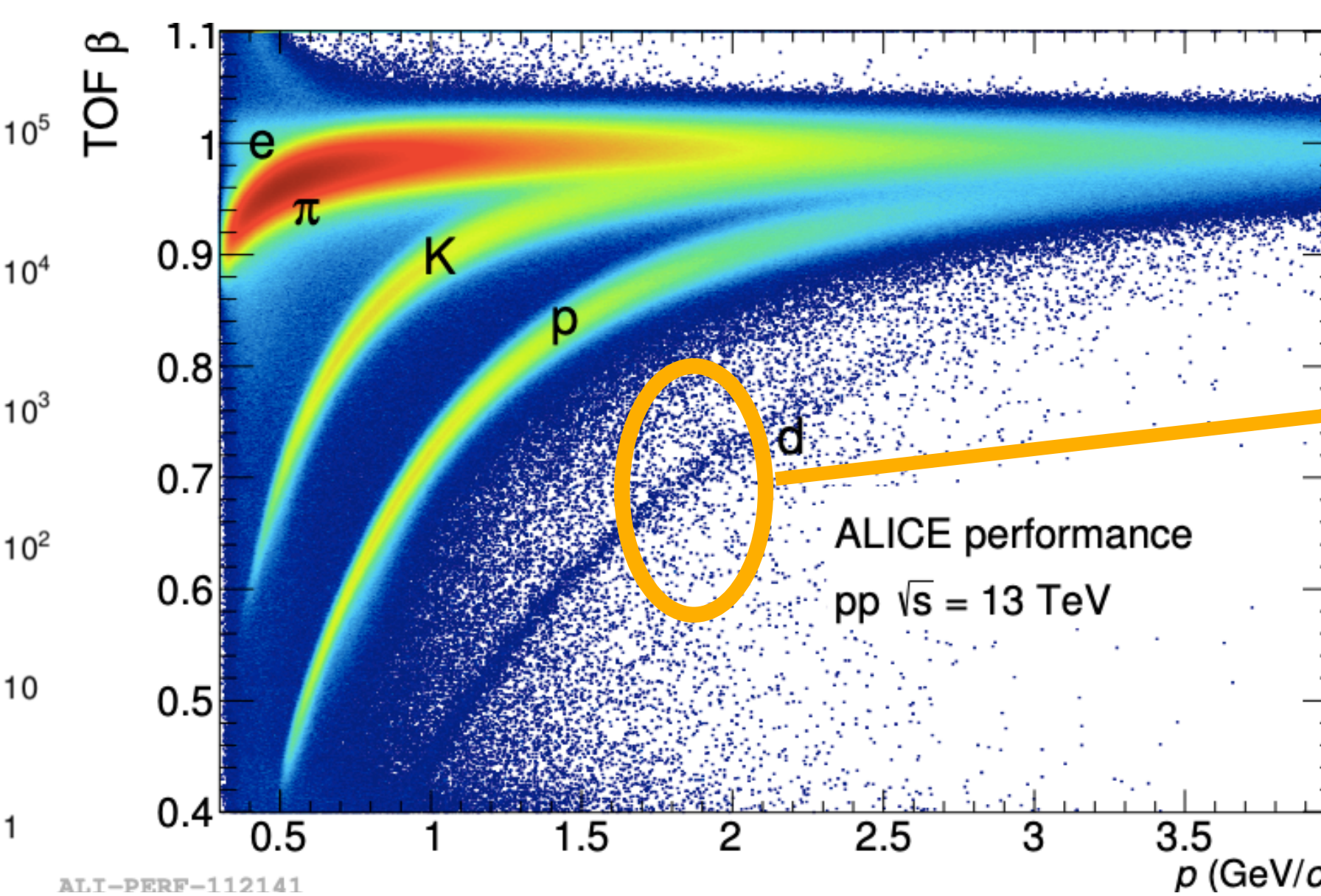
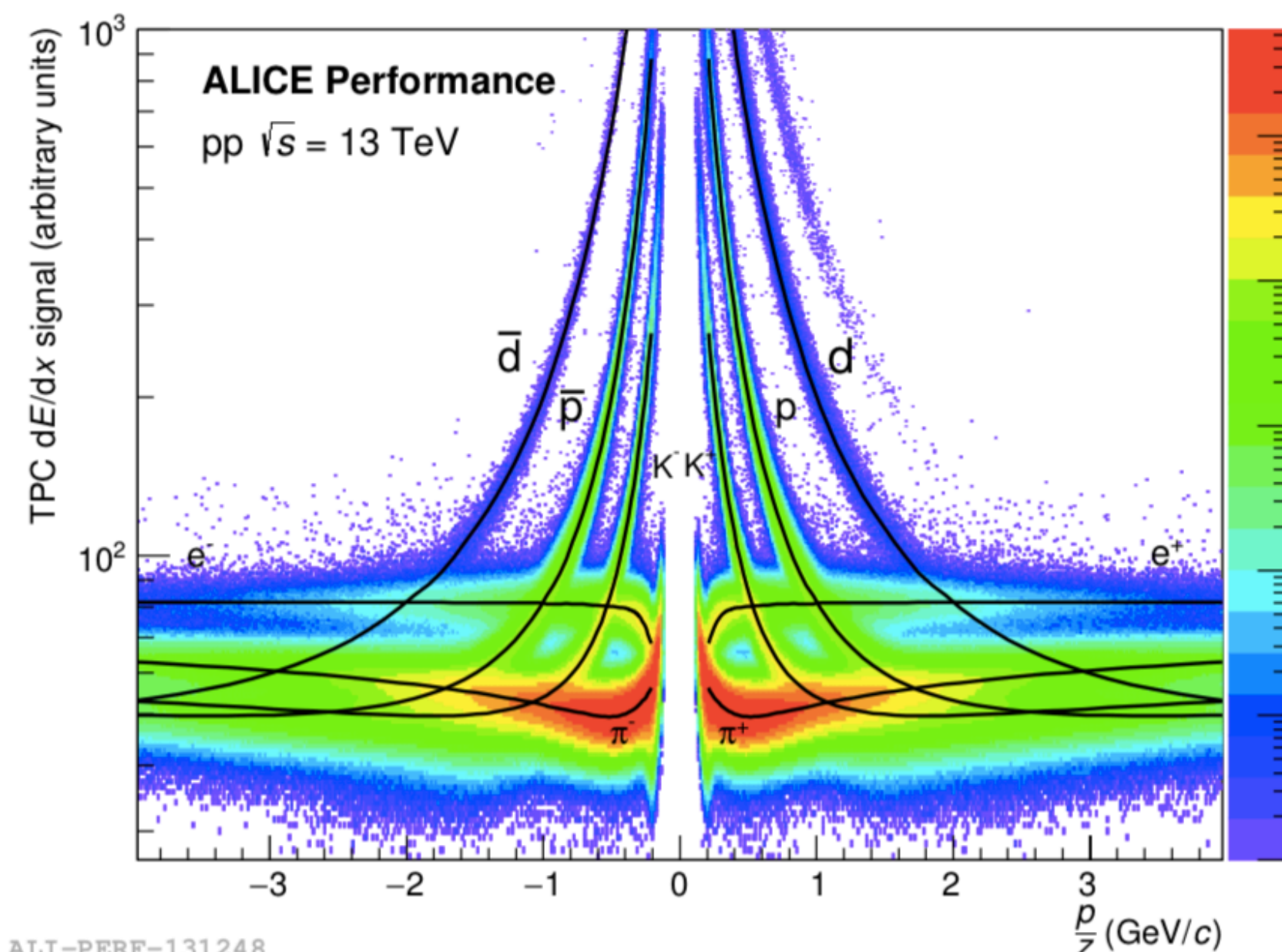
- TPC: dE/dx in gas
- TOF measurement $\beta = \frac{v}{c}$, $p = \gamma\beta mc \rightarrow$ mass



Particle identification in TPC and TOF

Complementary information from TPC and TOF detectors allows to select high purity (anti)particles:

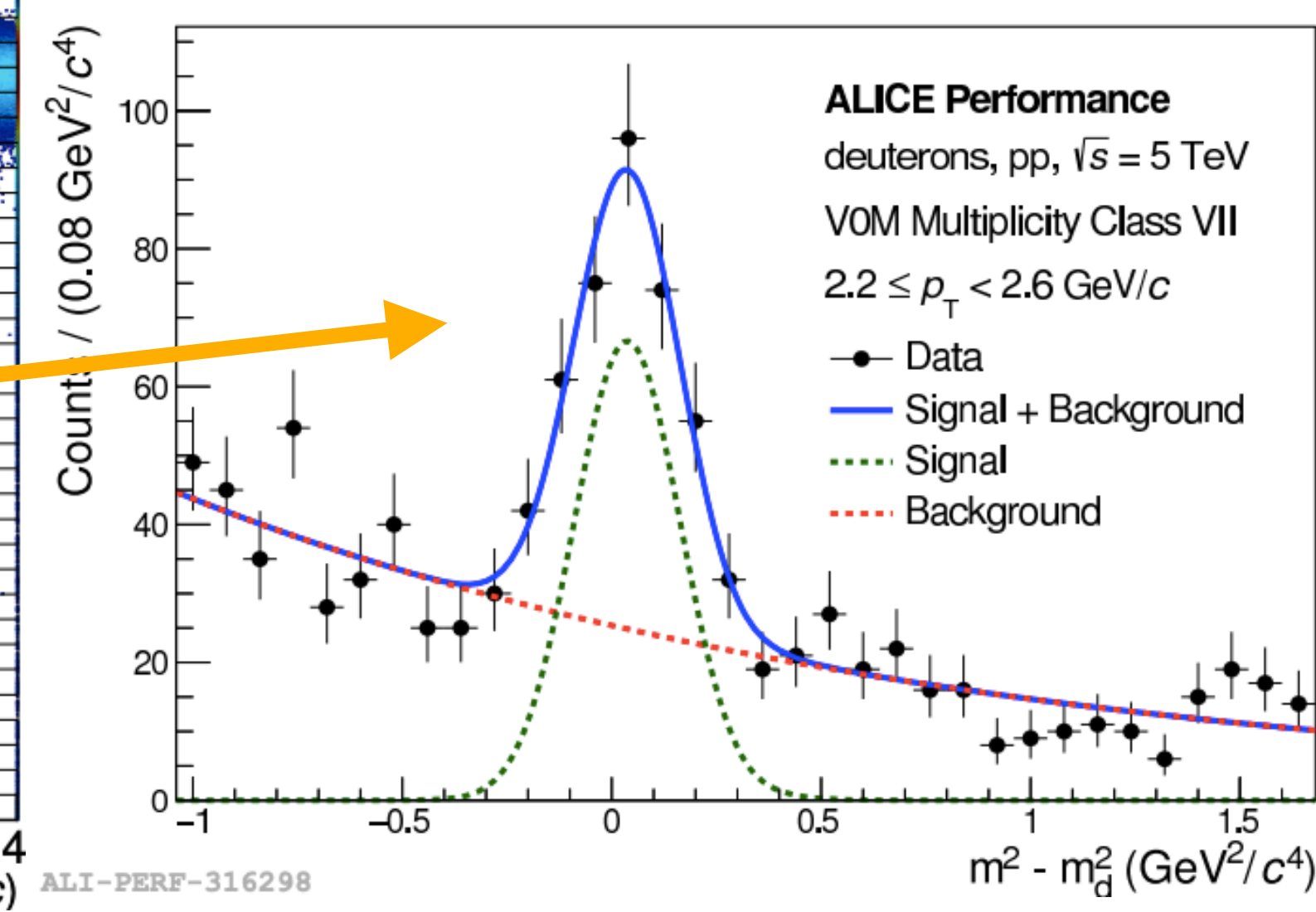
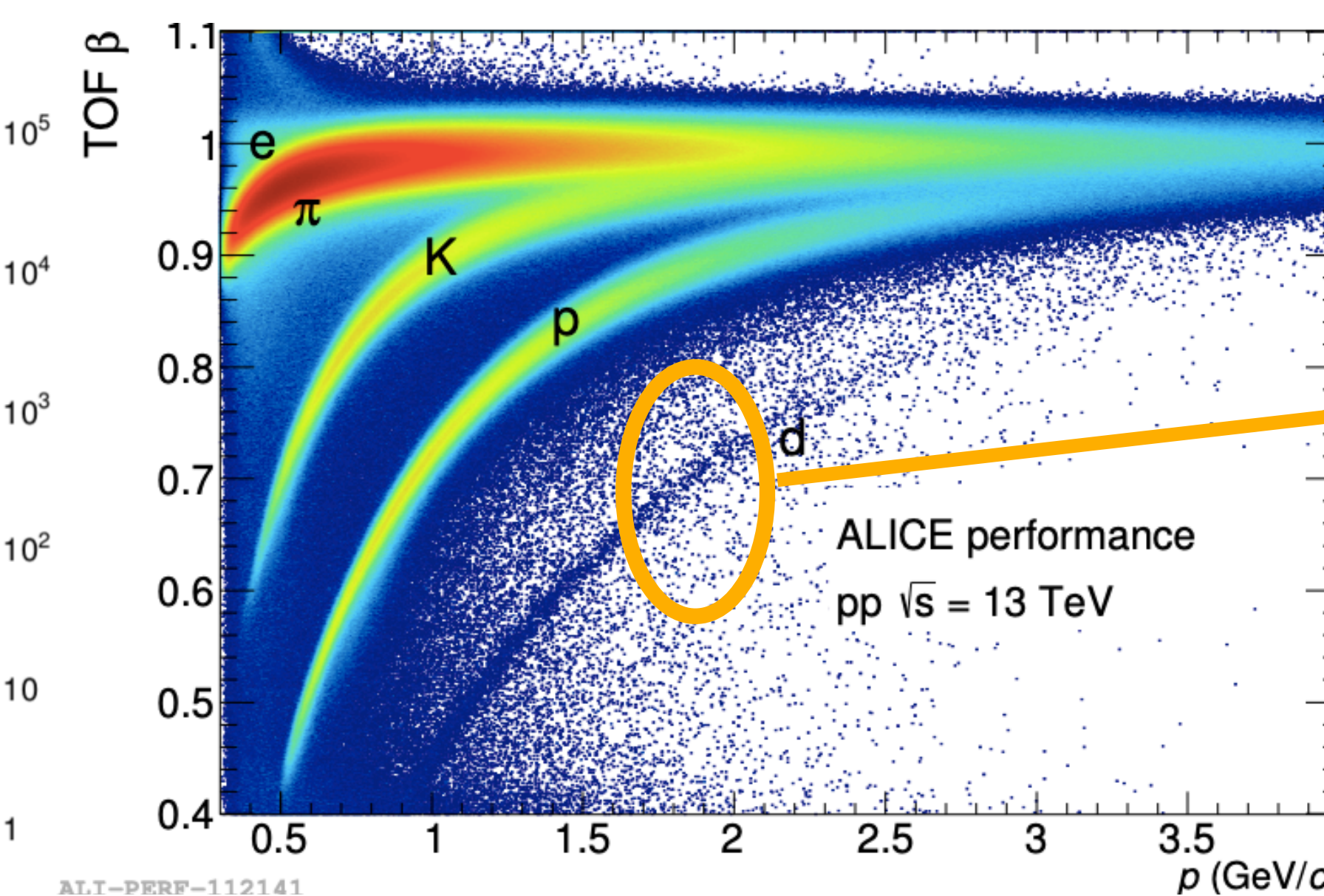
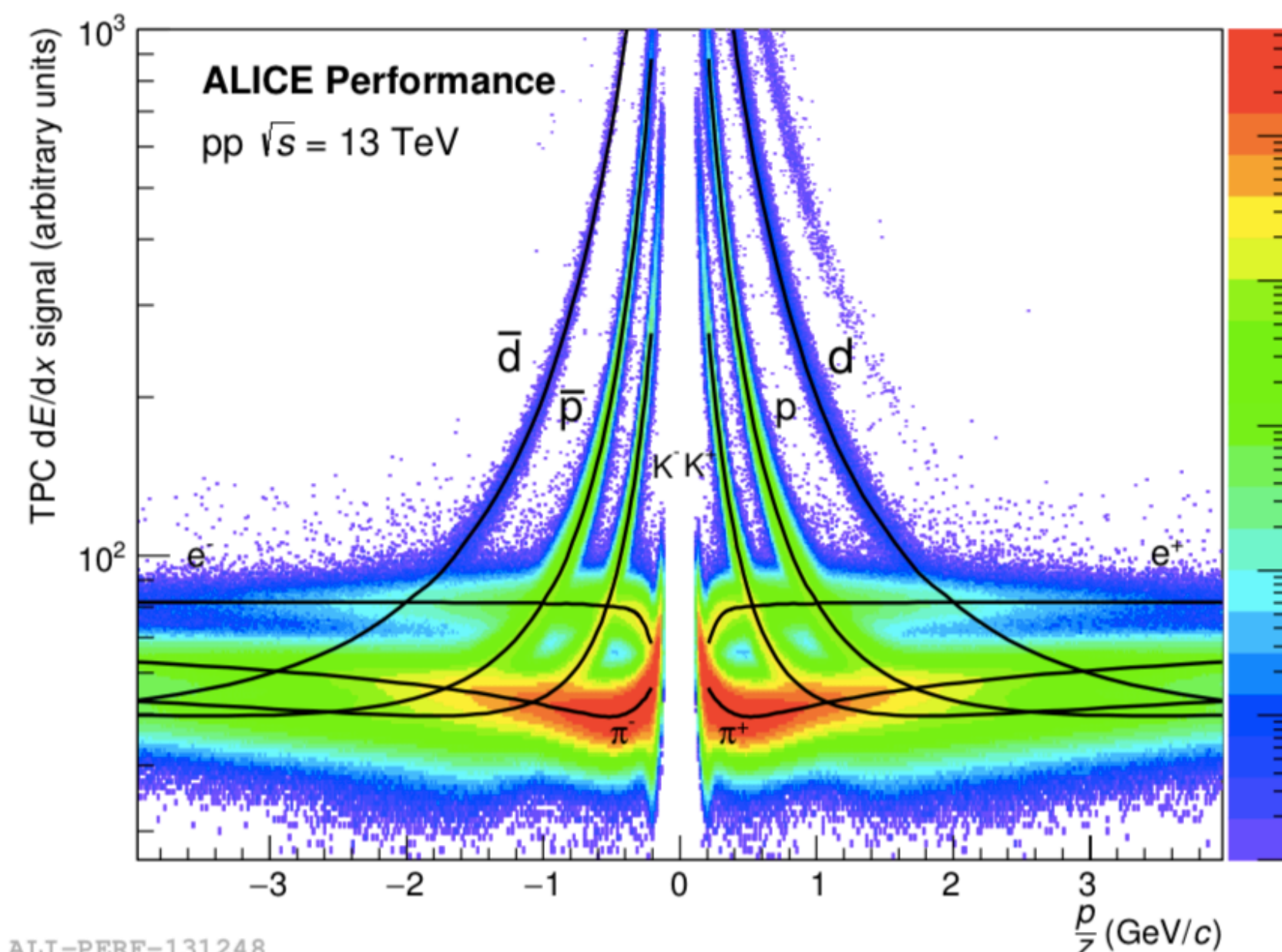
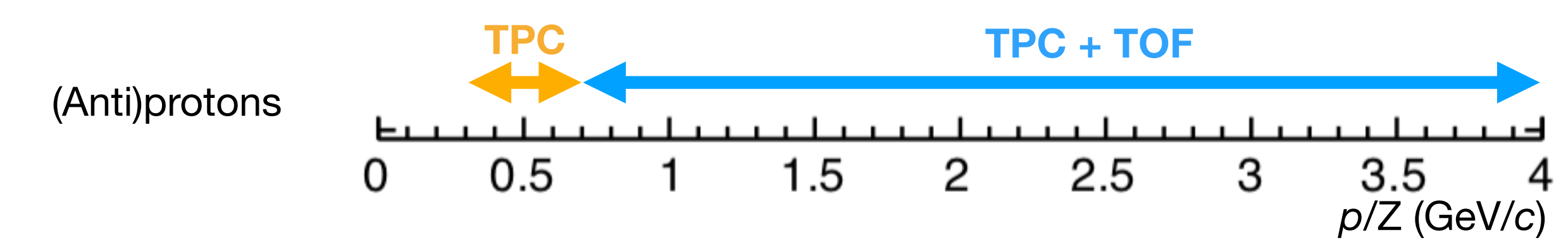
- TPC: dE/dx in gas
- TOF measurement $\beta = \frac{v}{c}$, $p = \gamma\beta mc \rightarrow$ mass



Particle identification in TPC and TOF

Complementary information from TPC and TOF detectors allows to select high purity (anti)particles:

- TPC: dE/dx in gas
- TOF measurement $\beta = \frac{v}{c}$, $p = \gamma\beta mc \rightarrow$ mass

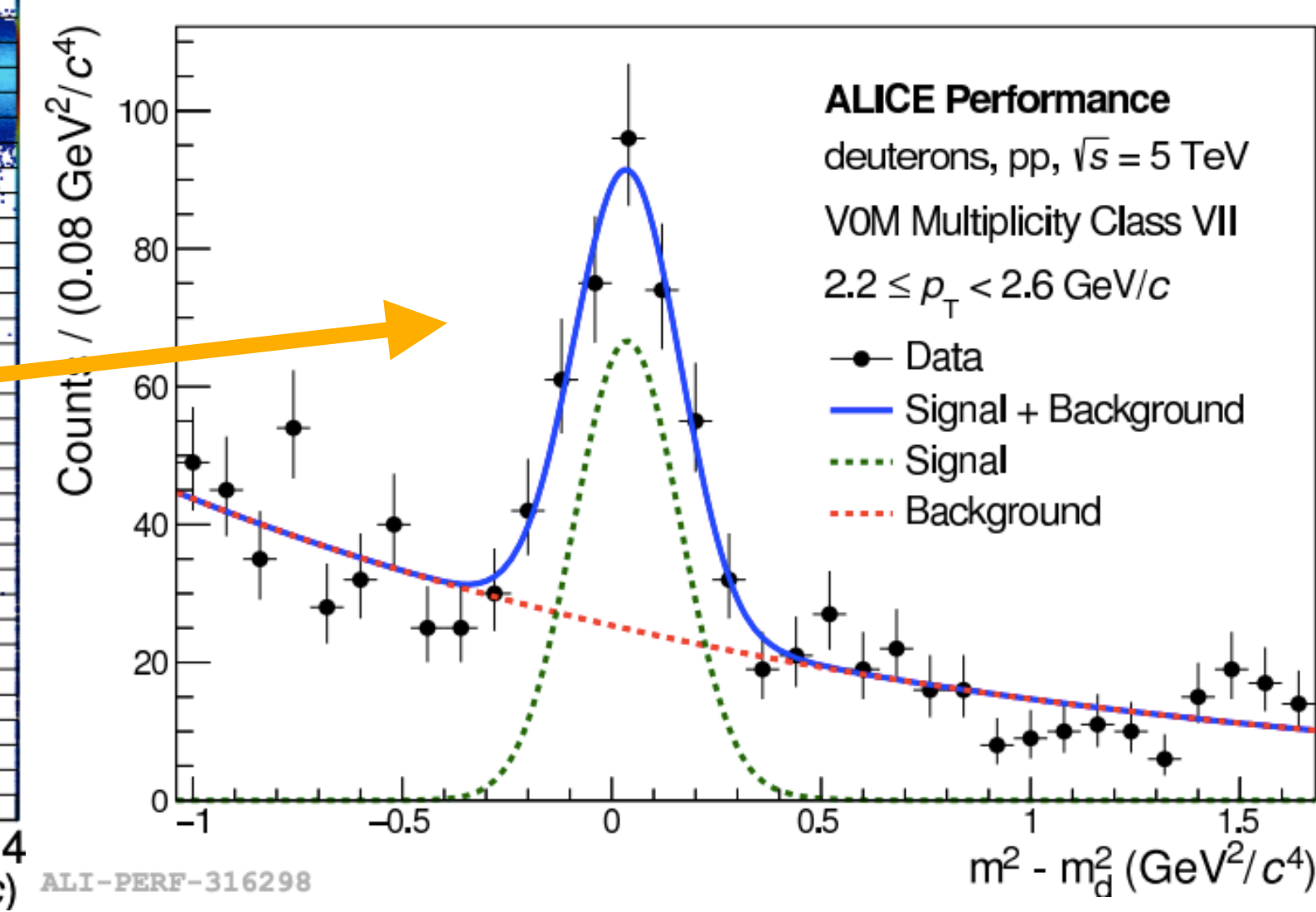
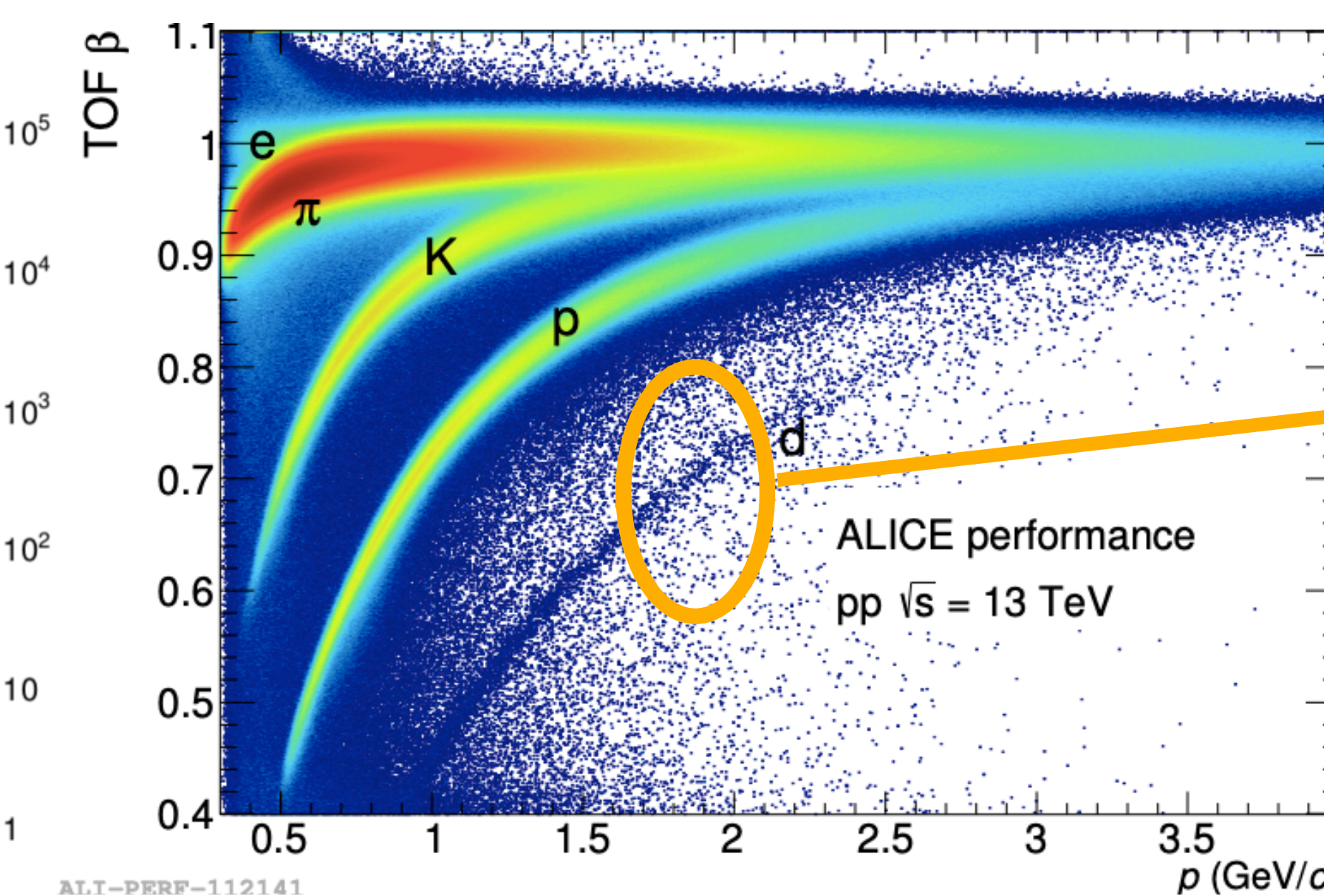
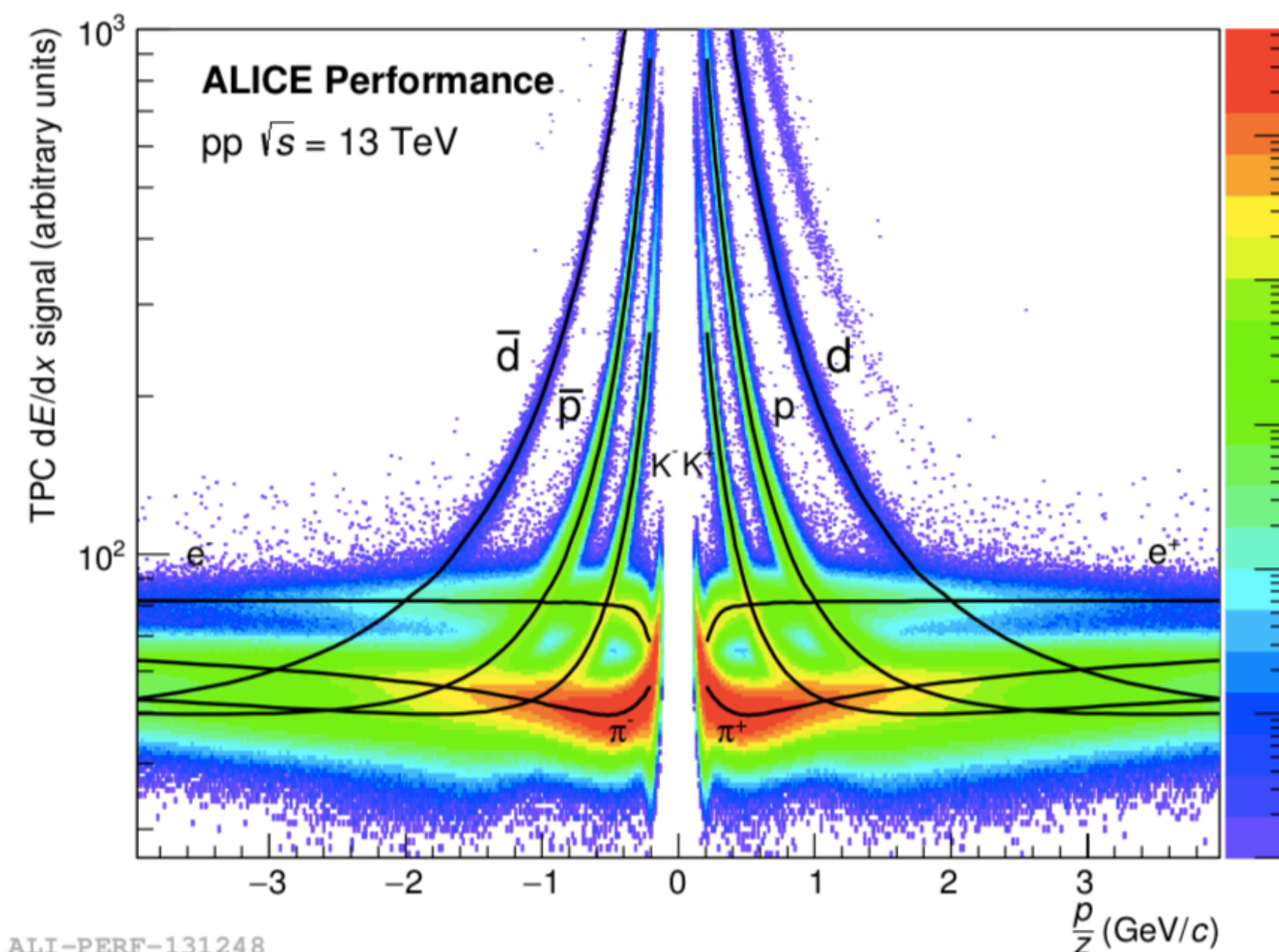
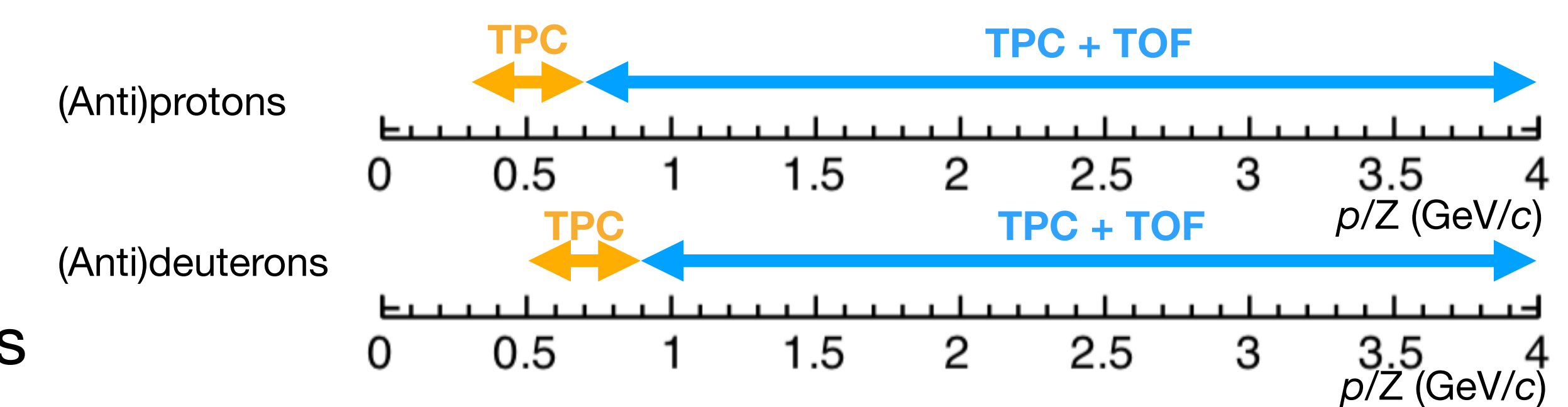


Particle identification in TPC and TOF

Complementary information from TPC and TOF detectors allows to select high purity

(anti)particles:

- TPC: dE/dx in gas
- TOF measurement $\beta = \frac{v}{c}$, $p = \gamma\beta mc \rightarrow$ mass

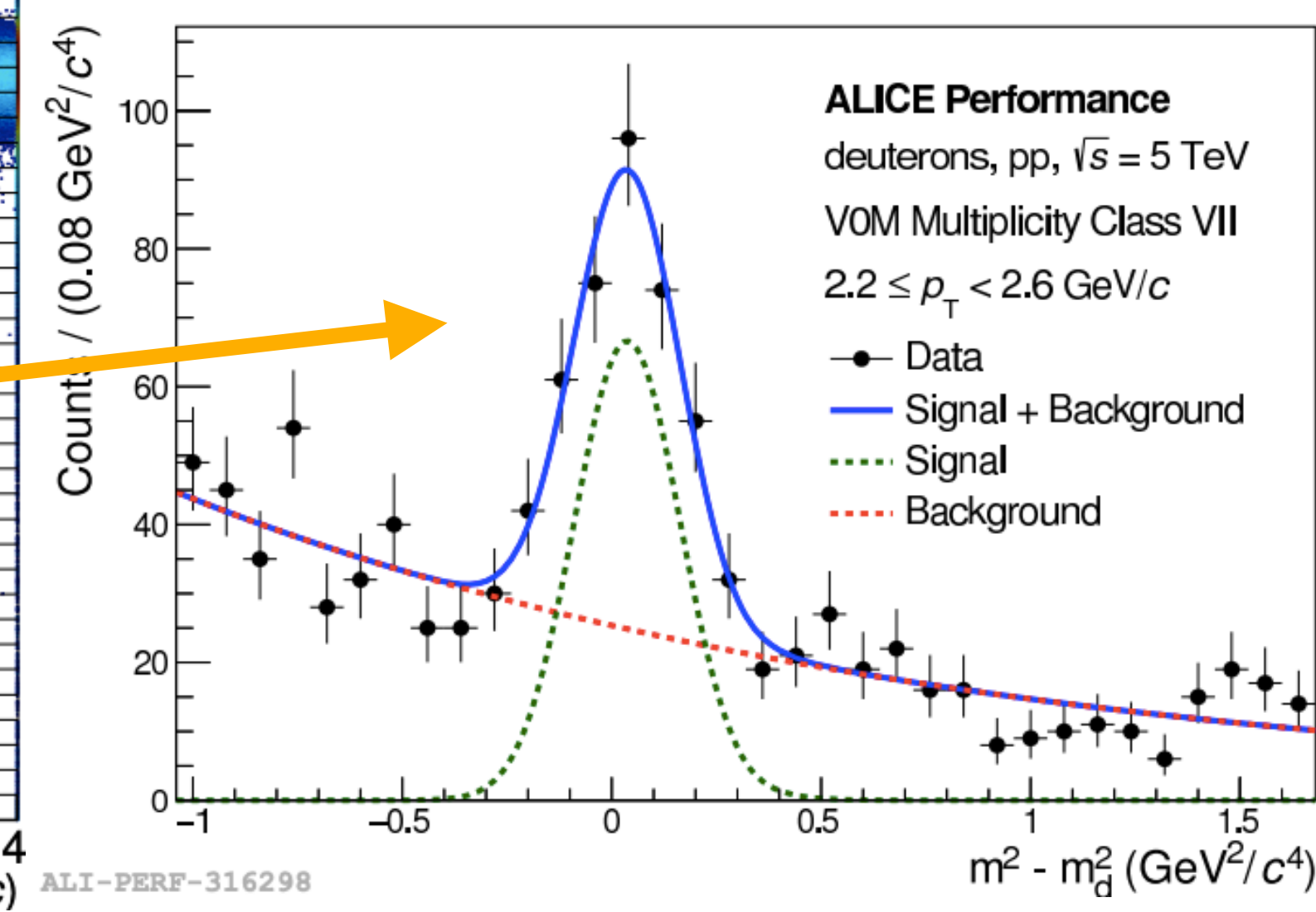
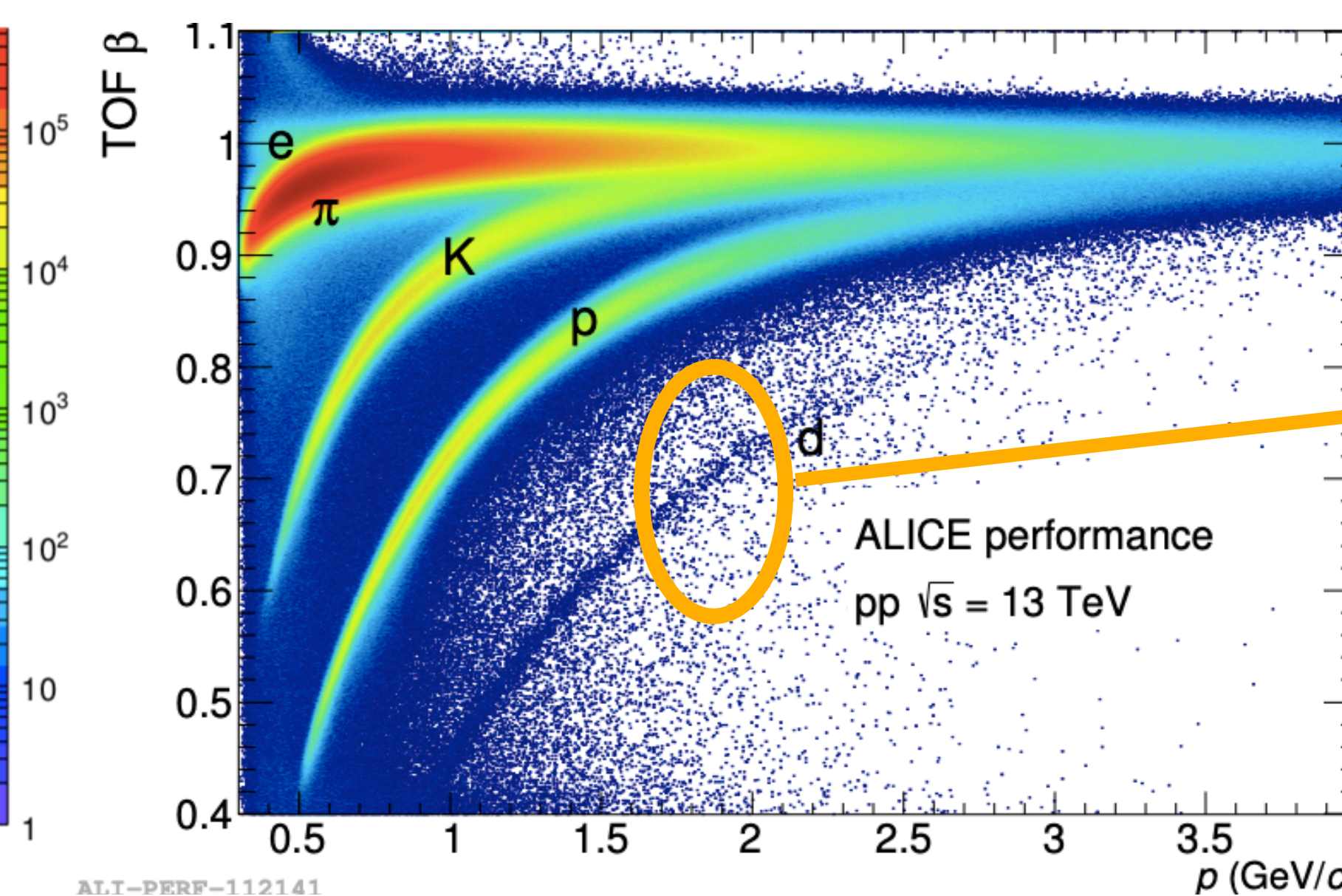
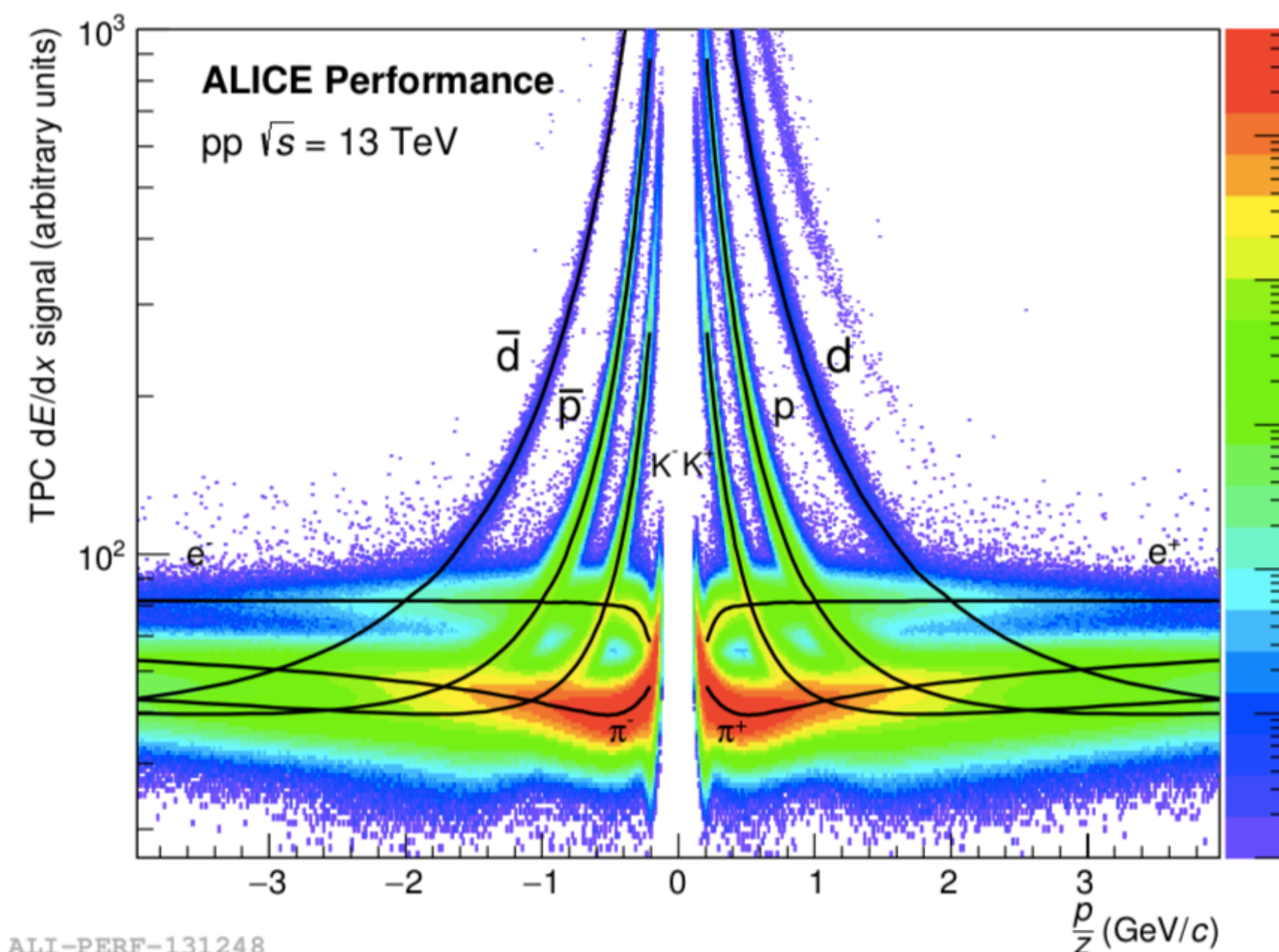
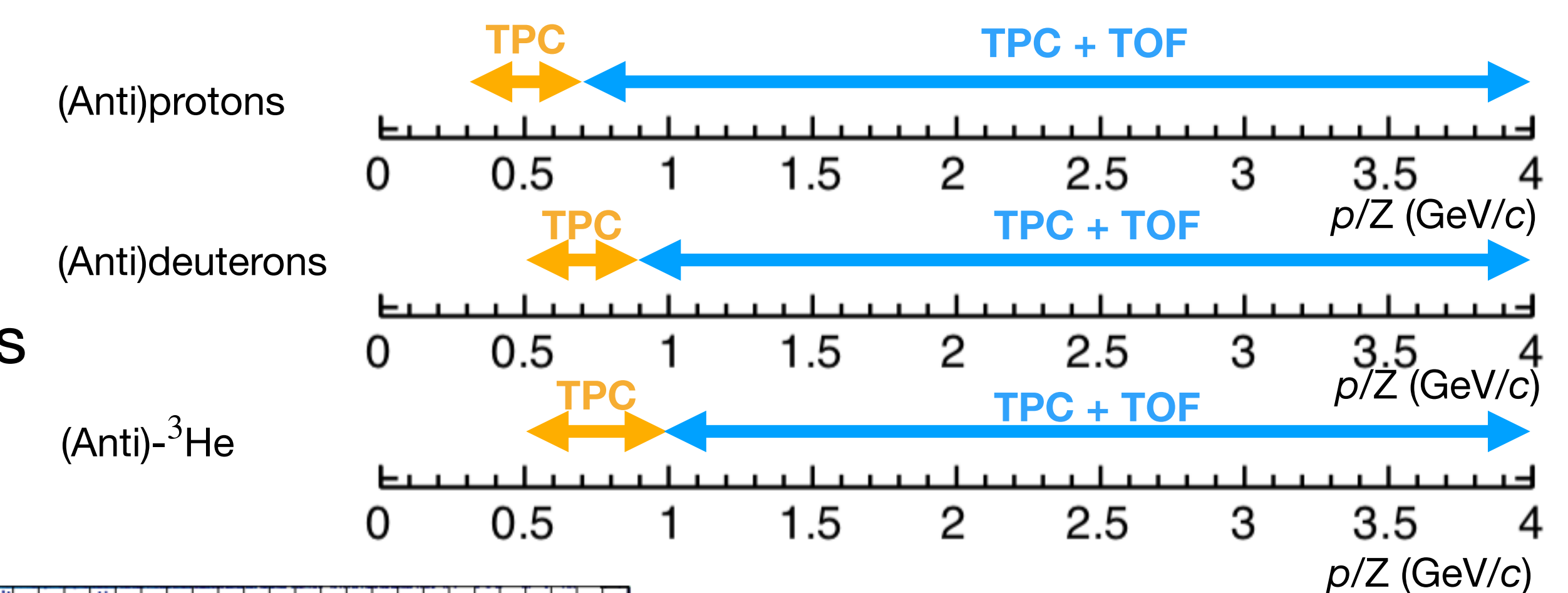


Particle identification in TPC and TOF

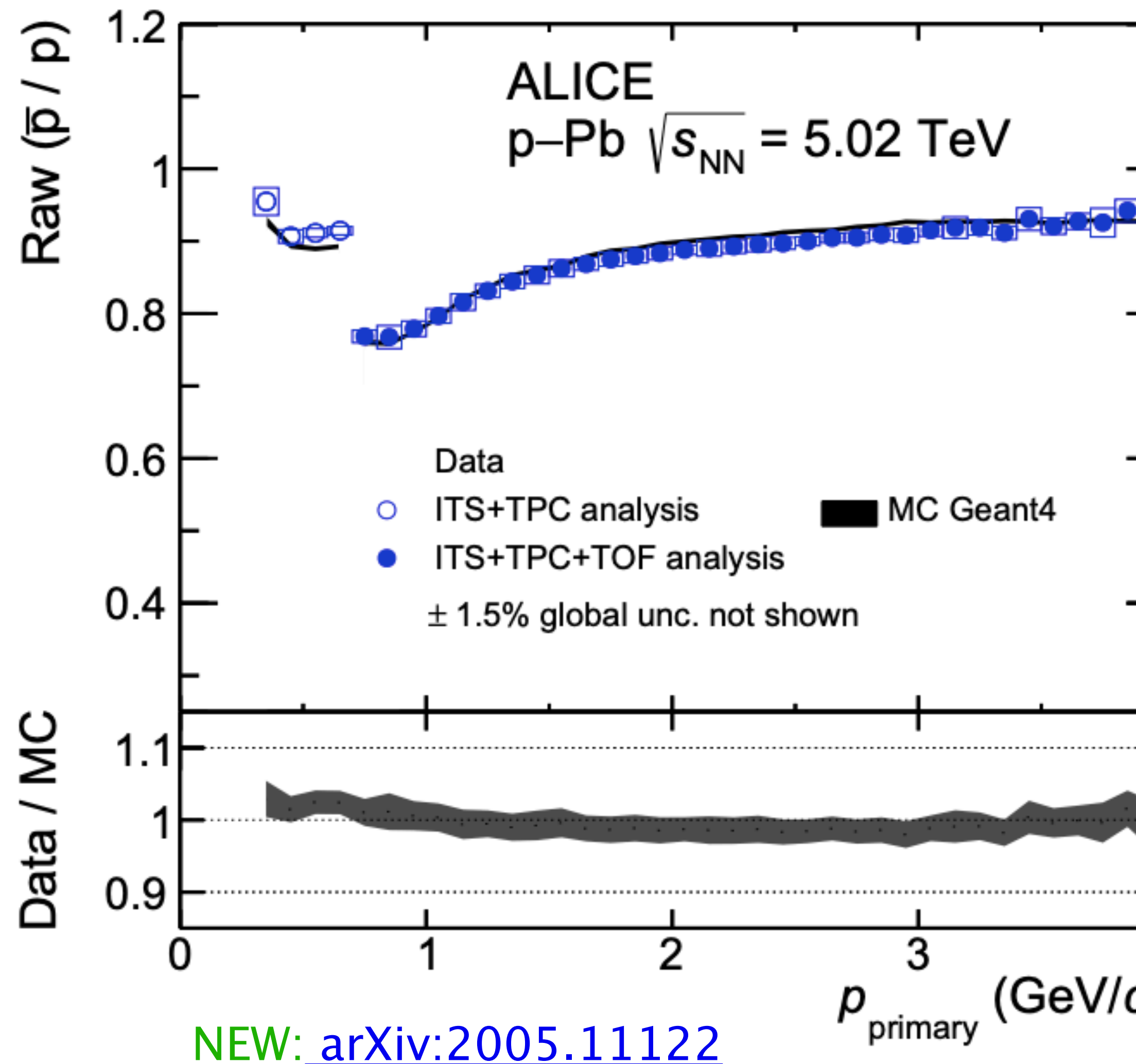
Complementary information from TPC and TOF detectors allows to select high purity

(anti)particles:

- TPC: dE/dx in gas
- TOF measurement $\beta = \frac{v}{c}$, $p = \gamma\beta mc \rightarrow$ mass

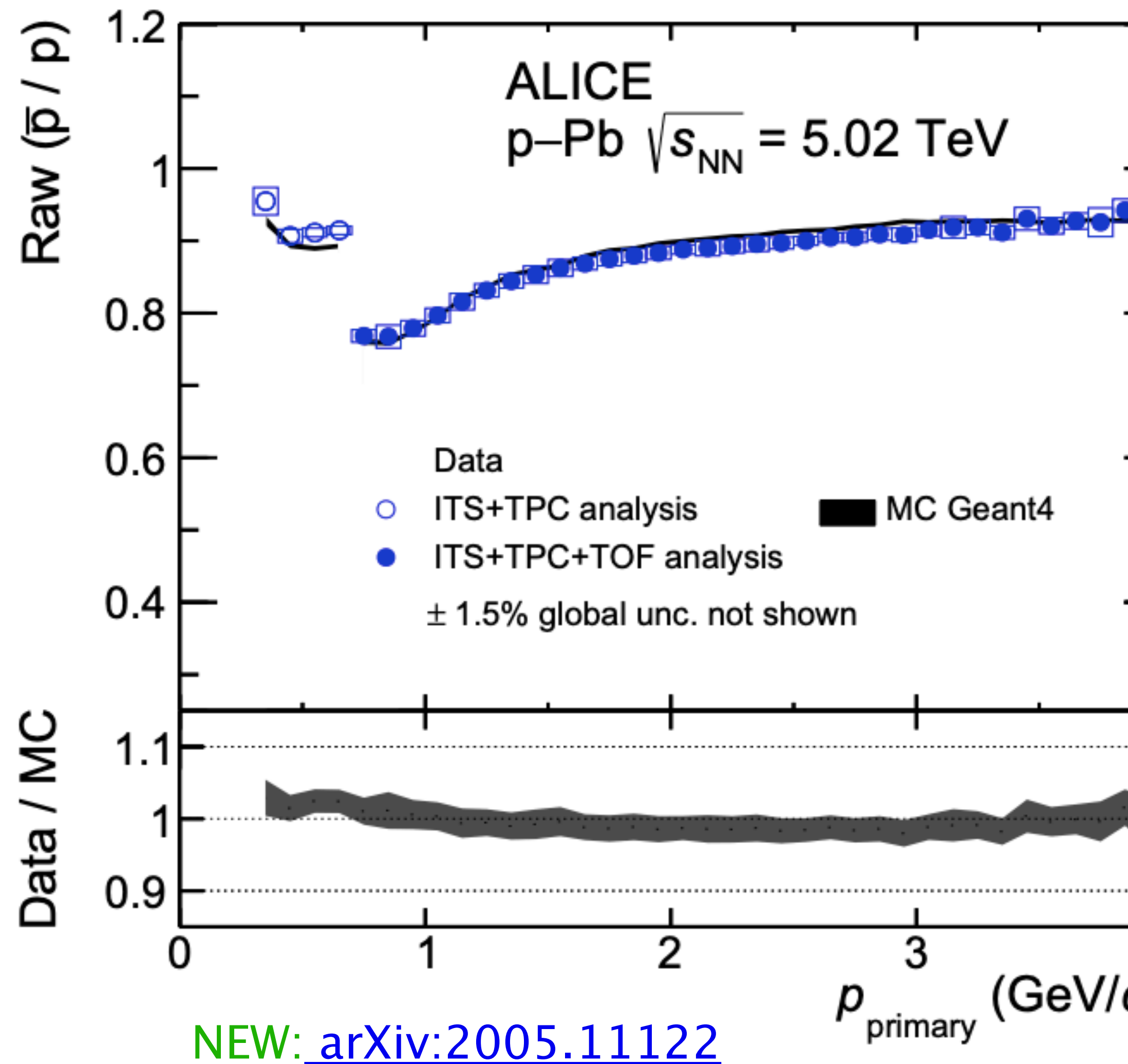


Raw primary antiproton-to-proton ratio



Raw primary \bar{p}/p ratio:

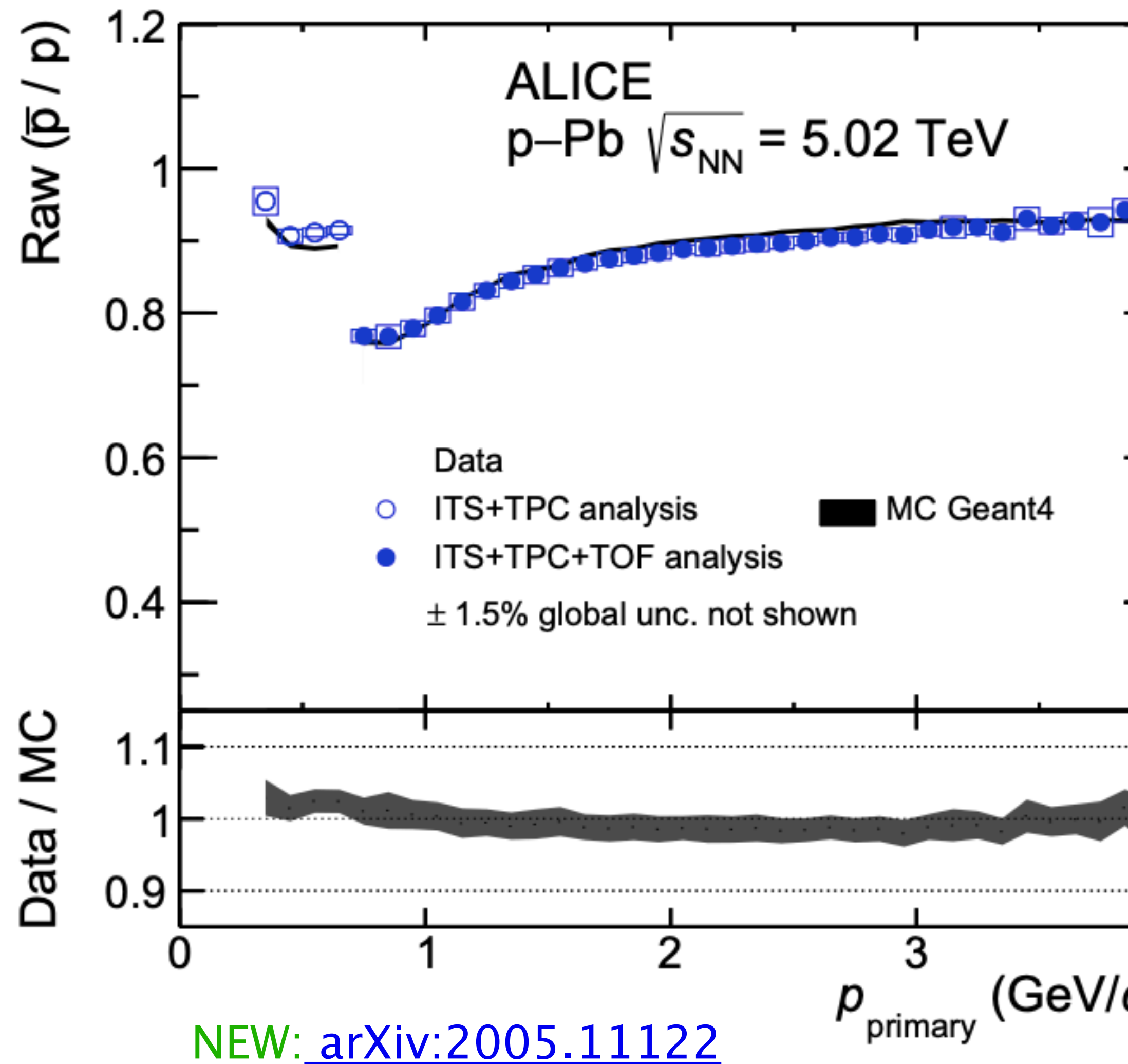
Raw primary antiproton-to-proton ratio



Raw primary \bar{p}/p ratio:

- Higher loss of antiprotons in detector material

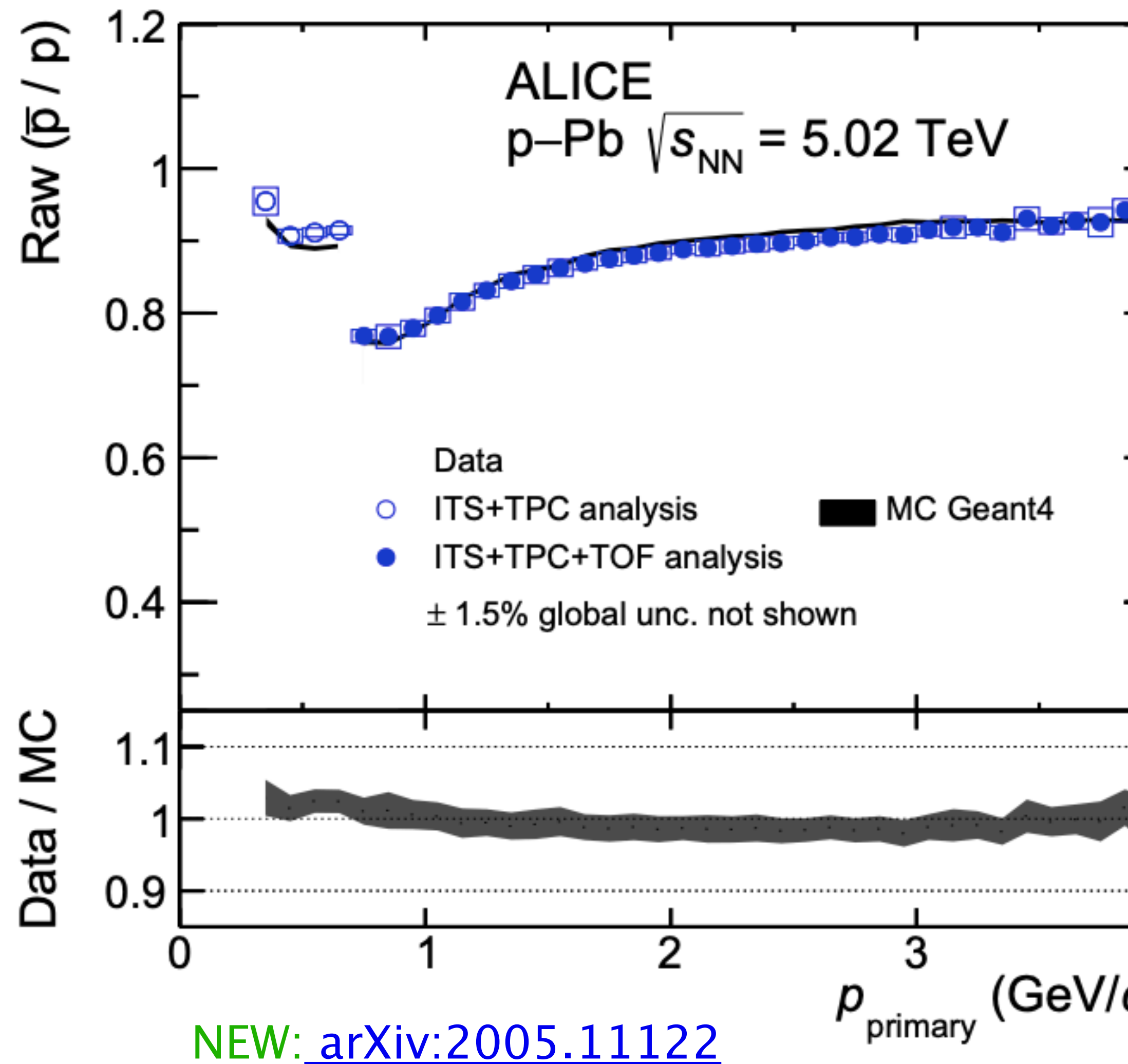
Raw primary antiproton-to-proton ratio



Raw primary \bar{p}/p ratio:

- Higher loss of antiprotons in detector material
- Step at 0.7 GeV/c due to additional detector material

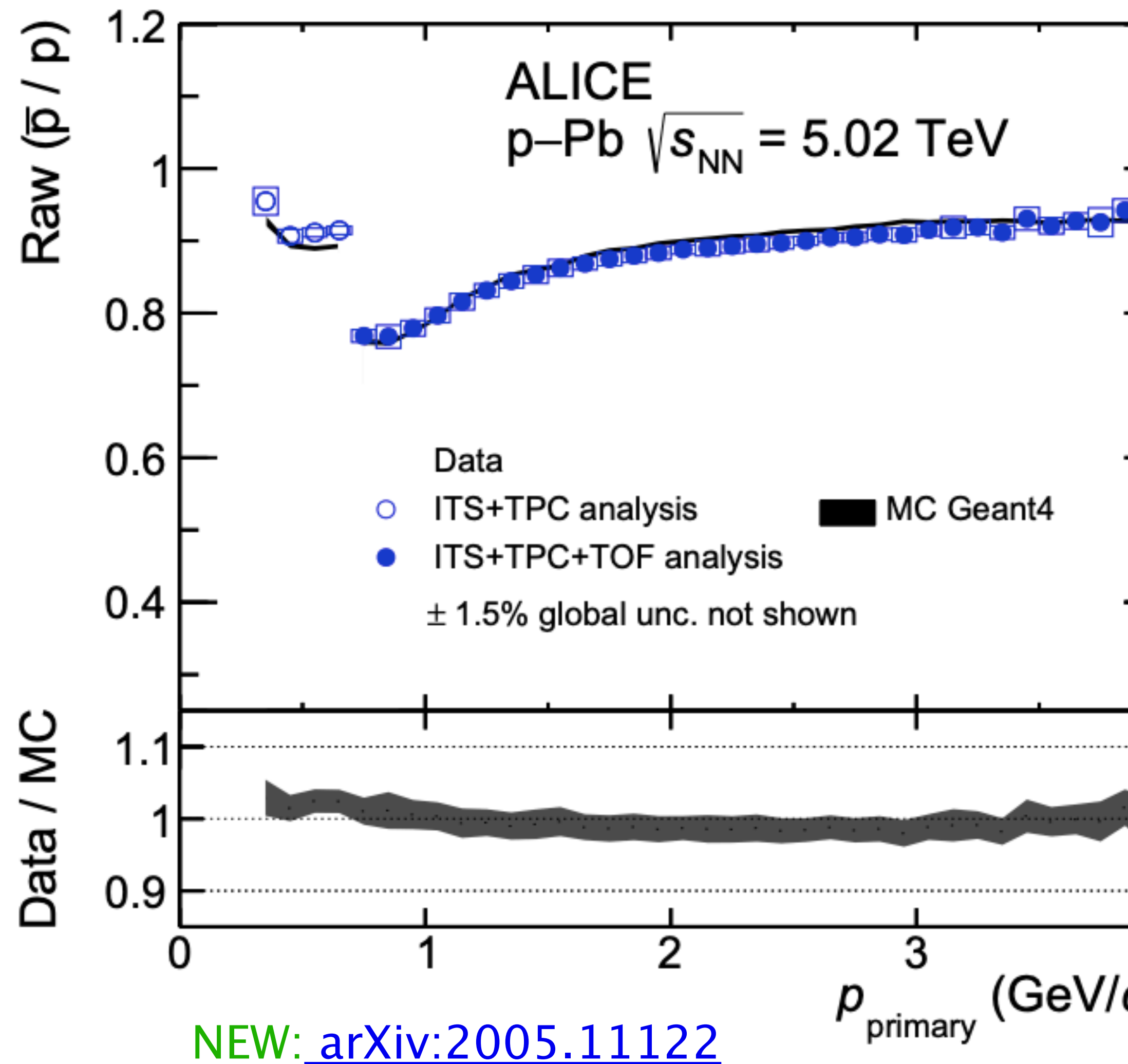
Raw primary antiproton-to-proton ratio



Raw primary \bar{p}/p ratio:

- Higher loss of antiprotons in detector material
- Step at 0.7 GeV/c due to additional detector material

Raw primary antiproton-to-proton ratio

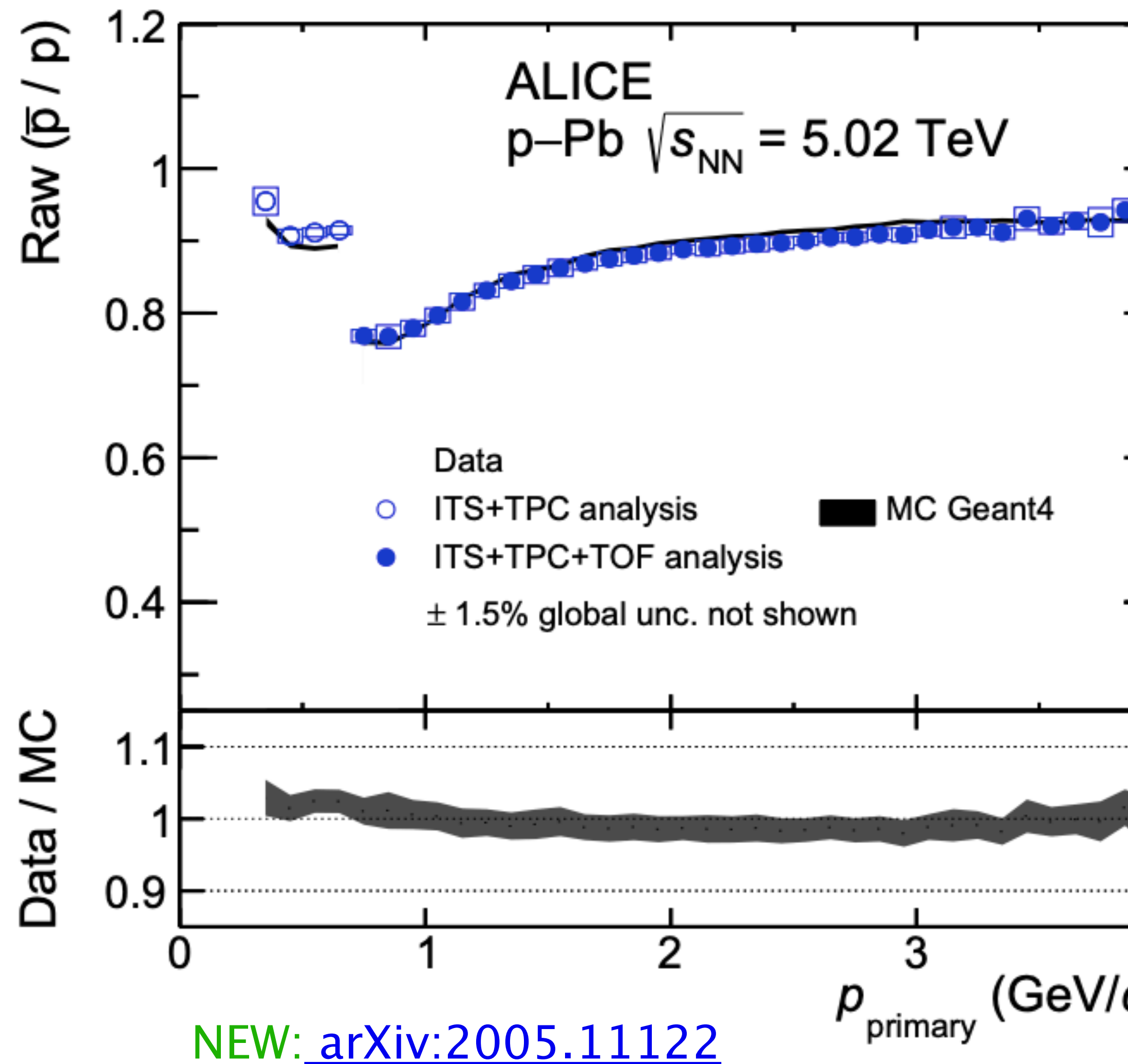


Raw primary \bar{p}/p ratio:

- Higher loss of antiprotons in detector material
- Step at 0.7 GeV/c due to additional detector material

Monte Carlo simulation:

Raw primary antiproton-to-proton ratio



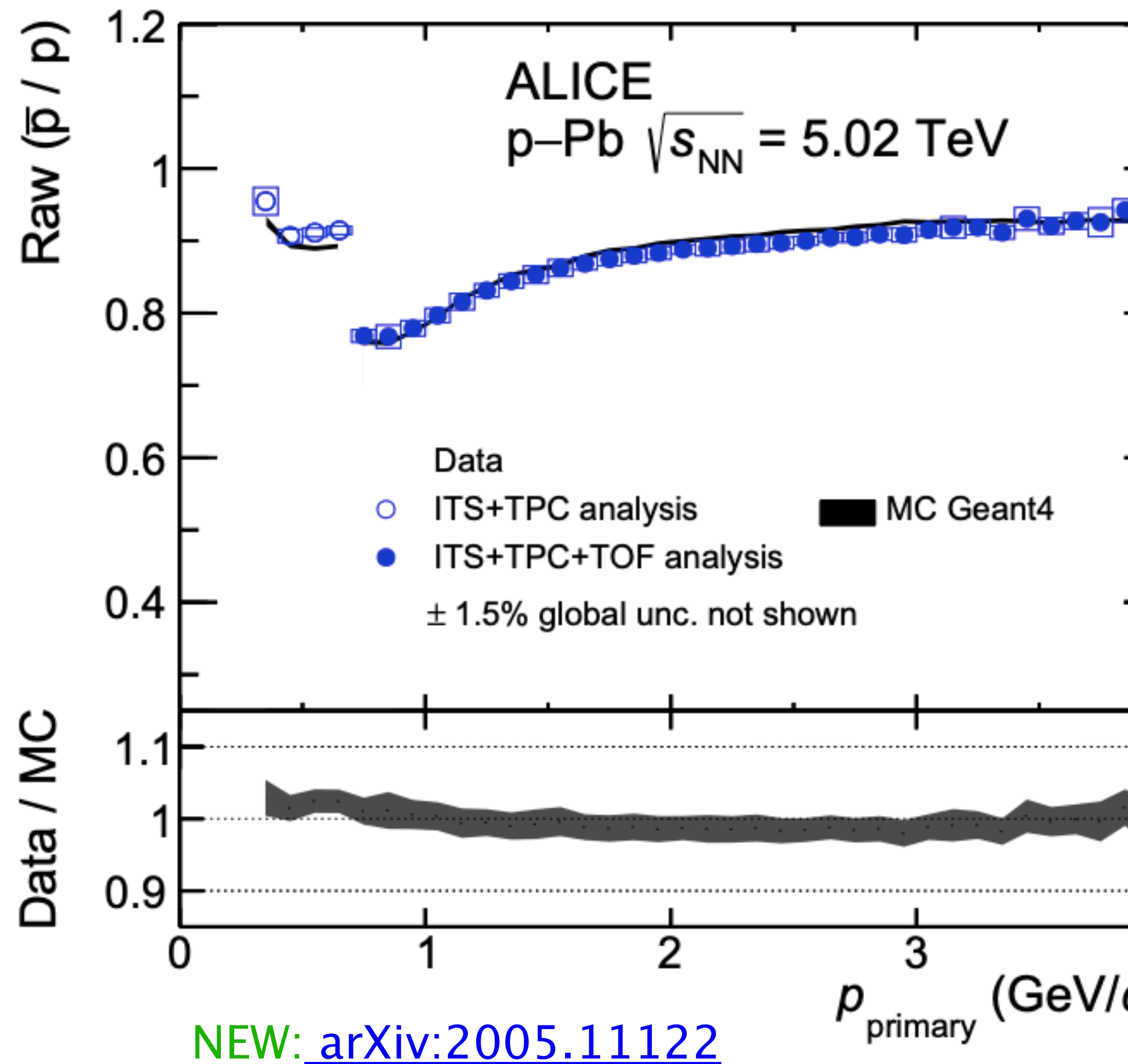
Raw primary \bar{p}/p ratio:

- Higher loss of antiprotons in detector material
- Step at $0.7 \text{ GeV}/c$ due to additional detector material

Monte Carlo simulation:

- Detailed simulations of the ALICE detector performance

Raw primary antiproton-to-proton ratio



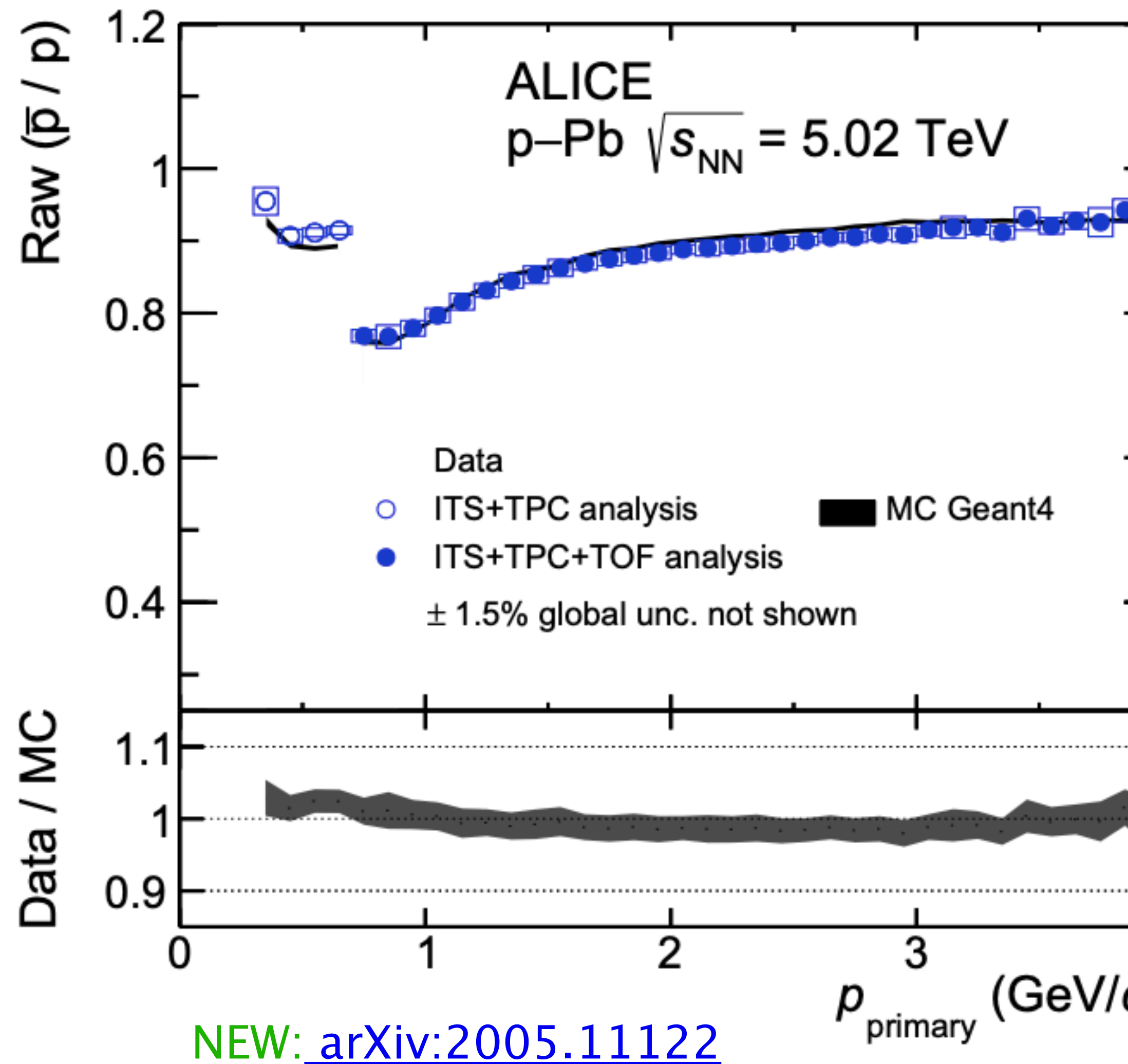
Raw primary \bar{p}/p ratio:

- Higher loss of antiprotons in detector material
- Step at 0.7 GeV/c due to additional detector material

Monte Carlo simulation:

- Detailed simulations of the ALICE detector performance
- Propagation with Geant4

Raw primary antiproton-to-proton ratio



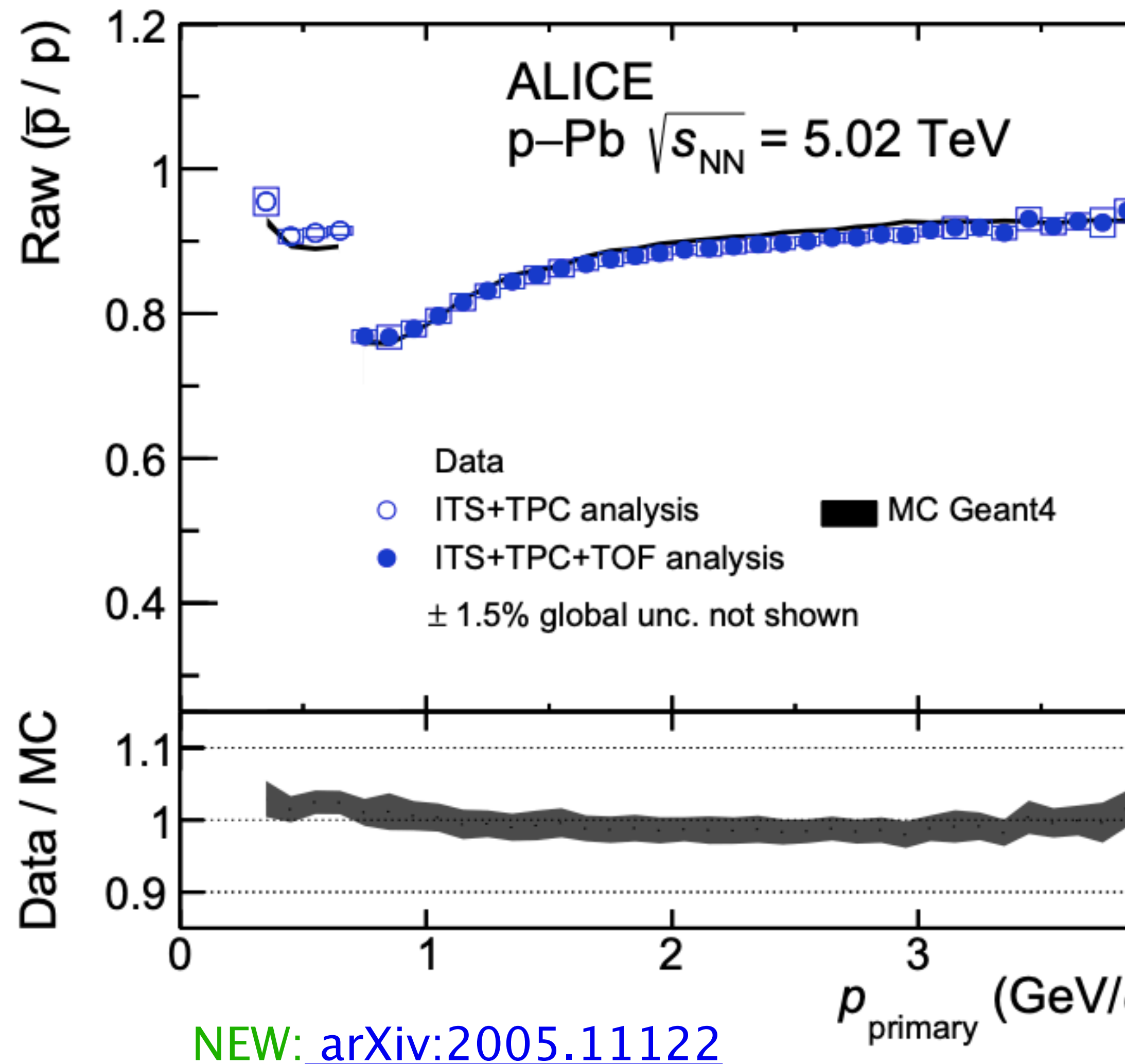
Raw primary \bar{p}/p ratio:

- Higher loss of antiprotons in detector material
- Step at 0.7 GeV/c due to additional detector material

Monte Carlo simulation:

- Detailed simulations of the ALICE detector performance
- Propagation with Geant4

Raw primary antiproton-to-proton ratio



Raw primary \bar{p}/p ratio:

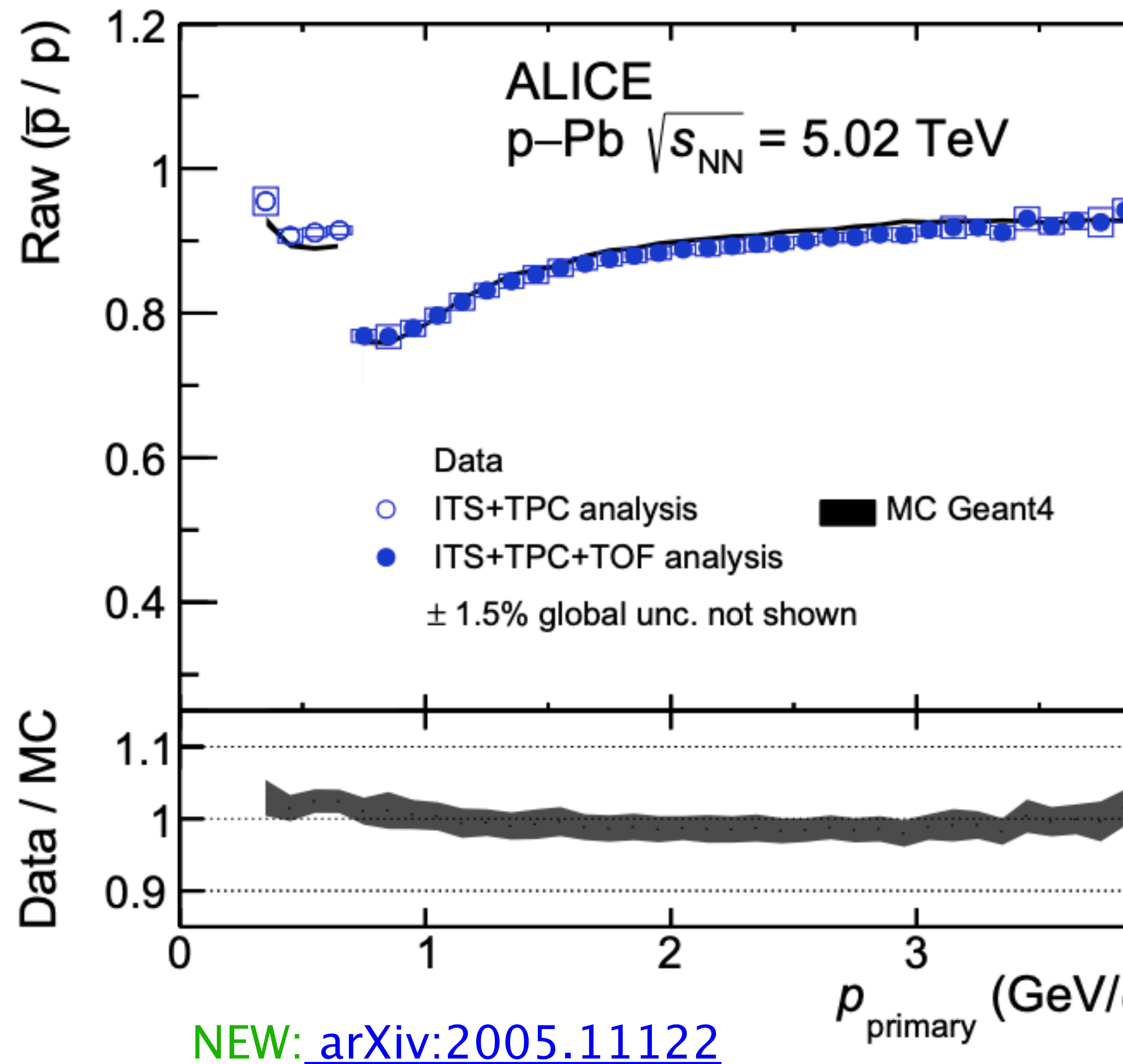
- Higher loss of antiprotons in detector material
- Step at 0.7 GeV/c due to additional detector material

Monte Carlo simulation:

- Detailed simulations of the ALICE detector performance
- Propagation with Geant4

Vary $\sigma_{\text{inel}}(\bar{p})$ in Geant4 based simulations until MC ratio is $\pm 1\sigma$ and $\pm 2\sigma$ away from experimental ratio -> measurement of $\sigma_{\text{inel}}(\bar{p})$

Raw primary antiproton-to-proton ratio



Raw primary \bar{p}/p ratio:

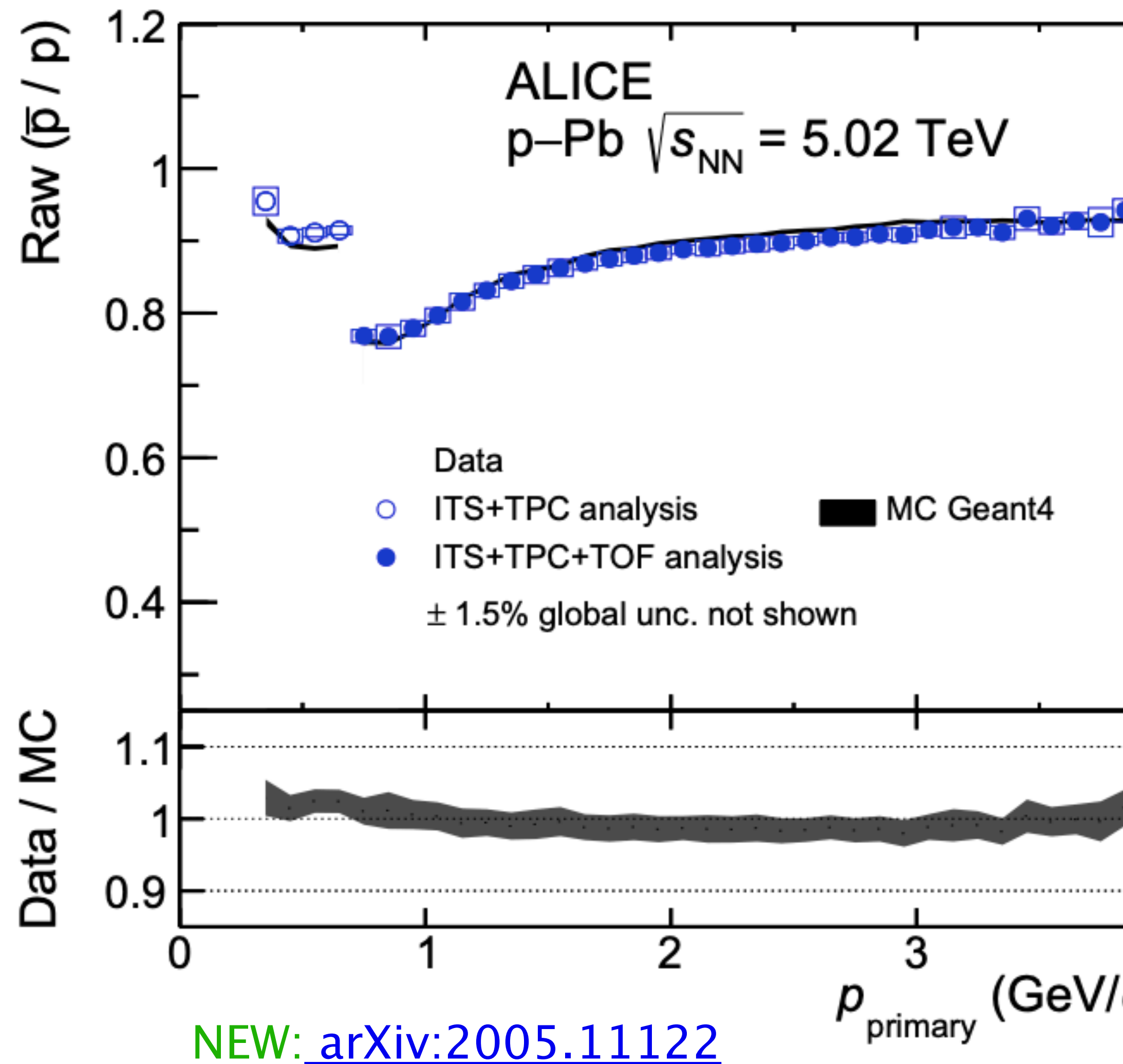
- Higher loss of antiprotons in detector material
- Step at 0.7 GeV/c due to additional detector material

Monte Carlo simulation:

- Detailed simulations of the ALICE detector performance
- Propagation with Geant4

Vary $\sigma_{\text{inel}}(\bar{p})$ in Geant4 based simulations until MC ratio is $\pm 1\sigma$ and $\pm 2\sigma$ away from experimental ratio -> measurement of $\sigma_{\text{inel}}(\bar{p})$

Raw primary antiproton-to-proton ratio



Raw primary \bar{p}/p ratio:

- Higher loss of antiprotons in detector material
- Step at 0.7 GeV/c due to additional detector material

Monte Carlo simulation:

- Detailed simulations of the ALICE detector performance
- Propagation with Geant4

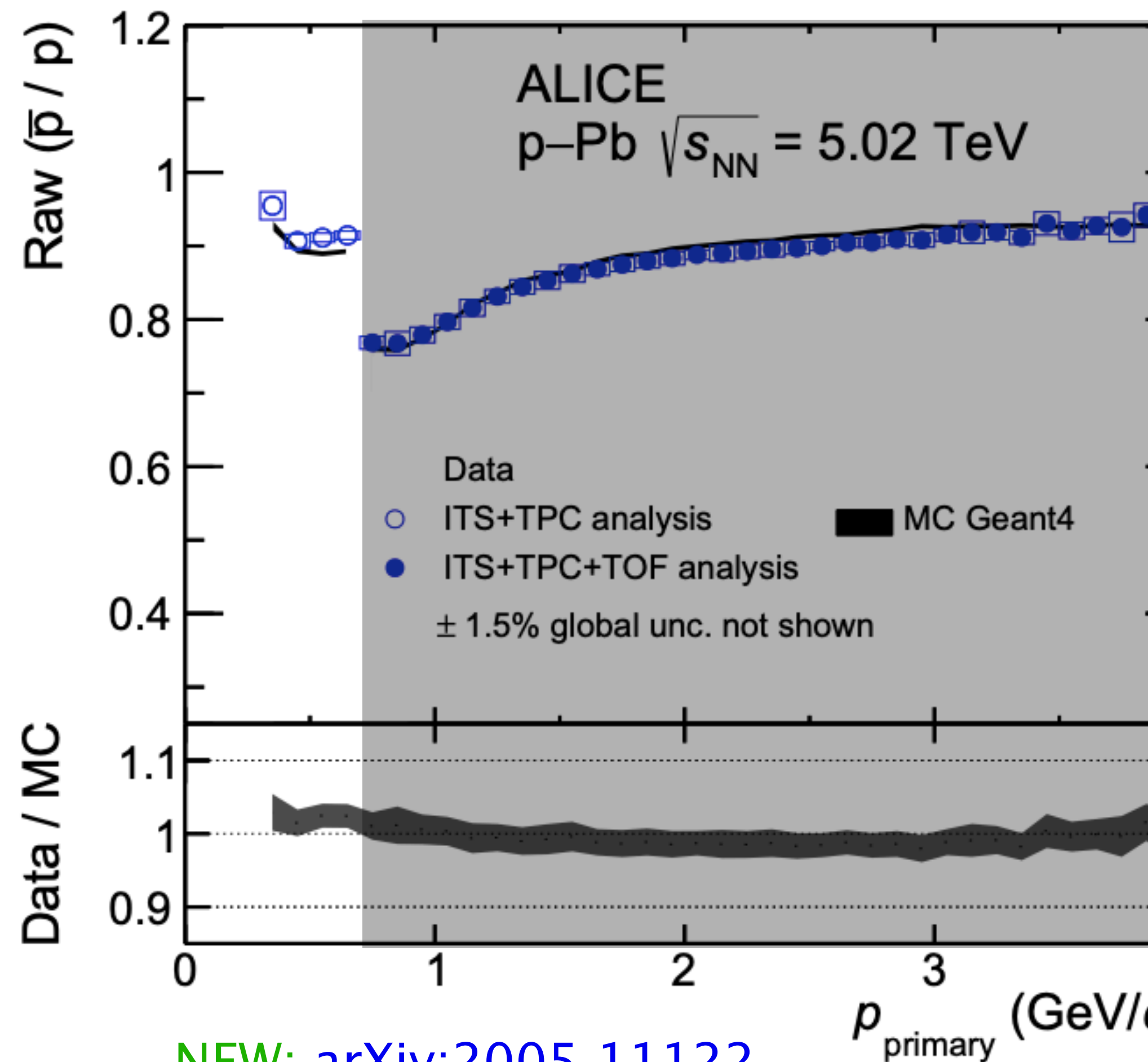
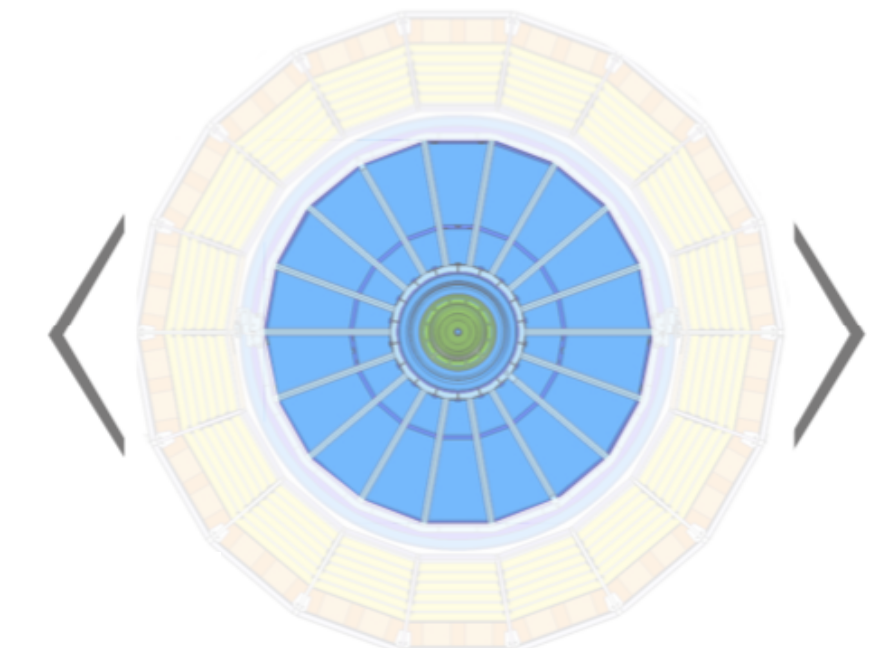
Vary $\sigma_{\text{inel}}(\bar{p})$ in Geant4 based simulations until MC ratio is $\pm 1\sigma$ and $\pm 2\sigma$ away from experimental ratio -> measurement of $\sigma_{\text{inel}}(\bar{p})$

→ Agreement with of the antiproton cross section obtained confirms the correctness of the procedure.

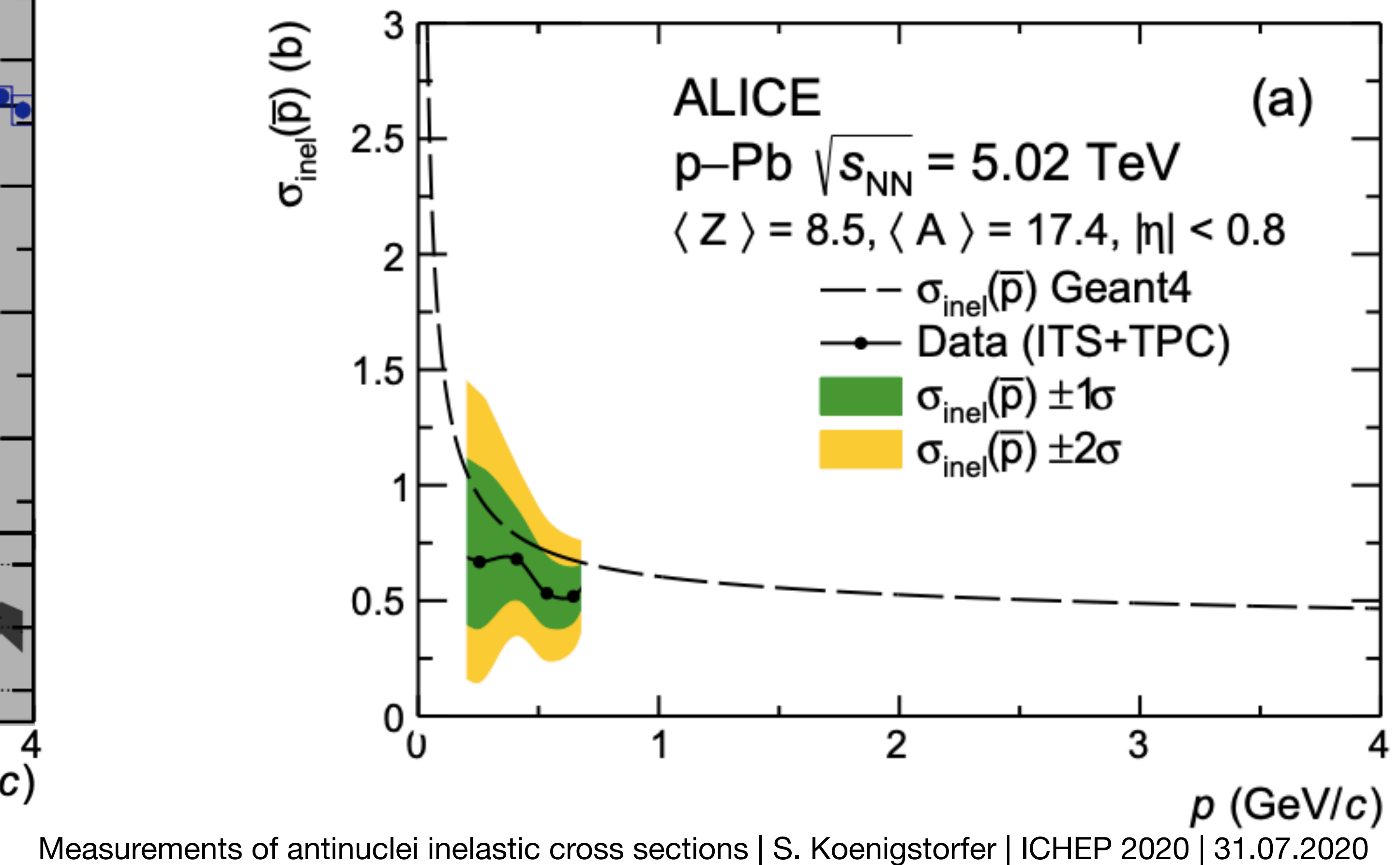
Antiproton inelastic cross section

$\sigma_{\text{inel}}(\bar{p})$ on average ALICE detector material.

Good agreement with Geant4 parameterization as expected.



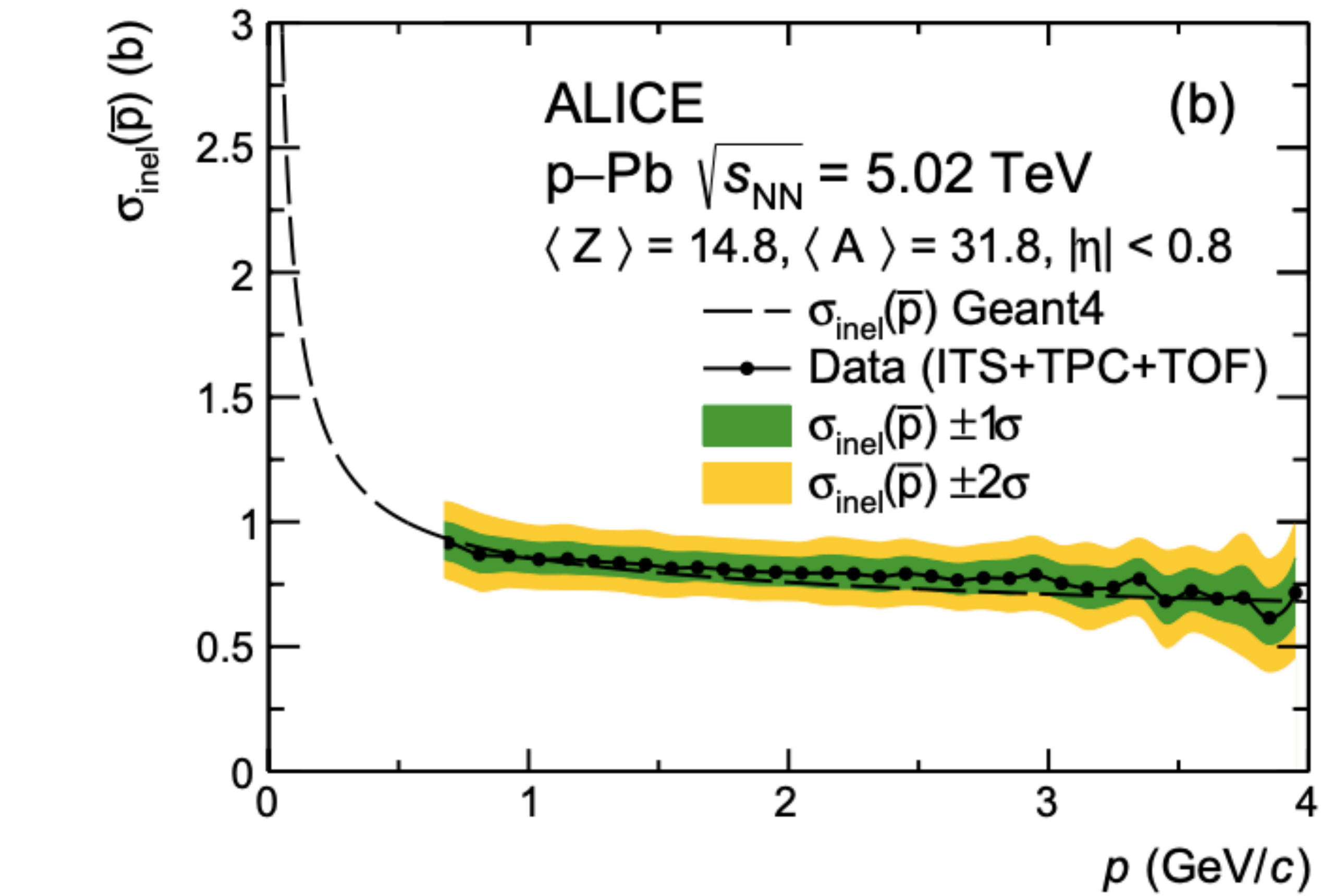
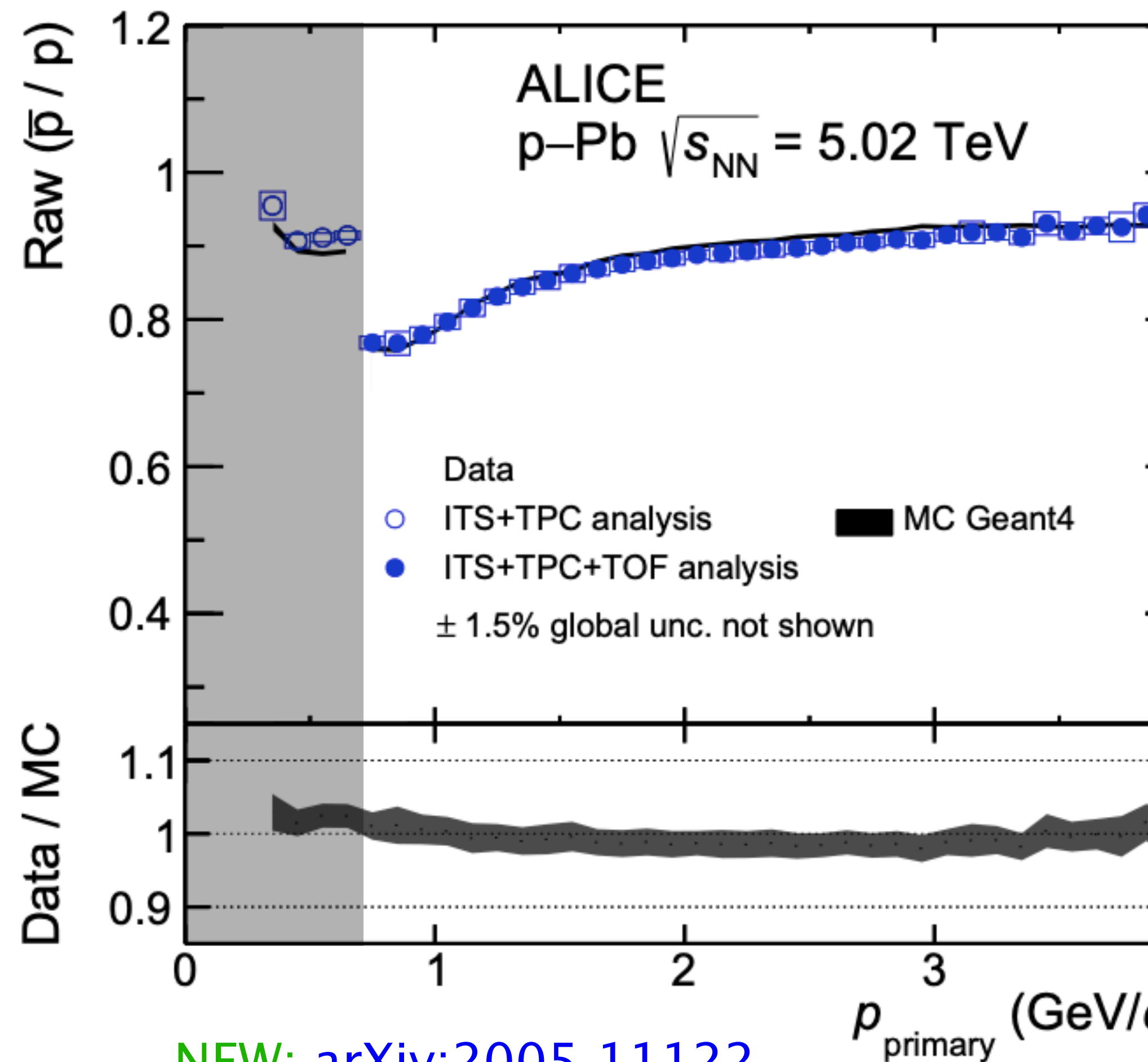
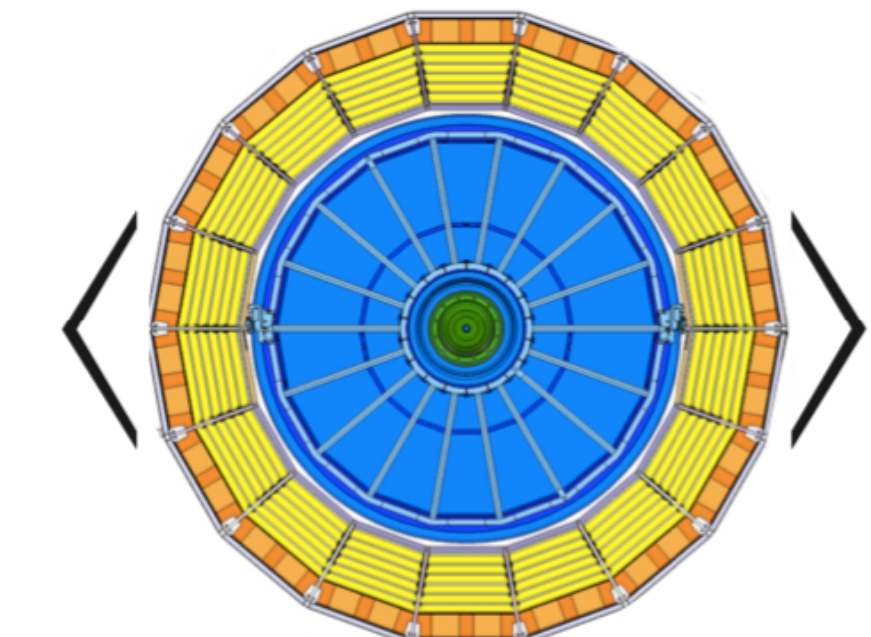
NEW: [arXiv:2005.11122](https://arxiv.org/abs/2005.11122)



Antiproton inelastic cross section

$\sigma_{\text{inel}}(\bar{p})$ on average ALICE detector material.

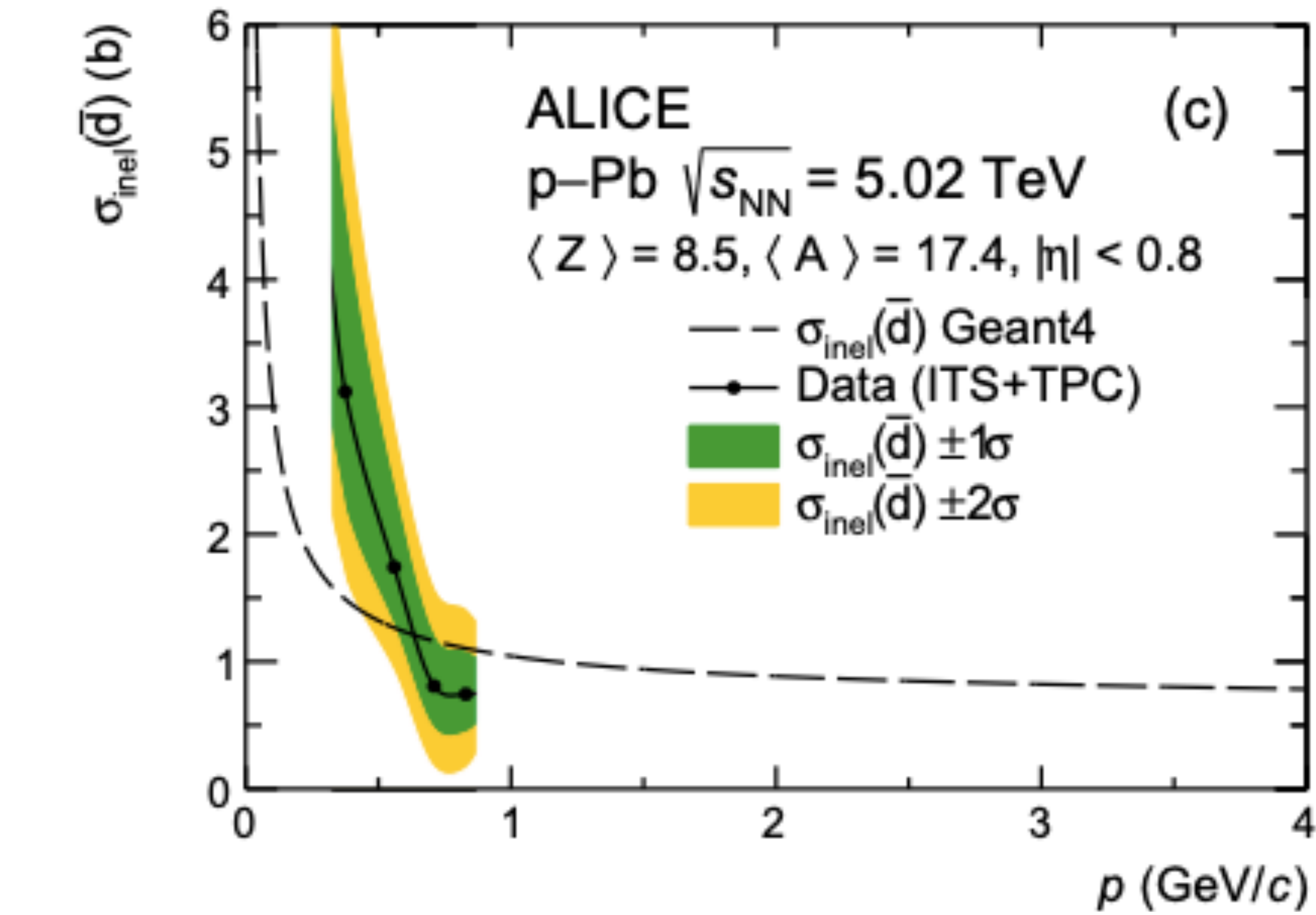
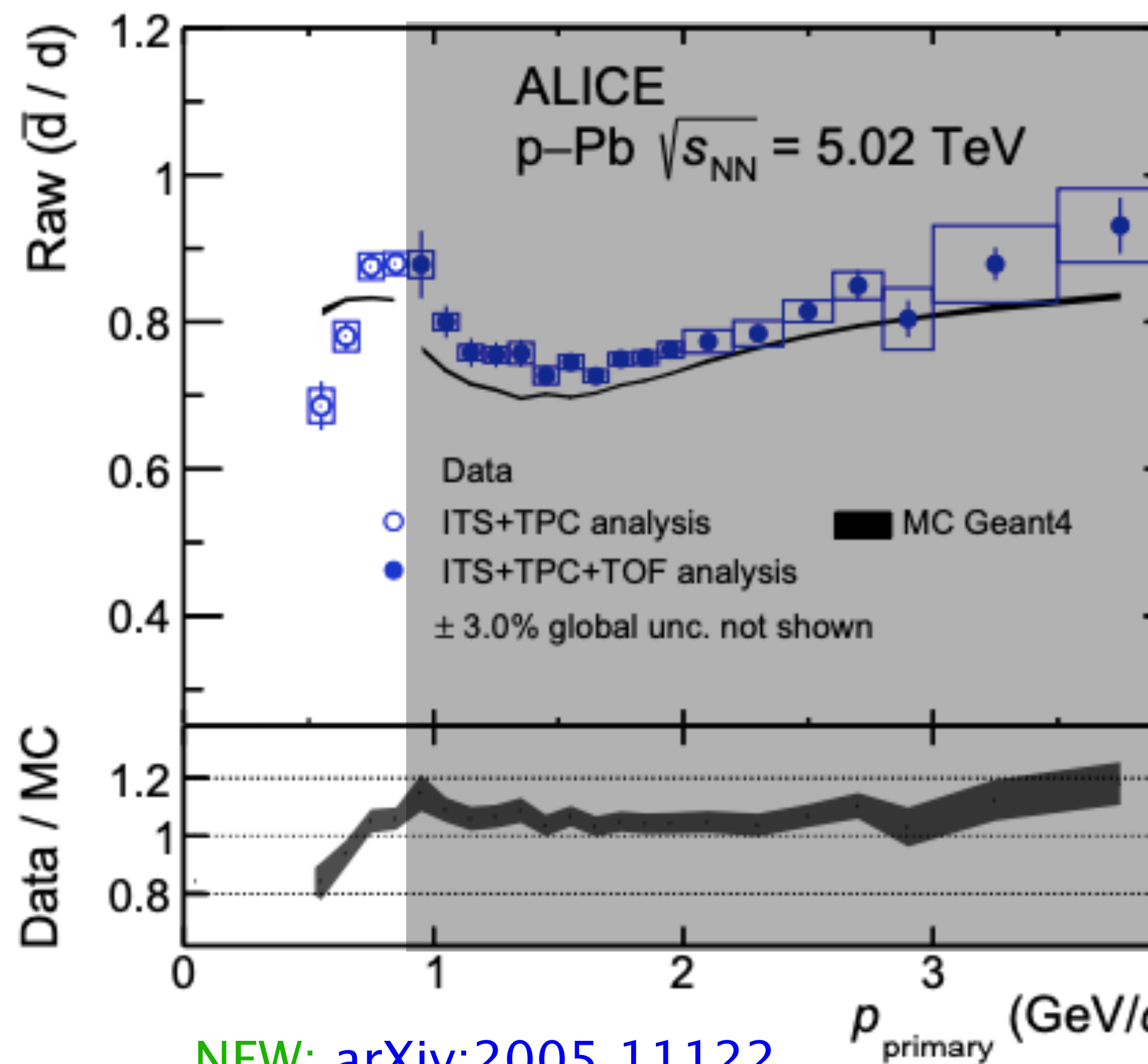
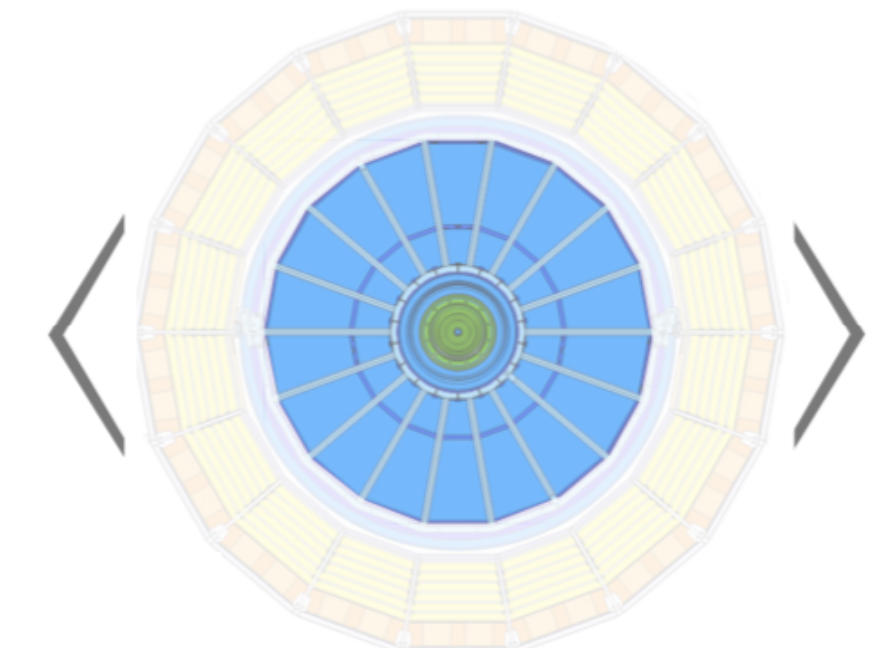
Good agreement with Geant4 parameterization as expected.



NEW: [arXiv:2005.11122](https://arxiv.org/abs/2005.11122)

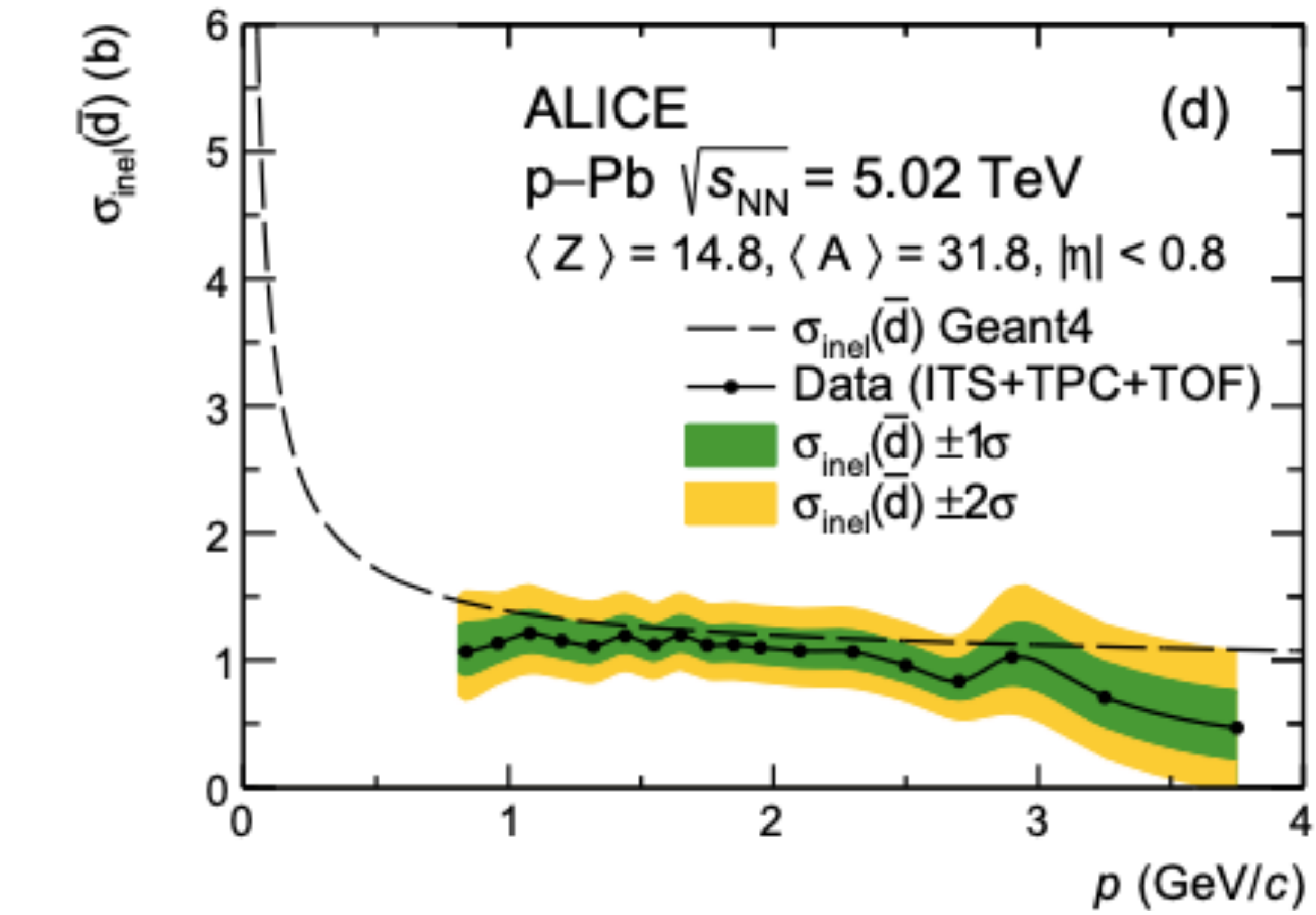
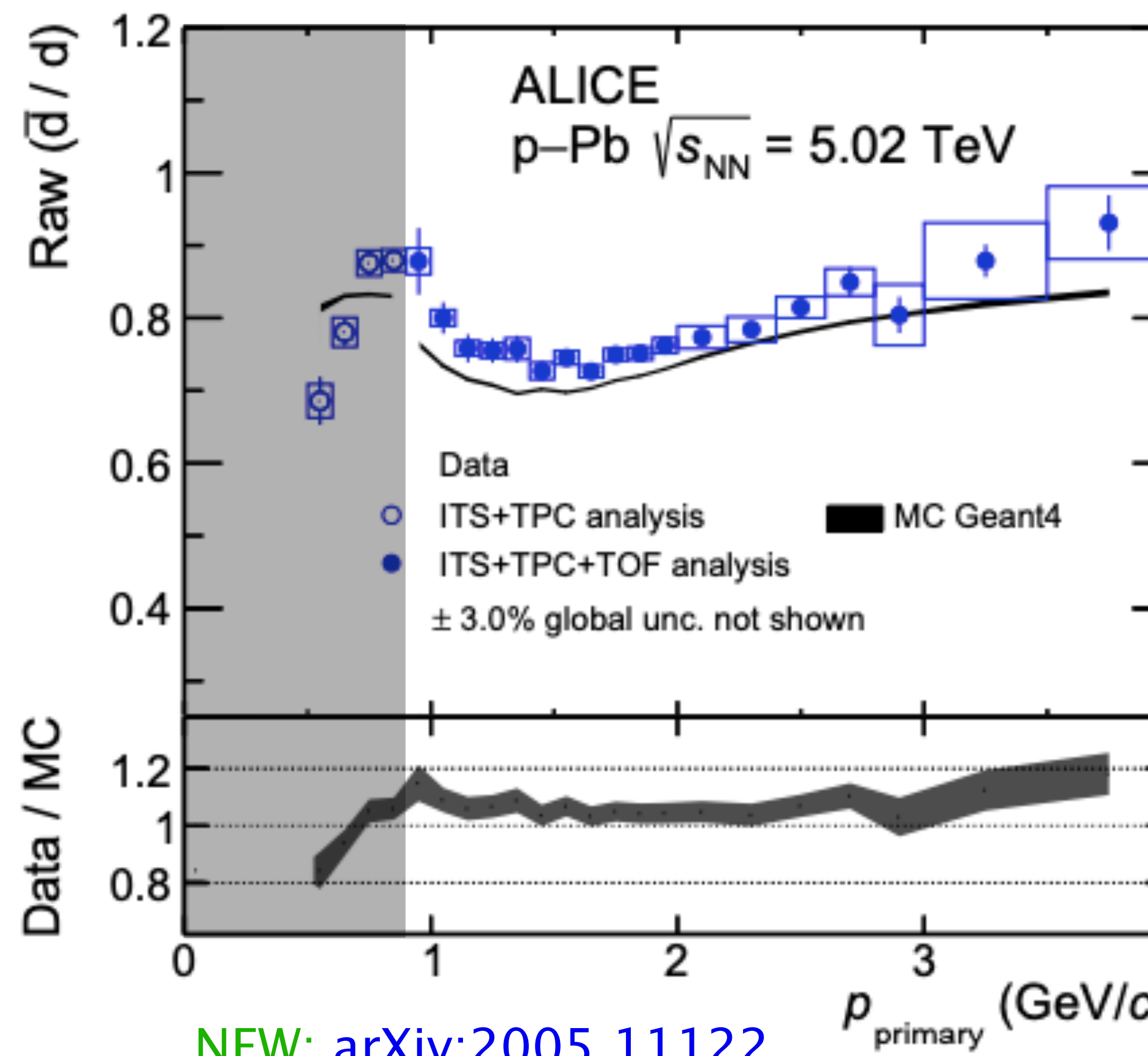
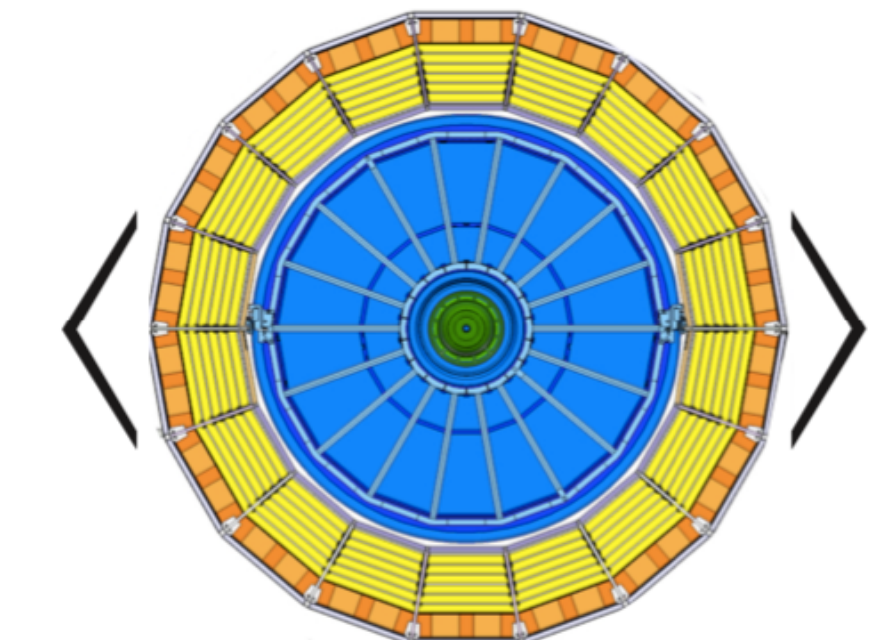
Antideuteron inelastic cross section

$\sigma_{\text{inel}}(\bar{d})$ on average ALICE detector material.
Hint at steeper rise at low momentum.



Antideuteron inelastic cross section

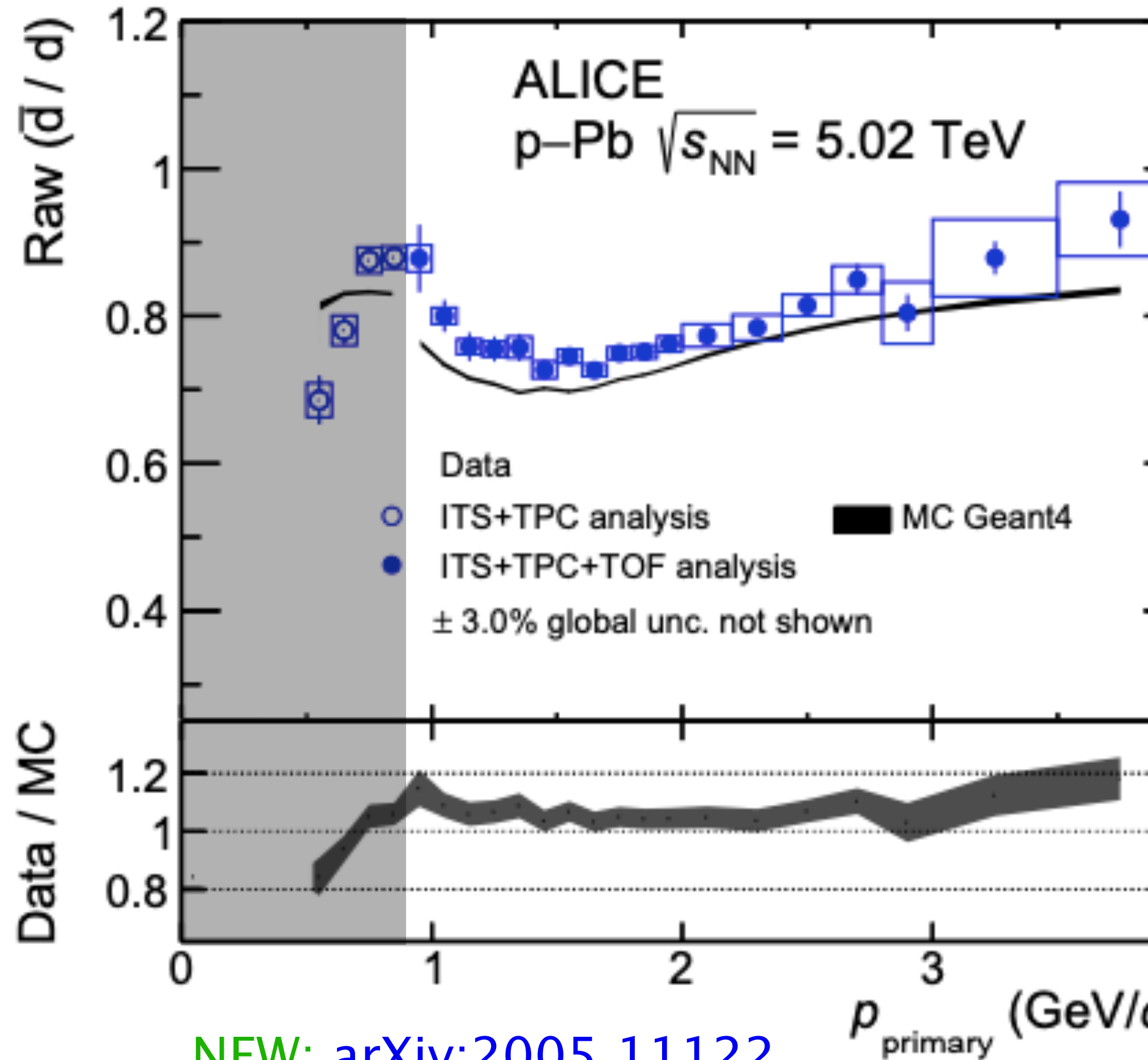
$\sigma_{\text{inel}}(\bar{d})$ on average ALICE detector material.
Hint at steeper rise at low momentum.



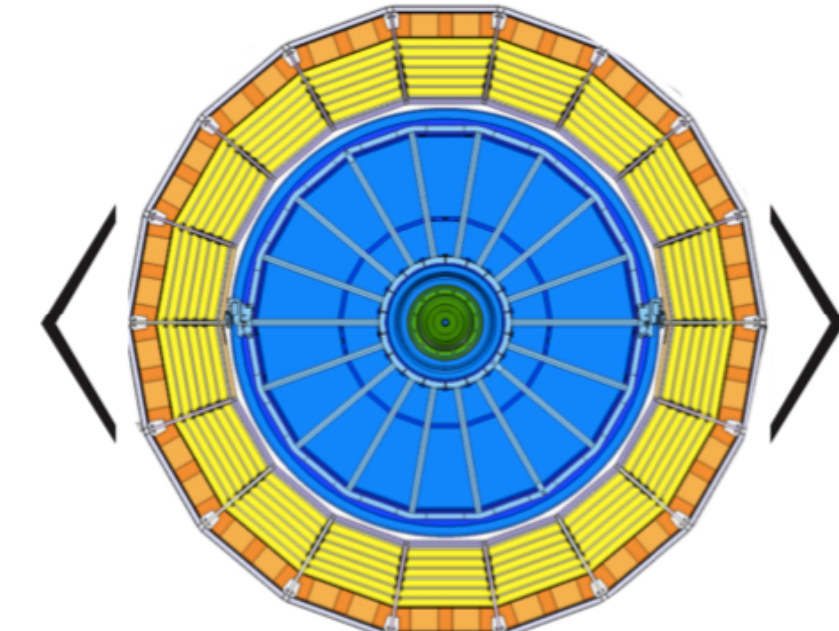
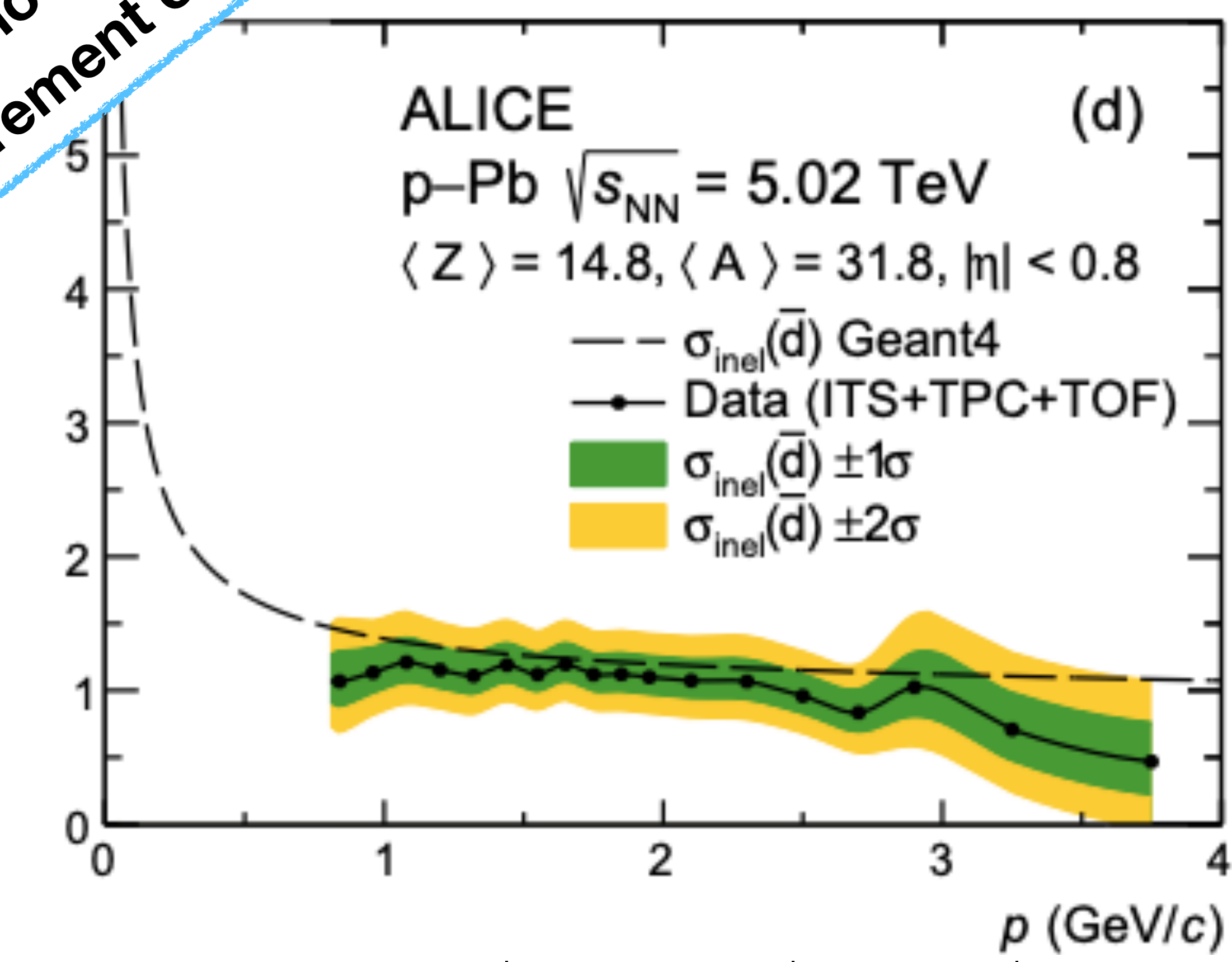
Antideuteron inelastic cross section

$\sigma_{\text{inel}}(\bar{d})$ on average ALICE detector material.

Hint at steeper rise at low momentum.



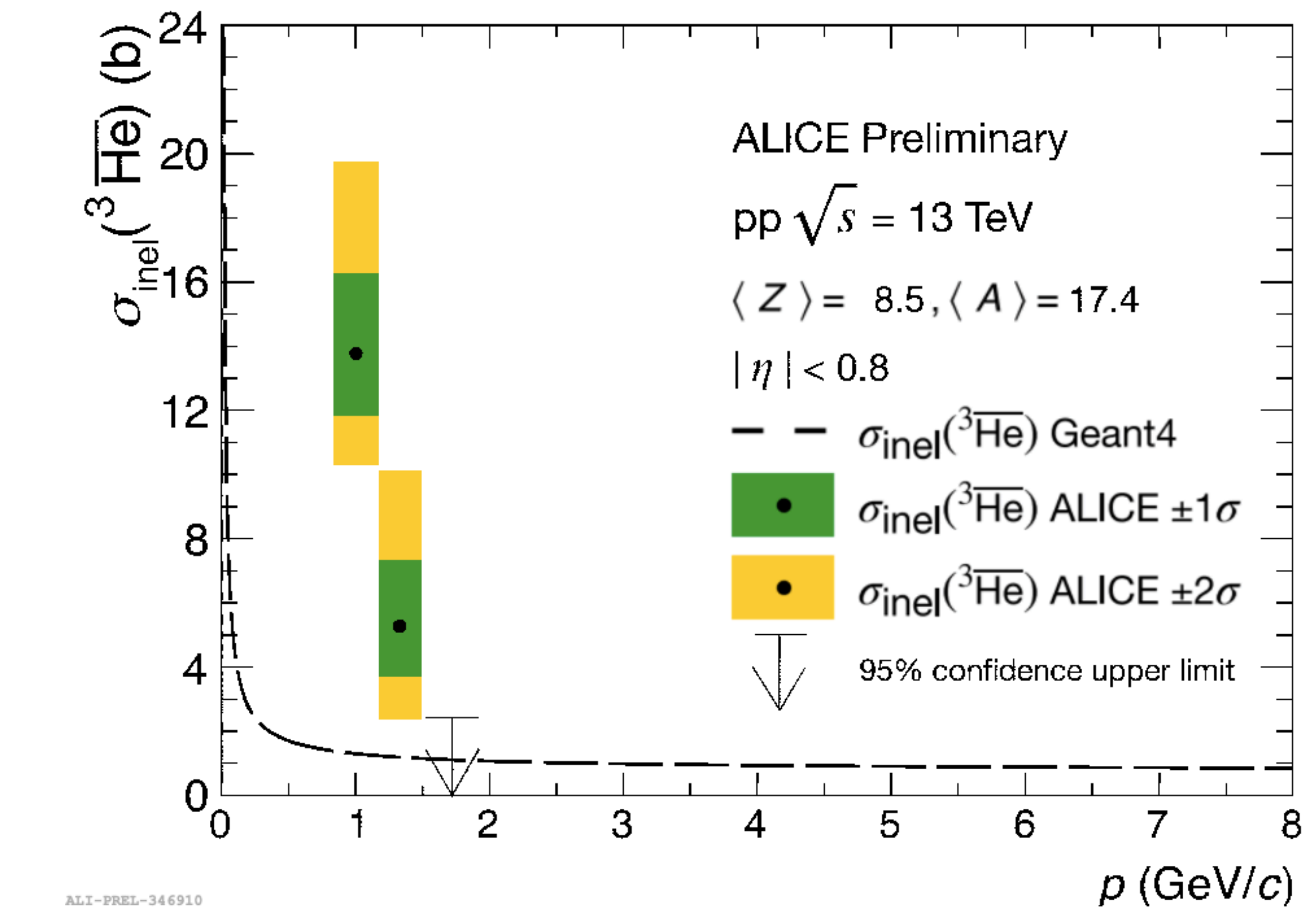
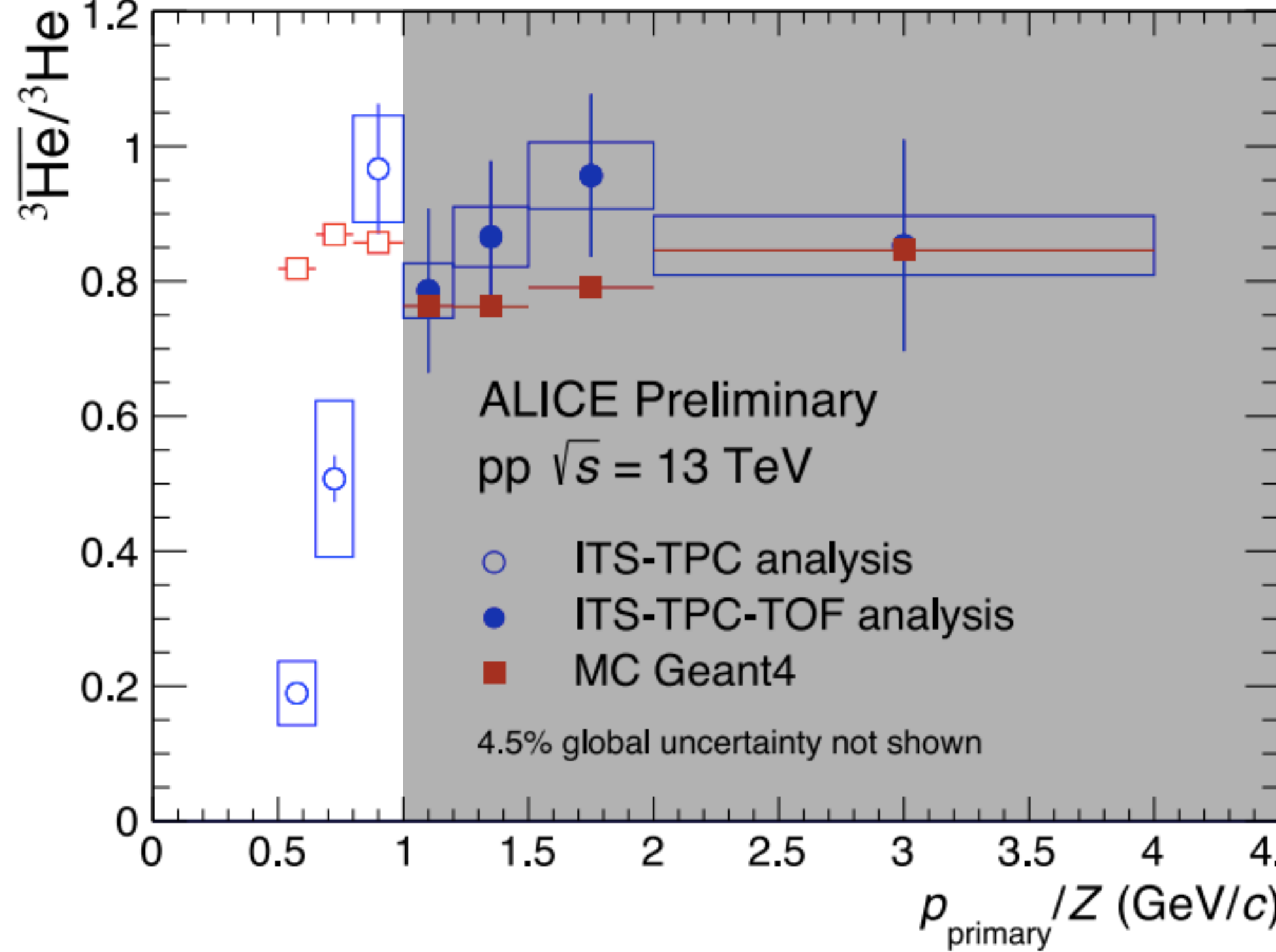
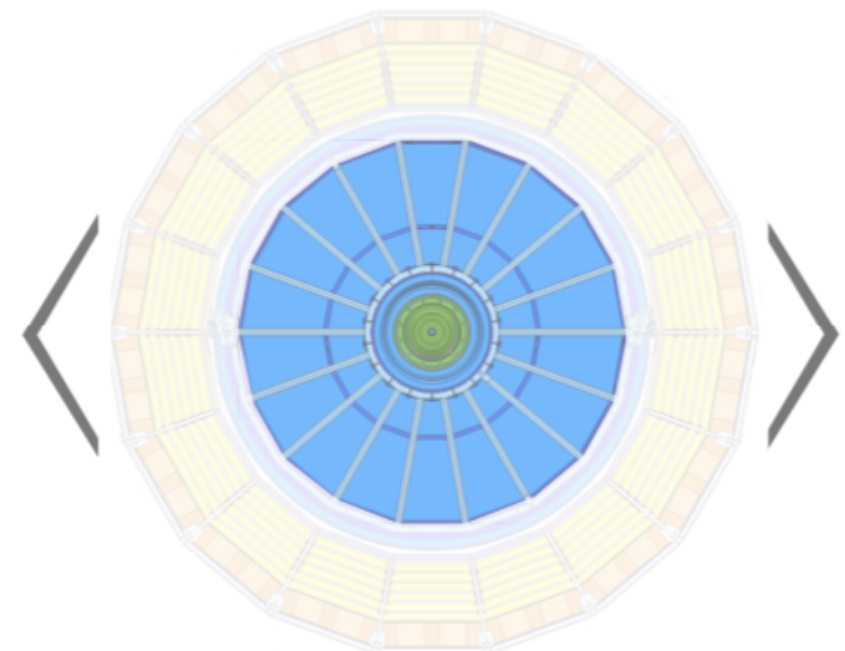
First low energy measurement of $\sigma_{\text{inel}}(\bar{d})$



Anti- ${}^3\text{He}$ inelastic cross section

$\sigma_{\text{inel}}({}^3\overline{\text{He}})$ on average ALICE detector material.

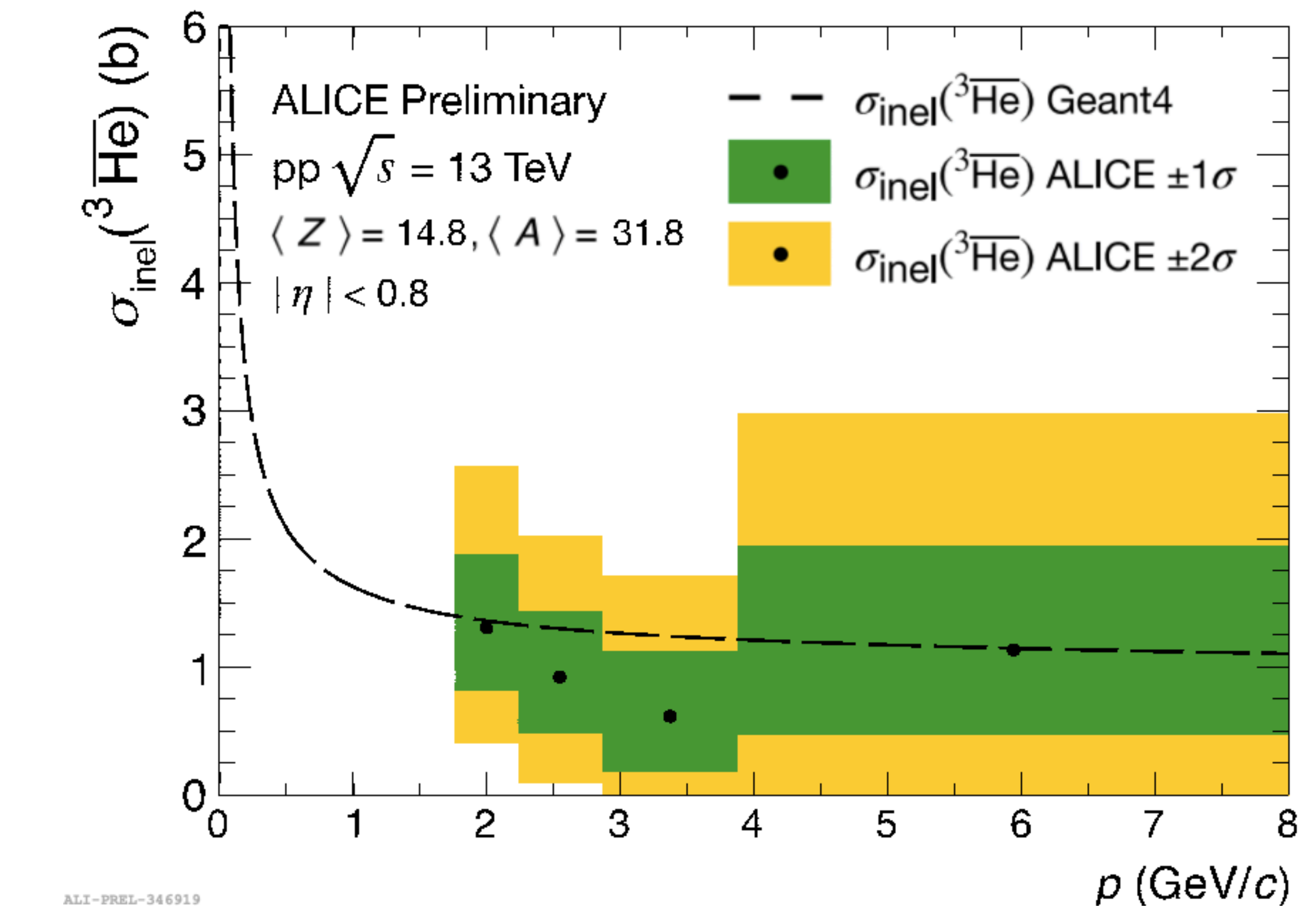
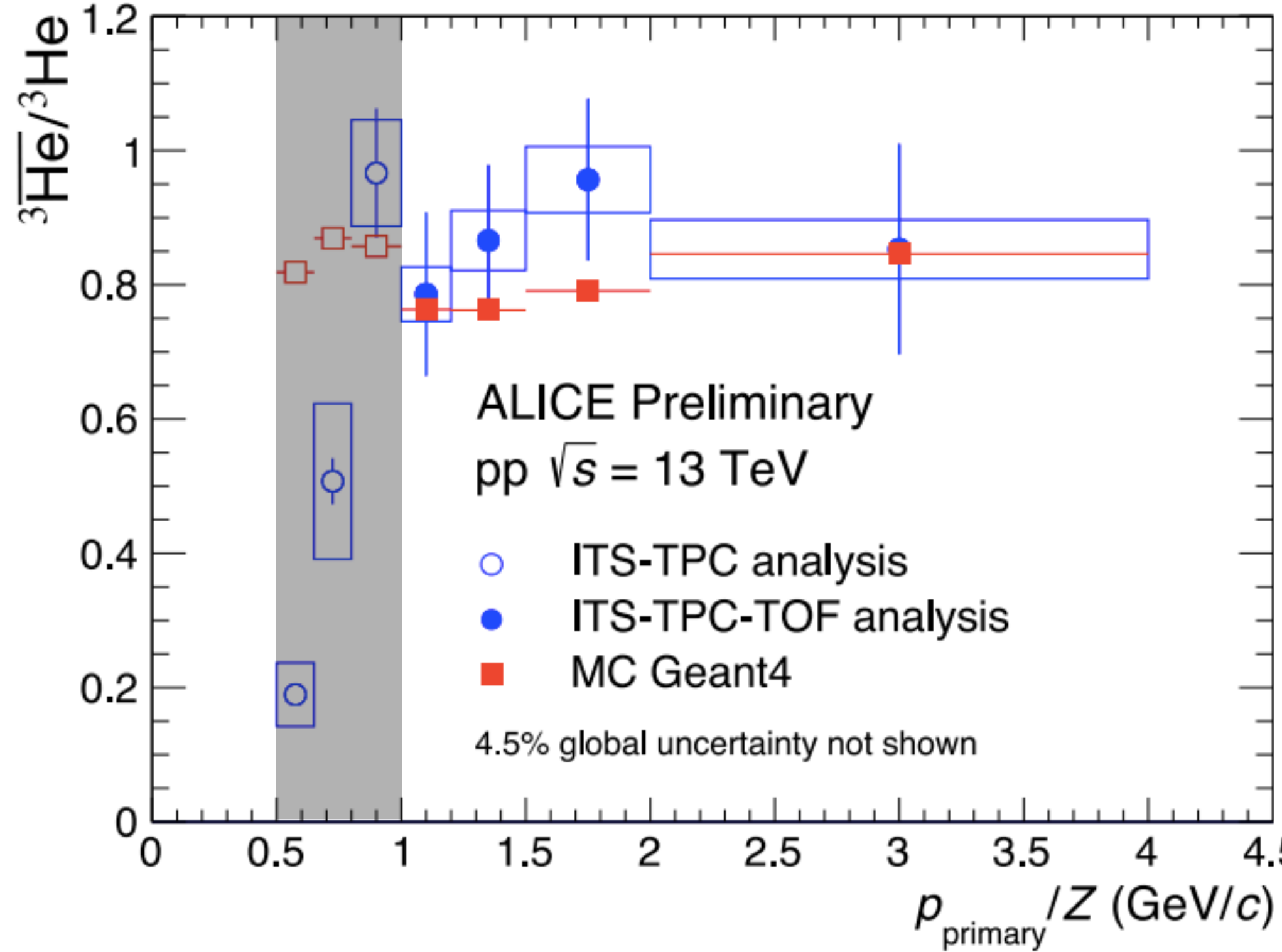
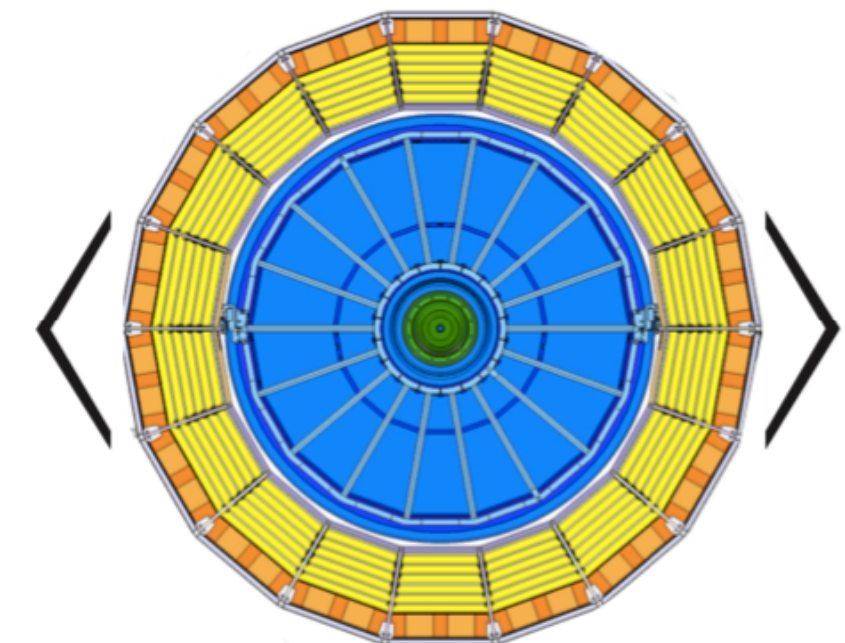
- Much steeper rise at low momentum
- Good agreement for momenta $> 1.5 \text{ GeV}/c$



Anti- ${}^3\text{He}$ inelastic cross section

$\sigma_{\text{inel}}({}^3\overline{\text{He}})$ on average ALICE detector material.

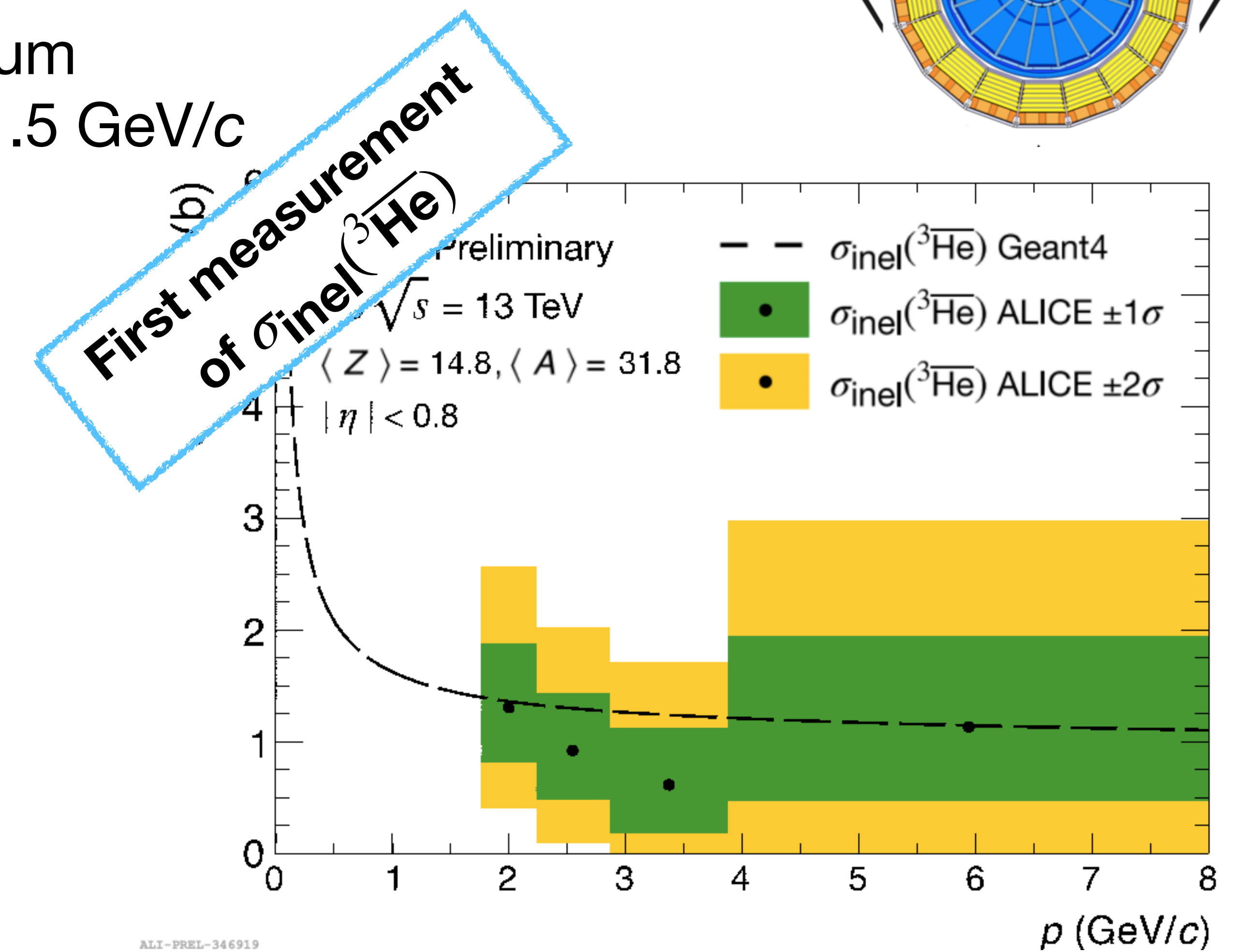
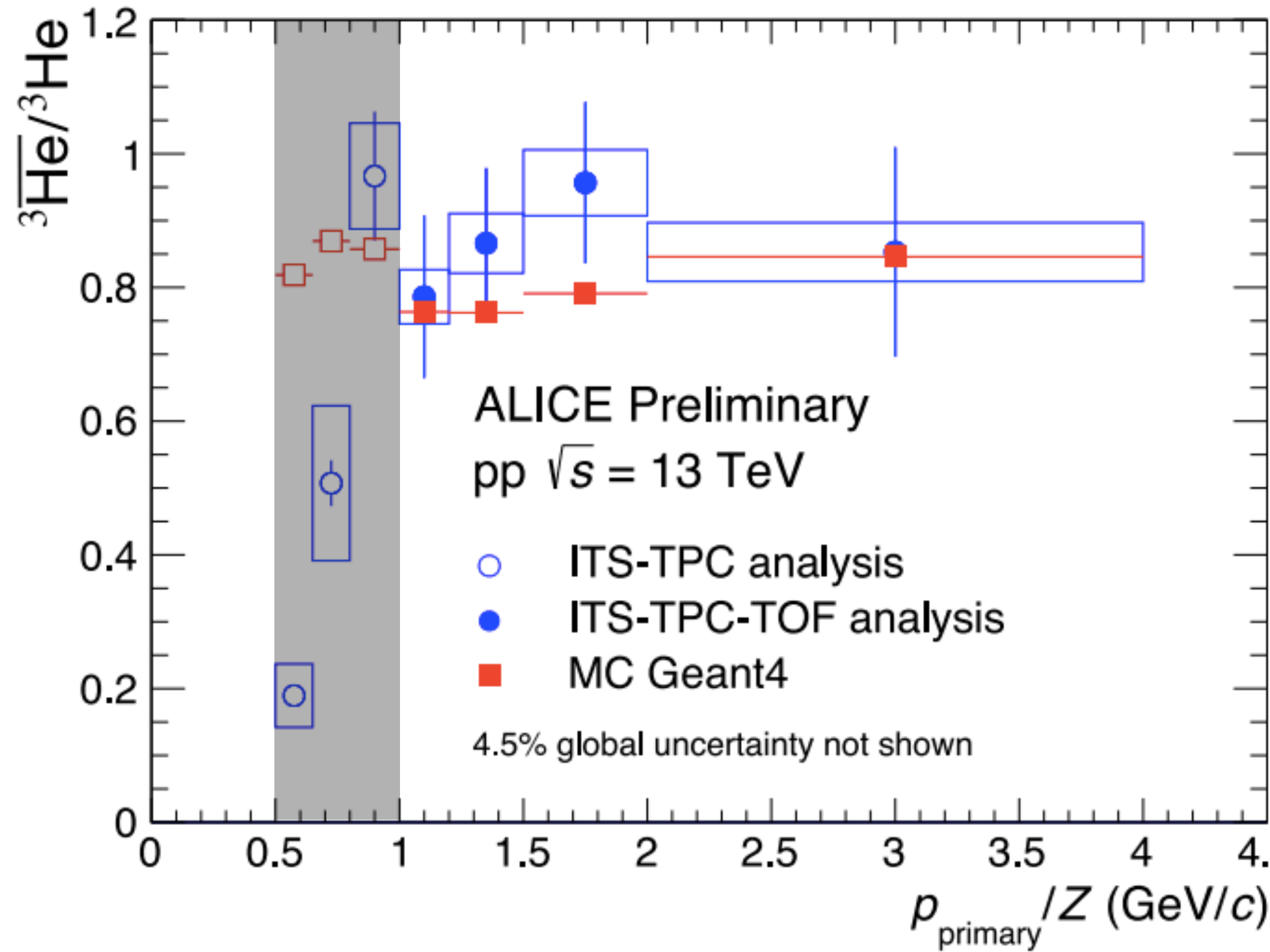
- Much steeper rise at low momentum
- Good agreement for momenta $> 1.5 \text{ GeV}/c$



Anti- ${}^3\text{He}$ inelastic cross section

$\sigma_{\text{inel}}({}^3\overline{\text{He}})$ on average ALICE detector material.

- Much steeper rise at low momentum
- Good agreement for momenta $> 1.5 \text{ GeV}/c$



Effect on antinuclei in cosmic rays

Effect on antinuclei in cosmic rays

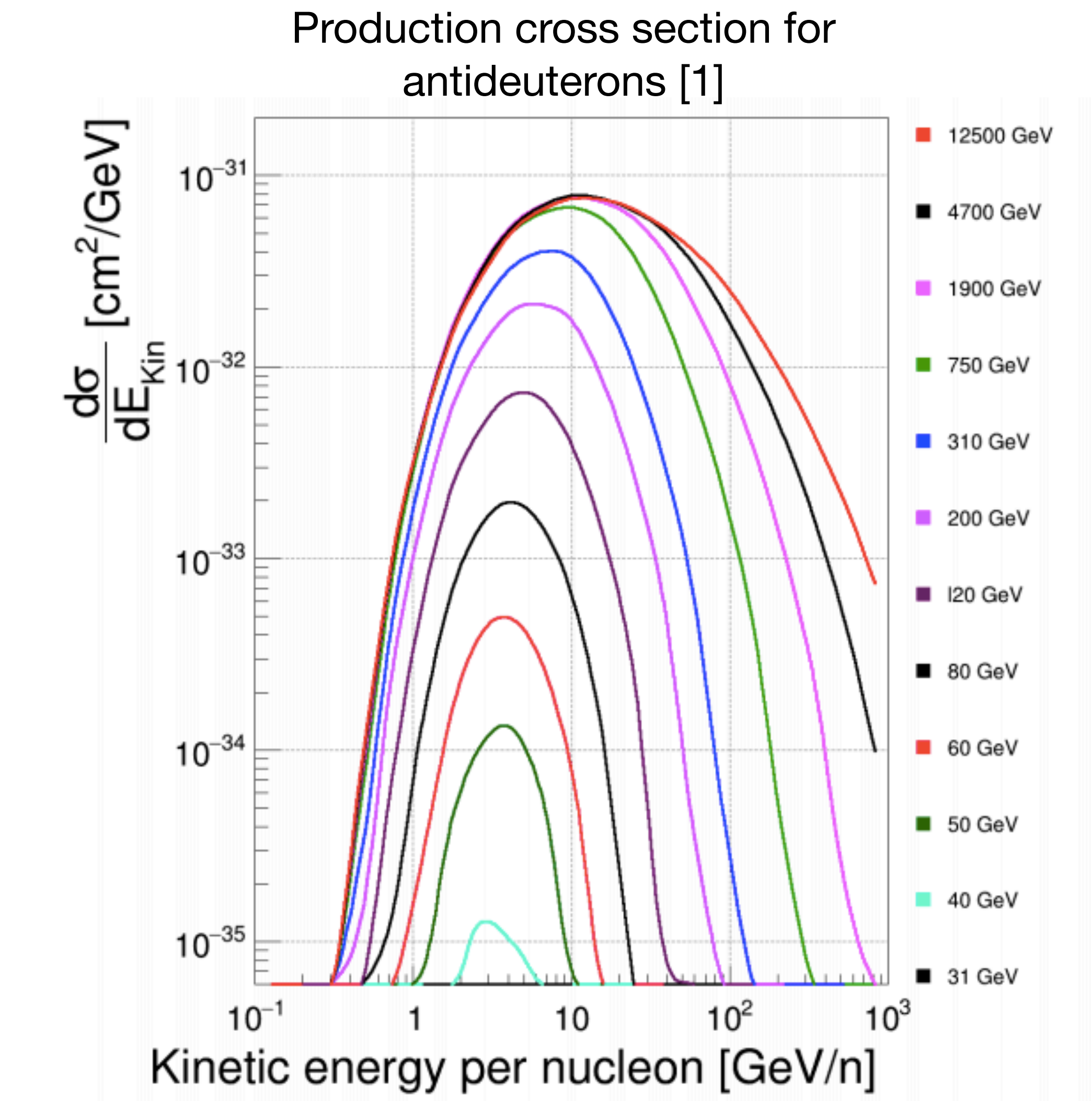
- Particles can get reshuffled to lower momenta due to energy loss effects

Effect on antinuclei in cosmic rays

- Particles can get reshuffled to lower momenta due to energy loss effects
- The flux is most sensitive to the cross section at the peak

Effect on antinuclei in cosmic rays

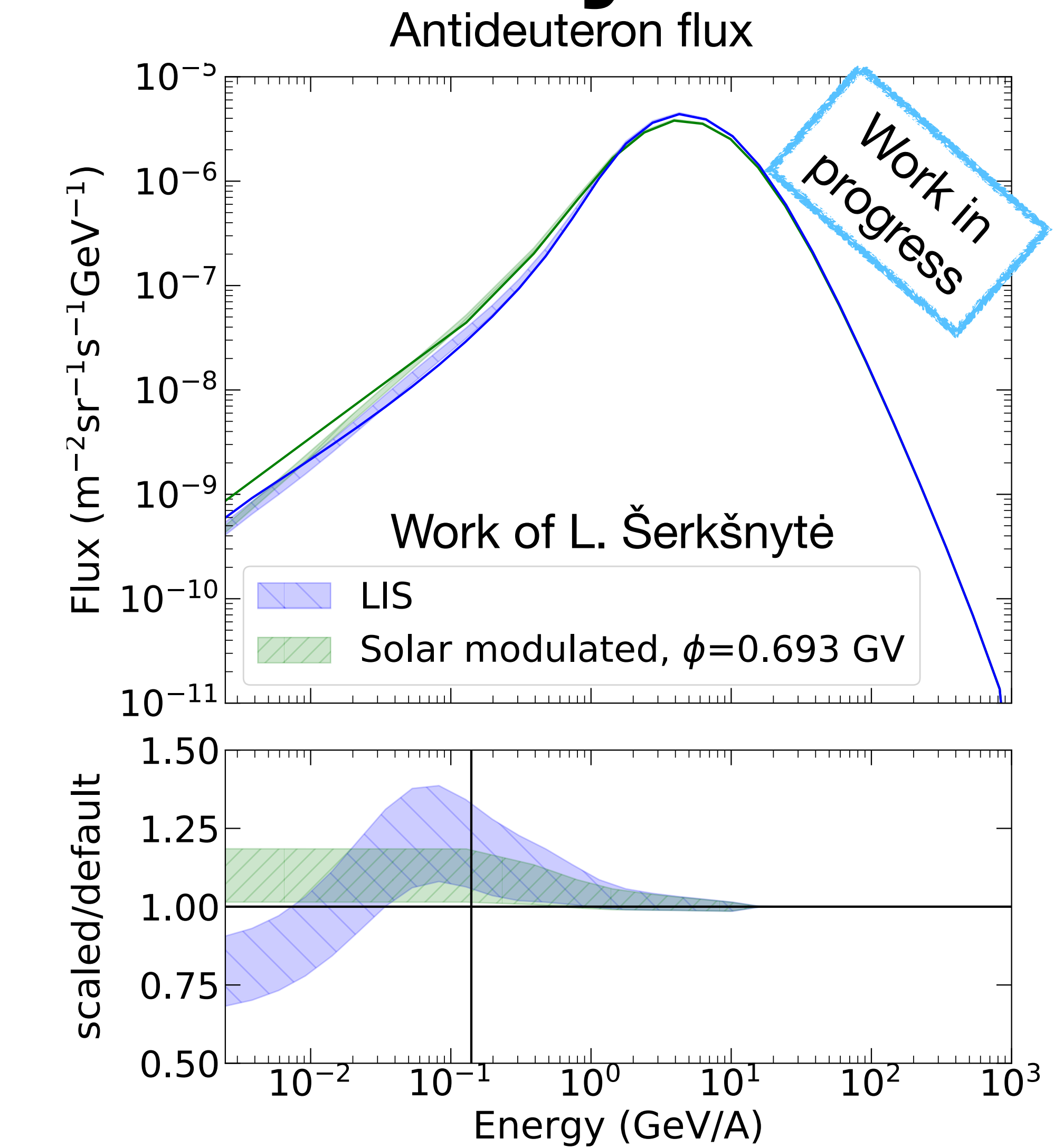
- Particles can get reshuffled to lower momenta due to energy loss effects
- The flux is most sensitive to the cross section at the peak



[1] Phillip von Doettinchem, [arXiv:2006.12707](https://arxiv.org/abs/2006.12707)

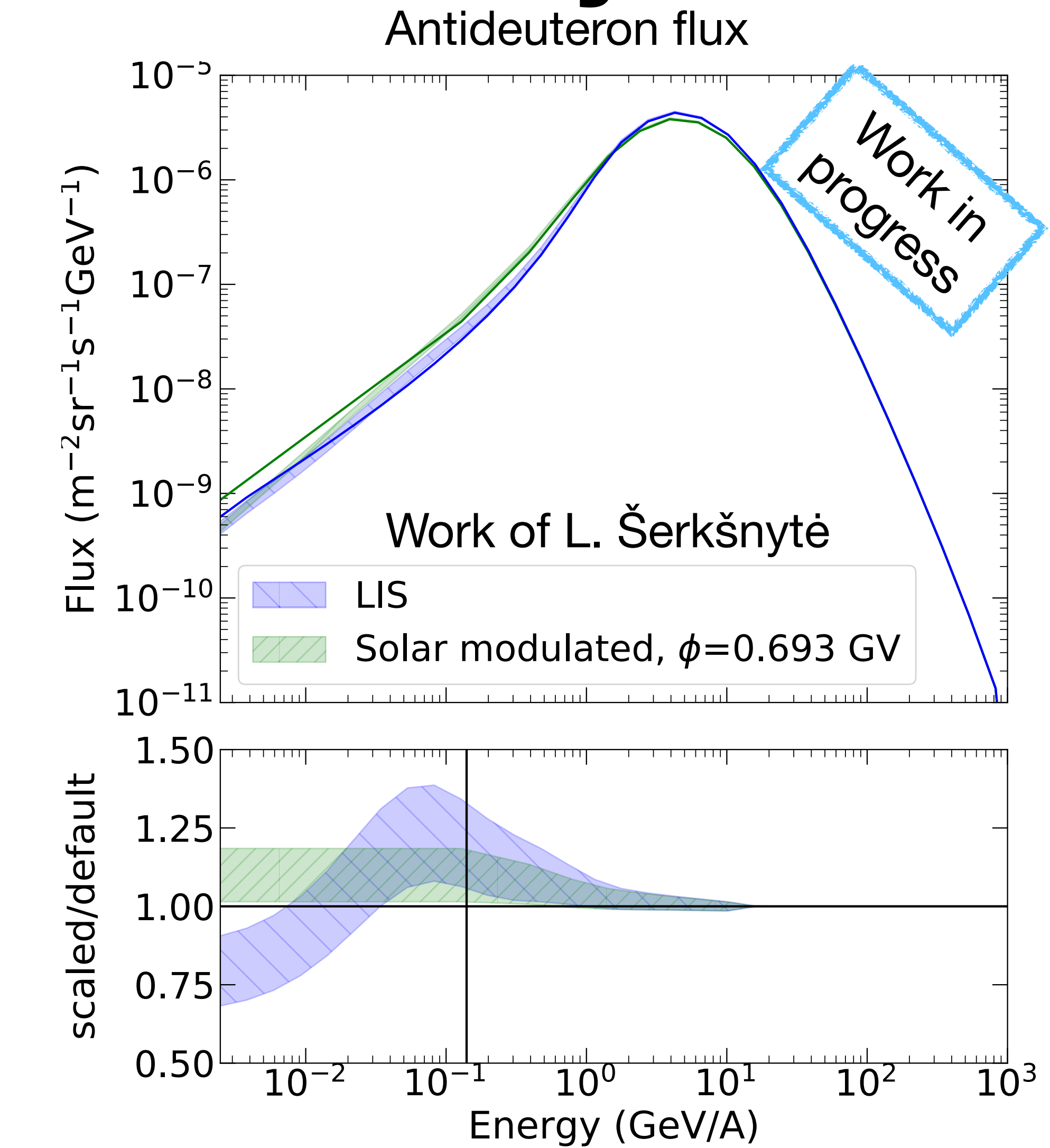
Effect on antinuclei in cosmic rays

- Particles can get reshuffled to lower momenta due to energy loss effects
- The flux is most sensitive to the cross section at the peak



Effect on antinuclei in cosmic rays

- Particles can get reshuffled to lower momenta due to energy loss effects
- The flux is most sensitive to the cross section at the peak
- Since this measurement agrees with current parameterization at the momentum where the peak of the flux is, the effect on the secondary spectrum is small



Effect on antinuclei in cosmic rays (cont.)

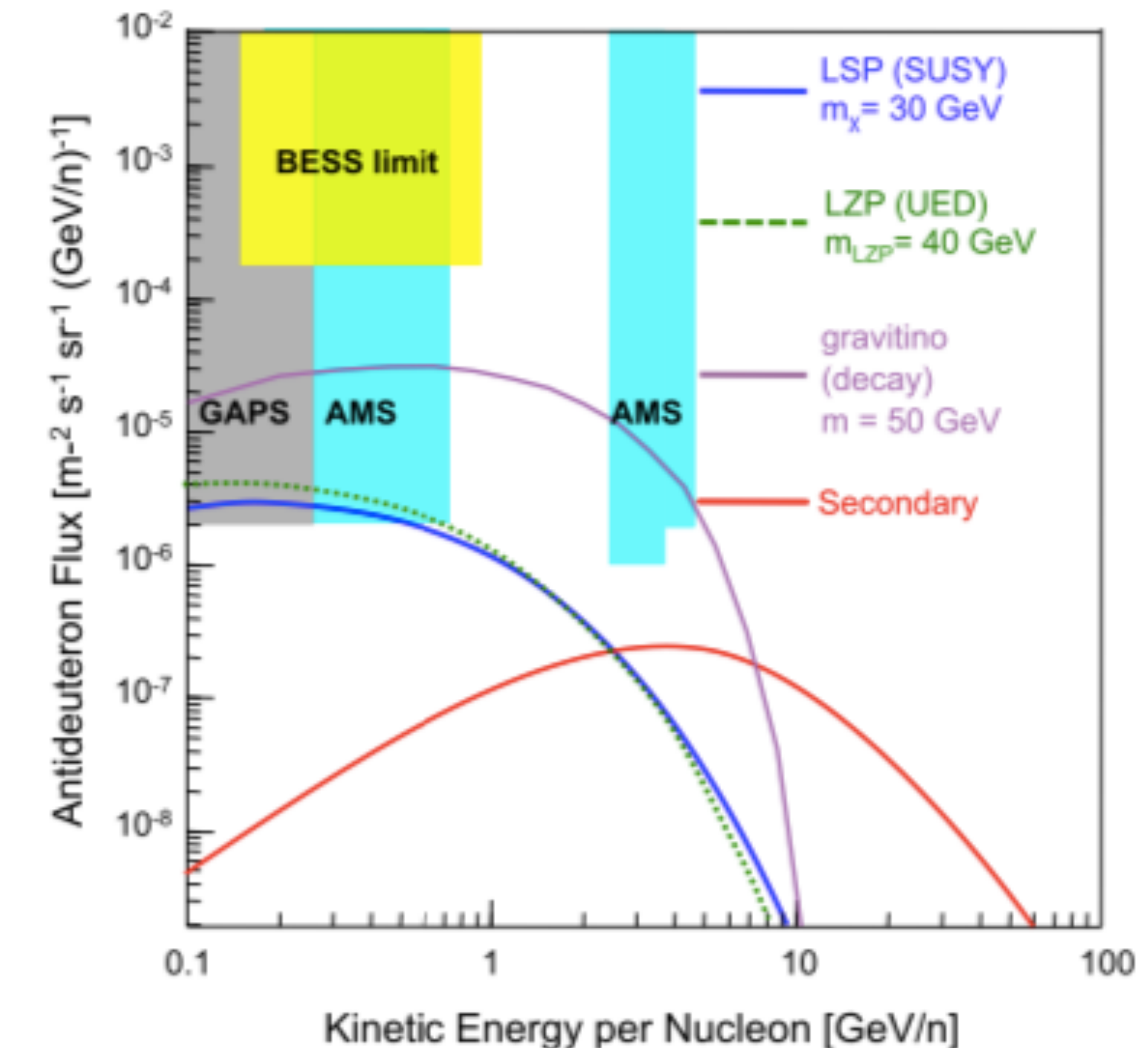
Effect on antinuclei in cosmic rays (cont.)

- Dark matter peak expected in/below this measurement range

Effect on antinuclei in cosmic rays (cont.)

- Dark matter peak expected in/below this measurement range

Predicted anti deutron flux near Earth [1]

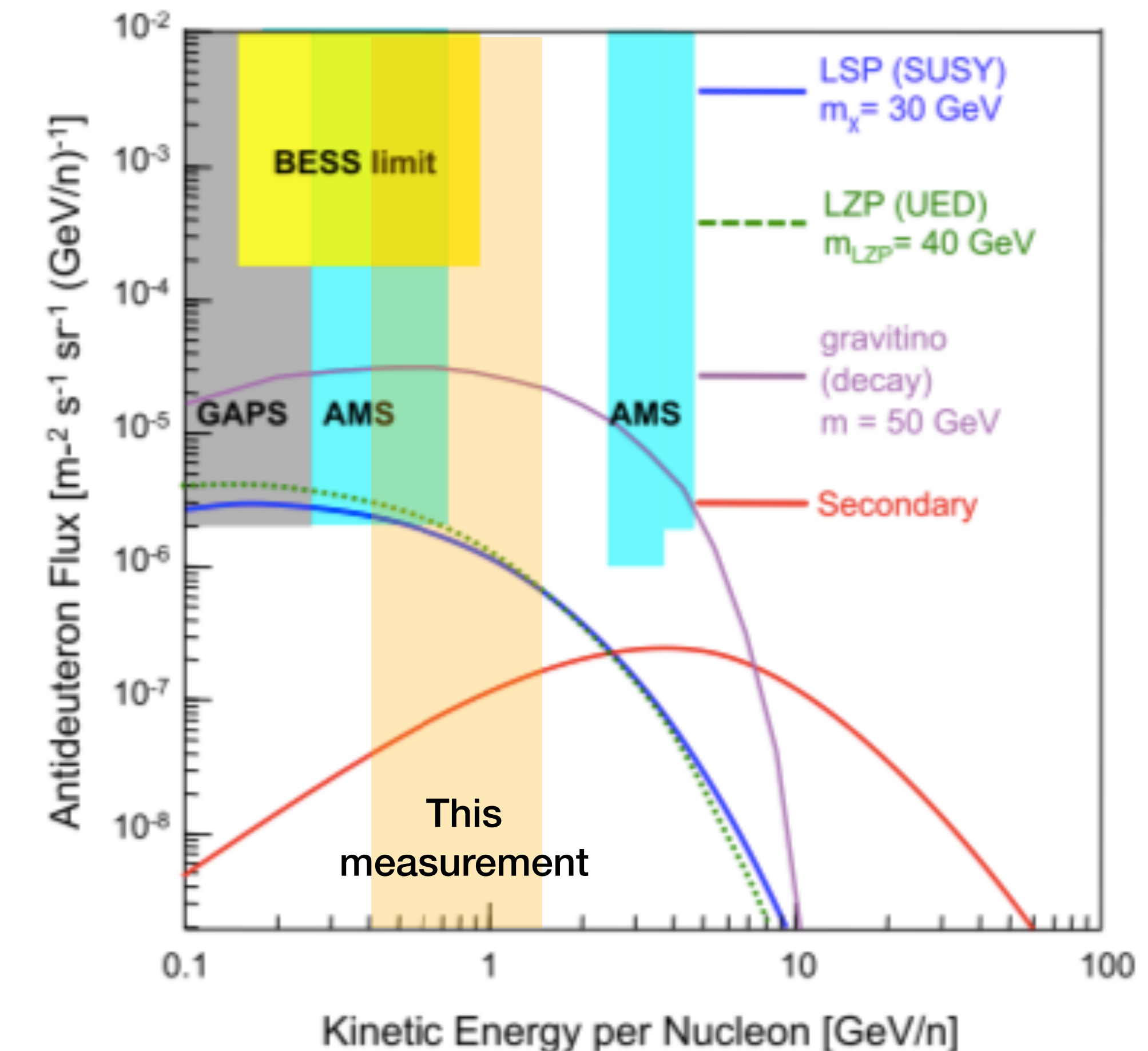


[1] Physics Report 618, 1

Effect on antinuclei in cosmic rays (cont.)

- Dark matter peak expected in/below this measurement range

Predicted anti deutron flux near Earth [1]

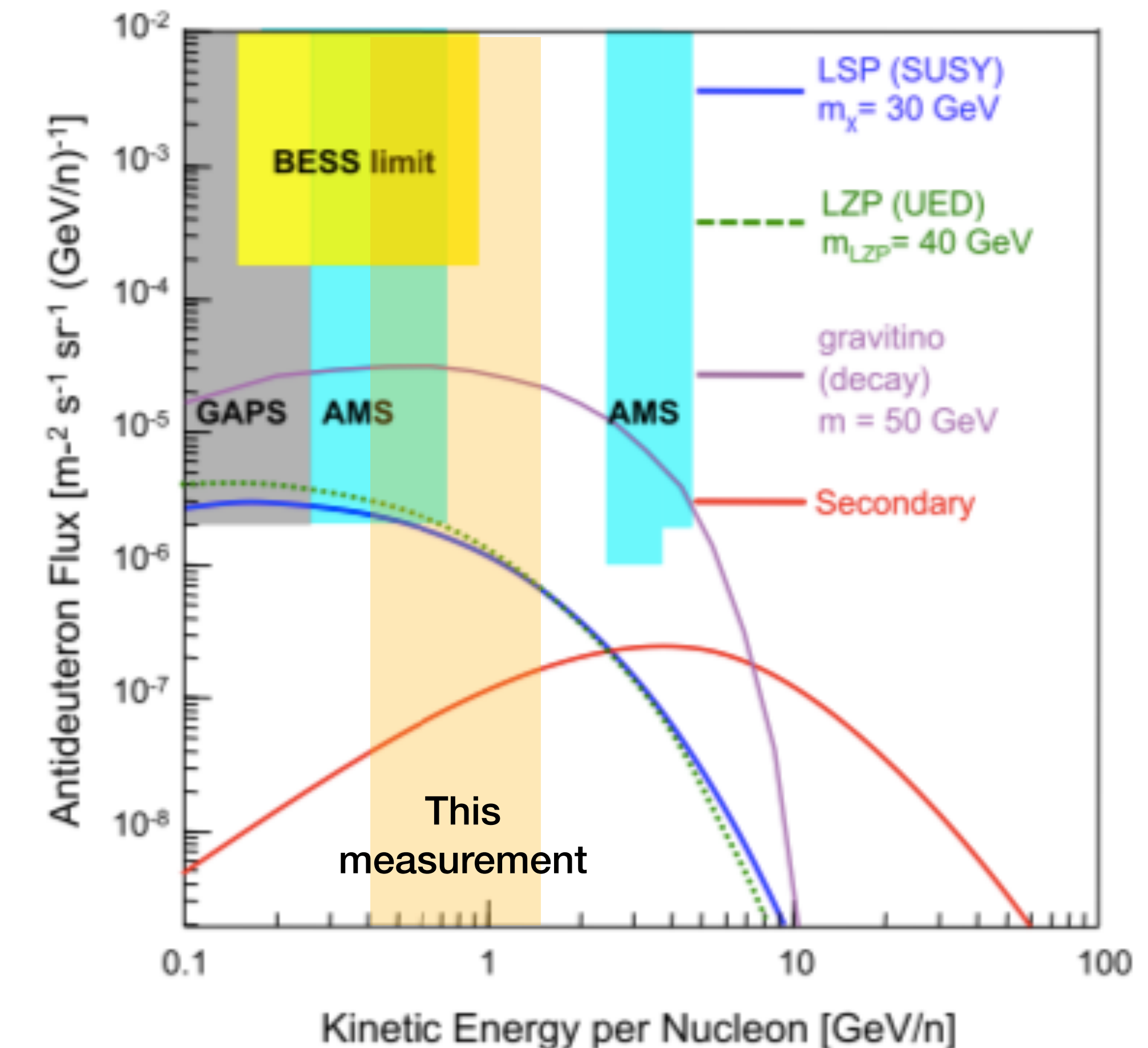


[1] Physics Report 618, 1

Effect on antinuclei in cosmic rays (cont.)

- Dark matter peak expected in/below this measurement range
- Increased cross section would reduce dark matter signal more than the background from secondaries

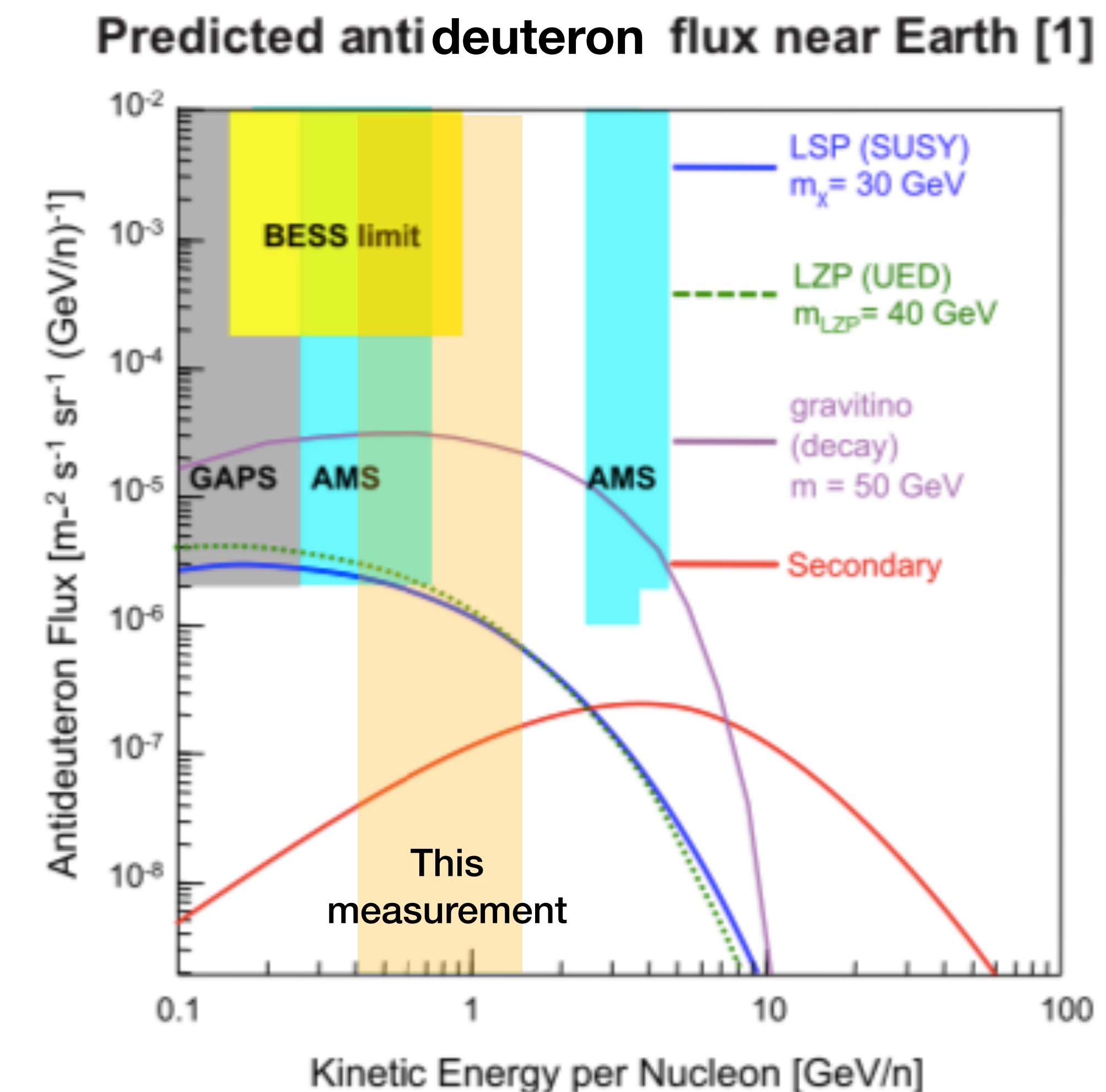
Predicted anti deutron flux near Earth [1]



[1] Physics Report 618, 1

Effect on antinuclei in cosmic rays (cont.)

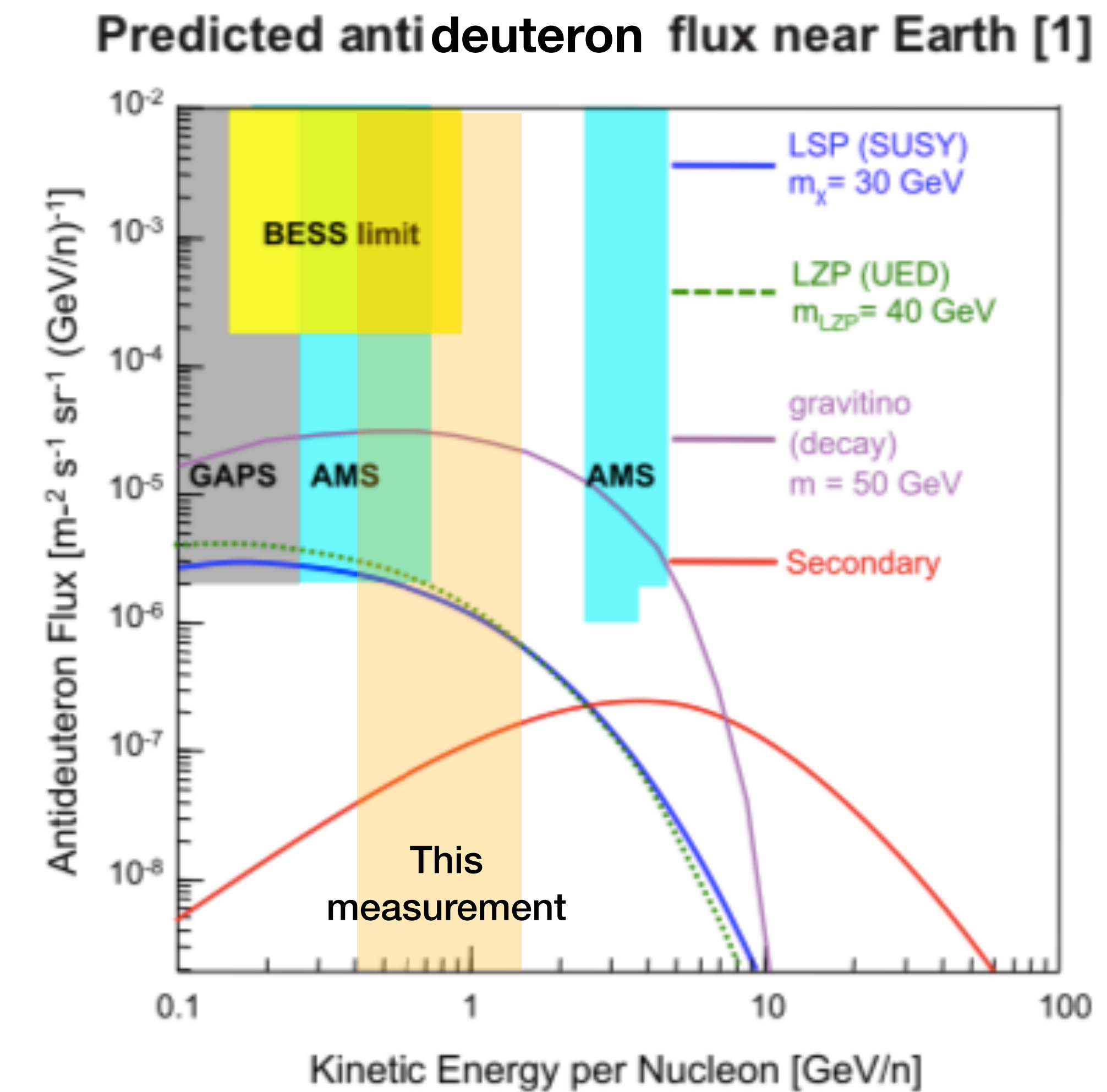
- Dark matter peak expected in/below this measurement range
- Increased cross section would reduce dark matter signal more than the background from secondaries
- This could reduce the signal/background ratio for a dark matter signal in cosmic ray antinuclei spectra



[1] Physics Report 618, 1

Effect on antinuclei in cosmic rays (cont.)

- Dark matter peak expected in/below this measurement range
- Increased cross section would reduce dark matter signal more than the background from secondaries
- This could reduce the signal/background ratio for a dark matter signal in cosmic ray antinuclei spectra

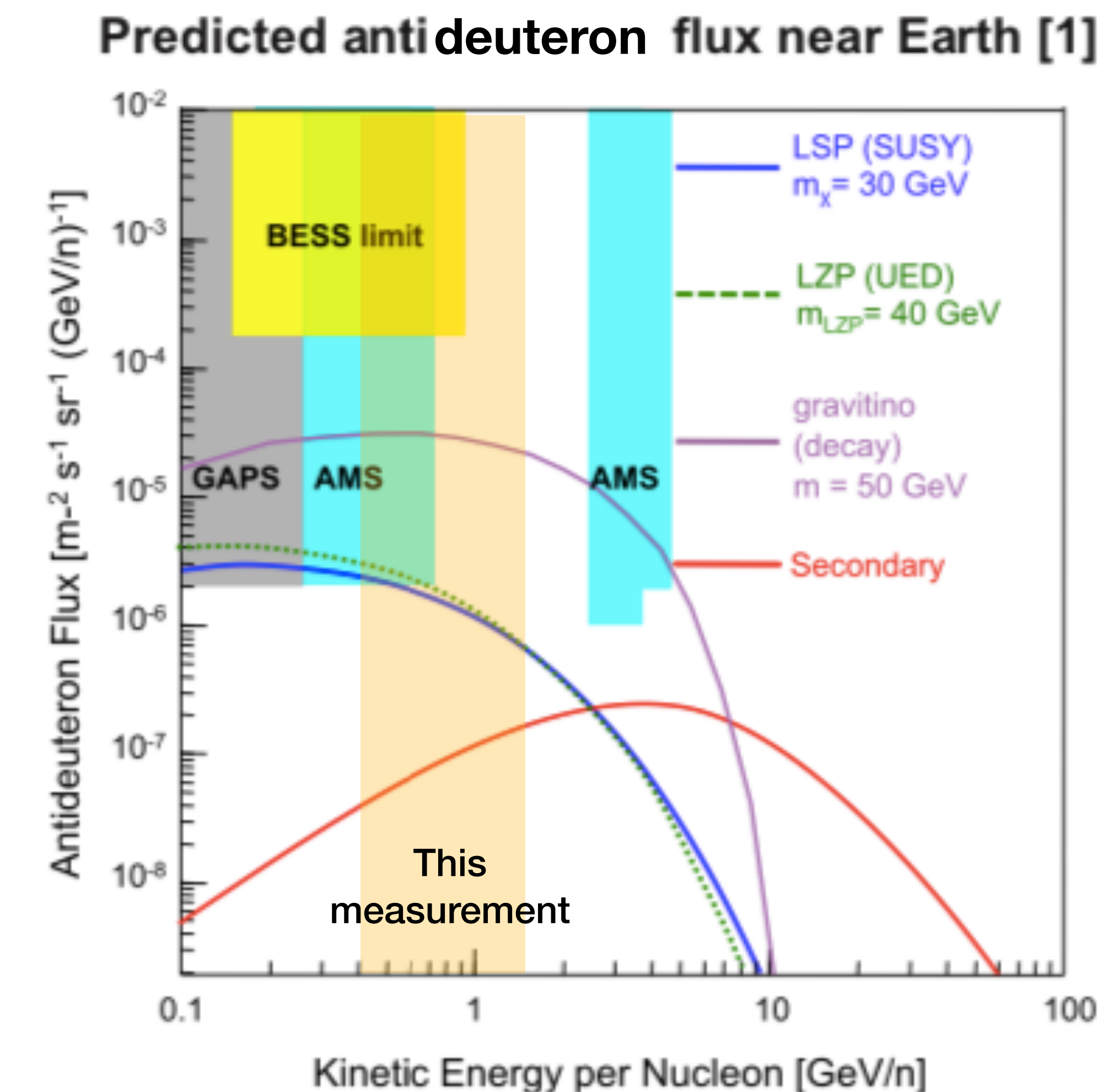


[1] Physics Report 618, 1

Effect on antinuclei in cosmic rays (cont.)

- Dark matter peak expected in/below this measurement range
- Increased cross section would reduce dark matter signal more than the background from secondaries
- This could reduce the signal/background ratio for a dark matter signal in cosmic ray antinuclei spectra

→ Potential lower antinuclei signals would be compatible with dark matter models!



[1] Physics Report 618, 1

Summary and outlook

Summary and outlook

Analysis of raw reconstructed \bar{p}/p , \bar{d}/d and ${}^3\overline{\text{He}}/{}^3\text{He}$ ratios.

- Measurement of σ_{inel} via comparison with detailed ALICE Monte Carlo simulations using Geant4

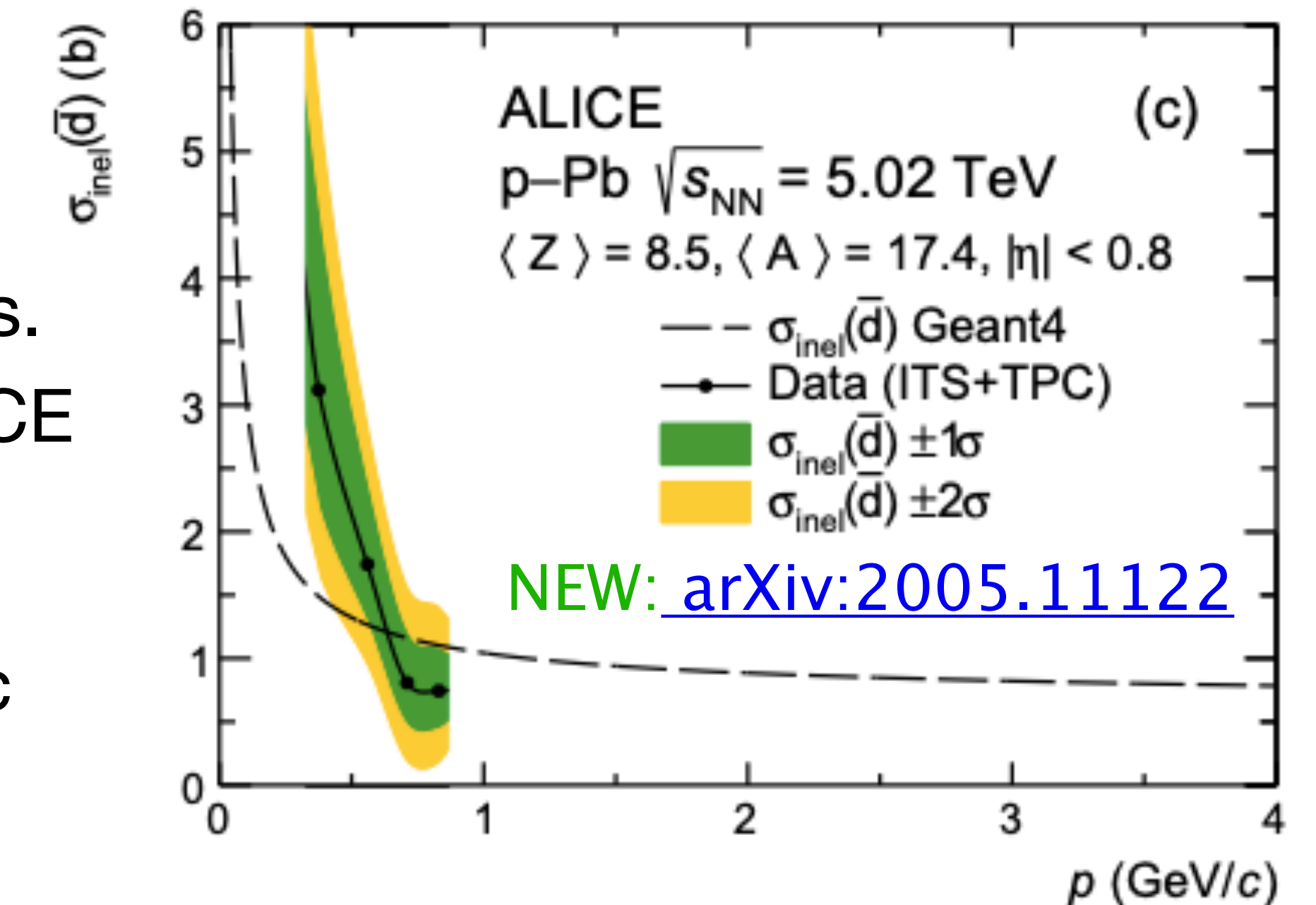
Summary and outlook

Analysis of raw reconstructed \bar{p}/p , \bar{d}/d and ${}^3\overline{\text{He}}/{}^3\text{He}$ ratios.

- Measurement of σ_{inel} via comparison with detailed ALICE Monte Carlo simulations using Geant4

First low energy measurement of the antideuteron inelastic cross section.

- Paper on [arXiv:2005.11122](https://arxiv.org/abs/2005.11122)



Summary and outlook

Analysis of raw reconstructed \bar{p}/p , \bar{d}/d and ${}^3\overline{\text{He}}/{}^3\text{He}$ ratios.

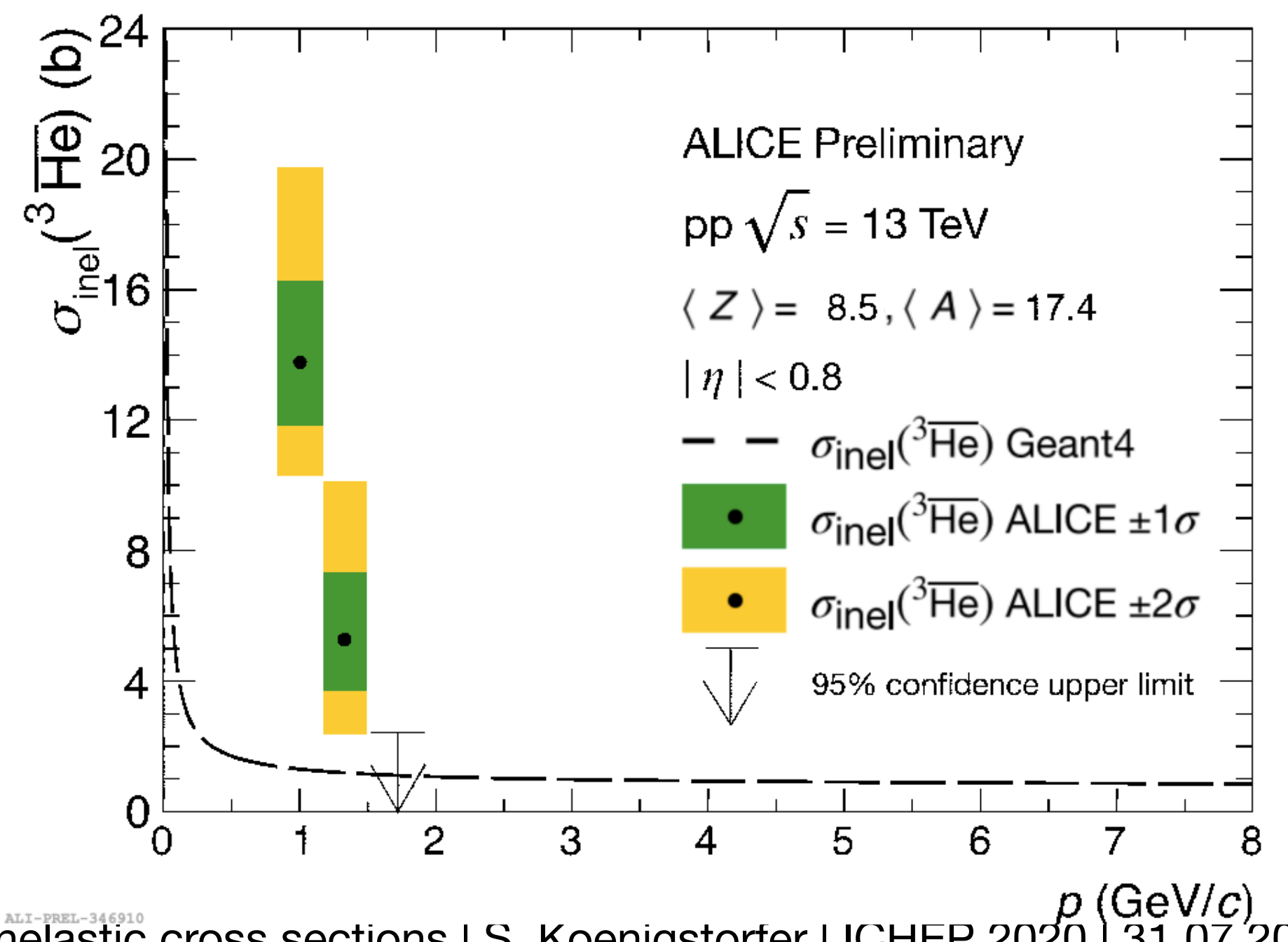
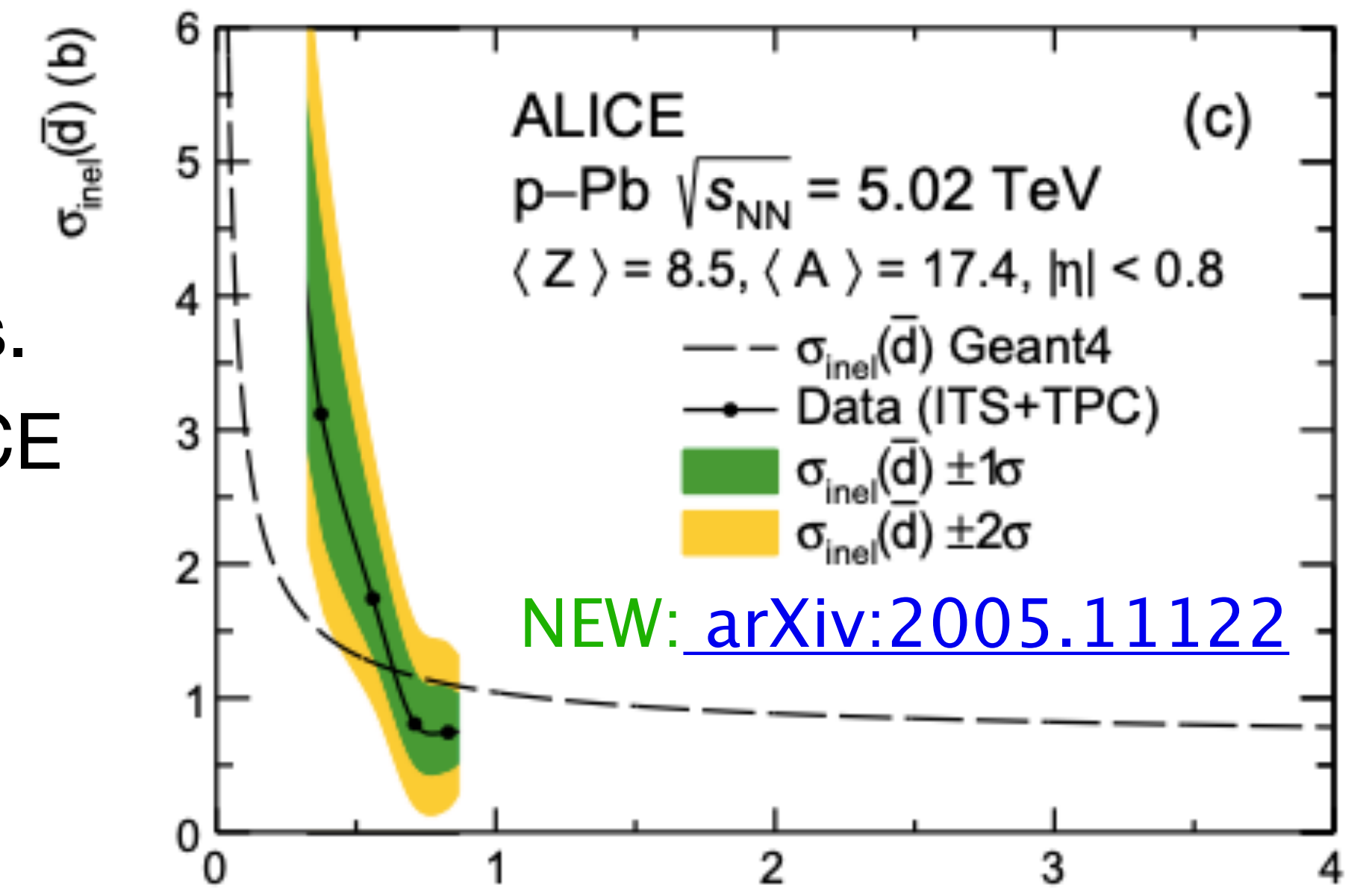
- Measurement of σ_{inel} via comparison with detailed ALICE Monte Carlo simulations using Geant4

First low energy measurement of the antideuteron inelastic cross section.

- Paper on [arXiv:2005.11122](https://arxiv.org/abs/2005.11122)

First measurement of the ${}^3\overline{\text{He}}$ inelastic cross section.

- Drastic difference to Geant4 for low momenta
- Paper in preparation



Summary and outlook

Analysis of raw reconstructed \bar{p}/p , \bar{d}/d and ${}^3\overline{\text{He}}/{}^3\text{He}$ ratios.

- Measurement of σ_{inel} via comparison with detailed ALICE Monte Carlo simulations using Geant4

First low energy measurement of the antideuteron inelastic cross section.

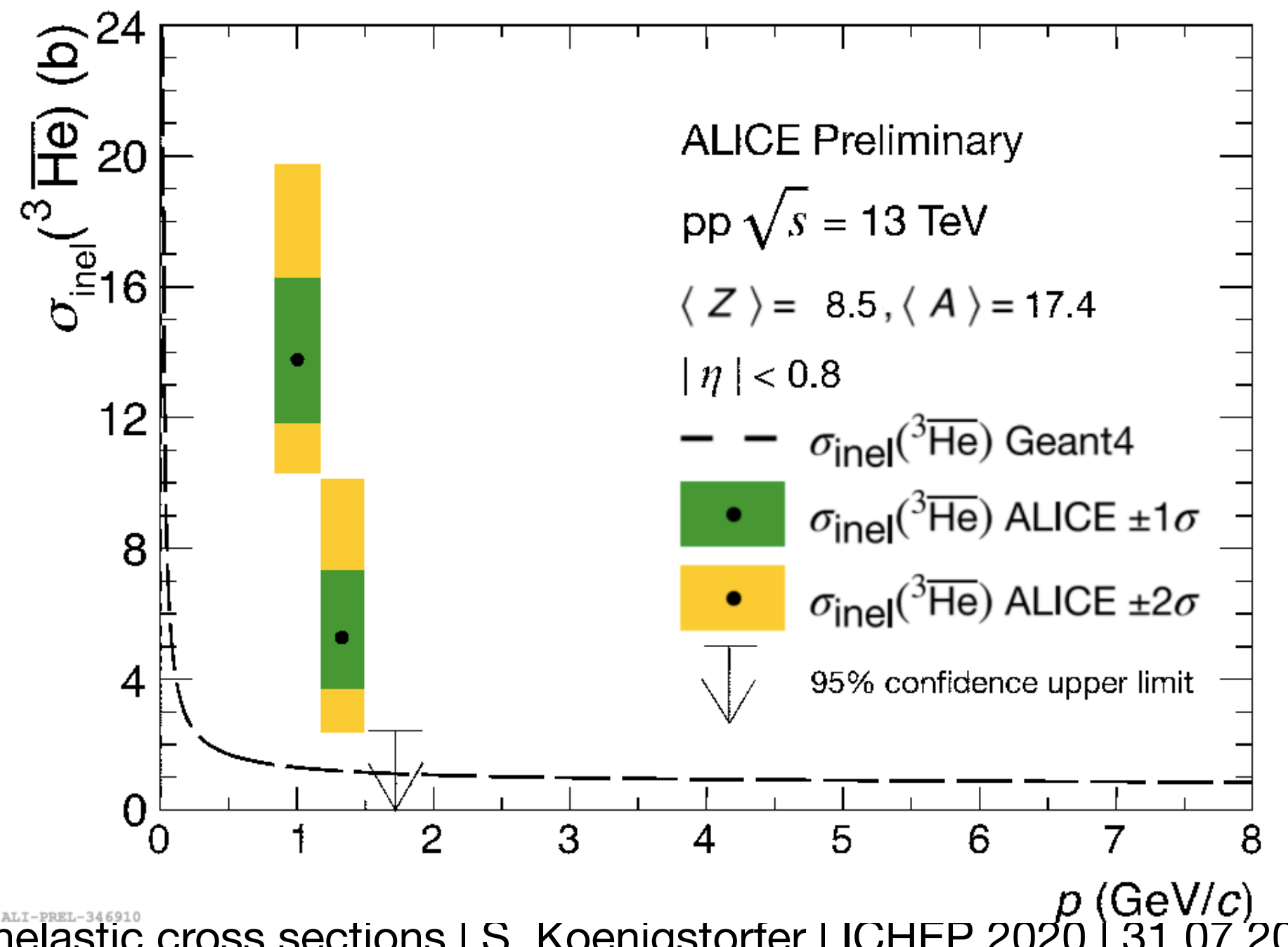
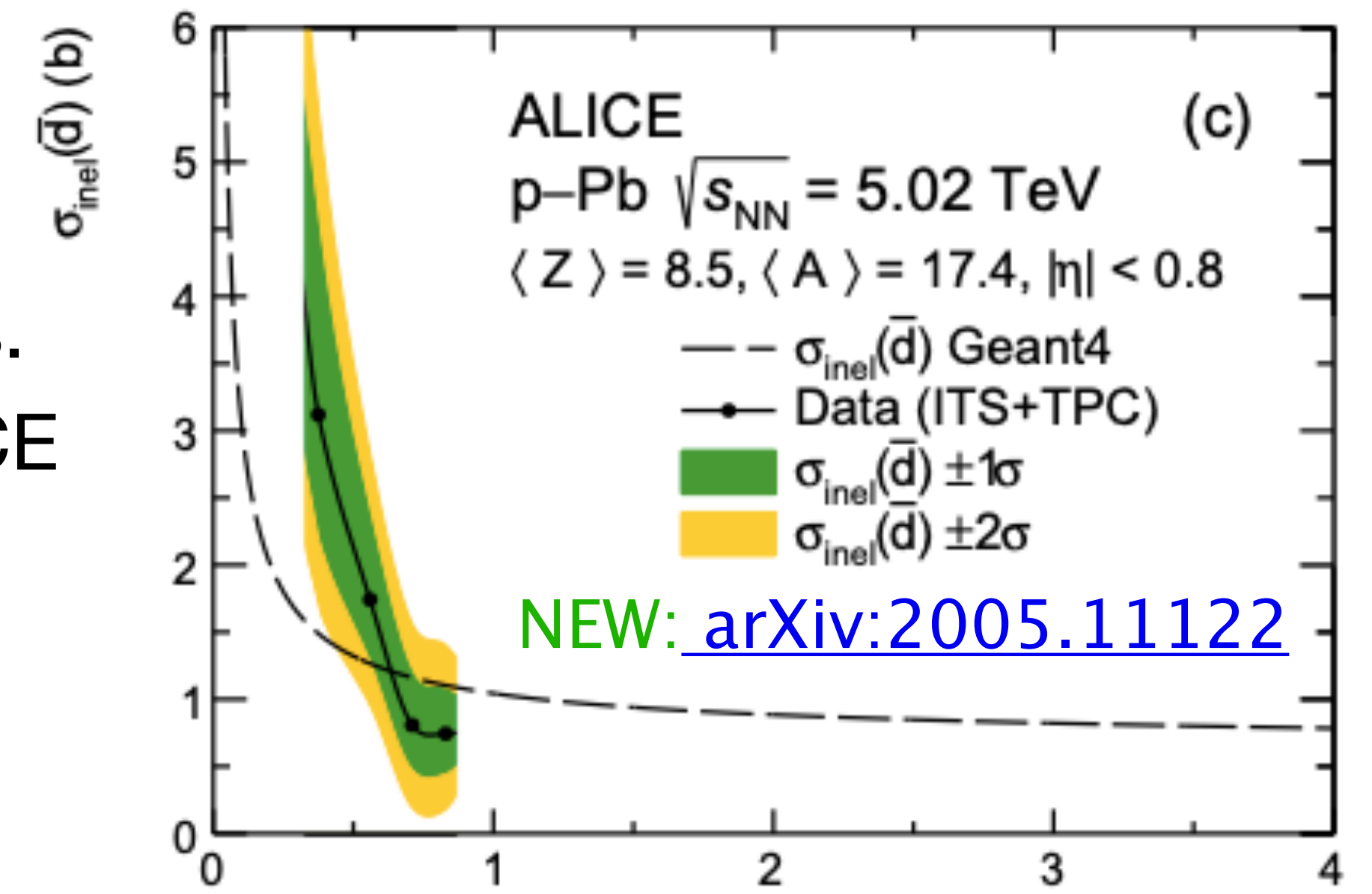
- Paper on [arXiv:2005.11122](https://arxiv.org/abs/2005.11122)

First measurement of the ${}^3\overline{\text{He}}$ inelastic cross section.

- Drastic difference to Geant4 for low momenta
- Paper in preparation

Work in progress:

- Influence of these results on expected antinuclei fluxes in cosmic rays is being investigated
- Extend the analysis to other antinuclei (\bar{t} , ${}^4\overline{\text{He}}$, ...)



Summary and outlook

Analysis of raw reconstructed \bar{p}/p , \bar{d}/d and ${}^3\overline{\text{He}}/{}^3\text{He}$ ratios.

- Measurement of σ_{inel} via comparison with detailed ALICE Monte Carlo simulations using Geant4

First low energy measurement of the antideuteron inelastic cross section.

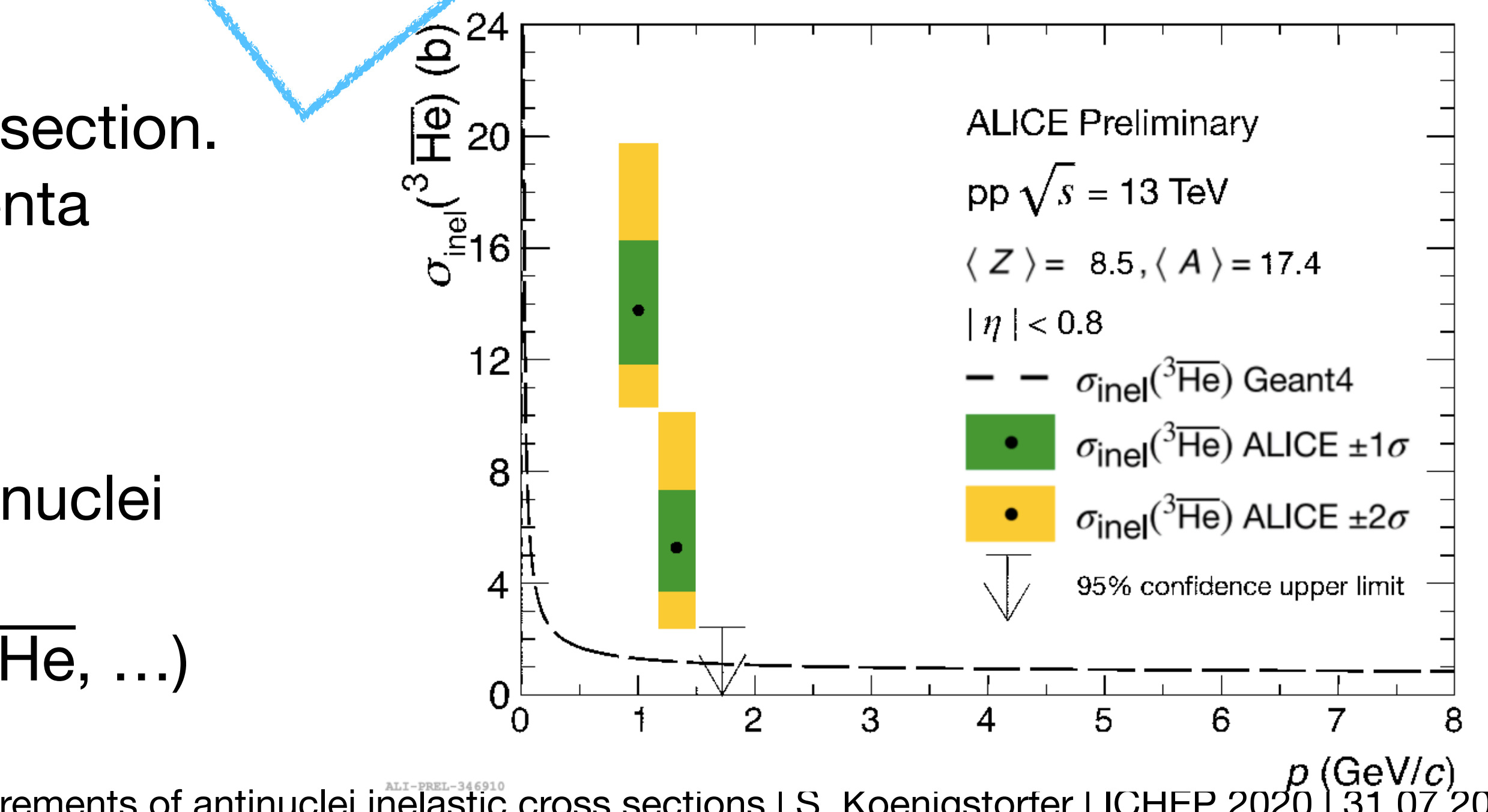
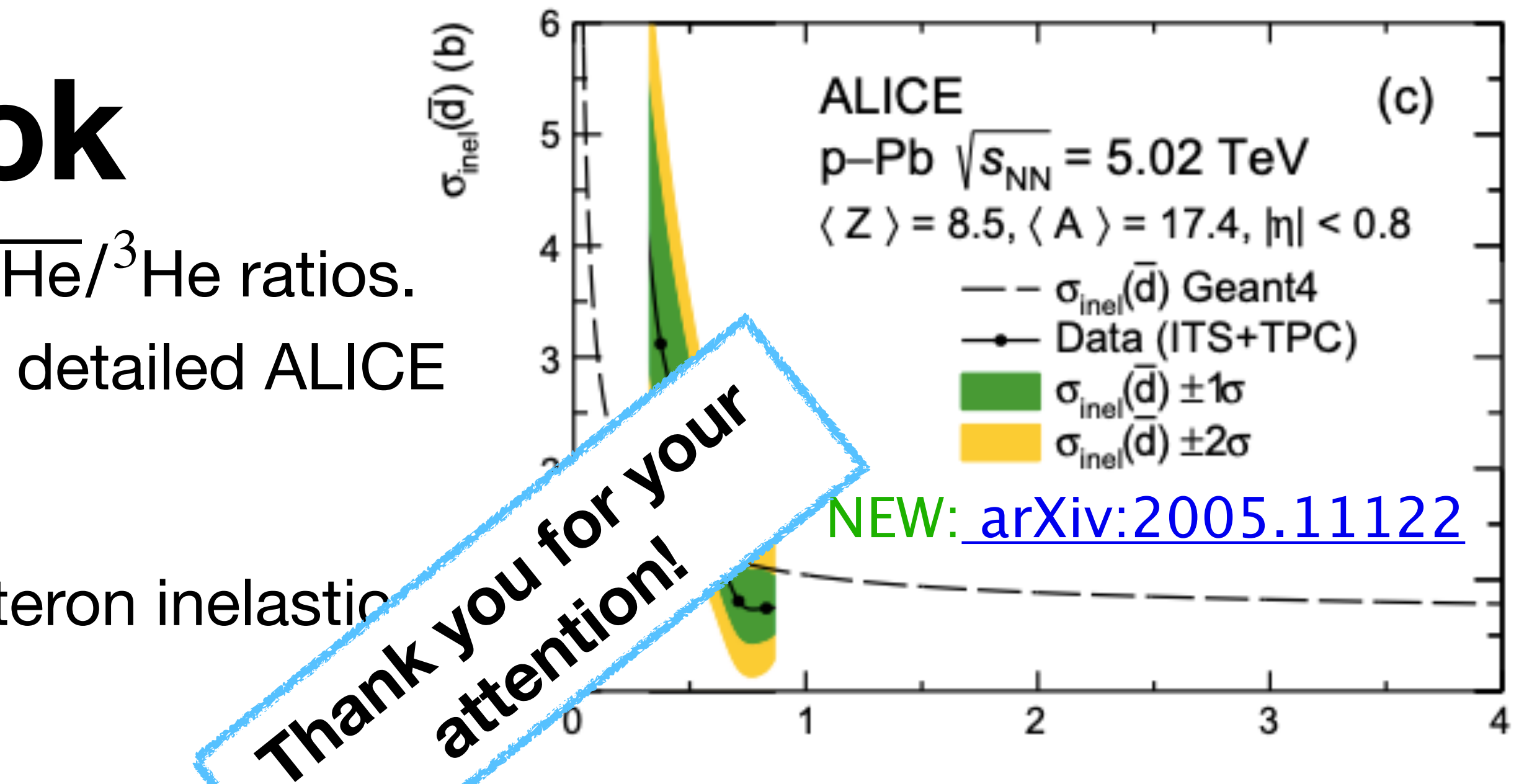
- Paper on [arXiv:2005.11122](https://arxiv.org/abs/2005.11122)

First measurement of the ${}^3\overline{\text{He}}$ inelastic cross section.

- Drastic difference to Geant4 for low momenta
- Paper in preparation

Work in progress:

- Influence of these results on expected antinuclei fluxes in cosmic rays is being investigated
- Extend the analysis to other antinuclei (\bar{t} , ${}^4\overline{\text{He}}$, ...)



Back-up slides

Parameterisations used in GEANT4

Direct Glauber calculations in GEANT4 in a run-time mode are too heavy
 → parametrise Glauber calculations with [1] :

$$\sigma_{hA}^{tot} = 2\pi R_A^2 \ln \left[1 + \frac{A\sigma_{hN}^{tot}}{2\pi R_A^2} \right]$$

$$\sigma_{hA}^{in} = \pi R_A^2 \ln \left[1 + \frac{A\sigma_{hN}^{tot}}{\pi R_A^2} \right],$$

$$\sigma_{BA}^{tot} = 2\pi (R_B^2 + R_A^2) \ln \left[1 + \frac{BA\sigma_{NN}^{tot}}{2\pi (R_B^2 + R_A^2)} \right]$$

$$\sigma_{BA}^{in} = \pi (R_B^2 + R_A^2) \ln \left[1 + \frac{BA\sigma_{hN}^{tot}}{\pi (R_B^2 + R_A^2)} \right],$$

R_A cannot be directly connected with known values due to some simplifications

Use equations as a determination of R_A having calculated σ_{hA} and σ_{BA} with Glauber

For total cross-section:

$$\bar{p}A R_A = 1.34A^{0.23} + 1.35/A^{1/3} \text{ (fm)},$$

$$\bar{d}A R_A = 1.46A^{0.21} + 1.45/A^{1/3} \text{ (fm)},$$

$$\bar{t}A R_A = 1.40A^{0.21} + 1.63/A^{1/3} \text{ (fm)},$$

$$\bar{\alpha}A R_A = 1.35A^{0.21} + 1.10/A^{1/3} \text{ (fm)}.$$

For inelastic cross-section:

$$\bar{p}A R_A = 1.31A^{0.22} + 0.90/A^{1/3} \text{ (fm)},$$

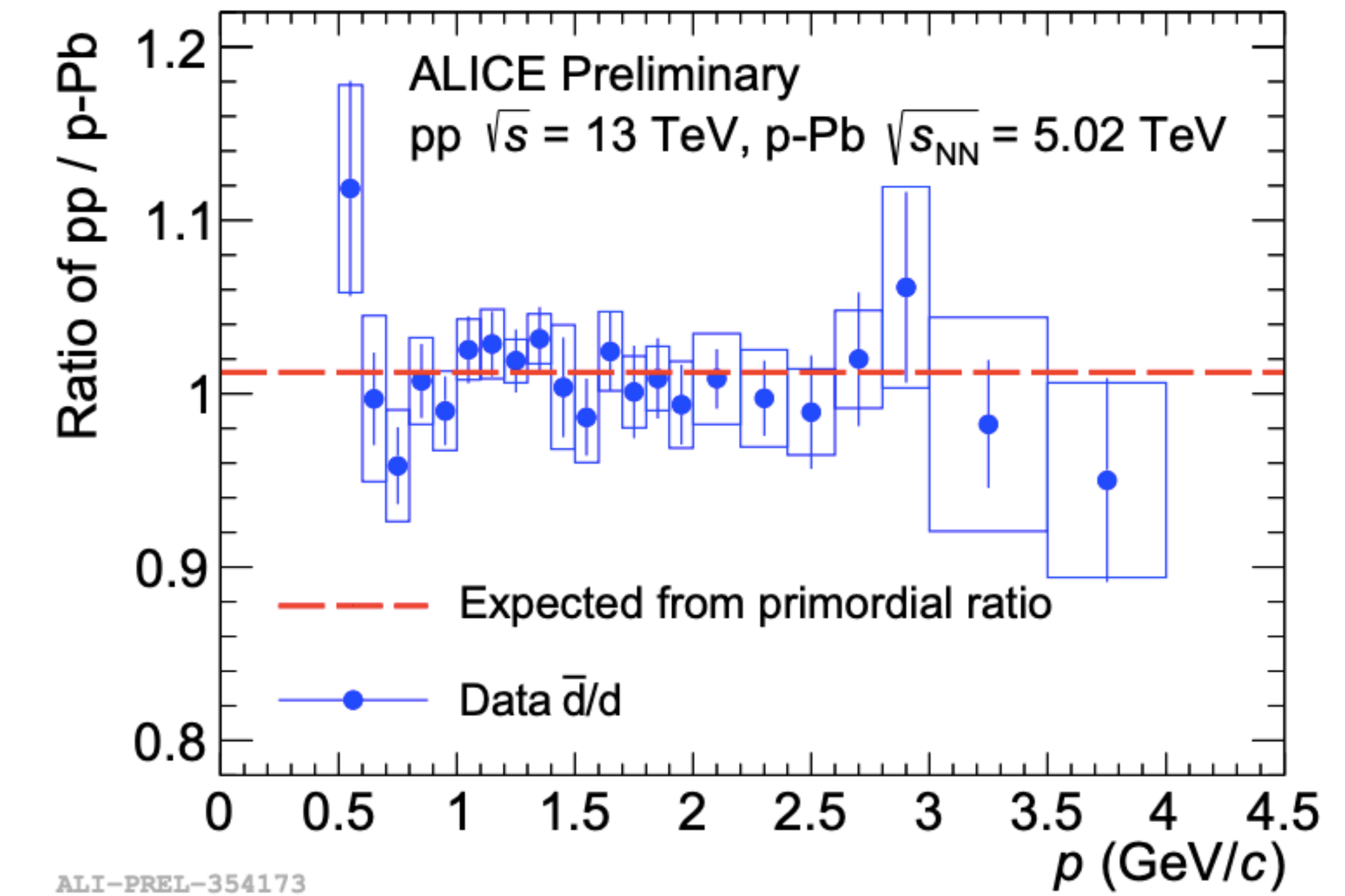
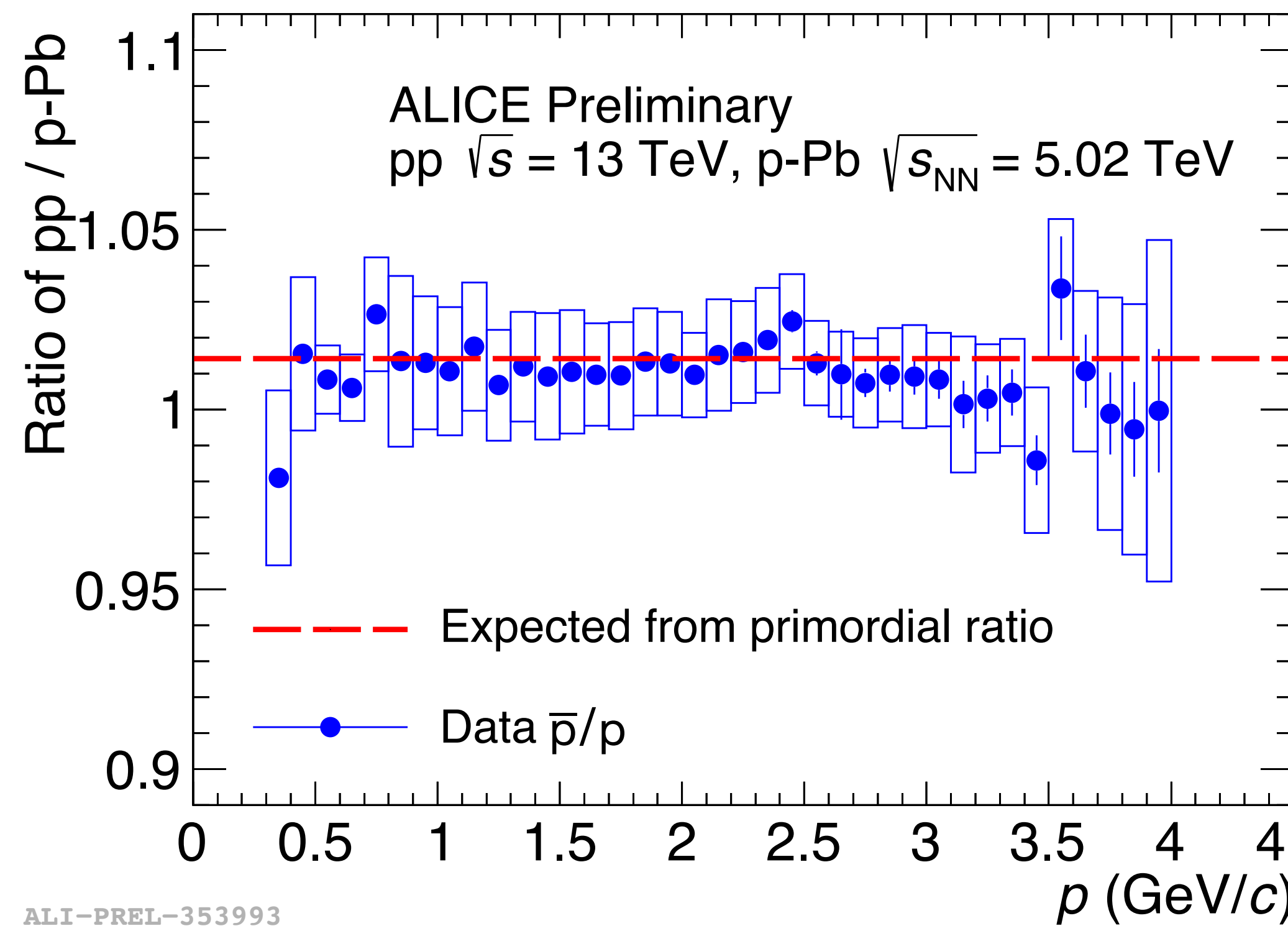
$$\bar{d}A R_A = 1.38A^{0.21} + 1.55/A^{1/3} \text{ (fm)},$$

$$\bar{t}A R_A = 1.34A^{0.21} + 1.51/A^{1/3} \text{ (fm)},$$

$$\bar{\alpha}A R_A = 1.30A^{0.21} + 1.05/A^{1/3} \text{ (fm)}.$$

[1] V.M. Grichine, Eur. Phys. J. C 62 (2009) 399, Nucl. Instrum. Methods B 267 (2009) 2460

Comparison of pp and p-Pb systems



Comparison of raw primary antiparticle-to-particle ratio in p-Pb and pp collisions.

- Consistent with the difference expected from primordial antimatter-to-matter ratio.
- The cross section measurements are independent of the collisions system, as expected.
- Analysis method is consistent.

Propagation in the galaxy

$$\frac{\partial \psi}{\partial t} = q(\mathbf{r}, p) + \mathbf{div}(D_{xx} \mathbf{grad} \psi - \mathbf{V} \psi) + \frac{\partial}{\partial p} p^2 D_{pp} \frac{\partial \psi}{\partial p} \frac{1}{p^2} - \frac{\partial}{\partial p} \left[\psi \frac{dp}{dt} - \frac{p}{3} (\mathbf{div} \cdot \mathbf{V}) \psi \right] - \psi \Gamma_{ann}$$

1

2

3

4

5

6

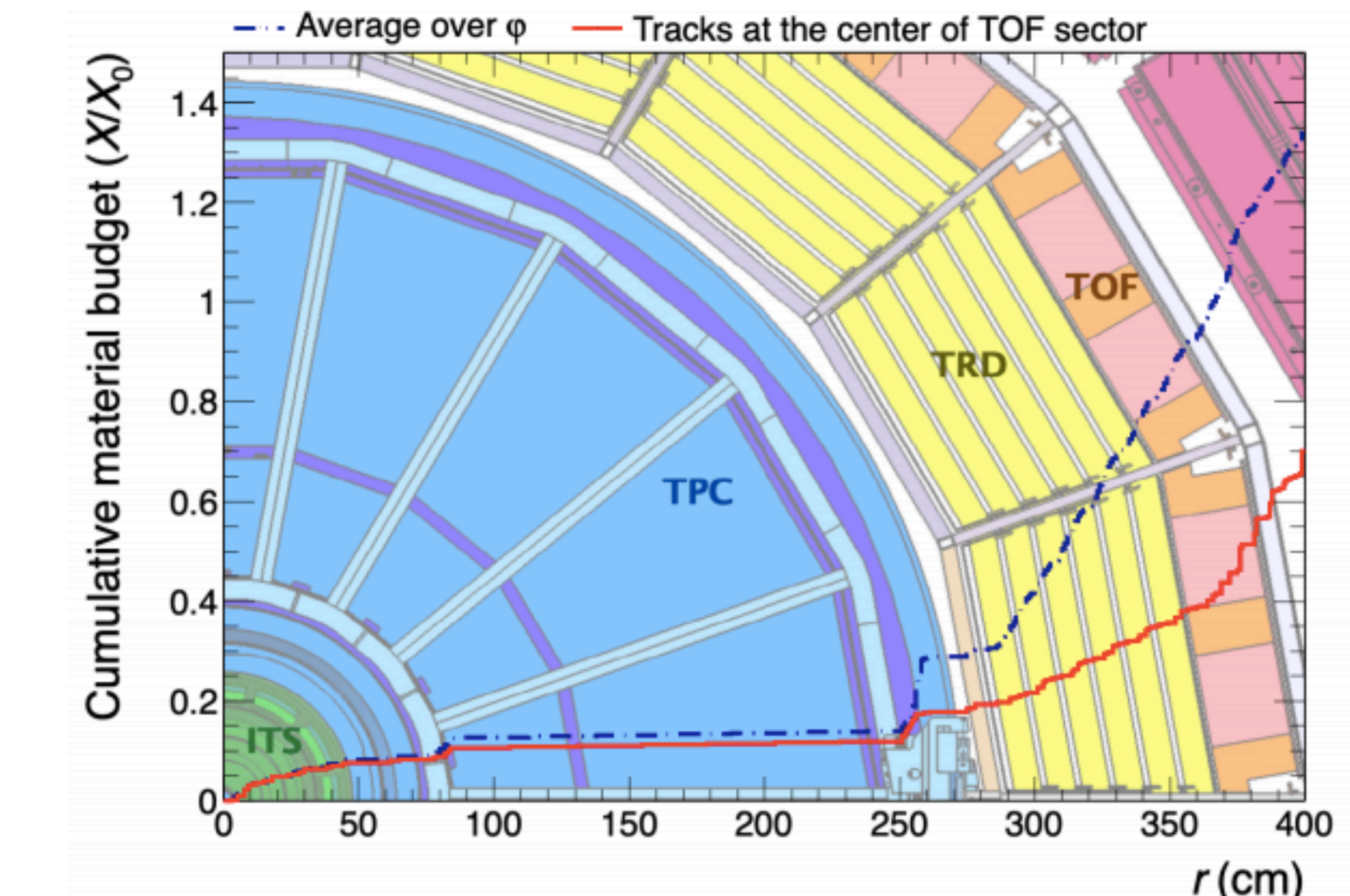
7

- 1 source function: PRIMARY OR SECONDARY
- 2 diffusion
- 3 convection
- 4 diffusive reacceleration
- momentum losses:
 - 5 via ionisation and bremsstrahlung
 - 6 adiabatic
- 7 annihilation

ALICE material budget

ALICE material budget at mid-rapidity [1]:

- **Beryllium beam pipe ($\sim 0.3\% X_0$)**
- **ITS ($\sim 8\% X_0$)**
- **TPC ($\sim 4\% X_0$)**
- **TRD ($\sim 25\% X_0$)**
- **Space frame ($\sim 20\% X_0$ between TPC and TOF)**

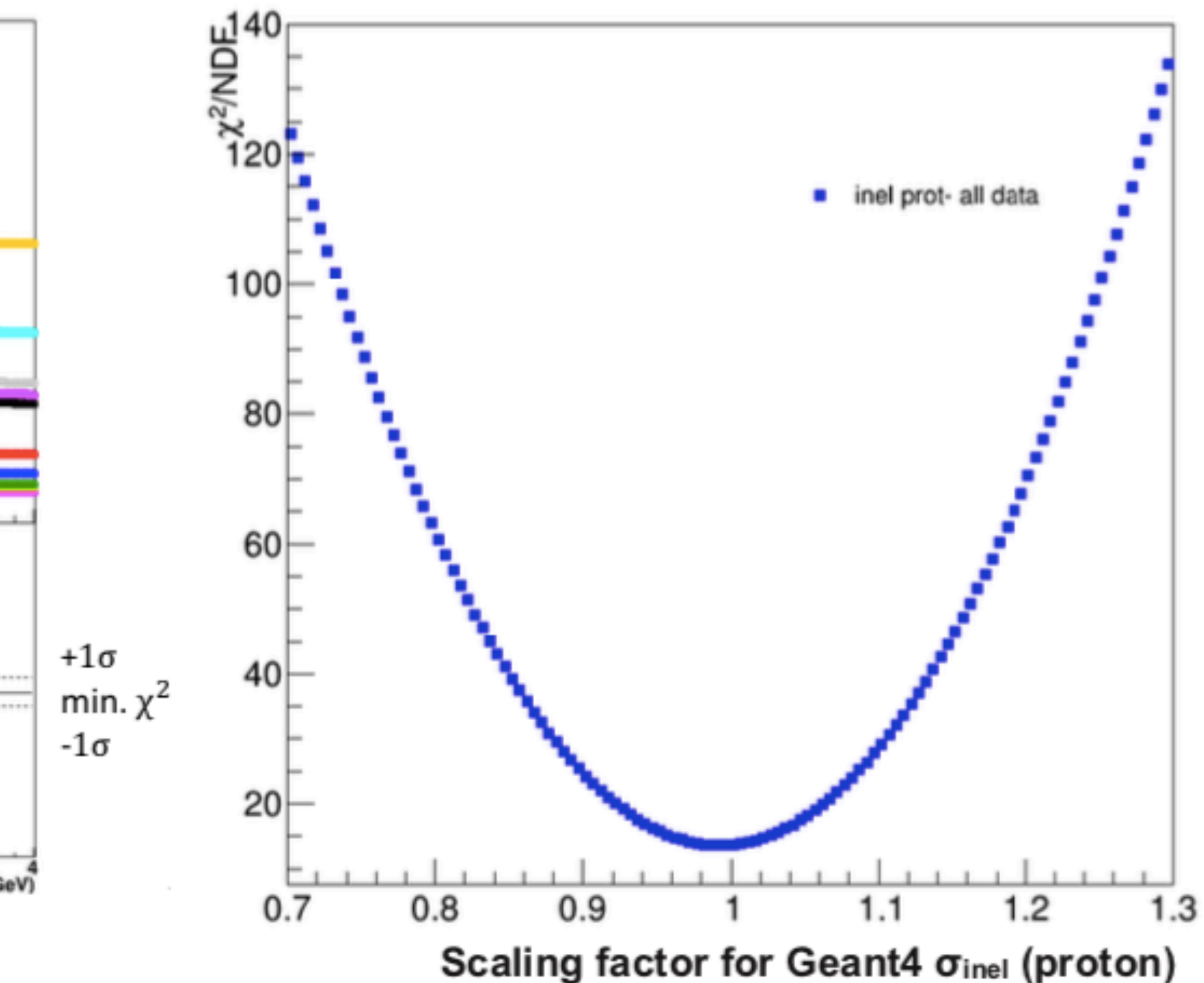
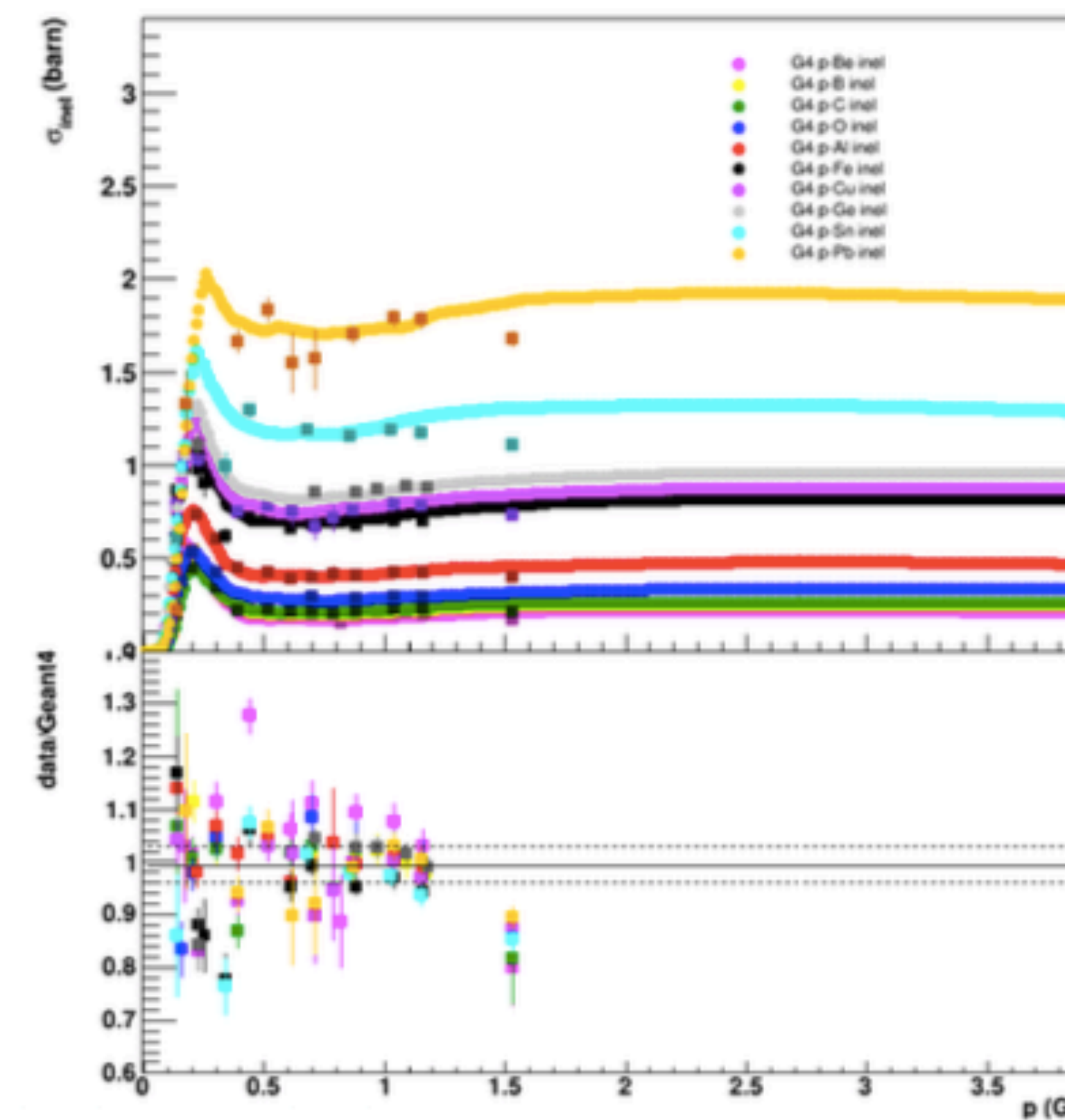


[arXiv:2005.11122](https://arxiv.org/abs/2005.11122)

Uncertainty due to σ_{inel} (proton)

How precise σ_{inel} (proton) is described by Geant4?

- Check available experimental data (Be,B,C,O,Al,Fe,Cu,Ge,Sn,Pb)
- Vary Geant4 parametrisation, calculate χ^2 for all data points
- Minimum χ^2 and $\pm 1\sigma$: **0.9925 $+0.0375$ -0.0325**



Variations of σ_{el} with simple Geant4 model

Vary each σ_{el} by $\pm 20\%$ in all combinations and check the final ratio

- σ_{el} contributes to scattering effects in ITS, TPC and TRD material
- Only a minor effect on the ratio ($\leq 1\%$ for \bar{p} / p , $\leq 2\%$ for \bar{d} / d)

For final results: cross-check the variations with full ALICE MC simulations

